

1 MARCH 1966

M-92-66-1

# STUDY OF THERMAL ISOLATION TECHNIQUES

## FINAL ENGINEERING REPORT

Contract No. JPL 950950

GPO PRICE \$ \_\_\_\_\_

CFSTI PRICE(S) \$ \_\_\_\_\_

Hard copy (HC) \$6.00

Microfiche (MF) 1.25

# 653 July 65

PREPARED FOR CALIFORNIA INSTITUTE OF TECHNOLOGY  
JET PROPULSION LABORATORY, PASADENA, CALIFORNIA

*Lockheed*

**MISSILES & SPACE COMPANY**

A GROUP DIVISION OF LOCKHEED AIRCRAFT CORPORATION

SUNNYVALE, CALIFORNIA

This work was performed for the Jet Propulsion Laboratory,  
California Institute of Technology, sponsored by the  
National Aeronautics and Space Administration under  
Contract NAS7-100.

N 66 24603

(ACCESSION NUMBER)

(PAGES)

(NASA CR OR TMX OR AD NUMBER)

(THRU)

(CODE)

(CATEGORY)

FACILITY FORM 602

1 MARCH 1966

M-92-66-1

# STUDY OF THERMAL ISOLATION TECHNIQUES

## FINAL ENGINEERING REPORT

Contract No. JPL 950950

PREPARED FOR CALIFORNIA INSTITUTE OF TECHNOLOGY  
JET PROPULSION LABORATORY, PASADENA, CALIFORNIA

*Lockheed*

**MISSILES & SPACE COMPANY**

A GROUP DIVISION OF LOCKHEED AIRCRAFT CORPORATION

SUNNYVALE, CALIFORNIA

This work was performed for the Jet Propulsion Laboratory,  
California Institute of Technology, sponsored by the  
National Aeronautics and Space Administration under  
Contract NAS7-100.

147  
PPG-2

## FOREWORD

This report covers work accomplished by the Lockheed Missiles & Space Company on the Study of Thermal Isolation Techniques (Contract JPL 950950) for the Jet Propulsion Laboratory, Pasadena, California, under the cognizance of the JPL Project Monitor, Robert Wengert. The study program was carried out by the Orbit Thermodynamics Department under the administration of H. Cohan.

The material presented in the report is arranged in three major sections that correspond to the three phases of the Thermal Isolation study. They are:

- Phase I - Evaluation of Thermal Isolation Techniques
- Phase II - Definition of Unique Problem Areas and Methods of Solution
- Phase III - Parametric Study of Selected Isolation Techniques for Typical Critical Components

Contributors to the study were:

G. R. Werth	Orbit Thermodynamics Study Leader
R. M. Vernon	Orbit Thermodynamics Principal Investigator
W. D. Moudy	Orbit Thermodynamics Feasibility of Thermoelectric Cooling
W. Hansen	Space Programs Component Sterilization Techniques
Dr. R. D. Reed	Physical Sciences Laboratory General Sterilization Problems
R. S. Hawkins	Material Sciences Laboratory Thermoelectric Devices Consultant
C. Waller	Orbit Thermodynamics Isolation System Design
B. W. Warner	Orbit Thermodynamics Computer Analysis

## CONTENTS

Section		Page
	FOREWORD	iii
	ILLUSTRATIONS	ix
	TABLES	xiii
	NOMENCLATURE	xv
1	INTRODUCTION	1-1
2	SUMMARY OF RESULTS AND RECOMMENDATIONS	2-1
	2.1 General Conclusions	2-1
	2.2 Recommendations	2-1
3	PHASE I - EVALUATION OF THERMAL ISOLATION TECHNIQUE	3-1
	3.1 Evaluation of Criteria for Feasibility of Thermal Isolation Methods	3-2
	3.1.1 Weight and Effectiveness	3-3
	3.1.2 Effect on Post-Launch Thermal Control	3-4
	3.1.3 Reliability	3-4
	3.1.4 Volume	3-5
	3.1.5 Aerospace Ground Equipment Requirements	3-5
	3.1.6 Other Considerations	3-5
	3.2 Weighting of Measurements of Feasibility Criteria	3-7
	3.3 Evaluation of Heat Flux Inputs for Unprotected General Components	3-7
	3.4 Passive Thermal Isolation	3-12
	3.4.1 Solid Insulation Materials	3-19
	3.4.2 Liquid Insulation Materials	3-25
	3.4.3 Gaseous Insulation Materials	3-25
	3.4.4 Feasibility of Passive Thermal Isolation	3-27



Section		Page
3.5	Fluid Circulation Cooling	3-27
3.5.1	Forced Fluid Circulation Systems	3-28
3.5.2	Cryogenic Fluid Boiloff Systems	3-38
3.5.3	Feasibility of Fluid Circulation Cooling	3-40
3.6	Phase Change Cooling	3-40
3.6.1	Solid Phase Change Materials	3-41
3.6.2	Liquid Phase Change Materials	3-44
3.6.3	Feasibility of Phase Change Cooling	3-48
3.7	Thermoelectric Cooling	3-49
3.7.1	Introduction	3-49
3.7.2	Application of Thermoelectric Cooling to Lander Module Thermal Isolation	3-51
3.7.3	Size of Thermoelectric Unit Required for Thermal Isolation	3-54
3.7.4	Feasibility of Thermoelectric Cooling	3-63
3.8	Summary and Relative Ranking of Candidate Thermal Isolation Methods	3-64
3.9	Conclusions – Phase I	3-68
3.10	References	3-68
4	PHASE II – DEFINITION OF PROBLEM AREAS AND METHODS OF SOLUTION	4-1
4.1	Preliminary Design of Isolation Systems	4-3
4.2	Interaction With Payload Design and Systems Integration	4-4
4.3	Interaction With Sterilization Facility and Lander Assembly Sequence	4-6
4.4	Detail Design of Isolation Devices	4-6
4.5	Program Plan and Milestones for Phase III	4-7
4.6	Conclusions – Phase II	4-9
4.7	References – Phase II	4-9
5	PHASE III – PARAMETRIC STUDY OF SELECTED ISOLATION TECHNIQUES FOR TYPICAL CRITICAL COMPONENTS	5-1
5.1	Preliminary Design of an Isolation System	5-1

Section	Page
5.1.1 Coolant Shield Design	5-8
5.1.2 Component Attachment to Adjacent Structure	5-10
5.1.3 Coolant Line Connection and Separation System	5-16
5.2 Interaction Between the Payload and Thermal Isolation Systems	5-19
5.2.1 Dry Heat Terminal Sterilization	5-20
5.2.2 Launch and Planetary Impact	5-24
5.2.3 Earth-Mars Cruise	5-25
5.2.4 Post-Landing	5-27
5.3 Interaction With Sterilization Facility and Lander Assembly Sequence	5-28
5.3.1 Sterilization Facility Design Requirements	5-28
5.3.2 Payload Assembly and Sterilization Processing	5-29
5.4 Detail Design of Isolation Devices	5-29
5.4.1 Coolant Shield and Auxiliary Isolation Mechanisms	5-32
5.4.2 Auxiliary Sterilization and Ground Equipment Requirements	5-34
5.4.3 Weight, Volume, and Reliability Penalties for the Thermal Isolation System	5-34
5.5 Conclusions - Phase III	5-37
5.6 References - Phase III	5-39

## Appendix

A	BASIC HEAT TRANSFER AND THERMOELECTRIC EQUATION DEVELOPMENT	A-1
A.1	Convective Heat Transfer to Non-Isolated Components	A-1
A.1.1	Cubical Volumes	A-1
A.1.2	Spherical Volumes	A-3
A.1.3	Long ( $L/D > 5$ ) Horizontal Cylinders	A-3
A.1.4	Short Horizontal or Vertical Cylinders	A-4
A.1.5	Long Vertical Cylinders	A-5
A.2	Summary of Relations for Fluid Circulation Cooling	A-6

Section	Page
A.3 Feasibility Analysis of Thermoelectric Cooling	A-7
A.3.1 Basic Relations for Analysis of Thermoelectric Cooling	A-8
A.3.2 Typical Material Parameters	A-11
A.3.3 Sample Calculations	A-12
A.3.4 Alternative Method of Analysis	A-14
B PHASE II ANALYTICAL OPERATIONS	B-1
B.1 Computer Thermal Analyses	B-1
B.1.1 References	B-16
B.2 Removable Thermoelectric Heat Shield	B-16
B.2.1 Heat Rejection Requirements	B-16
B.2.2 Sizing the Thermoelectric Unit	B-34
B.2.3 Application to Vidicon Tube Face	B-36

## ILLUSTRATIONS

Figure		Page
3-1	Convective Transfer Parameter vs. Surface Temperature (Natural Convection for Nitrogen at 293° F)	3-9
3-2	Free Convection Heat Transfer Correlation	3-10
3-3	Heat Flux Input to a Non-Isolated Body	3-11
3-4	Minimum Allowable Time Constant of Insulated Components as a Function of Initial and Maximum Component Temperatures	3-15
3-5	Minimum Insulation Resistance Required for Typical Sterilization Environment	3-18
3-6	Minimum Insulation Thickness Required for Passive Isolation as a Function of Component Properties and Insulation Thermal Conductivity	3-22
3-7	Minimum Insulation Thickness Required for Passive Isolation as a Function of Component Properties and Insulation Thermal Conductivity	3-23
3-8	Coolant Flow Rate vs. Spacing Between Component and Shield	3-32
3-9	Heat Transfer Coefficient vs. Shield Spacing	3-34
3-10	Shield Temperature vs. Shield Spacing	3-35
3-11	Heat Transfer Rate vs. Shield Spacing	3-36
3-12	Cryogenic Fluid Boiloff System	3-39
3-13	Vaporization of Liquid Phase-Change Materials at 1 Atmosphere Pressure	3-47
3-14	Typical Thermoelectric Heat Pump Couple	3-50
3-15	Maximum Hot Junction Temperature vs. Ratio of Insulation Area to Thermoelectric Pellet Area	3-57
3-16	Maximum Hot Junction Temperature vs. Ratio of Insulation Area to Thermoelectric Pellet Area	3-58
3-17	Thermoelectric Pellet Length vs. Ratio of Insulation Area to Thermoelectric Pellet Area	3-59

Figure		Page
3-18	Thermoelectric Pellet Length vs. Ratio of Insulation Area to Thermoelectric Pellet Area	3-60
3-19	Overall Characteristic Dimension and Minimum Thermoelectric Pellet Length vs. Component Characteristic Length	3-62
4-1	Design Considerations and Interface Effects	4-2
4-2	Thermal Analog Network for Simulation of Heat Flow Paths in Idealized Lander Configuration	4-5
5-1	Voyager-Lander Conceptual Design	5-2
5-2	Sterilization Shield Configuration	5-3
5-3	Battery Installation in Landed Payload	5-4
5-4	Life Detection Equipment in Landed Payload	5-5
5-5	Tape Recorder Installation in Landed Payload	5-6
5-6	Isolated Battery Installation	5-7
5-7	Isolated Component Concept Mockup	5-11
5-8	High Thermal Resistance Connection	5-13
5-9	High Thermal Resistance Connection	5-14
5-10	Thermal Expansion Joint Connection	5-15
5-11	Coolant Supply Line and Coolant Line Disconnect System	5-17
5-12	Thermal Response of Lander During Terminal Sterilization	5-21
5-13	Diagram of Sterilization Facility Functions	5-30
5-14	Diagram of Lander Sterilization Process	5-31
5-15	"In-Situ" Gulliver Design	5-33
5-16	Thermoelectric Isolation Device for Vidicon Tube Face	5-35
5-17	Thermoelectric Isolation Device, Second Concept	5-36
A-1	Heat Rejected and Convective Heat Transfer Rate vs. Thermoelectric Pellet Length-Area Ratio	A-17
B-1	Thermal Analyzer Input Data Listing for Terminal Sterilization Analysis	B-6
B-2	Thermal Analyzer Output	B-14
B-3	Thermal Analyzer Output	B-15
B-4	Thermal Analyzer Output	B-17
B-5	Martian Surface Temperature vs. Time	B-30

Figure		Page
B-6	Solar and Infrared Radiation Absorbed by Landed Payload Capsule	B-31
B-7	Convective Heat Transfer Coefficient vs. Film Temperature	B-33
B-8	Thermoelectric Pellet Length vs. Ratio of Insulation Area to Thermoelectric Pellet Area	B-35
B-9	Minimum Thermoelectric Pellet Length vs. Flat Plate Length	B-37

## TABLES

Table		Page
3-1	Typical Insulation Resistances Required for Passive Isolation	3-17
3-2	Insulation Resistances Required for Passive Isolation With Pre-Cooling	3-17
3-3	Thermal Conductivity of Typical Solid Insulating Materials and Potting Compounds	3-20
3-4	Thermal Conductivity of Liquid Insulation Materials at 70° F	3-20
3-5	Thermal Conductivity of Gaseous Insulation Materials at 100° F and Atmospheric Pressure	3-24
3-6	Maximum Component Surface Area-to-Thermal Capacity Ratios Allowable for Adequate Insulation Protection	3-24
3-7	Properties of Solid Phase Change Materials	3-42
3-8	Properties of Liquid Phase Change Materials	3-45
3-9	Numerical Values Assigned to Evaluation Criteria	3-65
3-10	Component Characteristics used for Isolation Rating Determination	3-65
3-11	Required Phase-Change Coolant Weights	3-65
3-12	Measures of Weight and Volume Requirements	3-66
3-13	Summaries of Ratings for Thermal Isolation Methods	3-66
4-1	Detailed Lander Component Specifications	4-3
5-1	Film Materials for Coolant Container Construction	5-9
5-2	Lander Temperatures During Cruise Phase	5-26
5-3	Lander Component Temperatures Six Hours After Planetary Impact	5-27
5-4	Isolation System Weight and Volume Requirements	5-37
B-1	Node Allocation for Voyager-Lander Network	B-2

## NOMENCLATURE

<u>Symbol</u>	<u>Definition</u>
A	Area, Convection Transfer Parameter
C	Thermal Capacitance
$c_p$	Specific Heat at Constant Pressure
D	Diameter, Annular Gap
$\mathcal{F}$	Interchange Factor for Gray-Body Radiative Transfer
g	Acceleration due to Gravity
Gr	Grashof Modulus
$\bar{h}$	Average Convective Heat Transfer Coefficient
H	Enthalpy
I	Electric Current
k	Thermal Conductivity
K	Thermal Conductance
L	Length
$L^*$	Characteristic Length
n	Number of Thermoelectric Couples
Nu	Nusselt Modulus
Pr	Prandtl Modulus
Q	Heat Flux
R	Thermal Resistance, Electrical Resistance
T	Temperature
$\bar{T}$	Mean Temperature
V	Volume
W	Weight
X	Ratio of Insulation Area to Area of Thermoelectric Element



## NOMENCLATURE (Cont.)

<u>Symbol</u>	<u>Definition</u>
Z	Thermoelectric Figure of Merit
$\alpha$	Seebeck Coefficient
$\beta$	Temperature Coefficient of Volume Expansion
$\epsilon$	Emittance
$\eta$	Dimensionless Measure of Feasibility
$\theta$	Time
$\theta^*$	Time Constant
$\mu$	Absolute Viscosity
$\rho$	Density, Electrical Resistivity, Reflectance
$\sigma$	Stefan-Boltzmann Constant
$\tau$	Thompson Coefficient
<u>Subscripts</u>	
a	Annular
AGE	Aerospace Ground Equipment
b	Bulk
C	Component, Cold Junction
COND	Conduction
CONV	Convection
E	Effectiveness
e	Effective
f	Fluid
G	Gas
H	Hot Junction
i,j	i <sup>th</sup> component, j <sup>th</sup> component
INT	Internal
IN	Inlet
I	Insulation

## NOMENCLATURE (Cont.)

<u>Subscripts</u>	<u>Definition</u>
MAX	Maximum
MIN	Minimum
n	n-type Thermoelectric Material
NI	Non-interference
OPT	Optimum
o	Initial
OUT	Outlet
P	Protected
p	p-type Thermoelectric Material
R	Reliability
RAD	Radiation
S	Shield, Outer Surface, Solid Material
ST	Sterilization
UNP	Unprotected
V	Volume
W	Weight

## Section 1

### INTRODUCTION

This report describes the results of the first phase of a program to develop thermal isolation techniques for heat sensitive components in a space vehicle during a terminal heat sterilization cycle. The development of successful isolation methods for operation under a severe sterilization environment will thus allow heat sensitive components to be included in the spacecraft's main structure during the thermal exposure. The major objective of this program was to investigate a wide range of candidate thermal isolation methods and their application to the protection of heat sensitive (pre-sterilized) components exposed to a prototype sterilization environment.

During Phase I of this study data was compiled on the proposed sterilization environment, typical spacecraft components, sterilization procedures and requirements; in addition a feasibility study was made of various isolation methods. The proposed sterilization environment for dry heat sterilization was specified in Ref. 1-1 and has been used as the basis for feasibility determination, as outlined in the next section. Spacecraft components which cannot withstand prolonged exposure to this sterilization environment were taken to be those typical of components used in a Mars Lander for a Mars-Voyager or Advanced Mariner system. Preliminary designs of Mars Lander modules are discussed in Refs. 1-2 and 1-3.

Previous studies of sterilization problems have been primarily devoted to specifying sterilization procedures which are effective in reducing the number of viable organisms remaining on the spacecraft below a certain level, or to handling and assembly techniques which do not allow contamination of sterilized components (see, for example, Ref. 1-4). The results of these studies have shown that dry-heat sterilization of the assembled, shrouded spacecraft is the most effective method of terminal sterilization. Procedures required for dry-heat sterilization are discussed in Ref. 1-5 and the design requirements of the sterilization canister or shroud are reviewed in Ref. 1-6. A detailed

study of the effects of the sterilization environment on the structural and thermal design of spacecraft is reported in Ref. 1-7, where a spacecraft configuration typical of proposed Mars Landers is analyzed. To date, however, no work appears to have been reported on the protection of pre-sterilized components during dry-heat terminal sterilization.

The results of the Feasibility Study presented in the Phase I Technical Summary Report provide the necessary background for a study of the design problems inherent in the application of thermal isolation devices to a typical Voyager Lander configuration. The primary objective of Phase II studies was the definition and categorization of these design problems, methods of approach to the solution of these problems, and the establishment of a work plan for the detailed studies that were performed during Phase III. Due to the lack of definition of a specific Lander design and the small amount of information available on sterilization facility designs, it became apparent that the most valuable output of the Thermal Isolation Study would be detailed information on the implementation of isolation systems and their associated weight and volume penalties, which could be applied to the preliminary design of Voyager systems. Requirements for thermal isolation can also be used as inputs in the design of a sterilization facility. Thus, the Phase III effort was planned to provide a limited parametric study of weight, volume, power requirements, and recommendations for packaging of thermal isolation devices. Because of the interaction of the isolation system with the spacecraft and sterilization facility systems, specific problems associated with the integration of these systems were investigated.

#### REFERENCES

- 1-1 JPL Specification No. XSO-30275-TST-A, Environmental Test Specification, Compatibility Test for Planetary Dry Heat Sterilization Requirements, dated 24 May 1963
- 1-2 Wooten, R. W., and Merz, E. J., "Mars-Voyager Systems," Preprints of Papers Presented at the AIAA Unmanned Spacecraft Meeting, Los Angeles, California, 1-4 March 1965

- 1-3 "Conceptual Design Studies of an Advanced Mariner Spacecraft," AVCO Corporation Report RAD-TR-64-36, AVCO Corp., Wilmington, Mass., 28 October 1964
- 1-4 Lockheed Missiles & Space Company, "Experimental Study of Sterile Assembly Techniques," Final Report Under Contract No. JPL-950993, LMSC M-56-65-1, 21 March 1965
- 1-5 Fried, E., and Kepple, R. J., "Spacecraft Sterilization - Thermal Considerations," AIAA Paper No. 65-427, July 1965
- 1-6 Tenney, J. B., and Crawford, R. G., "Design Requirements for the Sterilization Containers of Planetary Landers," AIAA Paper No. 65-387, July 1965
- 1-7 Tenney, J. B., and Fried, E., "Thermal Sterilization of Spacecraft Structures," Preprints of Papers Presented at the AIAA Unmanned Spacecraft Meeting, Los Angeles, California, 1-4 March 1965

## Section 2

## SUMMARY OF RESULTS AND RECOMMENDATIONS

LMSC has conducted a three-part study of Thermal Isolation Techniques. The overall objective of the study was to establish thermal isolation techniques that are feasible for protecting temperature sensitive materials and components in typical spacecraft instruments, equipment, systems and structures during a terminal heat sterilization cycle. Thermal isolation of some items may be necessary so that the entire assembled spacecraft can be subjected to the thermal exposure.

The results of the study should be of interest to both the engineering and biological communities since both are vitally concerned with meeting the recommendations of the Space Probe Sterilization Standards Study Group of COSPAR.

## 2.1 GENERAL CONCLUSIONS

1. Thermal isolation of temperature sensitive components during dry heat terminal sterilization is feasible from a thermodynamic viewpoint
2. Thermal isolation can best be accomplished, from a thermodynamic viewpoint, by circulating a liquid coolant through or around the component to be isolated. This method provides minimum total system weight and volume penalties.
3. The effects of efficacious thermal isolation systems on post-launch temperature control can be made negligible by proper thermal and mechanical design.
4. The isolation system interfaces between the landed payload, the lander module, and the sterilization facility require careful thermal and mechanical design to prevent biological contamination of the components to be isolated and to assure complete sterilization of adjacent non-isolated portions of the lander module.

## 2.2 RECOMMENDATIONS

It is recommended that future work be concentrated in the following three categories:

1. Preliminary design and evaluation of isolation techniques and mechanical devices for specific components or equipment packages that are to be included in planetary landers.
2. Preliminary design and evaluation of an integrated isolation system for a Lander module configuration under active consideration. The design would include all components and mobile units requiring thermal protection during terminal sterilization.
3. Preliminary design and evaluation of isolation system interface hardware such as coolant and/or electrical lines that originate in the sterilization facility and penetrate the lander module. Remotely actuated disconnect devices incorporating positive biological seals are included in this category. Ancillary equipment such as fluid conditioning units, vacuum pumps for evacuating the isolation system, and fluid charging equipment should be made a part of this category.

### Section 3

#### PHASE I - EVALUATION OF THERMAL ISOLATION TECHNIQUE

The initial task undertaken during Phase I of the study was to characterize the types of components for which thermal isolation would be required, and to delineate boundary conditions on sterilization environment and candidate isolation methods. As a result of meetings and communications with JPL, the following components were selected as representing the range of components requiring isolation:

- Type 1C Battery
- Tape Recorder
- Floating Rate Gyro
- Vidicon Tube
- Photomultiplier Tube
- Life Detection Experiment

The temperature limits and properties assumed for these components are summarized in Section 3.8. The materials used in the isolation technique must satisfy the following conditions:

- Materials shall be non-toxic and should not corrode or otherwise react with the spacecraft components or structure.
- Materials used in the isolation method must themselves be sterilizable.

A dry-heat terminal sterilization environment was taken to be that specified in Ref. 3-26, namely, exposure to a sterilization gas at 293° F for 36 hours. The sterilization gas was assumed to be dry nitrogen. Because of requirements for a shield or shroud surrounding the spacecraft, in addition to the fact that the outer shell of the lander module surrounds the lander components, it was assumed that natural, or free, convection of the sterilization gas was the primary mode of heat transfer to lander components.



The following candidate isolation methods were selected for investigation:

- Passive Thermal Isolation
- Fluid Circulation Cooling
- Phase Change Cooling
- Thermoelectric Cooling

The next step in the determination of feasibility of the candidate isolation methods was to establish the criteria by which feasibility of each method was to be evaluated. A numerical rating system was generated to provide a quantitative means of comparing isolation methods and rating their feasibility.

Each candidate isolation method was then examined to determine whether it could adequately protect components subjected to the proposed thermal environment. If the isolation method was shown to be adequate, the measures of feasibility criteria were then evaluated for each of the typical lander components. The results of this procedure and the numerical ratings of feasible isolation methods are summarized in the following sections.

### 3.1 EVALUATION OF CRITERIA FOR FEASIBILITY OF THERMAL ISOLATION METHODS

The criteria which were used to establish feasibility of candidate thermal isolation methods are as follows:

- Weight and Effectiveness
- Effect on Post-Launch Thermal Control
- Reliability
- Volume
- Aerospace Ground Equipment Required

These criteria must be evaluated for each type of component and for each isolation method. Numerical values are first established for each method as it is evaluated

with respect to a given type of component to be protected. These raw values are then adjusted by using appropriate weighting factors; the results are added together to provide a rating score ranging from zero to ten. Data pertinent to the use of this rating system are presented below.

### 3.1.1 Weight and Effectiveness

The coupling of weight and effectiveness criteria for each isolation method is one of the most significant measures of performance for each candidate method. However, the possibility of a favorable combination of methods having high effectiveness in conjunction with high weight should not be overlooked. Effectiveness as used here refers to operation of the isolation method solely during sterilization operations.

For any candidate thermal isolation scheme to be effective, it must be able to reject, insulate, or transport away heat fluxes, which would normally reach the body to be protected from the surrounding high temperature environment. A measure of effectiveness may thus be defined as a modified ratio of the heat flux input to an unprotected component to the heat flux input to a protected component; letting  $Q_P$  be the heat flux to the protected component, and  $Q_{UNP}$  be the heat flux to the unprotected component, we define an effectiveness,  $\eta_E$ , such that

$$\eta_E = \frac{1 - (Q_P/Q_{UNP})}{1 + (Q_P/Q_{UNP})} \quad (3.1)$$

Similarly, a measure of the weight penalty imposed by each type of isolation method may be defined as the ratio of the weight of the unprotected to the protected component:

$$\eta_W = \frac{W_{UNP}}{W_P} \quad (3.2)$$

obviously high values of both  $\eta_E$  and  $\eta_W$  are desirable. The value of  $W_P$  in Eq. (3.2) refers, of course, to the flight weight of the protected component.

### 3.1.2 Effect on Post-Launch Thermal Control

The effect of a particular isolation method on post-launch thermal control, and systems operation in general, must be minimized or eliminated. If a given isolation method is expected to have such effects, a complete evaluation of their importance requires a thermal analysis of the integrated vehicle and lander modules during the Earth orbit, transfer, and Mars orbit phases of the mission. For a preliminary evaluation, therefore, a qualitative scale of performance can be used with each isolation method ranked in order of desirability. A measure of "non-interference",  $\eta_{NI}$  is defined as follows:

<u>Non-Interference Parameter, <math>\eta_{NI}</math></u>	<u>Effect of Isolation Method on Thermal Control and/or System Performance</u>
1.0	Beneficial Effect
0.90	No Effect
0.70	Possible Performance Degradation
0.50	Allowable Performance Degradation
0.0	Prohibitive Effect

### 3.1.3 Reliability

Again, the reliability of a particular isolation scheme must be evaluated in conjunction with the components to which it is applied, the complexity of the isolation scheme, etc. As above, we establish a qualitative measure of reliability as follows:

<u>Reliability Parameter <math>\eta_R</math></u>	<u>Anticipated Reliability</u>
1.0	Fail-Safe
0.90	Inherently Reliable
0.50	Ordinarily Reliable
0.0	Notoriously Unreliable

### 3.1.4 Volume

A measure of the volume penalty imposed by a given isolation method is defined as follows:

$$\eta_V = \frac{V_{UNP}}{V_P} \quad (3.3)$$

where  $V_{UNP}$  refers to the original total volume of the component and  $V_P$  refers to the flight volume of the protected component. Again, high values of  $\eta_V$  are desirable.

### 3.1.5 Aerospace Ground Equipment Requirements

For this evaluation, a simple estimate of AGE requirements is made in terms of whether there is no AGE, a small amount, or a considerable amount is required.

$\eta_{AGE}$	Amount of AGE Required
1.0	None Required
0.5	Some Required
0.0	Large Amount Required

### 3.1.6 Other Considerations

A cursory review of the total problem is sufficient to reveal other factors that will influence the selection of a thermal isolation method. For example, the proposed measure for volume does not take into account any limitations on space availability in the lander capsule design. It appeared to be highly presumptuous, however, to impose such restrictions in this study since they would have been, of necessity, quite arbitrary in nature. Furthermore, since only feasibility was evaluated in this phase of the study care was taken not to preclude any possible solutions to the problem.

### 3.2 WEIGHTING OF MEASUREMENTS OF FEASIBILITY CRITERIA

In any preliminary investigation of feasibility, the importance given to each of the above criteria must be somewhat arbitrary and subjective. However, in order to systematize the determination of feasibility, weighting factors were assigned to each feasibility criterion. The table below summarizes the parameters which were established as measures of feasibility criteria. Included are the weighting factors and summaries of "ideal", or perfect, scores which a given isolation method could have when applied to a particular component.

<u>Criterion</u>	<u>Measure</u>	<u>Ideal Value</u>	<u>Worst Value</u>	<u>Weighting Factor</u>	<u>Maximum Value</u>
Effectiveness	$\eta_E$	1.0	0.0	2.5	2.5
Weight	$\eta_N$	1.0	0.0	2.0	2.0
Reliability	$\eta_R$	1.0	0.0	2.0	2.0
Non-Interference	$\eta_{NI}$	1.0	0.0	1.7	1.7
Volume	$\eta_V$	1.0	0.0	1.5	1.5
AGE Required	$\eta_{AGE}$	1.0	0.0	0.3	0.3

Weighted "Perfect Score" 10.0

### 3.3 EVALUATION OF HEAT FLUX INPUTS FOR UNPROTECTED GENERAL COMPONENTS

For a general type of component, when not protected by some thermal isolation method the heat flux input will be given by

$$(Q_j)_{UNP} = \sum_{\substack{i=1 \\ i \neq j}}^n \frac{T_i - T_j}{R_{ij}} + (Q_j)_{INT} \quad (3.4)$$

where  $(Q_j)_{INT}$  is the internally generated heat flux of the  $j^{th}$  component, and  $R_{ij}$  represents the total thermal resistance due to combined radiative, convective and conductive inputs from the  $(n - 1)$  sources of heat transfer to the  $j^{th}$  component.

For a detailed effectiveness evaluation it is necessary to account for these separate modes of heat transfer; however, in order to establish feasibility, it was assumed that the unprotected component is completely isolated from conductive and radiative heat inputs, and that it has zero internal heat dissipation. In addition, it was assumed that each component can be approximated by a general shape exposed to natural convection heat inputs from nitrogen gas at 293° F. This simplifies the evaluation of  $\eta_E$  and allows a unified presentation of heat inputs to unprotected components. As shown in Ref. 3-1

$$R = \frac{1}{\bar{h}A_{CONV}} \quad (3.5)$$

and Eq. (3.4) reduces to

$$(Q_j)_{UNP} = \bar{h}A_{CONV} (293 - T_j) \quad (3.6)$$

The heat transfer coefficient,  $\bar{h}$ , has been evaluated for several general shapes, as shown in Appendix A. As a result of this evaluation, the following general method was obtained for the correlation of natural convection heat transfer. Representing the heat transfer coefficient,  $\bar{h}$ , as

$$\bar{h} = \frac{K_f Nu}{L^*} \quad (3.7)$$

and the product of Grashof and Prandtl numbers as

$$(Gr Pr)_{UNP} = 0.71 AL^{*3} (293 - T) \quad (3.8)$$

the Nusselt number is determined from the calculated value of  $(Gr Pr)_{UNP}$  and the correlations shown in Figs. 3-1 and 3-2 according to the following table:

<u>Geometry</u>	<u>Characteristic Length, <math>L^*</math></u>	<u>Correlation</u>
Cube, Side $L$	$L/2$	Fig. 3.2
Sphere, Diameter $D$	$D/2$	Fig. 3.2
Long Horizontal Cylinder, Diameter $D$	$D$	Fig. 3.2
Short Horizontal or Vertical Cylinders, Length $L$ , Diameter $D$	$L/1 + (L/D)$	Fig. 3.2
Long Vertical Cylinders, Height $H$	$H$	$Nu = 0.555 (Gr Pr)^{1/4}$

Using this method, the values of heat flux per unit area have been plotted as a function of body surface temperature in Fig. 3-3. Using these results, initial evaluations of effectiveness may be made for general shapes for each candidate thermal isolation scheme. In addition, the values of heat flux inputs shown in Fig. 3-3 determine the amount of heat which must be absorbed by the protective mechanism for a given outer surface temperature of the protected assembly. For example, if a fluid circulation scheme is proposed to protect a cubical component whose sides are 0.2 feet in length, and the outer surface temperature of the cooling jacket is 150° F, then the circulating fluid must be capable of absorbing at least 222 BTU/Hr-Ft<sup>2</sup> in order that the protected component be maintained at a constant temperature. Of course, the inner surface temperature of the cooling jacket must also be below the maximum allowable component temperature.

In the following sections, approximate measures of feasibility criteria are developed for specific isolation methods in the following general classes:

- Passive Thermal Isolation
- Fluid Circulation Cooling
- Phase Change Cooling
- Thermoelectric Cooling

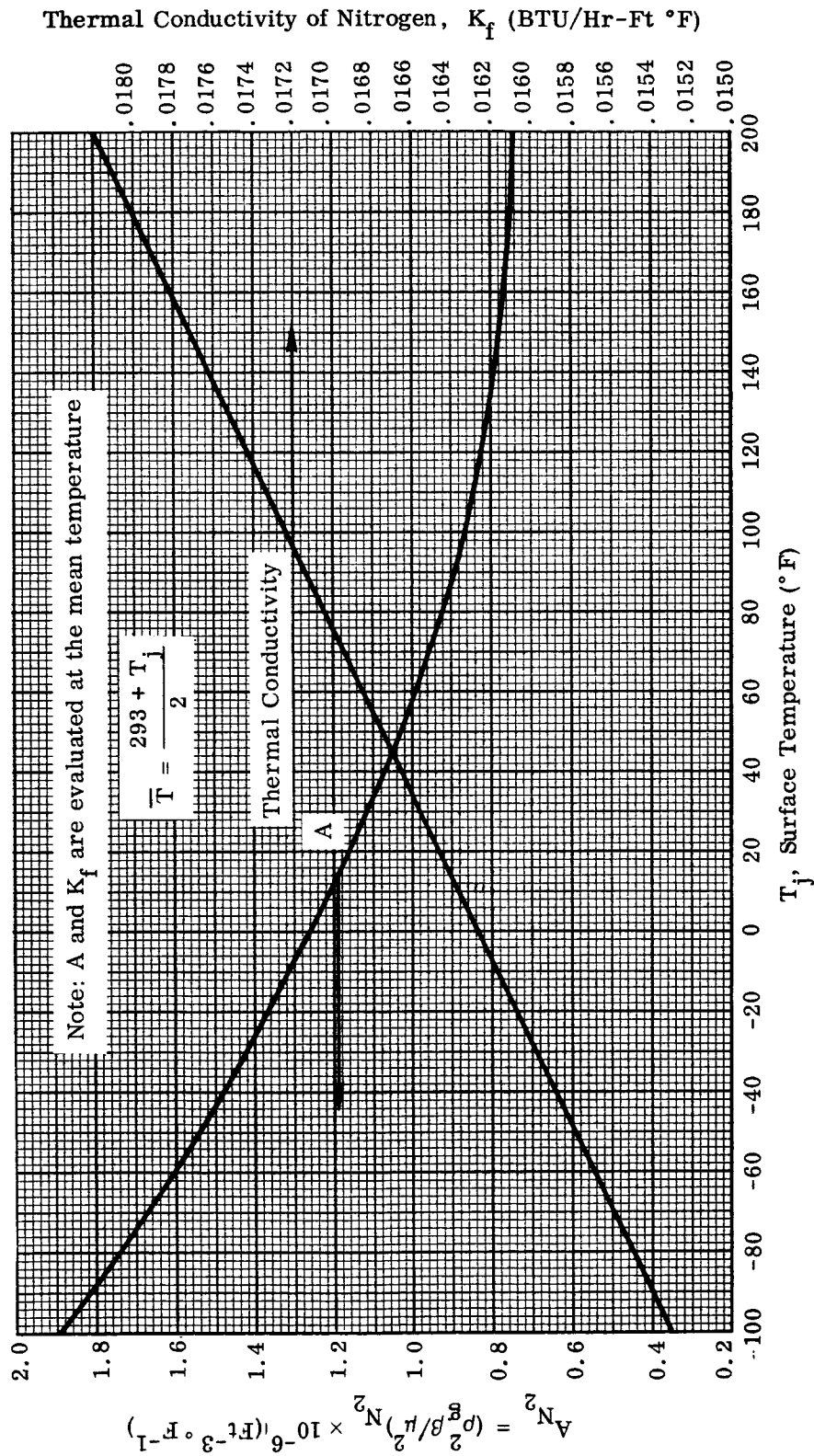


Fig. 3-1 Convective Transfer Parameter vs. Surface Temperature (Natural Convection for Nitrogen at 293°F)



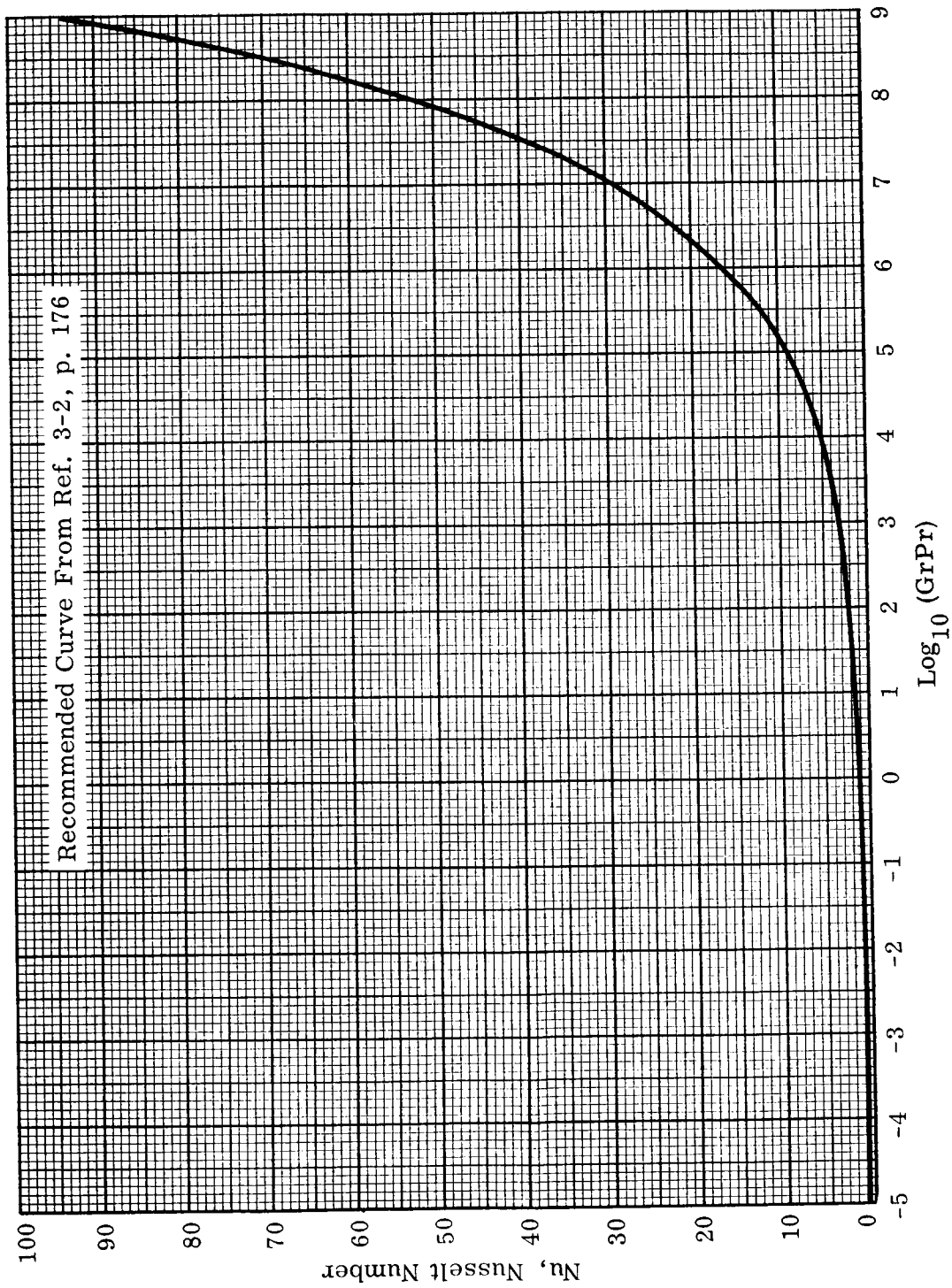


Fig. 3-2 Free Convection Heat Transfer Correlation

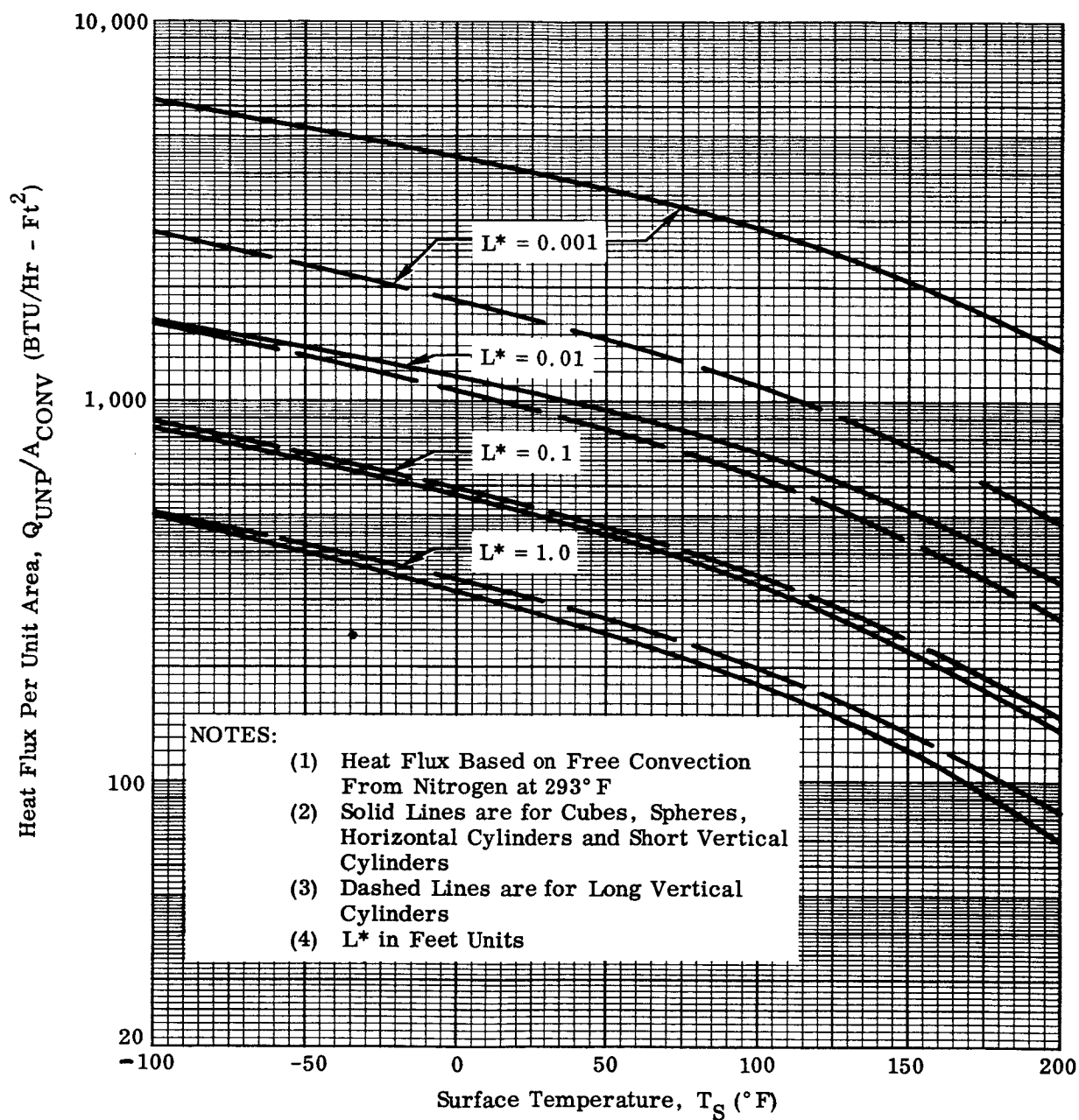
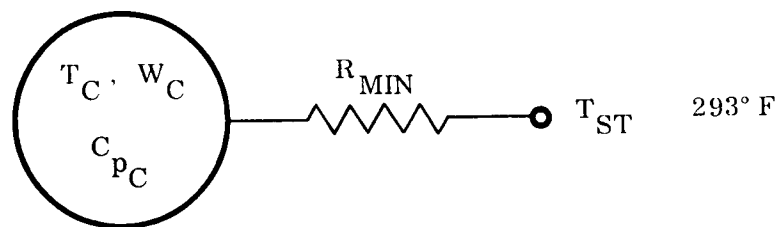


Fig. 3-3 Heat Flux Input to a Non-Isolated Body

In all cases, it is assumed that the component to be protected is not dissipating heat internally. Also, the effects of heat inputs through auxiliary connections, wiring, etc., required by the isolation method are neglected.

### 3.4 PASSIVE THERMAL ISOLATION

Passive thermal isolation schemes include the use of insulation surrounding the component to be protected, as well as the combination of component precooling or mechanical disconnects in conjunction with insulation. For any of these isolation schemes, the minimum requirement for feasibility is that the protected component remain below its maximum allowable temperature,  $T_{MAX}$ . This requirement may be interpreted as a lower bound on the thermal resistance of the insulation. To obtain this minimum required resistance, the component is idealized as a lumped thermal capacitance,  $C$ , connected to its environment through a thermal resistance  $R_{MIN}$ , as sketched below.



For insulation schemes using solid insulation materials, the resistance,  $R_{MIN}$ , is the conductive thermal resistance;

$$(R_{MIN})_S = \left( \frac{L_{COND}}{K_S A_{COND}} \right)_{MIN} \quad (3.9)$$

For liquid insulation materials, it is the combination of the conductive and convective thermal resistances in parallel:

$$(R_{\text{MIN}})_L = \left[ \frac{1}{\left( \frac{K_L A_{\text{COND}}}{L_{\text{COND}}} \right) + \bar{h}_L A_{\text{CONV}}} \right]_{\text{MIN}} \quad (3.10)$$

and for gaseous insulation materials, it is the combination of conductive, convective and radiative resistances in parallel:

$$(R_{\text{MIN}})_G = \left[ \frac{1}{\frac{K_G A_{\text{COND}}}{L_{\text{COND}}} + \bar{h}_G A_{\text{CONV}} + \frac{\sigma A_{\text{RAD}} \mathcal{F}(\bar{T}_C^4 - T_{\text{ST}}^4)}{T_C - T_{\text{ST}}}} \right] \quad (3.11)$$

In Eq. (3.11), it is assumed that the insulating gas is contained around the component by a metallic shield which is at the temperature of the sterilization fluid,  $T_{\text{ST}}$ . This assumption is desirable since, in preliminary studies reported in Ref. 3-1, it was shown that the isolation effectiveness of gaseous insulators contained by insulating shields is less than those contained by highly conductive, thin shields.

As shown in Ref. 3-1, if  $T_{\text{ST}}$  is constant, the minimum required resistance may be calculated from

$$\frac{T_{\text{MAX}} - T_{\text{ST}}}{T_0 - T_{\text{ST}}} = e^{-\theta_{\text{ST}}/RC}$$

or

$$R_{\text{MIN}} = \frac{\theta_{\text{ST}}}{C \ln \frac{T_{\text{ST}} - T_o}{T_{\text{ST}} - T_{\text{MAX}}}} \quad (3.12)$$

where  $\theta_{\text{ST}}$  is the maximum duration of the sterilization period. Equation (3.12) may be rewritten to yield another parameter which provides a direct physical interpretation of the isolation scheme:

$$\theta_{\text{MIN}}^* = (RC)_{\text{MIN}} = \frac{\theta_{\text{ST}}}{\ln \frac{T_{\text{ST}} - T_o}{T_{\text{ST}} - T_{\text{MAX}}}} \quad (3.13)$$

where  $\theta^* = RC$  is the time constant of the system; i.e., the time in which the component temperature rise has reached 63 percent of the difference between its initial temperature,  $T_o$ , and the sterilization temperature,  $T_S$ . Thus

$$\frac{T - T_o}{T_S - T_o} = 0.632 \text{ when } \theta = \theta^* \quad (3.14)$$

It should be noted that in the idealized model described above, no allowance has been made for the thermal capacitance of the insulation. This is a conservative factor in that the thermal capacity of the insulation would cause an added time lag in heat flux input to the component.

The dimensionless ratio  $(\theta_{\text{MIN}}^*/\theta_{\text{ST}})$  has been evaluated as a function of the dimensionless ratios  $(T_{\text{MAX}}/T_{\text{ST}})$  and  $(T_o/T_{\text{ST}})$  from Eq. (3.13) and the results plotted in Fig. 3-4. These curves establish the minimum allowable time constant and, for a given component, the minimum thermal resistance of insulation required to maintain

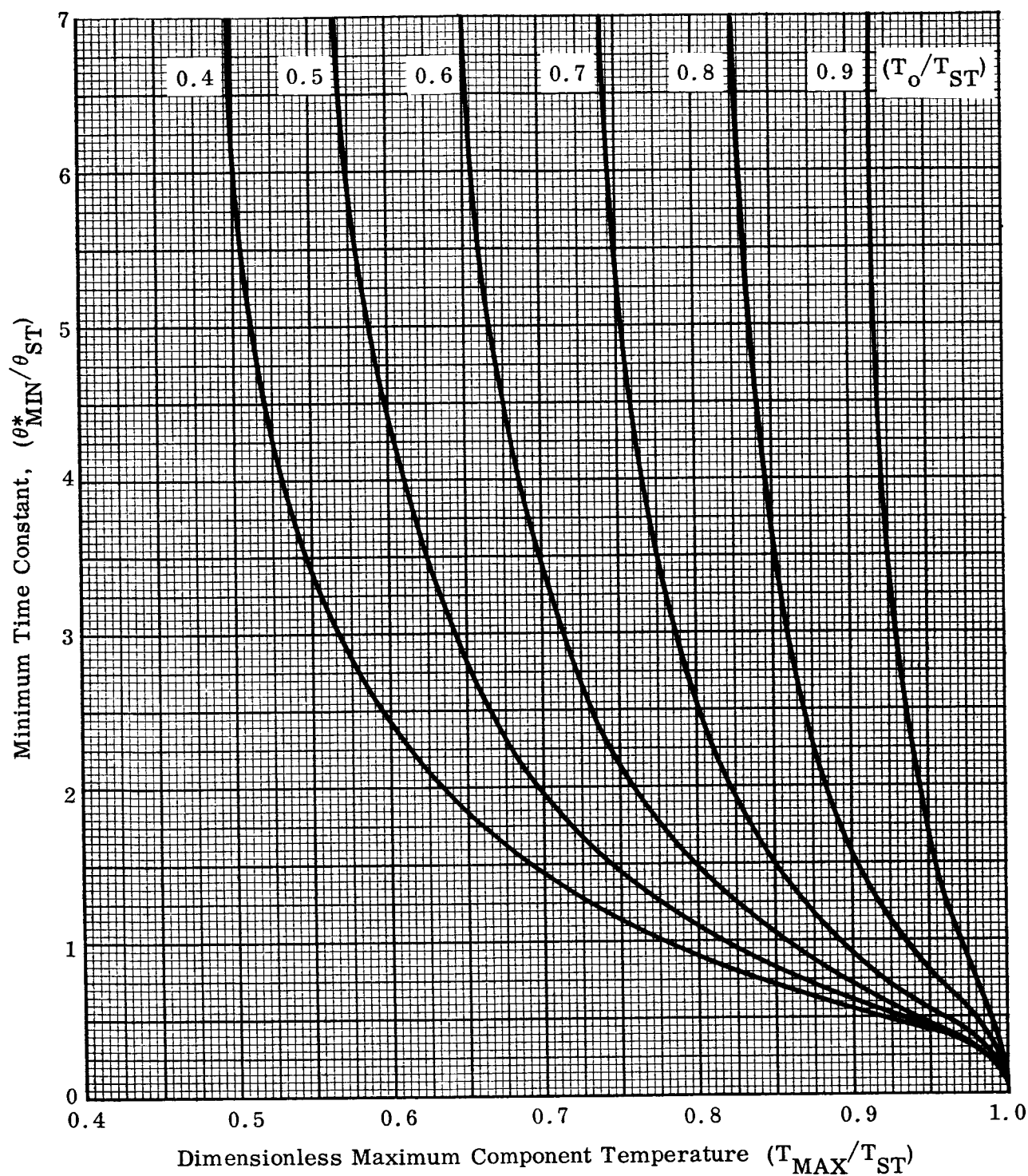


Fig. 3-4 Minimum Allowable Time Constant of Insulated Components as a Function of Initial and Maximum Component Temperatures

the component below a temperature  $T_{MAX}$ , with a sterilization environment temperature  $T_{ST}$  and an initial component temperature  $T_O$ .

In order to determine the range of thermal resistances required for feasible insulation schemes, we consider some typical components which would require protection during sterilization. These components and their estimated weights, average specific heats, and upper temperature limits are listed in Table 3-1. Also indicated are the values of  $R_{MIN}$  required as computed using the following assumptions:

$$T_{ST} = 293^{\circ}F = 753^{\circ}R$$

$$T_O = 67^{\circ}F = 527^{\circ}R$$

$$\theta_{ST} = 36 \text{ hours}$$

These results show that, for components with low thermal capacitances, the high insulation resistances required prohibit the use of this method of isolation.

The dramatic effect of pre-cooling the same components (with  $T_{ST}$  and  $\theta_{ST}$  as before) is shown in Table 3-2 where it has now been assumed that  $T_O = -8^{\circ}F$ . In most cases, the required insulation resistances have been reduced by about a factor of two. Indeed, for the component with the largest thermal capacity (the type IC battery), the required conductive resistance may be obtained with a gaseous insulation material such as air. This was discussed earlier in Ref. 3-1. The minimum required insulation resistance has been plotted as function of thermal capacity in Fig. 3-5, where it has been assumed that

$$T_{ST} = 293^{\circ}F$$

$$T_{MAX} = 142^{\circ}F$$

$$T_O = -8^{\circ}F \text{ and } +67^{\circ}F$$

$$\theta_{ST} = 36 \text{ hours}$$

Table 3-1

TYPICAL INSULATION RESISTANCES REQUIRED FOR  
PASSIVE ISOLATION

Component	Weight (lb)	$C_p$ (BTU/Lb° F)	$T_{MAX}$ (° F)	$\theta^*_{MIN}$ (hr)	$R_{MIN}$ (BTU/Lb° F)	$R_{MIN}$ (° F/watt)
Type IC Battery	118.0	0.186	140	93.6	4.26	14.55
Tape Recorder	17.0	0.20	158	70.1	20.6	70.3
Gyro Package	~10.0	0.20	140	93.6	46.8	159.6
Vidicon Tube (Including coils)	~ 0.6	0.20	212	35.9	299.0	1,020.0
Photomultiplier Tube	0.375	0.20	100	266.3	3,020.0	10,300.0

NOTE: Initial temperature =  $T_o = 67^\circ F$ ; sterilization temperature =  $T_{ST} = 293^\circ F$ ;  
duration of exposure to sterilization environment =  $\theta_{ST} = 36$  hours.

Table 3-2

INSULATION RESISTANCES REQUIRED FOR PASSIVE  
ISOLATION WITH PRE-COOLING

Component	$\theta^*_{MIN}$ (hr)	$R_{MIN}$ (Hr° F/BTU)	$R_{MIN}$ (° F/watt)	$(R_{MIN})_{T_o = -8^\circ F}$
				$(R_{MIN})_{T_o = 67^\circ F}$
Type IC Battery	52.9	2.41	8.22	0.565
Tape Recorder	44.3	13.03	44.4	0.632
Gyro Package	52.9	26.4	90.0	0.564
Vidicon Tube	27.0	225.0	768.0	0.753
Photomultiplier Tube	81.8	1,090.0	3,720.0	0.362

NOTE: Initial temperature =  $T_o = -8^\circ F$ ;  $T_{ST} = 293^\circ F$ ;  $\theta_{ST} = 36$  hours.



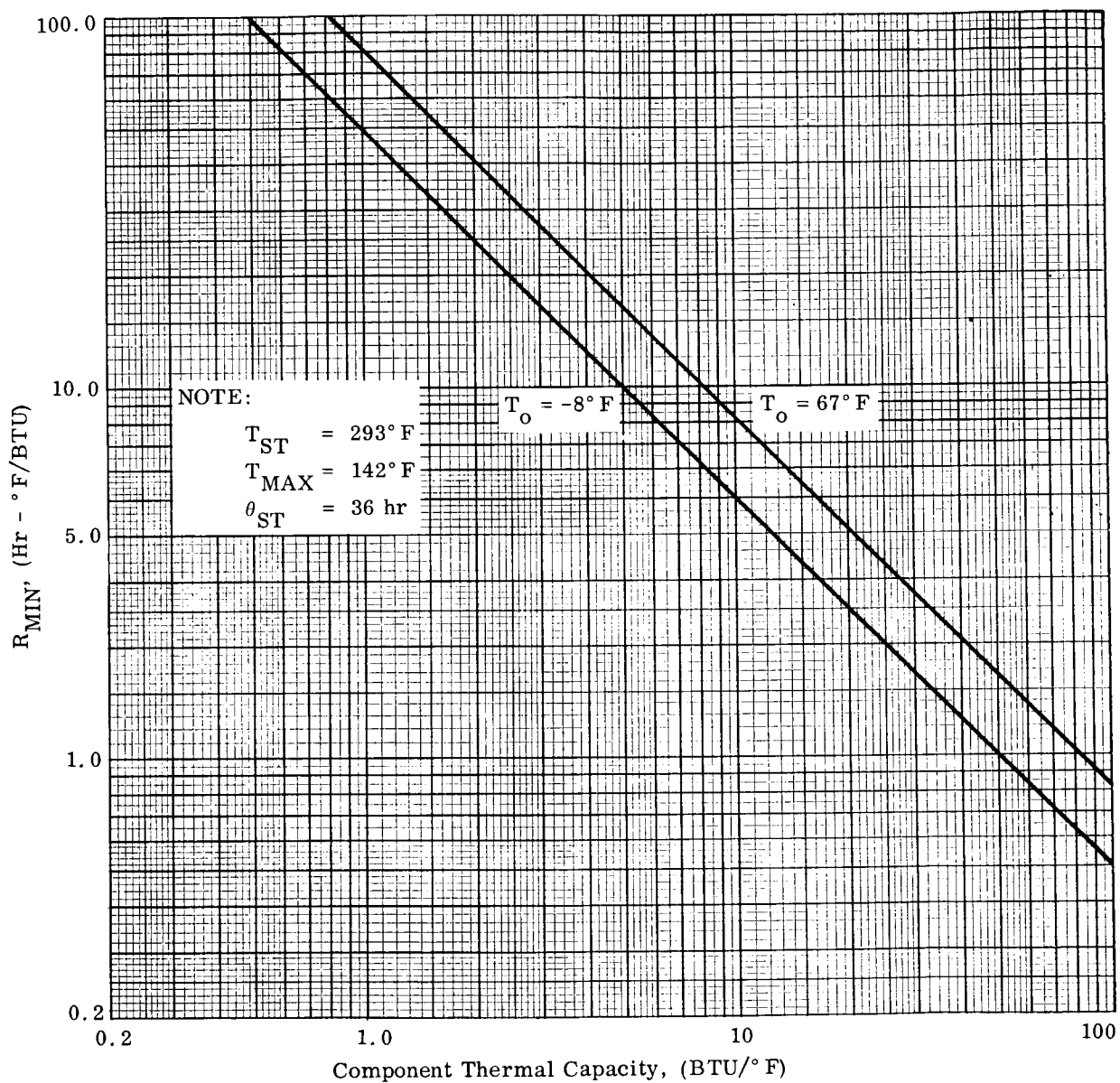


Fig. 3-5 Minimum Insulation Resistance Required for Typical Sterilization Environment

The minimum resistance values shown in Fig. 3-5 can be used to determine the adequacy of typical solid, liquid, and gaseous insulation materials.

### 3.4.1 Solid Insulation Materials

The thermal resistance of a solid material is given by

$$R_S = \frac{L_{COND}}{K_S A_{COND}} \quad (3.15)$$

where  $A$  is the average area for conductive heat transfer. For reasonable insulation thicknesses we may approximate this area by the external surface area of the component, if the component is large ( $L^* > 0.2$ , for example). Table 3-3 shows the thermal conductivity of some typical insulation materials at room temperature.

Assuming that a material having a thermal conductivity of 0.01 BTU/Hr-Ft° F is available, the minimum required insulation thickness may be calculated for several typical components. This has been done using Eq. (3.15) and Fig. 3-5, assuming that  $T_o = -8^\circ\text{F}$ . The results are tabulated below.

Component	$A_{COND}$ (ft <sup>2</sup> )	$C$ (BTU/° F)	$(R_{MIN})_{T_o = -8^\circ\text{F}}$ (Hr° F/BTU)	$L_{MIN}$ (in)
Battery	6.0	21.95	2.35	1.69
Tape Recorder	3.3	3.4	15.2	6.03
Gyro Package	1.0	2.0	26.0	3.12
Vidicon Tube	0.15	0.12	225.0	4.05
Photomultiplier Tube	0.25	0.075	1090.0	32.75

From these results it may be seen that reasonable insulation thicknesses are obtainable only for components having high thermal capacitances and small surface areas. Indeed, for any isolation scheme using an insulation material through which conduction is the primary mode of heat transfer, the minimum insulation thickness is given by

Table 3-3

THERMAL CONDUCTIVITY OF TYPICAL SOLID INSULATING  
MATERIALS AND POTTING COMPOUNDS

<u>Material</u>	<u>Thermal Conductivity (BTU/Hr-Ft-° F)</u>	<u>Reference</u>
Alkyd-Isocyanate Foam	0.03	3-5
Alumina (48.7% porosity)	8.7	3-3
Asbestos	0.092	3-4
Butadiene-Styrene Foam	0.018	3-2
Butyl Rubber	0.05	3-2
Min-K	0.011 - 0.015	3-6
Natural Rubber	0.08	3-2
Natural Rubber Foam	0.025	3-2
Polyester Urethane Foam	0.023	3-7 & 3-8
Polystyrene Epoxy Foam, Rigid	0.02	3-2
Quartz Felt	0.02	3-9 & 3-10
Silicone Foams, Rigid	0.025	3-2
Silicone Foam, R-7002	0.018	3-11
Silicone Rubber	0.12	3-2
Urethane, Foamed-in-Place, Rigid	0.01 - 0.03	3-2

Table 3-4

THERMAL CONDUCTIVITY OF LIQUID INSULATION  
MATERIALS AT 70° F

<u>Material</u>	<u>Thermal Conductivity (BTU/Hr-Ft-° F)</u>	<u>Reference</u>
Water	0.347	3-12
Commercial Aniline	0.100	3-12
Ammonia	0.293	3-12
Freon 12, CC1 <sub>2</sub> F <sub>2</sub>	0.041	3-12
n-Butyl Alcohol	0.097	3-12
Benzene	0.086	3-14
Glycerin	0.165	3-12
Petroleum Oils	0.07 - 0.08	3-14
Acetic Acid	0.099	3-14
Acetone	0.102	3-14
Alcohol	0.091 - 0.097	3-14
Nitromethane	0.096	3-14

$$L = \left( \frac{A_{\text{COND}} K}{C} \right) \left[ \frac{\theta_{\text{ST}}}{\ln \left( \frac{1 - T_{\text{O}}/T_{\text{ST}}}{1 - T_{\text{MAX}}/T_{\text{ST}}} \right)} \right] \quad (3.16)$$

Equation (3.16) is plotted in Figs. 3-6 and 3-7, with thermal conductivity as a parameter, where it has been assumed that

$$\theta_{\text{ST}} = 36 \text{ hours}$$

$$T_{\text{ST}} = 293^{\circ} \text{F}$$

$$T_{\text{MAX}} = 142^{\circ} \text{F}$$

$$T_{\text{O}} = -8^{\circ} \text{F and } +67^{\circ} \text{F}$$

The approximate range of thermal conductivities for solid, liquid and gaseous insulation materials has been indicated; these ranges have been obtained from the data in Tables 3-3, 3-4, and 3-5. If an arbitrary limit of 2 inches is set on the insulation thickness, the maximum value of the component surface area-to-thermal capacity ratio may be found from Figs. 3-6 and 3-7, for solid, liquid, and gaseous insulation materials. The A/C values, shown in Table 3-6, indicate the type of components for which passive insulation provides adequate protection during terminal sterilization, with and without pre-cooling. These results, of course, are strictly applicable only to solid insulation materials, since the effects of convective and radiative transfer are neglected in Eq. (3.16). This implies that even smaller values of A/C are required for adequate liquid and gaseous insulation protection, as noted in Table 3-6. Estimated A/C values for some typical components are as follows:

<u>Component</u>	<u>Approximate A/C</u>
Battery	0.27
Tape Recorder	0.97
Gyro Package	0.50
Vidicon Tube	1.25
Photomultiplier Tube	3.33

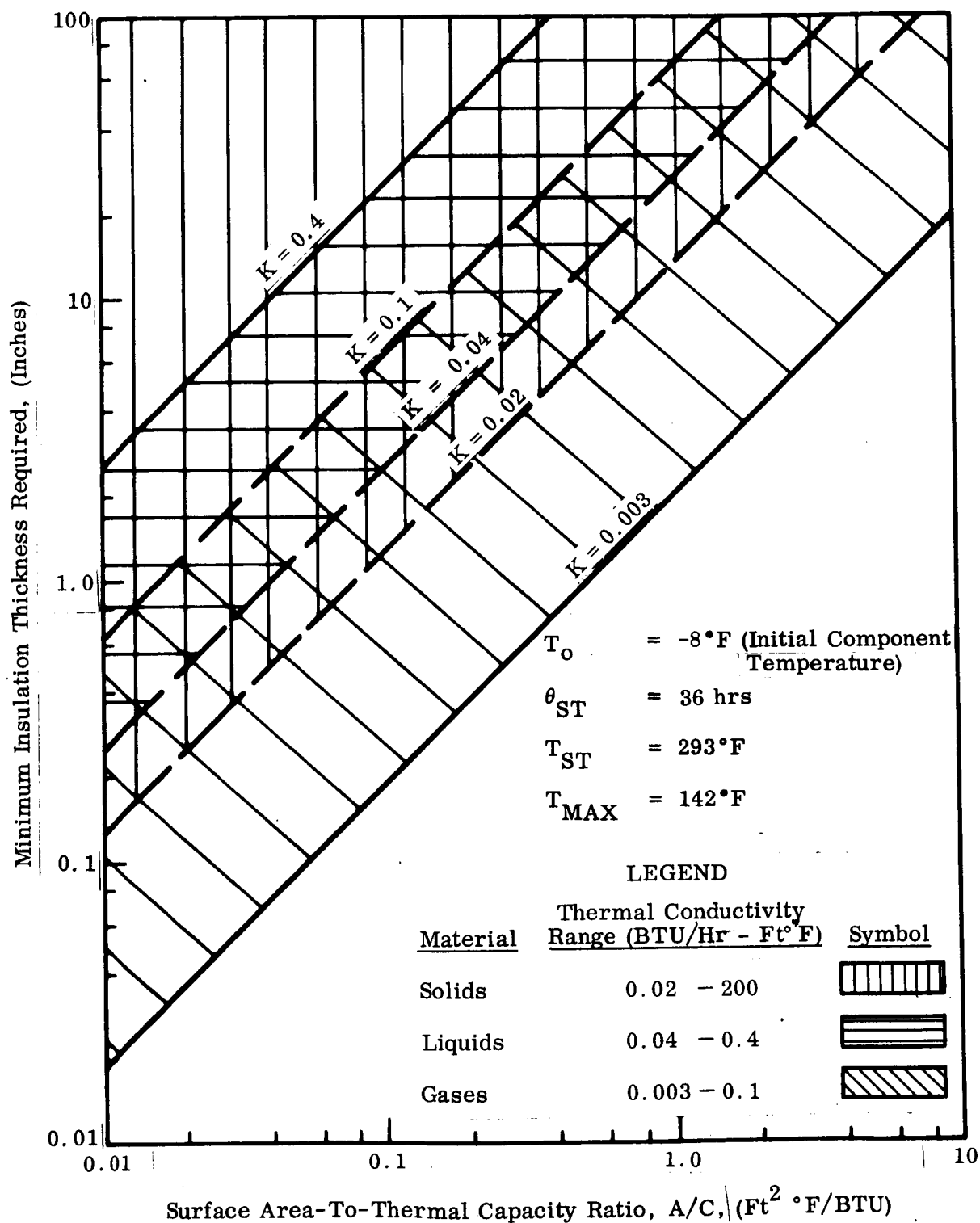


Fig. 3-6 Minimum Insulation Thickness Required for Passive Isolation as a Function of Component Properties and Insulation Thermal Conductivity

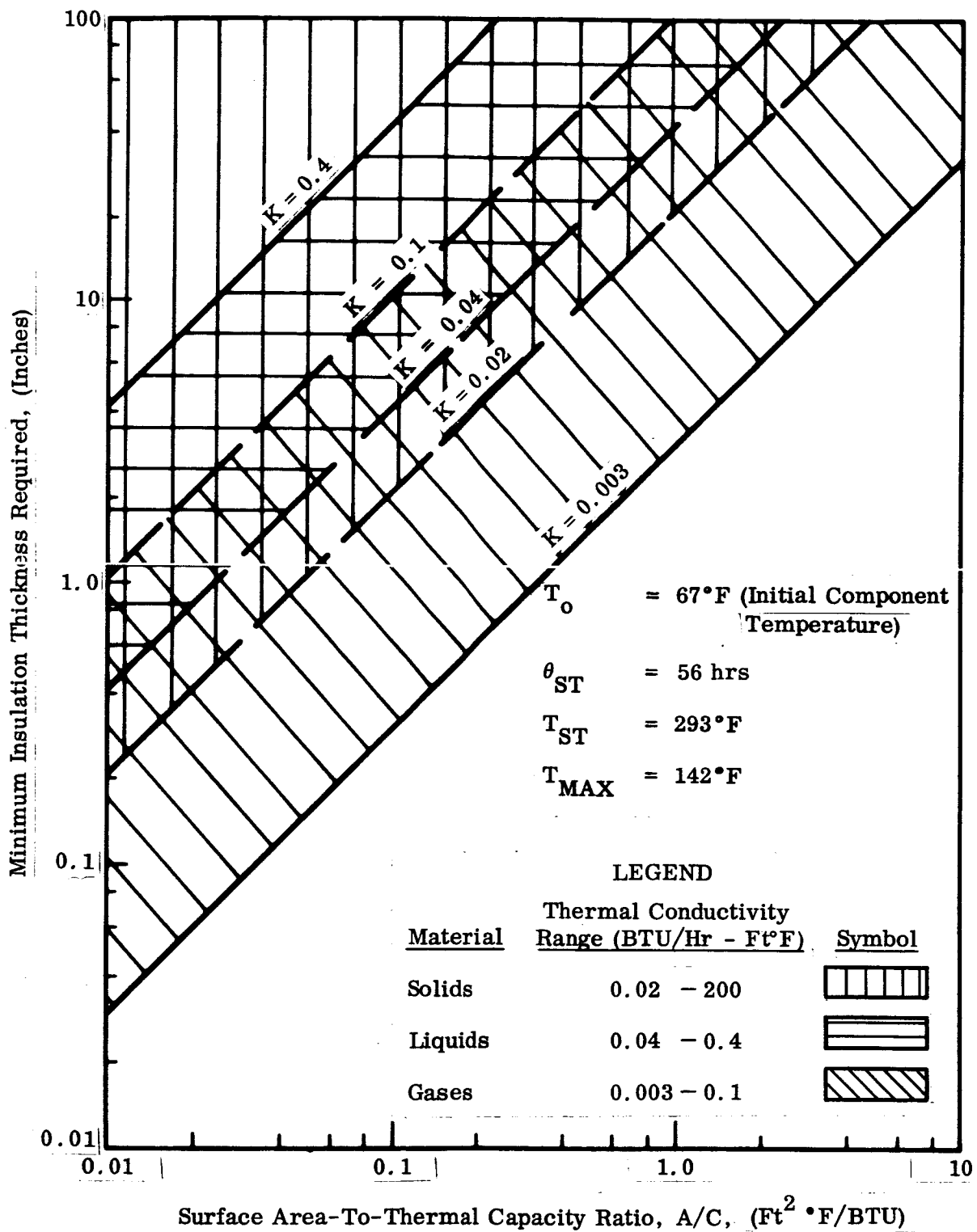


Fig. 3-7 Minimum Insulation Thickness Required for Passive Isolation as a Function of Component Properties and Insulation Thermal Conductivity

Table 3-5

THERMAL CONDUCTIVITY OF GASEOUS INSULATION MATERIALS  
AT 100° F AND ATMOSPHERIC PRESSURE

<u>Material</u>	<u>Thermal Conductivity (BTU/Hr-Ft ° F)</u>	<u>Reference</u>
Air	0.0154	3-12
Oxygen	0.0159	3-12
Carbon Monoxide	0.0149	3-12
Carbon Dioxide	0.0100	3-12
Argon	0.0941	3-13
Methane	0.0157	3-13
Nitrous Oxide	0.00847	3-13
Nitrogen	0.0154	3-12
Sulfur Dioxide	0.0055	3-14
Neon (32° F)	0.00256	3-14
Carbon Disulfide	0.0046	3-14

Table 3-6

MAXIMUM COMPONENT SURFACE AREA-TO-THERMAL CAPACITY  
RATIOS ALLOWABLE FOR ADEQUATE INSULATION PROTECTION

Type of Insulation <sup>(3)</sup>	Maximum Allowable A/C <sup>(2)</sup>	
	Component Pre-cooled (T <sub>O</sub> = -8° F)	No Pre-cooling (T <sub>O</sub> = 67° F)
Solid	0.16	0.096
Liquid	0.08	0.048
Gas	1.07	0.64

NOTES: (1) Insulation thickness assumed to be 2.0 inches.  
 (2) Units of A/C are ft<sup>2</sup> ° F/BTU. (3) Results for liquid and gases should be lower since effects of convection and radiation are neglected. (4) Components exposed to sterilization environment at 293° F for 36 hours. (5) Upper limit on component temperature assumed to be 142° F.

Thus, using the criteria shown in Table 3-6, neither solid or liquid insulation materials provide adequate protection for these types of components.

### 3.4.2 Liquid Insulation Materials

Further investigation of liquid insulation materials was not pursued in view of the conclusions of Section 3.4.1.

### 3.4.3 Gaseous Insulation Materials

By combining Eqs. (3.11) and (3.12), the minimum gas layer thickness for adequate thermal isolation is obtained:

$$(L_{\text{MIN}})_G = \frac{K_G A_{\text{COND}}}{\frac{C}{\theta_{\text{ST}}} \ln \left( \frac{T_{\text{ST}} - T_o}{T_{\text{ST}} - T_{\text{MAX}}} \right) - \bar{h}_G A_{\text{CONV}} - \sigma A_{\text{RAD}} \mathcal{F} \frac{(T_{\text{ST}}^4 - \bar{T}^4)}{(T_{\text{ST}} - \bar{T})}} \quad (3.17)$$

where  $\bar{T}$  is the average component temperature for radiative transfer (fourth-root mean temperature). For small ( $< 200^\circ \text{F}$ ) differences in temperature between the gas and the component, the emissivity and absorptivity of the gas is approximately equal, so that the effects of emitted and absorbed radiation by the gas balance out. In any case, the most conservative estimate of insulation thickness required is obtained if it is assumed that the gas is transparent to thermal radiation. The gas containment shield may be designed to have a low emittance on its inner surface, say  $\epsilon_{\text{shield}} = 0.1$ ; if the emittance of the component surface is  $\epsilon_C = 0.8$ , then

$$\left[ \frac{\sigma \mathcal{F} T_{\text{ST}}^4 - T_C^4}{T_{\text{ST}} - T_C} \right]_{\text{MAX}} \approx 0.1714 \times 0.08 \frac{[(7.53)^4 - (4.52)^4]}{(293 + 8)}$$

$$= 0.1264 \text{ BTU/Hr-Ft}^2 \cdot ^\circ \text{F}$$



where it has been assumed that the component is at its initial temperature  $T_o = -8^\circ \text{F}$ . Assuming that the insulation gas is nitrogen, and using the procedure outlined in Section 3.3, with a characteristic length  $L^* = 1 \text{ ft}$ , then

$$\bar{h}_G = 0.0438 \text{ BTU/Hr-Ft}^2 \text{ } ^\circ \text{F}$$

and with  $(A/C) = 0.5$ ,  $\theta_{ST} = 36 \text{ hr}$ ,  $T_{ST} = 293^\circ \text{F}$ ,  $T_o = -8^\circ \text{F}$  and  $T_{MAX} = 142^\circ \text{F}$ , then

$$\frac{(C/A)}{\theta_{ST}} \ln \left( \frac{T_{ST} - T_o}{T_{ST} - T_{MAX}} \right) = 0.0385 \text{ BTU/Hr-Ft}^2 \text{ } ^\circ \text{F}$$

The radiative, conductive, and convective components in the denominator of Eq. (3.17) all appear to be significant in the determination of  $L_{MIN}$ . In fact, from the above calculations, it appeared that radiative transfer alone would make the use of gaseous insulation (with a transparent gas) completely ineffective. This possibility was checked by calculating the component temperature at which

$$h_{RAD} = \frac{\sigma \mathcal{F} (T_{ST}^4 - T_C^4)}{(T_{ST} - T_C)} = 0.0385 \text{ BTU/Hr-Ft}^2 \text{ } ^\circ \text{F} \quad (3.18)$$

Using  $\epsilon_{shield} = 0.1$ ,  $\epsilon_C = 0.8$  and  $T_{ST} = 293^\circ \text{F}$ , as before, the solution to Eq. (3.18) was found to be

$$T_C = 292.67^\circ \text{F}$$

Thus the radiative transfer coefficient,  $h_R$ , is so large that radiation transfer alone would completely overcome the conductive insulation provided by the gas, without considering the deleterious effects of natural convection transfer.

Gaseous Insulation with Multiple Radiation Shields. It has been suggested that the use of multiple shields to contain the insulating gas could effectively reduce the radiative

heat transferred to the component to a negligible quantity. Test data obtained at LMSC and elsewhere indicate that the effective thermal conductivity of multilayer insulation at atmospheric pressure is about

$$K_E = 5 \times 10^{-2} \text{ BTU/Hr-Ft}^2 \text{ } ^\circ \text{F}$$

so that the minimum required thickness of multilayer insulation would be

$$L_{\text{MIN}} = \frac{K_C}{\frac{(C/A)}{\theta_{\text{ST}}} \ln \left( \frac{T_{\text{ST}} - T_0}{T_{\text{ST}} - T_{\text{MAX}}} \right)} = \frac{5 \times 10^{-2}}{3.85 \times 10^{-2}} = 1.3 \text{ ft}$$

Therefore, the thickness of multilayer insulation required would be prohibitively large.

#### 3.4.4 Feasibility of Passive Thermal Isolation

On the basis of the considerations in Sections 3.4.1 through 3.4.3, it was concluded that the use of passive isolation schemes does not provide adequate protection from the proposed sterilization environment. In addition to these considerations, passive isolation systems would also have a large effect on post-launch thermal operation. If it were possible to adequately isolate a component during sterilization by means of insulation techniques, a means of "re-connecting" the component to its supporting structure would need to be provided to allow internally generated heat to escape from the component during post-launch operation. Therefore, the use of insulation techniques does not appear to be feasible for passive thermal isolation under the given boundary conditions.

#### 3.5 FLUID CIRCULATION COOLING

A fluid circulation cooling system is an obvious candidate for the protection of previously sterilized components during over-all vehicle sterilization. Such a scheme utilizes either a hermetically sealed shield or a double walled heat exchanger surrounding the component to be protected, the cooling fluid being circulated either around the

component enclosed in the single shield or through the heat exchanger. The cooling fluid may be supplied from a single line through a manifold in the sterilization chamber wall to the separate components to be cooled. The use of individual temperature sensors in conjunction with flow rate controls for each component would provide for efficient utilization of the cooling fluid. By use of a proportional control system, the coolant flow would be controlled on a demand basis for individual components. Alternatively, the coolant fluid may be supplied from a source within the sterilization chamber by the use of expendable fluid or cryogenic fluid boiloff systems.

For the purpose of feasibility determination, the following classification of fluid circulation systems has been used:

- Forced Fluid Circulation Systems
- Cryogenic Fluid Boiloff Systems

In these systems, it has been assumed that no change of phase of the coolant fluid occurs within the enclosure or heat exchanger surrounding the component.

It was anticipated that fluid circulation systems, in general, would prove to be compatible with active cooling systems designed for orbital temperature control of packages in either the Mars lander modules, the orbiter, or both. The latter possibility cannot presently be evaluated, but may ultimately be the basis for selection of a thermal isolation system where several candidate systems appear to be equally effective.

### 3.5.1 Forced Fluid Circulation Systems

As described above, a forced circulation system provides for fluid circulation through a single-walled chamber enclosing the component, or through a double-walled heat exchanger surrounding the component to be protected. Use of a single-walled jacket affords some advantages in that the coolant fluid flows directly over the component surfaces, providing for more efficient heat transfer between the circulating fluid and the component than with the use of the double-walled heat exchanger. Some possible

disadvantages of the former system are that the cooling fluid must not contaminate, corrode, or react with the component materials. Thus, depending on the coolant fluid selected, and the component material characteristics, either one or both types of cooling jackets may be used.

Since, for sufficiently high coolant flow rates and a reasonable selection of coolants, the heat input to the protected component may be reduced to zero, we assume  $\eta_E = 1.0$  for forced circulation systems in which the component is completely enclosed by the cooling jacket. In the following discussion it has been assumed that the cooling jacket material (whether single- or double-walled) is highly conductive. This assumption, in addition to simplifying the analysis, implies a minimal effect of the cooling jacket on post-launch thermal operation. In the following analysis, it was assumed that the heat input to the shield enclosing the protected component is equal to that for an unprotected component having the dimensions of the outer shield.

Coolant Flow Rate Requirements. Assuming only sensible heat absorption by the coolant as it passes through the shield (no change of phase)

$$Q_S = Q_F = \dot{W}_f C_{p_f} (T_{f_{OUT}} - T_{f_{IN}}) \quad (3.19)$$

where we must have

$$T_{f_{OUT}} = T_{MAX} \quad (3.20)$$

so that the required coolant flow rate is

$$\dot{W}_f = \frac{Q_S}{C_{p_f} (T_{MAX} - T_{f_{IN}})} \quad (3.21)$$

where  $Q_S$  is a function of the shield surface area, geometry and average surface temperature,

$$Q_S = (Q_{UNP})_S = f(A_S, L_S^*, T_S) \quad (3.22)$$

The solution to Eq. (3.22) is given by the plot shown in Fig. 3-3. The shield surface temperature is obtained from Eq. (3.23).

$$Q_S = Q_f = 0.25 A_S \frac{(293 - \bar{T}_S)^{1.25}}{(L_S^*)^{0.27}}, \quad 0.01 \leq L_S^* \leq 1.0 \quad (3.23)$$

This equation is an approximation to the curves for unprotected components shown in Fig. 3-3, and yields an average shield temperature which corresponds to an average convective heat transfer coefficient between the hot gas and the shield.

For convective heat transfer between the shield and the fluid (or the component and the fluid) we use the correlation for laminar flow

$$h_{Sf} = 0.667 \frac{\dot{W}_f (C_{p_f})_b}{A_a Re_f^{1/2} Pr_f^{2/3}} \quad (3.24)$$

so that

$$Q_{Sf} = Q_S = Q_f = h_{Sf} A_S \Delta T_M = h_{Sf} A_S (\bar{T}_S - T_b) \quad (3.25)$$

where the subscript b refers to properties evaluated at the fluid bulk temperature

$$T_b = \frac{T_{MAX} + T_{fIN}}{2} \quad (3.26)$$

and the subscript f refers to properties evaluated at the average film temperature of the fluid  $T_f$  defined as

$$T_f = \frac{\bar{T}_S + T_b}{2} \quad (3.27)$$

For simplicity, rather than using a log-mean temperature difference in Eq. 3.25, we will use the approximation

$$\Delta T_M = \bar{T}_S - T_b \quad (3.28)$$

Now, for fixed values of  $T_{MAX}$  and  $T_{fIN}$ , Eq.(3.21) implies that the lowest coolant flow rates will be required for fluids having high specific heats. Conversely, Eq.(3.24) implies that high specific heat fluids will produce high values of  $h_{Sf}$ , which in turn implies large values of  $Q_{Sf}$  and  $h_{Sf}$ . Thus, an iterative procedure is required to determine coolant flow rate as a function of the coolant thermal properties and the component and cooling jacket geometry. This calculation has been performed for three candidate fluids (water, carbon dioxide, and nitrogen) using the following assumptions:

- $T_{MAX} = 130^\circ F$ ,  $T_{fIN} = 70^\circ F$
- The component is a cube whose sides are 1.0 foot long
- The cooling jacket (shield) is a hollow cube whose sides are spaced a distance,  $D_S$ , from the sides of the component.
- Heat is transferred to the coolant only by convection between the shield and the coolant as the coolant flows in the annular space between the shield and sides of the component.

Using Eqs.(3.19),(3.23) and (3.25), coolant flow rates were computed as a function of shield spacing,  $D_S$ , for three candidate coolant fluids. The results of these calculations are shown in Fig. 3-8. These results show that, except for extremely large shield spacings ( $> 1.5$  inches), a lower weight flow is required with water than for

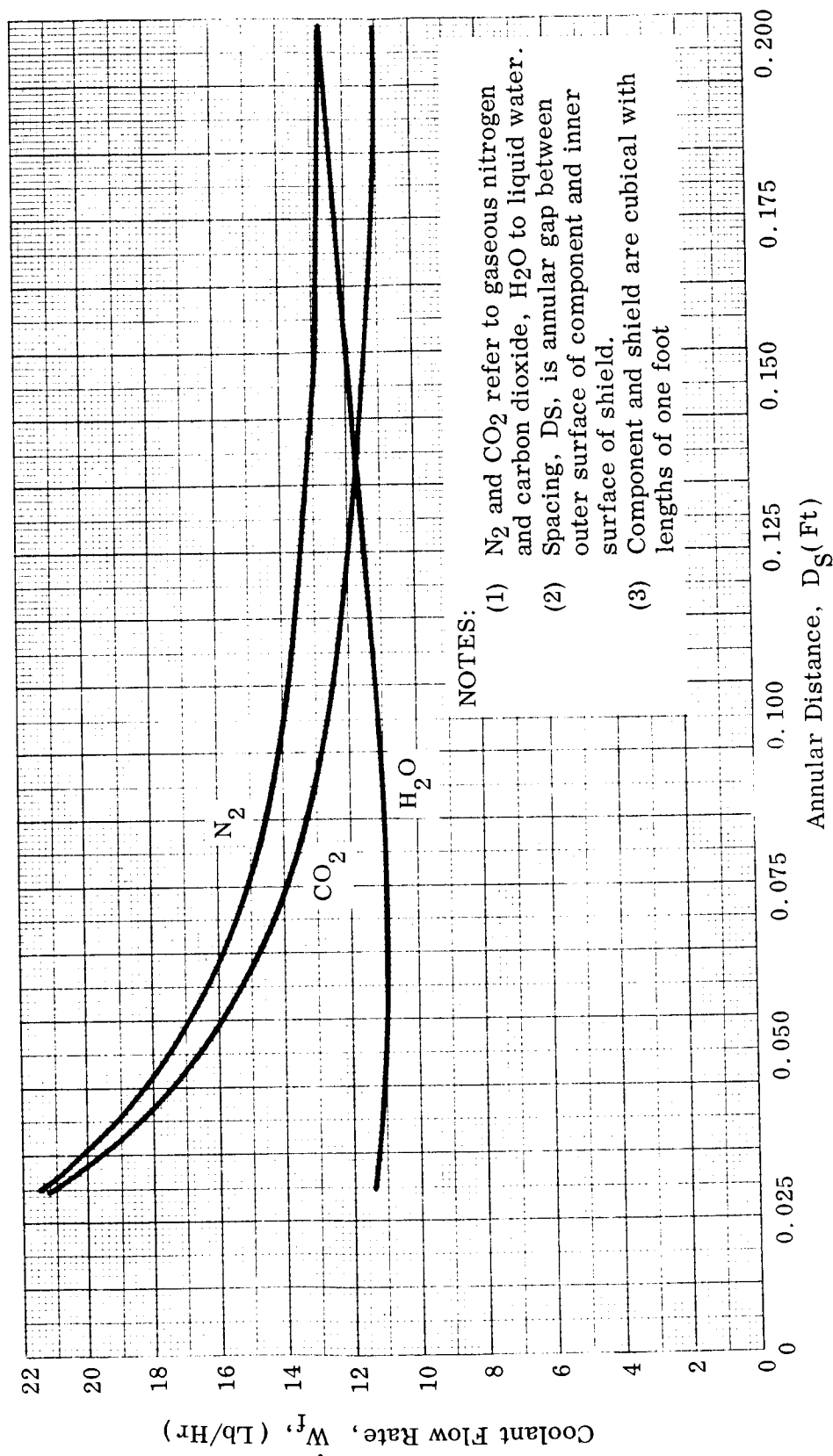


Fig. 3-8 Coolant Flow Rate vs. Spacing Between Component and Shield

the two gaseous coolants investigated. In the course of calculating coolant flow rate requirements, an iterative solution technique was employed which resulted in the intermediate results shown in Figs. 3-9 through 3-11. These plots, some of which are used below, show the variation with shield spacing of the heat transfer coefficient between the shield and the coolant, shield temperature and heat transfer rate into the shield, respectively. In general, it may be seen that water is much more effective than the gaseous coolants in absorbing the heat flux into the shield, although the heat transfer rates into the shield are much lower for gaseous coolants than for water.

Radiation Effects with Gaseous Coolants. The coolant flow rate requirements shown in Fig. 3-8 do not reflect the effects of radiative exchange between the shield and the component when gaseous coolants are used. The inclusion of these effects results in a higher coolant flow rate requirement for gaseous coolants. To obtain an accurate evaluation of the effect requires a complex iterative solution; however, an estimate of increase in flow rate may be obtained by using the shield temperatures shown in Fig. 3-10 for, say,  $D = 0.10$  feet, to calculate the magnitude of the radiative heat transfer to the component and to derive an approximate value for the increase in flow rate required to absorb the heat flux. The results of such a calculation indicate that an increase of about 1.5 lb/hr in coolant flow rate will account for the added heat load due to radiation transfer between the shield and the component.

Weight and Volume Penalties of Forced Fluid Circulation Isolation. Under the assumption of annular geometry, an estimate of weight and volume penalties may be made for various types of components. Again, for purposes of feasibility determination, we neglect the effect of supporting structure bracketry and fittings.

For a cylindrical component, assuming a shield constructed of 0.1 inch thick aluminum, the volume of the isolated installation is

$$\frac{V_P}{L_C} = \frac{\pi}{4} \left( D_C + 2D_S + \frac{0.2}{12} \right)^2 = 0.785 (D_C + 2D_S + 0.0167)^2$$



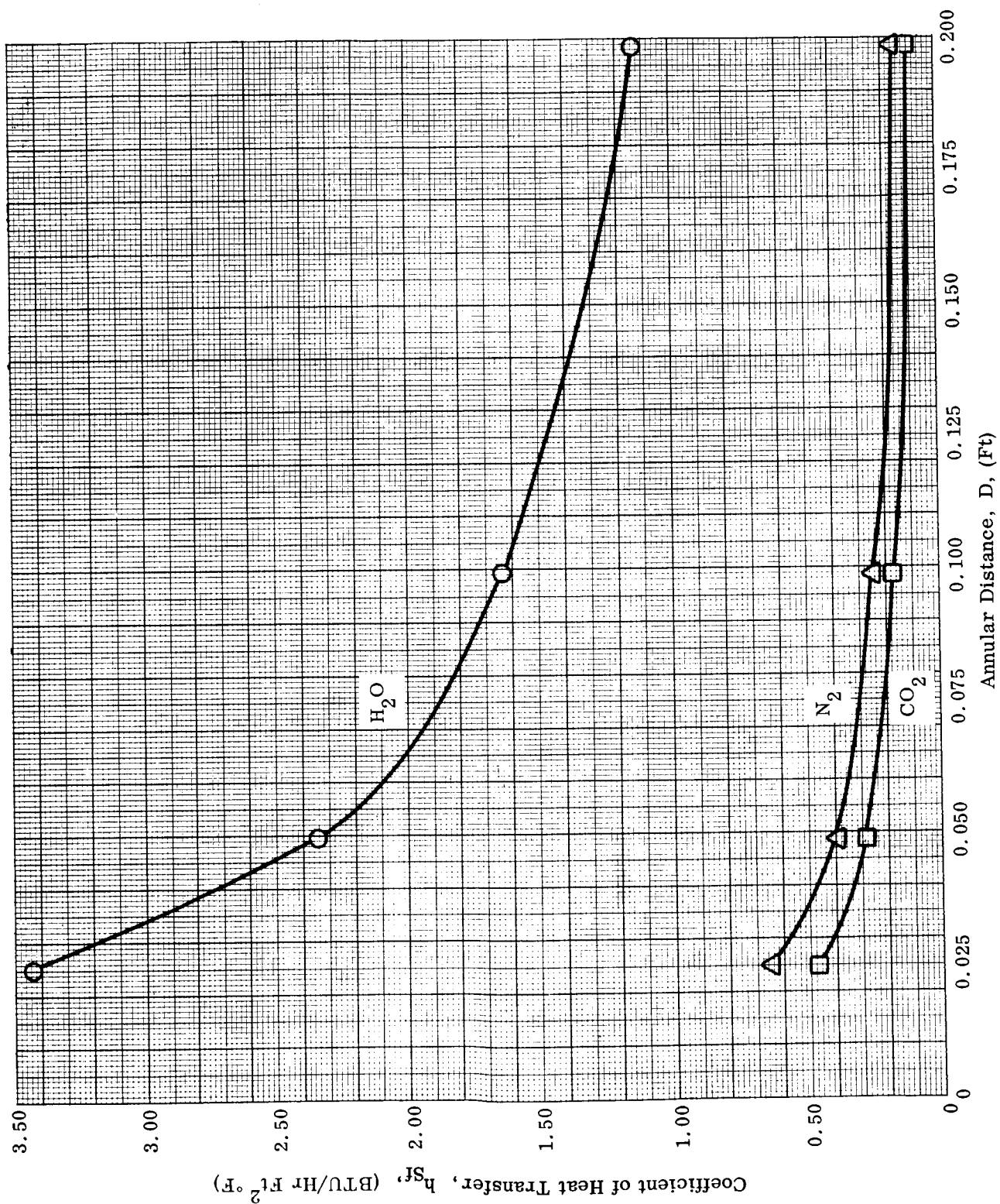


Fig. 3-9 Heat Transfer Coefficient vs. Shield Spacing

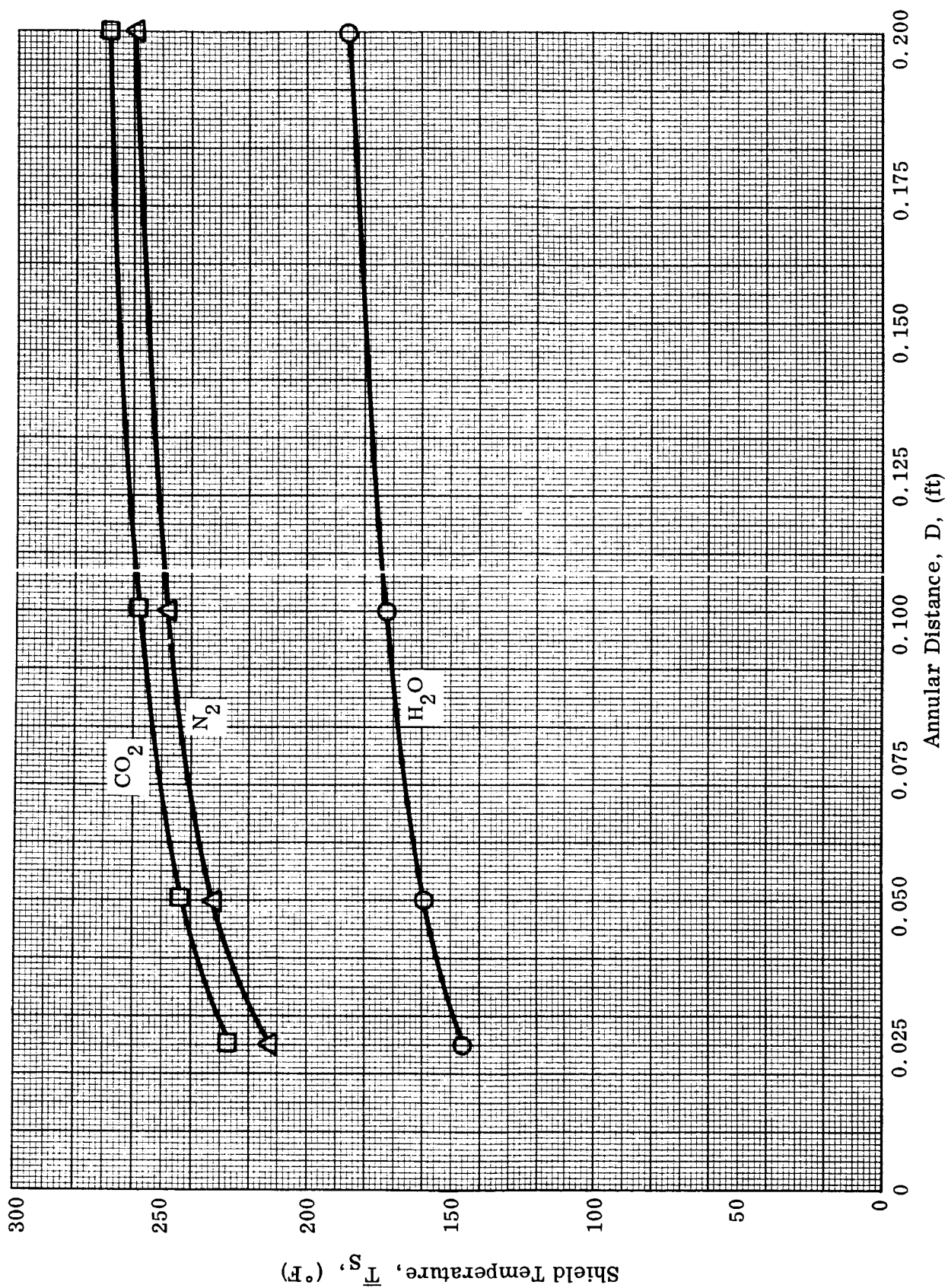


Fig. 3-10 Shield Temperature vs. Shield Spacing

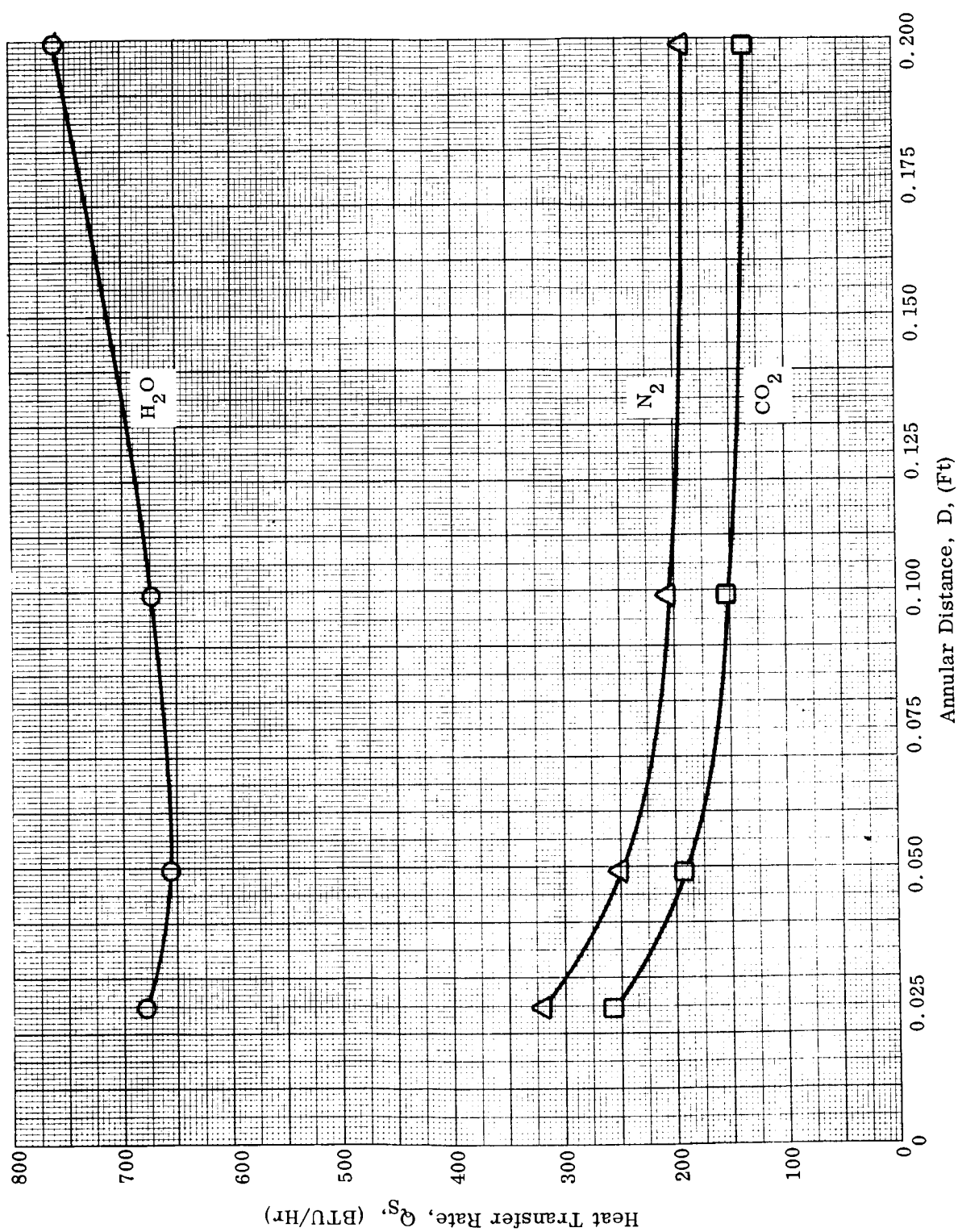


Fig. 3-11 Heat Transfer Rate vs. Shield Spacing

while the volume of the unprotected component is

$$\frac{V_{\text{UNP}}}{L_C} = 0.785 D_C^2$$

so that

$$\eta_V = \frac{V_{\text{UNP}}}{V_P} = \left( \frac{D_C}{D_C + 2D_S + 0.0167} \right)^2$$

similarly

$$\eta_W = \frac{W_{\text{UNP}}}{W_P} = \frac{W_C}{W_C + W_S}$$

where

$$W_S = \rho_S V_S \cong 4.45 D_S L_S$$

For a cubical component, the volume of the isolated installation is

$$\frac{V_P}{L_S} = (L_C + 2D_S)^2$$

so that

$$\eta_V = \frac{1}{\left( 1 + \frac{2D_S}{L_C} \right)^2}$$

and

$$W_S = 5.66 L_C (L_C + 2D_S)$$

These relations are used in Section 3.8 to evaluate the measures of feasibility used for comparison with other isolation methods.

### 3.5.2 Cryogenic Fluid Boiloff Systems

Cryogenic fluid boiloff systems refer to the circulation of the vapor from a very cold, evaporating liquid around the component to be protected. Since the boiling points of these liquids are low, the vapors can absorb large amounts of heat before reaching normal component temperatures. In applying such a boiloff system to thermal protection during terminal sterilization, an arrangement similar to that shown in Fig. 3-12 would be used. The cryogenic fluid is supplied to a heat exchanger where it absorbs heat; by virtue of this heat absorption, the liquid evaporates and the resultant vapor flows through the cooling jacket. A thermostatically operated valve controls the flow of vapor to the component, the latter being enclosed in a shield or jacket as in the forced fluid circulation system. The heated vapor is then vented outside the sterilization chamber.

The primary virtues of a cryogenic fluid boiloff system are simplicity of fluid supply and the availability of a low temperature gas coolant. If the coolant supply line connecting the coolant reservoir and the cooling jacket is perfectly insulated, the temperature of the gaseous coolant at the inlet to the cooling jacket is close to the boiling point of the cryogenic liquid. In the case of nitrogen, this temperature would be  $-320^{\circ}\text{F}$ . For such a low coolant inlet temperature, it is obvious that if the coolant impinges directly on the component, very low local component temperatures would result. For this reason, a system of multiple shields, as shown in Fig. 3-12, has been suggested.

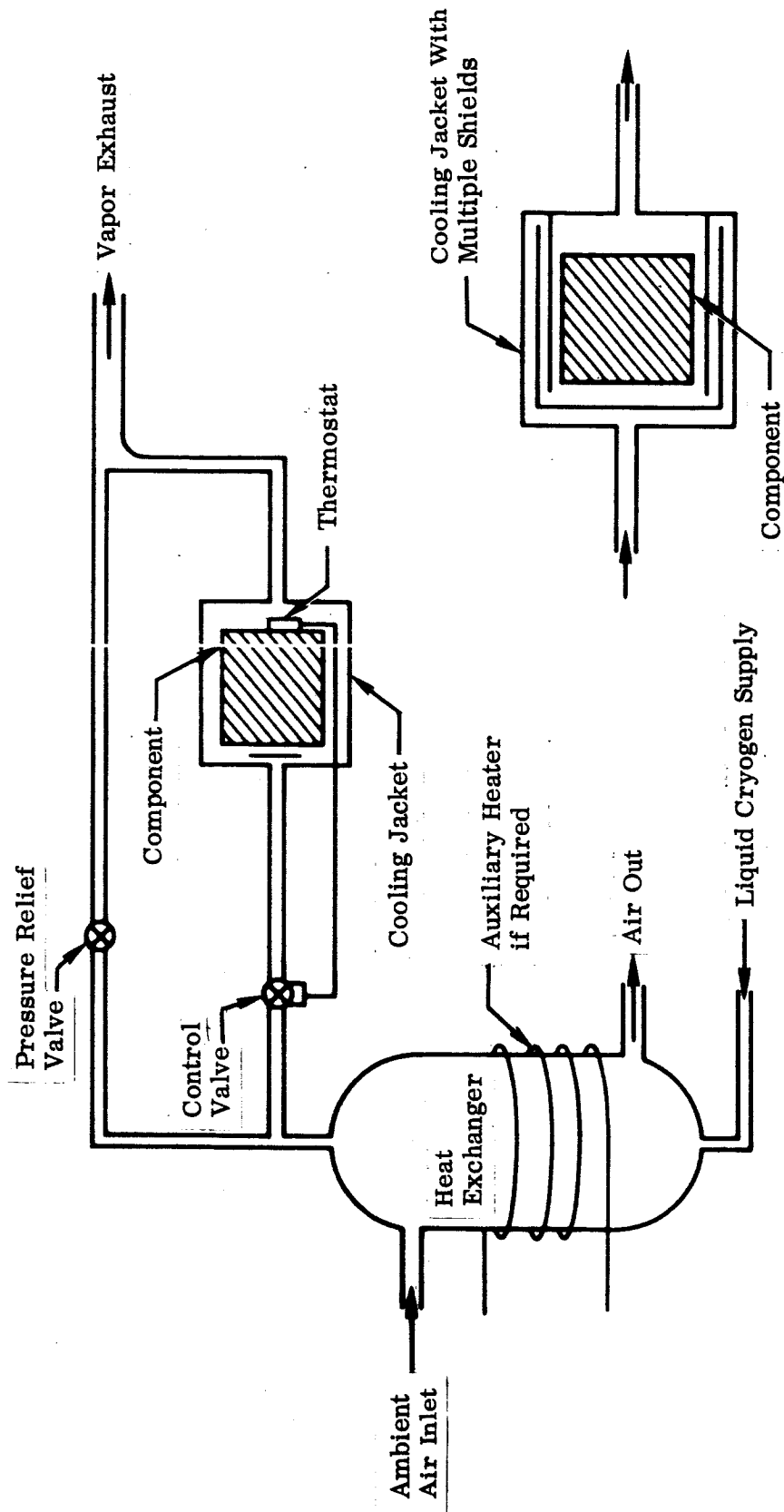


Fig. 3-12 Cryogenic Fluid Boil-off System

Approximate calculations of the heat transfer in the inlet stagnation region indicate that, by proper selection of the shield material, extreme local cooling of the component can be avoided. A detailed analysis of the complex fluid flow and heat transfer relations in the multiple shield configuration requires the generation of a computer program to perform the iterative solutions involved. Such an analysis exceeds the level of effort allocated for feasibility determination, and was not attempted in Phase I.

Since the component cooling jacket weight and volume penalties for cryogenic boiloff systems are comparable to those for forced fluid circulation, a separate determination of these penalties was not made for boiloff systems.

### 3.5.3 Feasibility of Fluid Circulation Cooling

On the basis of the foregoing analysis, fluid circulation cooling appears to be adequate for component thermal isolation during terminal sterilization. Under the assumptions indicated in Section 3.5.1, a forced fluid circulation system using water as a coolant appears to be most desirable, a flow rate of less than 11 pounds per hour being required for adequate isolation of a cubical component whose sides are 1 foot in length. Fluid cooling during terminal sterilization can be integrated with fluid circulation systems designed for post-launch thermal control. With such a system only the weight of a small number of valves and short lengths of coolant supply lines are charged to the thermal isolation system required during sterilization.

Cryogenic boiloff systems also appear to be adequate for thermal isolation, however, a more complex system of shielding is required than with a forced fluid circulation system. The boiloff system weight and volume penalties appear to be comparable to those for forced fluid circulation cooling.

## 3.6 PHASE CHANGE COOLING

The application of phase-change cooling to spacecraft components implies the encapsulation of the component in a material which changes phase (i. e. , melts, sublimates,

or vaporizes) upon absorption of a sufficient amount of heat. Ideally, by virtue of this phase change, the exposed coolant surface is continually renewed by the natural transport of the molten or vapor phase of the coolant away from the heated surfaces. Therefore, this investigation was concentrated on the study of those materials which sublime or vaporize in the appropriate temperature range, producing a vapor phase which is vented or ducted into or outside of the sterilization chamber. The isolation effectiveness of these materials is based primarily on their latent heat of fusion, vaporization or sublimation and vapor pressure-temperature characteristics. However, secondary properties such as chemical behavior and toxicity must also be considered.

### 3.6.1 Solid Phase Change Materials

Thermal isolation by means of fusible solid materials has been discussed extensively in Refs. 3-18, 3-19, and 3-22. In the application of this method, the component to be protected is surrounded by the phase change material (PCM) which, in turn, is surrounded by a shield which serves to contain the PCM in its molten state. Table 3-7 shows the properties of some candidate phase change materials as given in Refs. 3-19 and 3-22. It may be seen that the highest value of latent heat of fusion (130 BTU/Lb) is much less than the latent heat of vaporization of many liquids. Water at atmospheric pressure, for example, absorbs 970 BTU/Lb while evaporating at 212° F.

In order to accurately evaluate the adequacy of solid PCM isolation systems, it is necessary to calculate the heat transferred to the component through the liquid and solid phases of the material as a function of time. This analysis has been performed in Ref. 3-22 using a numerical finite difference solution technique for a cyclic heat flux into the isolated component. In lieu of such an analysis, we will use some simplifying assumptions to estimate the weight of phase change material required per unit area of the exposed shield surface. Assuming that a sufficient amount of PCM is available to absorb the heat flux through the shield, a heat balance gives

$$\int_0^{\theta_f} \left( \frac{Q_s}{A_s} \right) d\theta = \int_0^{\theta_f} Q_f \dot{W}_f d\theta \quad (3.29)$$



Table 3-7

PROPERTIES OF SOLID PHASE CHANGE MATERIALS<sup>(1)</sup>

<u>Material</u>	<u>Fusion Temperature (° F)</u>	<u>Latent Heat of Fusion (BTU/Lb)</u>
Tristearin <sup>(2)</sup>	132.8	82.1
Tristearin	162.5	98.1
Hydrogenated Cottonseed Oil	144.0	79.7
Beeswax	143.2	76.1
Technical Eicosane	94.6	71.2
Pentacosane	129.1	96.4
Heneicosane	105.4	94.5
Paraffins	126.0	63.1
Camphene	124.0	102.8
Sodium Dibasic Phosphate	98.0	120.0
Polyethylene Glycol	68-77	63.0
Transit Heet 86 <sup>(3)</sup>	86.0	130.0

NOTES: (1) Materials selected have melting points between 70° F and 150° F with latent heats of fusion greater than 50 BTU/Lb.

(2) Tristearin exhibits the double melting point characteristic common to most glycerides, with a solid ( $\beta$ ) phase existing between the two fusion temperatures.

(3) A proprietary formulation manufactured by Cryo-Therm, Inc.

where  $Q_f$  is the latent heat of fusion of the PCM, and  $\dot{W}_f$  is the weight rate of material melted per unit area. From Eq. (3.23),

$$\frac{Q_S}{A_S} \doteq \frac{(293 - \bar{T}_S)^{1.25}}{4 (L_S^*)^{0.27}} \quad (3.30)$$

Assuming a linear shield temperature variation with time,

$$\bar{T}_S(\theta) \doteq T_f + \left( \frac{\Delta \bar{T}_S}{\Delta \theta} \right) \theta, \quad \bar{T}_S < 293^\circ \text{F}, \quad (3.31)$$

From the results of Ref. 3-22, we estimate

$$\frac{\Delta \bar{T}_S}{\Delta \theta} \doteq 50^\circ \text{F/Hr} \quad (3.32)$$

so that  $T_S = 293^\circ \text{F}$  after  $\theta_f = (5.86 - T_f/50)$  hours.

Using  $T_f = 86^\circ \text{F}$ ,  $L_S^* = 1.0$ , and  $Q_f = 130 \text{ BTU/Lb}$ , and substituting Eqs. (3.30) and (3.32) into (3.29),

$$W_f = \int_0^{\theta_f} \dot{W}_f d\theta = \frac{1}{520} \int_0^{\theta_f} (207 - 50\theta)^{1.25} d\theta \quad (3.33)$$

where  $\theta_f = 4.14$  hours and  $W_f$  is the total weight of PCM required per unit shield area. After  $\theta = \theta_f = 4.14$  hours and the shield temperature has reached  $293^\circ \text{F}$ , the bulk of the PCM will have melted and will act as a passive insulation material. Evaluating Eq. (3.33), we find that

$$W_f = 1,445 \text{ lb/ft}^2$$

Thus, on the basis of this calculation alone, it appears that the weight penalty imposed by the use of solid phase change materials would be prohibitive.

In addition to high weight and volume requirements of solid PCM systems, a satisfactory thermal isolation system using solid phase change materials would require integration of the isolation system with the spacecraft thermal control system, unless the isolation system were removed from the spacecraft after terminal sterilization. Considering the above limitations, it may be concluded that the use of solid phase change materials for thermal isolation during sterilization is not generally feasible.

### 3.6.2 Liquid Phase Change Materials

The application of liquid phase change materials to thermal isolation requires the containment of an expendable liquid coolant around the component by a shield or cooling jacket similar to that used in fluid circulation cooling. The selection of evaporative fluids is discussed at length in Ref. 3-15, and portions of the following analysis are abstracted from that reference.

Table 3-8 gives the boiling point at one atmosphere pressure and the latent heat of vaporization of a number of candidate liquid coolants. It may be seen that those liquids with the highest heats of vaporization also have boiling points (at atmospheric pressure) which are outside the desired component temperature limits (32° F to 160° F). The following evaluation includes the use of a mixture of the two fluids having the highest latent heats shown in Table 3-8, namely, water and ammonia. As pointed out in Ref. 3-15, ammonia-water mixtures have relatively high heats of solution and, during evaporation, the heat of solution is reabsorbed by the mixture. Because of these characteristics an ammonia-water mixture appears to be very desirable for use as an evaporative coolant. A possible disadvantage of this coolant is that aqueous ammonia tends to corrode copper and nickel-silver alloys, so that some components will require use of a double-walled cooling jacket or a protective surface coating. Two additional coolants were evaluated; water, for those components whose upper temperature limit is greater than or equal to 212° F, and methyl alcohol for those components whose upper temperature limit is greater than or equal to 148° F.

Table 3-8

## PROPERTIES OF LIQUID PHASE CHANGE MATERIALS

<u>Material</u>	<u>Boiling Point*</u> (° F)	<u>Heat of Vaporization</u> (BTU/Lb)
Water	212	970
Ammonia	-28.3	589
Methyl Alcohol	148.5	473
Methylamine	20	460
Ethyl Alcohol	173	368
Acetonitrile	176	313
n-Propyl Alcohol	207	295
Iso Propyl Alcohol	180	286
Ethylamine	61.9	263
Ethylene Oxide	51.3	250
Acetaldehyde	69.8	245
Propionitrile	206.6	241
Tert-Butyl Alcohol	181	235

---

\*At one atmosphere pressure.

As with fluid circulation cooling, we assume that the evaporative cooling system is designed to absorb all the heat flux into the coolant container during a 36 hour sterilization period, so that  $\eta_E = 1.0$  by design. We also assume that the coolant is stored in a container (shield) completely surrounding the component, that the heat absorbed by the component from the fluid coolant is negligible and that the fluid bulk temperature is equal to the average shield temperature. It is also assumed that the fluid container is vented to the atmosphere and that pressure drops out the vent line, entrainment losses, etc., are negligible. The heat flux into the shield will then be equal to the heat flux absorbed by the fluid.

$$Q_S = Q_f = W_f C_{p_f} \frac{dT_f}{d\theta} = \frac{d}{d\theta} (W_f H_f) \quad (3.34)$$

The heat input to the shield,  $Q_S$ , may be obtained as a function of shield temperature,  $T_S$ , from Fig. 3-2. Thus, for single component fluids having a fixed boiling point, the right-hand side of Eq. (3.34) is a constant equal to the heat of vaporization times the weight rate of fluid vaporized. For a two-component liquid mixture, the boiling point changes continuously during the evaporation process as the more volatile component is vaporized. Thus, the right-hand side of Eq. (3.34) varies with time for a two-component mixture.

The vaporization of both single- and two-component liquids is illustrated in Fig. 3-13, where the fluid temperature (assumed equal to the container temperature) is plotted as a function of time, the coolant container being assumed to be a one-foot cube. For single-component fluids evaporating at constant pressure,

$$W_f = \int_0^\theta \dot{W}_f d\theta = W_f \theta = \frac{\theta Q_S}{H_f} \quad (3.35)$$

so that  $W_f$  is the total weight of liquid which is vaporized at the end of the evaporation process.

## NOTES:

- (1)  $W_f$  = Total weight of fluid at start of vaporization or distillation, for single component fluids  $W_f$  is equal to the weight of fluid vaporized after 36 hrs.
- (2) Ammonia completely vaporized after 36 hrs.
- (3) Approximately 72 mol percent of ammonia evaporated after 36 hrs.
- (4) Coolant container is assumed to be a tube whose sides are 1 ft long.

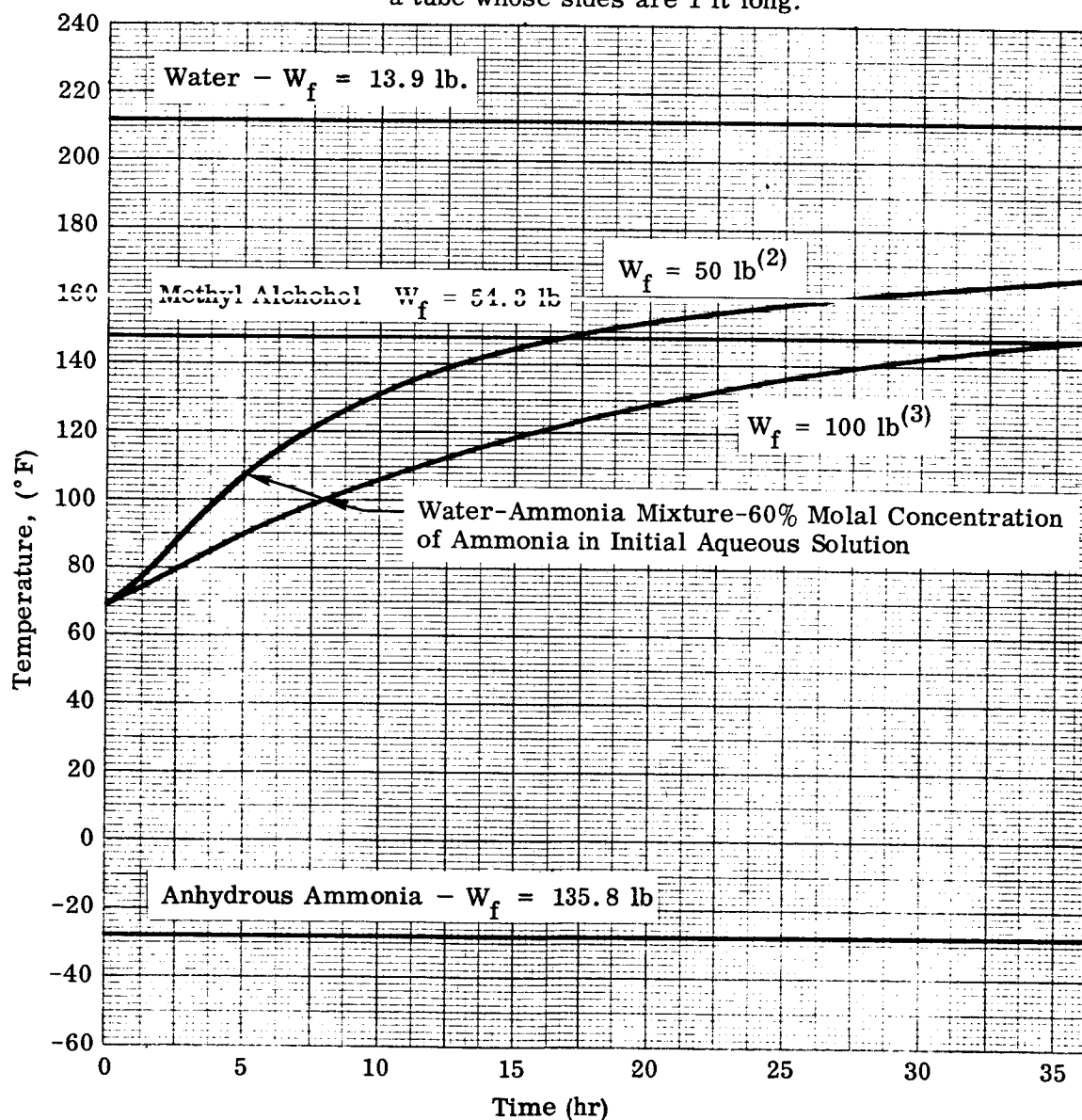


Fig. 3-13 Vaporization of Liquid Phase-Change Materials at 1 Atmosphere Pressure

For two-component mixtures, Eq. (3.34) may be written

$$\frac{dT_f}{d\theta} = \frac{Q_S}{W_f \left( \frac{dH_f}{dT_f} \right) \Big|_{T=T_f}} \quad (3.36)$$

Equation (3.36) was integrated for a water-ammonia mixture using a second order Runge-Kutta method by obtaining  $(dH_f/dT_f)$  from the temperature-enthalpy plots shown in Ref. 3.15 and  $Q_S$  from Fig. 3-3. The upper water-ammonia curve shown in Fig. 3.13 indicates the temperature-time curve for a weight of mixture such that the ammonia has been completely evaporated at the end of 36 hours. The second curve ( $W_f = 100$  lb) shows the reduction in temperature obtained by doubling the total weight of the mixture. In this case, the distillation process is not completed at the end of 36 hours, with about 28 mol percent of ammonia remaining in the liquid phase. On the basis of this result, it would appear that more effective use is made of the water-ammonia mixture by increasing the initial ammonia concentration to obtain a lower final temperature than by increasing mixture weight. Since the final fluid temperature at the end of the distillation process corresponds to the component upper temperature limit, the coolant mixture may be tailored to each component by varying the ammonia concentration in the mixture. Thus, as the component upper temperature limit varies between  $-28^\circ\text{F}$  and  $212^\circ\text{F}$ , the required coolant weight varies between 136 pounds and 14 pounds.

### 3.6.3 Feasibility of Phase Change Cooling

On the basis of the foregoing analysis it has been concluded that thermal isolation by means of a liquid phase change cooling system is a feasible method of thermal isolation, with liquid coolants being available for use over the anticipated range of component temperatures. The use of available solid phase change materials is much less effective on a weight basis than that of the liquids, and is not feasible for the contemplated component sizes due to the prohibitively large coolant weight required.

### 3.7 THERMOELECTRIC COOLING

#### 3.7.1 Introduction

The application of thermoelectric cooling devices to thermal isolation during terminal sterilization would make use of its ability to act as a "thermal shield"; the component to be protected is shielded by the thermoelectric device whose cold junctions remain at the desired component temperature, while the hot junctions operate at a temperature high enough to reject heat to the surrounding sterilization gas.

The "pumping" of heat from cold to hot junctions is due to the Peltier effect whereby thermal energy, in addition to the Joule heat, is absorbed or evolved at the thermoelectric junctions through which an electric current is flowing. When a voltage is applied to a thermoelectric heat pump couple as shown in Fig. 3-14, the device absorbs heat at the cold junction (source) while the electrical energy consumed plus the absorbed heat is rejected from the hot junction (sink).

The temperature differential between hot and cold junctions is shown in Appendix A, Section A.3, to be

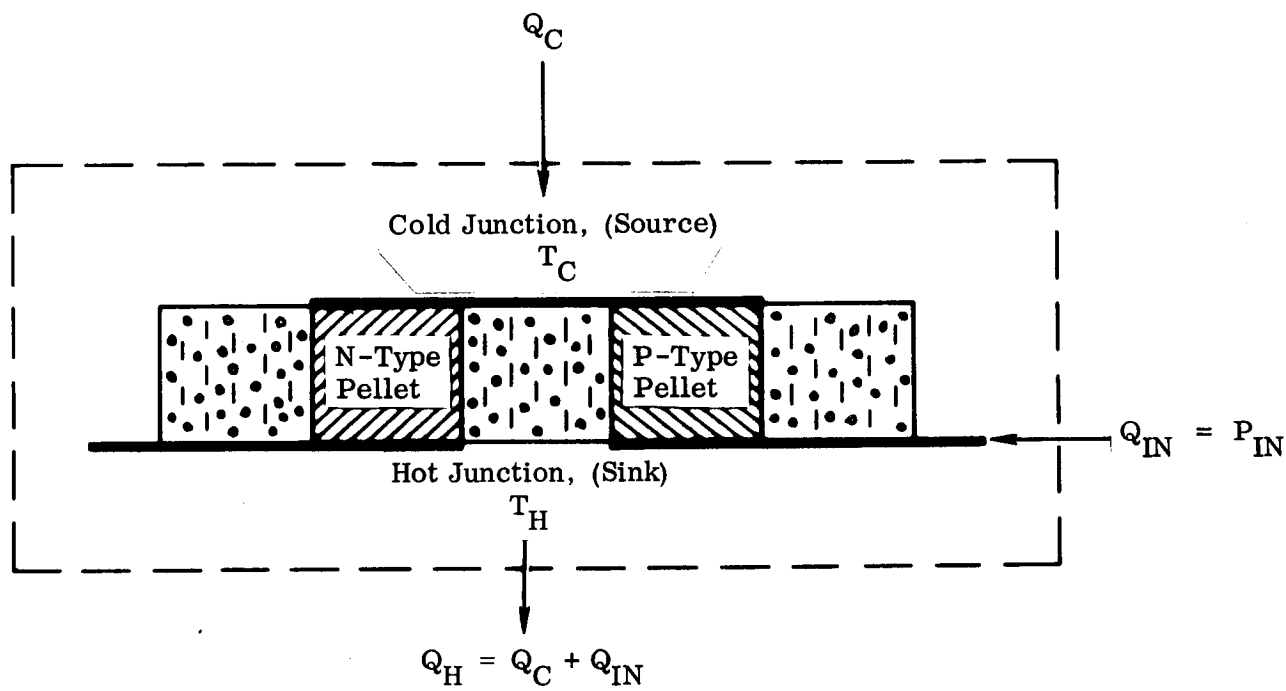
$$\Delta T = T_H - T_C = \frac{I \alpha T_C - \frac{1}{2} I^2 R - Q_C}{K} \quad (3.37)$$

It is seen that for a given input current, the maximum value of  $\Delta T$  is obtained for  $Q_C = 0$ .

The current which produces a maximum  $\Delta T$  is termed the optimum current,  $I_{OPT}$ , and may be found by setting  $Q_C = 0$ , holding  $T_C$  constant, and differentiating Eq. (3.37) with respect to  $I$ , giving

$$I_{OPT} = \frac{\alpha T_C}{R} \quad (3.38)$$





## LEGEND





-  N-Type Thermoelectric Material
-  P-Type Thermoelectric Material
-  Insulation
-  Conductive Metal

Fig. 3-14 Typical Thermoelectric Heat Pump Couple

The maximum temperature differential may then be found by substituting the optimum current into Eq. (3.37) with  $Q_C = 0$ , giving

$$\Delta T_{MAX} = \frac{1}{2} \frac{\alpha^2 T_C^2}{RK} \quad (3.39)$$

### 3.7.2 Application of Thermoelectric Cooling to Lander Module Thermal Isolation

Component Temperature Control. In determining the feasibility of applying a thermoelectric heat pump to component isolation during terminal sterilization, some simplifying assumptions have been made. It has been assumed that the thermoelectric heat pump device is in direct contact with the component to be protected and the temperatures of the junctions on the cold and hot sides are equal to the final temperature of the surfaces where heat is absorbed and rejected, respectively, i.e.,  $T_C$  = component temperature and  $T_H$  = temperature of surface exposed to the sterilizing gas. Thermal resistance due to joints and connecting straps is considered small and has been neglected. It has also been assumed that the components to be protected during terminal sterilization are not dissipating heat. This implies that the net heat absorbed at the cold junctions of the thermoelectric unit,  $Q_C$ , must be equal to zero in order to maintain a constant component temperature. With conservation of energy, the heat rejected at the hot junctions of the thermoelectric unit,  $Q_H$ , is equal to the energy input,  $Q_{IN}$ , plus the net heat absorbed,  $Q_C$ ; i.e.,  $Q_H = Q_{IN} + Q_C$ . Therefore, for the case of  $Q_C = 0$ , the heat rejected is equal to the energy input,  $(Q_H) = Q_{IN}$ .

Removal of Heat Rejected. In general, there is no guarantee that a given component in the lander module will be exposed to forced circulation of the sterilization gas. Therefore, natural convection heat transfer was assumed for removal of heat rejected by the thermoelectric unit to the sterilization gas. This implies that the natural convection heat transfer rate,  $Q_S$ , of the nitrogen gas must be equal to the heat rejected by the thermoelectric heat pump device, where  $Q_S$  is given by equation (3.23) in metric units:

$$Q_S = 4.14 \times 10^{-4} \frac{A_S (T_H - 418)^{1.25}}{(L_S)^{0.27}} \quad (3.40)$$

where

- $A_S$  = total surface area exposed to the sterilizing nitrogen gas,  $\text{cm}^2$   
 $L_S$  = characteristic dimension of a configuration consisting of a component surrounded by a thermoelectric unit,  $\text{cm}$   
 $418$  = temperature of the sterilizing nitrogen gas,  $^\circ\text{K}$

Equation (3.40) implies that the hot junction temperatures,  $T_H$ , must be greater than  $418^\circ\text{K}$  for removal of rejected heat from the thermoelectric device. This restricts the operation of the thermoelectric unit to high values of  $\Delta T$  in order to maintain reasonable component temperature.

Minimization of Weight and Volume. From both a weight and volume standpoint, the length of the thermoelectric unit in the direction of heat flow should be as small as possible. If  $Q_C = 0$  so that  $Q_H = Q_{IN}$ , it is shown in Appendix A that

$$(Q_H)_{Q_C=0} = I\alpha\Delta T + I^2 R \quad (3.41)$$

where  $R = 2\rho L/A$ . Here it is assumed that the n-type and p-type thermoelectric pellet sizes and material parameters are identical and independent of temperature, so that

$$\alpha_n = \alpha_p, \text{ and } \alpha = |2\alpha_n| = |2\alpha_p| = \text{Seebeck Coefficient, volts}/^\circ\text{K}$$

$$K = K_n = K_p = \text{Thermal conductivity, watts/cm } ^\circ\text{K}$$

$$\rho = \rho_n = \rho_p = \text{Resistivity, ohm-cm}$$

$A = A_n = A_p =$  Thermoelectric pellet cross-sectional area perpendicular to heat and current flow,  $\text{cm}^2$

$L = L_n = L_p =$  Thermoelectric pellet length in direction of heat and current flow, cm

The Thompson effect may be neglected since the Thompson Coefficient,  $\tau = T d\alpha/dT = 0$  from  $\alpha \neq \alpha(T)$  assumed above. Solving Eq. (3.41) for  $L$ ,

$$L = \frac{A}{2\rho I^2} \left[ (Q_H)_{Q_C=0} - I\alpha\Delta T \right] \quad (3.42)$$

we see that the thermoelectric pellet length can be minimized by maximizing both  $I$  and  $\Delta T$ , for a given value of heat rejected. We now have two arguments in favor of operating with a maximum  $\Delta T$  and  $I = I_{OPT}$ . The restrictions imposed on  $\Delta T$  discussed above imply that any advantage in operating with currents other than  $I_{OPT}$  would not justify the increased complexity of the analysis necessary for a more general solution.

Defining  $Q_H^*$  as the heat rejected under the conditions of  $Q_C = 0$  and  $I = I_{OPT}$ , it is seen from Appendix A that  $Q_H^* = (Q_{IN})_{OPT}$ , or

$$Q_H^* = 2K \frac{T_H}{T_C} \Delta T_{MAX} \quad (3.43)$$

Thus, requirements for satisfactory application of a thermoelectric heat pump to thermal isolation may be summarized as follows:

- $Q_H = Q_{IN}$ , since  $Q_C$  must be zero in order to maintain a constant component temperature.
- Removal of heat rejected by the thermoelectric unit by natural convection requires  $Q_S = Q_H$  and large  $\Delta T$ .

- Minimization of weight and volume requires a minimum thermoelectric pellet length  $L$ , or large  $I$  and  $\Delta T$ , therefore  $I = I_{OPT}$ ,  $\Delta T = \Delta T_{MAX}$  and  $Q_S = Q_H^*$ .

### 3.7.3 Size of Thermoelectric Unit Required for Thermal Isolation

The importance of size and weight considerations suggests using thermoelectric pellet length as a function of component size as a criterion for the feasibility of thermoelectric cooling for thermal isolation. The following analysis, based on the requirements listed above, was used in evaluating this measure of feasibility.

The surface area per p-n couple exposed to the sterilization gas includes both the thermoelectric pellet area,  $2A$ , and the insulation area,  $A_I$ . The total surface area exposed to the sterilization gas is therefore

$$A_S = (2A + A_I) n \quad (3.44)$$

where

- $A$  = pellet cross-sectional area perpendicular to heat and current flow,  $\text{cm}^2$
- $A_I$  = insulation cross-sectional area perpendicular to heat flow,  $\text{cm}^2$
- $n$  = number of p-n couples

The insulation area may be defined as a function of the area covered by thermoelectric material as follows:

$$A_I = X (2A) \quad (3.45)$$

where

$$X = \frac{\text{Area covered by insulation}}{\text{Area covered by thermoelectric material}}$$

Then Eq. (3.44) reduces to

$$A_S = 2 n A (1 + X) \quad (3.46)$$

Combining Eqs. (3.39) and (3.43), multiplying by  $n$ , the number of p-n couples used, and solving for  $n (A/L)$  yields

$$\frac{nA}{L} = \frac{2\rho Q_H^*}{\alpha^2 T_C T_H} \quad (3.47)$$

Using typical material parameters, Eq. (3.47) reduces to

$$\frac{nA}{L} = 1.632 \times 10^4 \frac{Q_H^*}{T_C T_H} \quad (3.48)$$

Assuming that the insulation and pellet lengths are equal, Eqs. (3.46) and (3.48) may now be combined to eliminate  $n$  and  $A$  giving

$$L = 3.06 \times 10^{-5} \frac{A_S T_C T_H}{Q_H^* (1 + X)} \quad (3.49)$$

Applying the condition that  $Q_S = Q_H^*$ , Eqs. (3.40) and (3.49) may be combined to give Eq. (3.50):

$$L = \frac{0.0740 T_C T_H (L_S)^{0.27}}{(T_H - 418)^{1.25} (1 + X)} \quad (3.50)$$

The relationship between  $T_C$ ,  $T_H$  and  $X$  for  $\Delta T_{MAX}$  may be found from Eq. (3.39).

For

$$R = 2\rho \frac{L}{A}, \quad K = 2\frac{A}{L}(K + XK_I)$$

and typical material parameters (see A.3.2)

$$\left(T_H - T_C\right)_{MAX} = \frac{1.333 \times 10^{-3} T_C^2}{1 + 0.0226 X} \quad (3.51)$$

Equation (3.51) may be used to determine the maximum possible range of  $T_H$  and  $X$  for various values of  $T_C$ . For the case of perfect insulation, the surface area covered by insulation can be neglected (since no heat would be conducted to the cold junctions through the insulation) and  $X = 0$ . For this case, the maximum values of  $\Delta T_{MAX}$  and  $T_H$  are obtained.

There are also minimum values of  $\Delta T_{MAX}$  and  $T_H$  corresponding to a maximum amount of surface area covered by insulation, i.e., if the area covered by insulation exceeds a certain value, heat leak through the insulation will cause the maximum hot junction temperature to approach the temperature of the sterilization gas, at which point  $Q_s = 0$  and no convective heat transfer to the sterilization gas is possible.

These relationships are shown in Figs. 3-15 and 3-16 for two values of the cold junction (or component) temperature,  $T_C$ .

Equations (3.50) and (3.51) may now be combined to give  $L = L(L_S, T_C, X)$ . By taking the derivative of  $L$  with respect to  $X$ , the optimum value of  $X$ , i.e.,  $X$  for minimum  $L$ , may be found for any given value of  $T_C$ . This is shown graphically in Figs. 3-17 and 3-18 showing  $X_{OPT}$  to be approximately 3.1 and 31 for  $T_C$  equal to 100° F and 200° F, respectively.

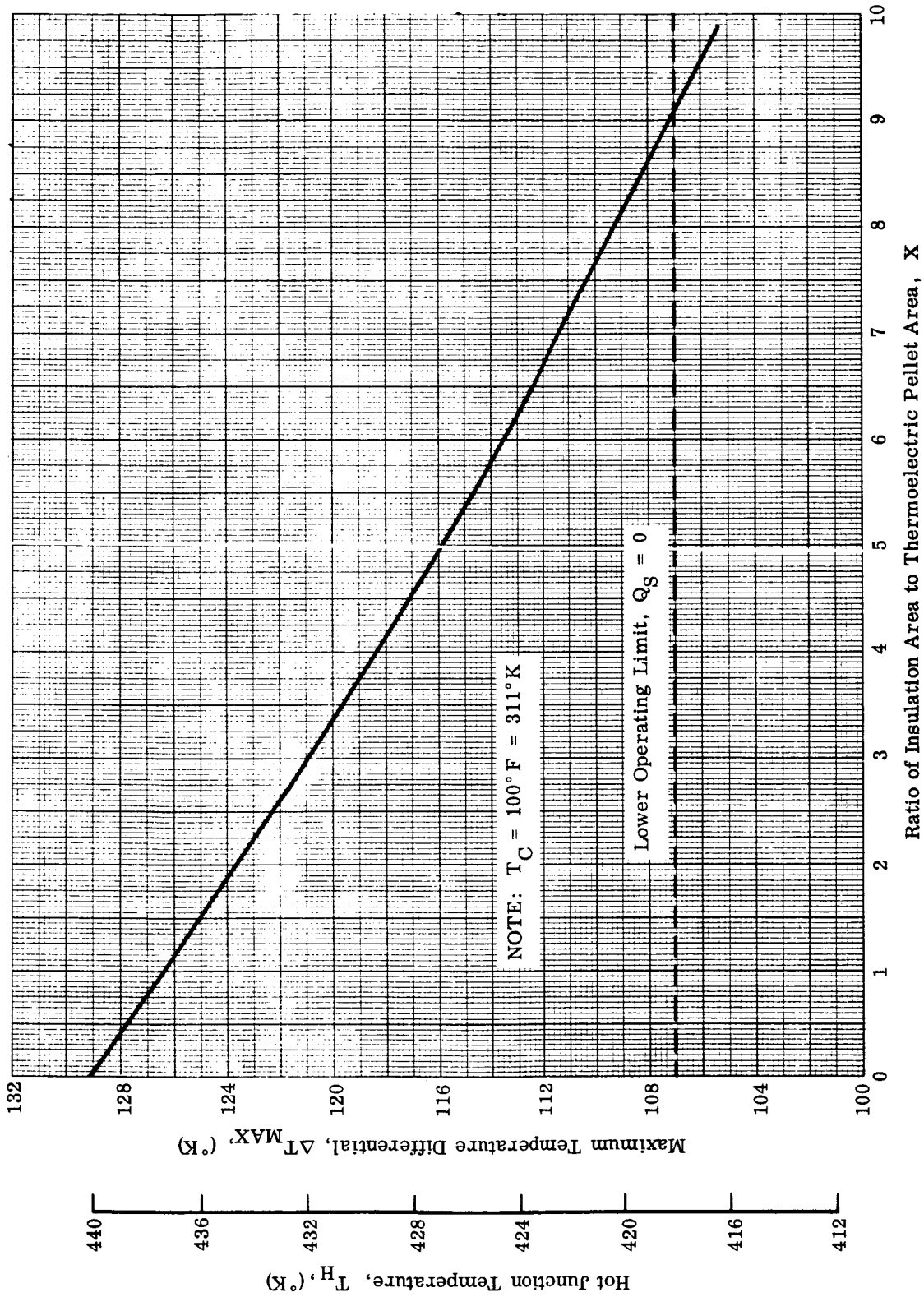


Table 3-15 Maximum Hot Junction Temperature vs. Ratio of Insulation Area to Thermoelectric Pellet Area



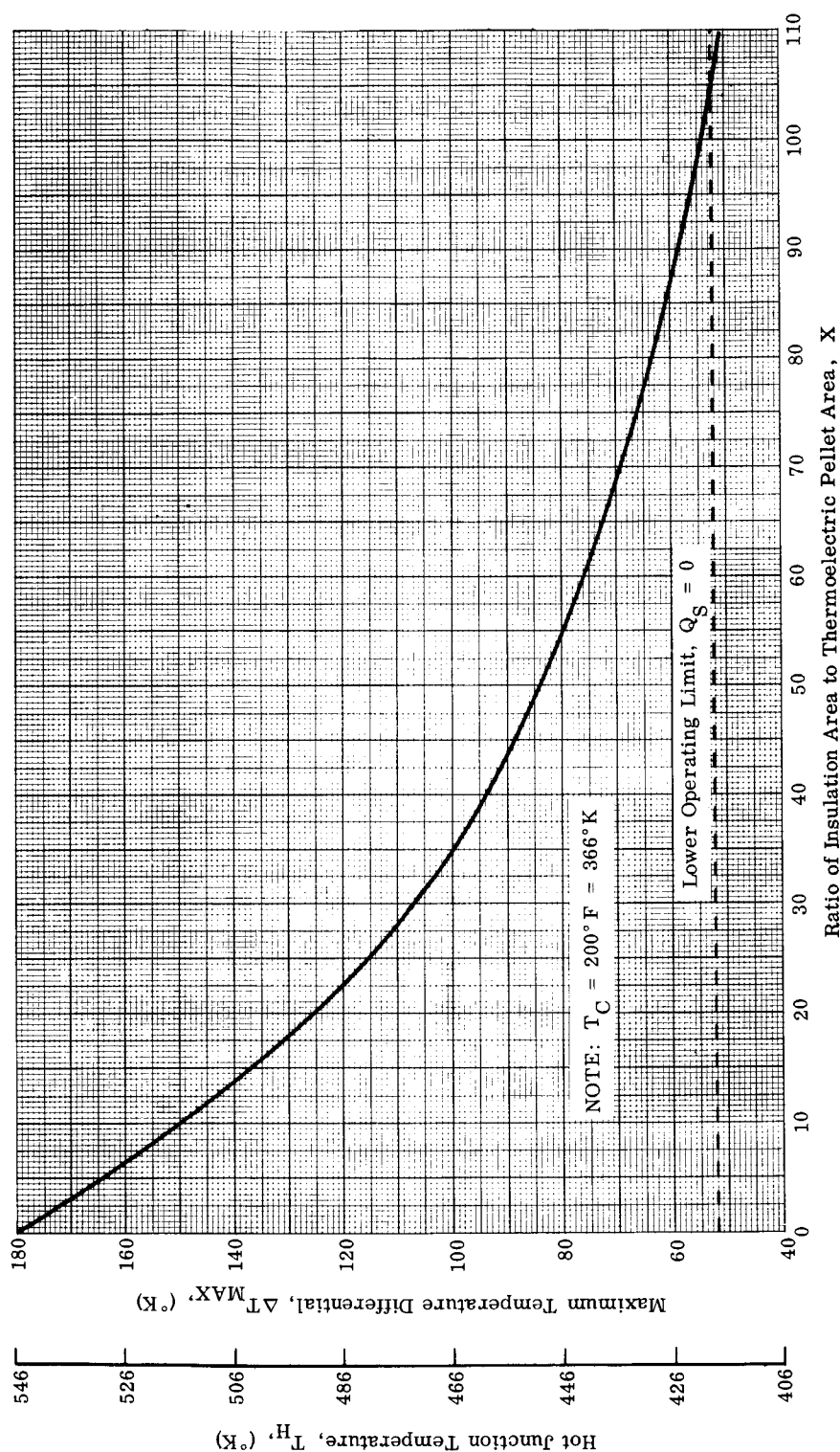


Fig. 3-16 Maximum Hot Junction Temperature vs. Ratio of Insulation Area to Thermoelectric Pellet Area

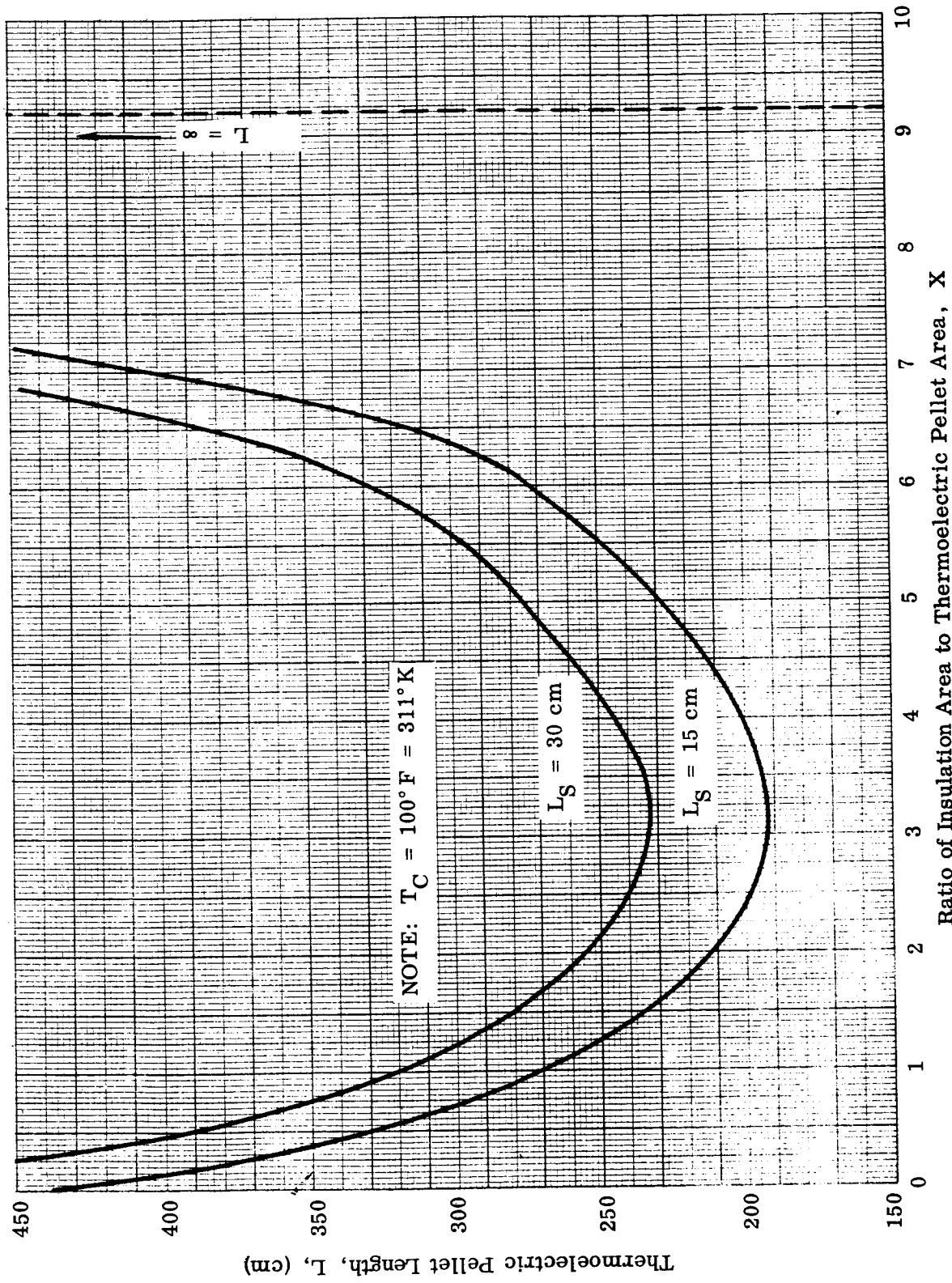


Fig. 3-17 Thermoelectric Pellet Length vs. Ratio of Insulation Area to Thermoelectric Pellet Area

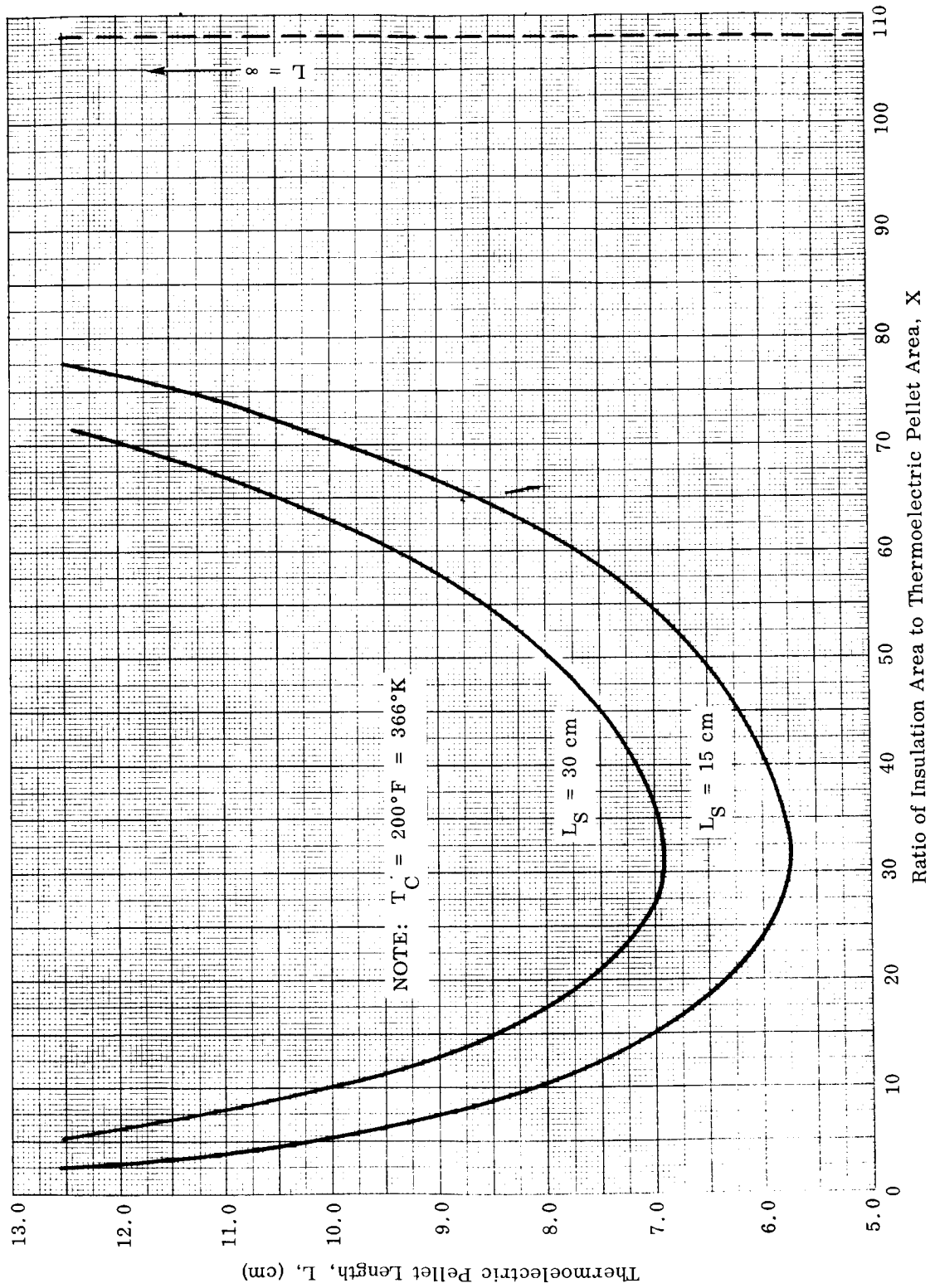


Fig. 3-18 Thermoelectric Pellet Length vs. Ratio of Insulation Area to Thermoelectric Pellet Area

Since  $X_{OPT}$  is not a function of component size, an optimum ratio of insulation area to thermoelectric pellet area may be found for each component, based on its upper temperature limit only.

Using the above values of  $X$  and the corresponding values of  $T_H$  from Figs. 3-15 and 3-16, the minimum thermoelectric pellet length,  $L_{MIN}$ , may be derived from Eq. (3.50) as a function of characteristic dimension only, i.e.,

$$\left(L_{MIN}\right)_{T_C = 100^\circ F} = 93.1 (L_S)^{0.27} \quad (3.52)$$

and

$$\left(L_{MIN}\right)_{T_C = 200^\circ F} = 2.79 (L_S)^{0.27} \quad (3.53)$$

The characteristic dimension,  $L_S$ , as used in the above analysis defines the characteristic length of the surface exposed to the sterilization gas and includes both the component characteristic,  $L_S^*$ , and the thermoelectric pellet length,  $L$ . The component characteristic length is given by

$$L_S^* = L_S - L \quad (3.54)$$

Weight and volume penalties may now be illustrated by incorporating the definition of  $L_S^*$  from Eq. (3.54) in Eqs. (3.52) and (3.53). This yields the minimum thermoelectric pellet length and the characteristic length of component surrounded by a thermoelectric unit as functions of component size as shown in Eqs. (3.55)–(3.58).

For  $T_C = 100^\circ F$

$$L_{MIN}^{3.7} - 1.90 \times 10^7 L_{MIN} - 1.90 \times 10^7 L_S^* = 0 \quad (3.55)$$

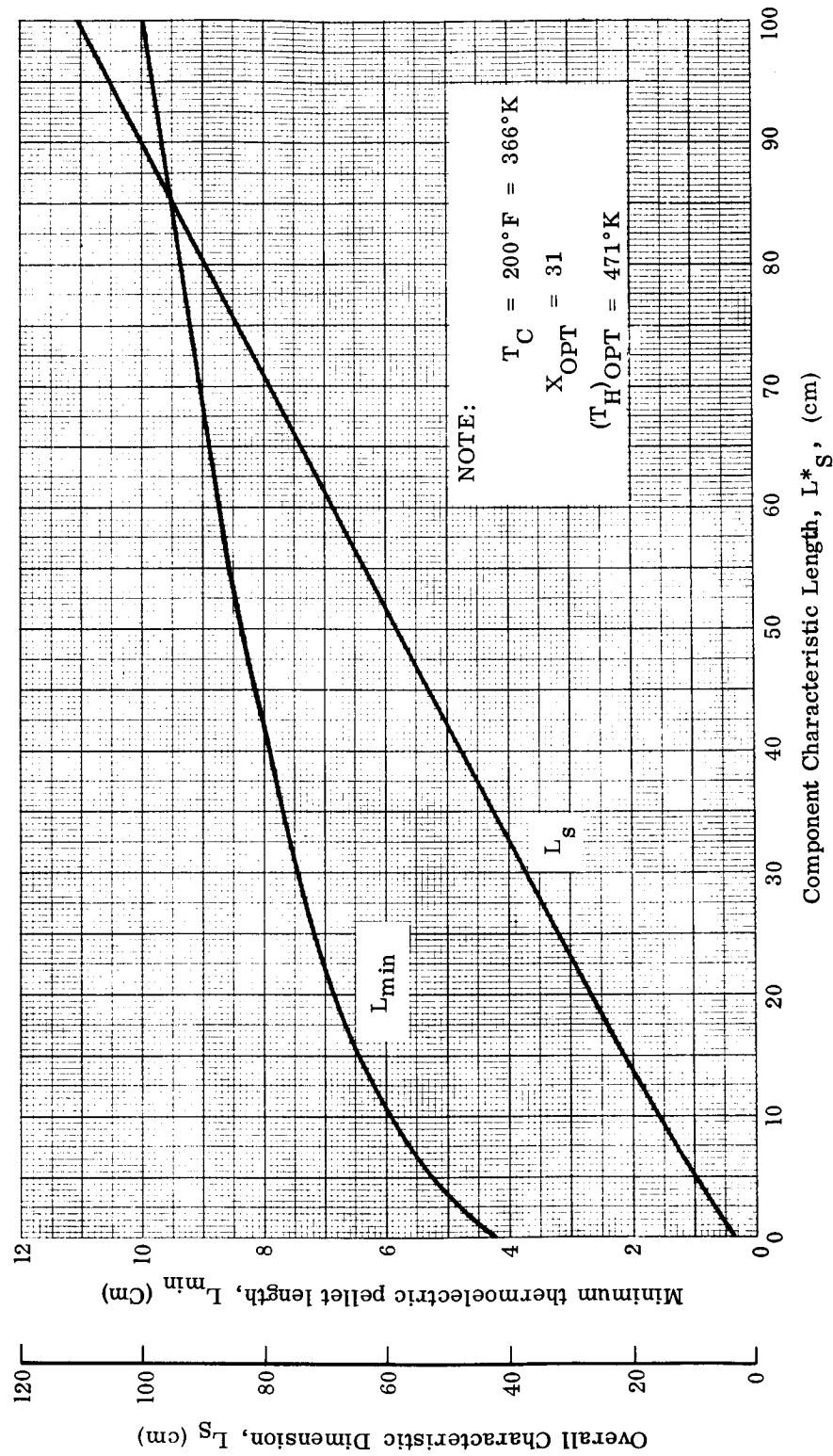


Fig. 3-19 Overall Characteristic Dimension and Minimum Thermoelectric Pellet Length vs. Component Characteristic Length

$$L_S - 93.1 (L_S)^{0.27} - L_S^* = 0 \quad (3.56)$$

For  $T_C = 200^\circ \text{F}$

$$L_{\text{MIN}}^{3.7} - 44.7 L - 44.7 L_S^* = 0 \quad (3.57)$$

$$L_S - 2.79 (L_S)^{0.27} - L_S^* = 0 \quad (3.58)$$

Equations (3.55) and (3.56) show that protecting a component of negligible size would require a thermoelectric pellet length of 500 cm. This implies that protecting a component at  $100^\circ \text{F}$  is not feasible for the operating conditions during terminal sterilization. Equations (3.57) and (3.58), plotted in Fig. 3-19, give much lower, but still impractical, values of  $L_{\text{MIN}}$  and  $L_S$  for a component temperature of  $200^\circ \text{F}$ .

A sample calculation for a cubical component one foot on a side having an upper temperature limit of  $200^\circ \text{F}$  is included in Appendix A. Using the measures of weight and volume penalties defined in Section 3.1, it is found that

$$\eta_W = 0.612 \quad \text{and} \quad \eta_V = 0.350$$

where the ideal ratios would be 1.0. Comparing these values with the measures of weight and volume for fluid circulation ( $\eta_W = 0.91$ ,  $\eta_V = 0.95$ ) shows the relatively high weight and volume penalties involved in thermoelectric cooling for the operating conditions required during terminal sterilization.

#### 3.7.4 Feasibility of Thermoelectric Cooling

On the basis of the foregoing analysis and sample calculations, the application of a thermoelectric heat pump device as a thermal shield is not considered to be feasible for the operating conditions assumed during terminal sterilization.

Because only one of the proposed lander components has an upper temperature limit above 200° F, it was concluded that prohibitive sizes of thermoelectric devices would be required for thermal isolation of the remainder of the components. For this reason, thermoelectric devices are not included in the comparison of candidate isolation methods discussed in the following section.

### 3.8 SUMMARY AND RELATIVE RANKING OF CANDIDATE THERMAL ISOLATION METHODS

For reasons cited in Sections 3.4 and 3.7, thermal isolation by means of passive isolation and thermoelectric cooling does not provide feasible protection for components exposed to the dry-heat sterilization environment. Thus, only fluid circulation and phase change cooling have been evaluated using the criteria given in Section 3.1. The rating system derived in Section 3.2 has been implemented in order to obtain a quantitative comparison of the thermal isolation methods that survived the test for feasibility. Several of the criteria employed in this rating system must be evaluated primarily on the basis of engineering experience and judgment, rather than component cooling requirements. The numerical values assigned to measures of these criteria and their weighted scores are shown in Table 3-9.

The remaining measures of weight and volume required by the candidate isolation method, are functions of several variables. For the two remaining isolation methods, fluid circulation and phase-change cooling, the weight penalty incurred is due to the cooling jacket or coolant container required to contain the circulating fluid or the phase change coolant, plus any associated bracketry, piping, and fixtures.

In order to compare the two remaining isolation methods, only the weight of the cooling jacket was considered, and each component was idealized to have either a cubical or cylindrical geometry. The size, weight (unprotected), assumed upper temperature limit, and shape of these components is shown in Table 3-10.

The cooling jacket was in all cases assumed to be a 0.1-inch-thick aluminum shield. For evaluation of phase change isolation, the phase change coolants were selected

Table 3-9

## NUMERICAL VALUES ASSIGNED TO EVALUATION CRITERIA\*

Criterion	Measure	Numerical Value		Weighted Score	
		Fluid Circulation	Phase Change	Fluid Circulation	Phase Change
Effectiveness	$\eta_E$	1.0	1.0	2.50	2.50
Reliability	$\eta_R$	0.8	0.8	1.60	1.60
Noninterference	$\eta_{NI}$	0.5	0.6	0.85	1.02
AGE Required	$\eta_{AGE}$	0.3	0.7	0.09	1.21

\*Partial List - See Text

Table 3-10

COMPONENT CHARACTERISTICS USED FOR ISOLATION  
RATING DETERMINATION

Component	Maximum Temperature (° F)	Weight (lb)	Size and Shape
Battery	148	118	1 ft cube
Tape Recorder	158	17	1 ft cube
Floating Rate Gyro	148	10	0.5 ft cube
Vidicon Tube	212	0.6	Cylinder, 0.1 ft diam. 0.4 ft long
Photomultiplier Tube	122	0.375	Cylinder, 0.17 ft diam. 0.45 ft. long
Life Detection Experiment	122	7.5	0.5 ft cube

Table 3-11

## REQUIRED PHASE-CHANGE COOLANT WEIGHTS

Component	Coolant	Coolant Weight (lb)
Battery	Methyl Alcohol	54.3
Tape Recorder	Ammonia-Water Mixture*	47.0
Floating Rate Gyro	Methyl Alcohol	18.3
Vidicon Tube	Water	0.4
Photomultiplier Tube	Ammonia-Water Mixture**	17.3
Life Detection Experiment	Ammonia-Water Mixture**	90.0

Notes: \*60% initial molal concentration of ammonia

\*\*90% initial molal concentration of ammonia



Table 3-12

## MEASURES OF WEIGHT AND VOLUME REQUIREMENTS

Component	$\eta_V$		$\eta_W$	
	Fluid Circulation	Phase Change	Fluid Circulation	Phase Change
Battery	0.91	0.48	0.95	0.90
Tape Recorder	0.91	0.52	0.74	0.56
Gyro	0.83	0.25	0.87	0.65
Vidicon Tube	0.36	0.33	0.98	0.66
Photomultiplier Tube	0.52	0.02	0.95	0.09
Life Detection Experiment	0.83	0.06	0.83	0.34

Table 3-13

## SUMMARIES OF RATINGS FOR THERMAL ISOLATION METHODS

Isolation Method Component	Fluid Circulation Cooling	Phase Change Cooling
Battery	8.30	7.85
Tape Recorder	7.88	7.23
Floating Rate Gyro	8.03	7.01
Vidicon Tube	7.54	7.15
Photomultiplier Tube	7.72	5.54
Life Detection Experiment	7.95	6.10

individually for each component, corresponding to the component's upper temperature limit. The coolants selected and the required coolant weights are tabulated in Table 3-11.

Using the required coolant weights and specific volumes, measures of weight and volume requirements were computed using the following definitions:

$$\eta_W = \frac{\text{Weight of Unprotected Component}}{\text{Weight of Protected Component}}$$

$$\eta_V = \frac{\text{Volume of Unprotected Component}}{\text{Volume of Protected Component}}$$

Obviously, the ideal value of these ratios is 1, while the worst possible value is 0. The computed values of these measures of weight and volume penalties are tabulated in Table 3-12 for the two candidate isolation methods.

It may be seen that, on a weight basis, phase change cooling compares favorably with fluid circulation cooling only when used with the heaviest component, where small variations in system weight penalties are overshadowed in the comparison shown. On an absolute basis, the cooling jacket weight for fluid circulation cooling of the battery is only 6.3 pounds, while the phase change system requires 13 pounds for the coolant container, almost twice the weight penalty. On a volume basis, the phase change cooling system compares favorably with the fluid circulation system only when applied to isolation of the vidicon tube, where water is the most favorable coolant due to the high maximum allowable temperature of the vidicon tube.

The results shown in Tables 3-9 and 3-12 have been combined to yield a summary of the weighted measures as shown in Table 3-13. This table compares the overall ratings for each system, where a "perfect score" of 10 is considered to be the ideal system.

### 3.9 CONCLUSIONS - PHASE I

An analysis of passive isolation techniques and thermoelectric cooling devices has shown that these two methods are not suitable for achieving thermal isolation during sterilization.

Of the two remaining candidate isolation methods, (phase change and fluid circulation cooling), fluid circulation cooling appears to be feasible for the three coolant fluids investigated, while phase change cooling is feasible only when liquid coolants are used. Cryogenic fluid boiloff systems require a more complex system of shielding than fluid circulation cooling, while incurring similar weight and volume penalties.

The results of a numerical comparison of fluid circulation and phase change cooling show that, for the types of components considered, fluid circulation cooling appears to be the most favorable system for thermal isolation during terminal sterilization. However, because of the possibility that more sophisticated analyses and inclusion of additional system design considerations may disclose favorable applications of phase-change cooling, it was recommended that both thermal isolation methods be investigated more thoroughly. Furthermore, thermoelectric cooling may be useful in certain special cases such as protecting the face of a vidicon tube.

### 3.10 REFERENCES - PHASE I

- 3-1 Werth, G. R., "Technical Status Report - Thermal Isolation Study," LMSC/A748637, dated 10 May 1965
- 3-2 Materials in Design Engineering, Materials Selector Issue, Reinhold Publishing Corp., October 1964
- 3-3 Goldsmith, Alexander, et al, "Thermophysical Properties of Solid Materials," Wright Air Development Center, Wright-Patterson AFB, Ohio, 1959
- 3-4 Marks, L. S., "Mechanical Engineers' Handbook," 1951

- 3-5 O'Brien, F. R., Oglesby, S., Jr., "Investigation of Thermal Properties of Plastic Laminates, Cores, and Sandwich Panels, Part 1," WADC TR 54-306, November 1955
- 3-6 Johns-Manville Data, New York, N. Y.
- 3-7 Nopco Chemical Co. Data, North Arlington, New Jersey
- 3-8 "Properties of Rigid and Semi-Rigid Urethane Foams," du Pont de Nemours and Co., Inc., Wilmington, Delaware, 1957
- 3-9 Gaumer, G. R., and Kummer, D. L., "Thermal Properties of Materials," Report 5926, McDonnell Aircraft Corp., St. Louis, Mo., 3 February 1958
- 3-10 Insulation Product Information #IN-304A, Johns-Manville, New York, N. Y.
- 3-11 Howse, P. T., Jr., Pear, C. D., Oglesby, S., Jr., "The Thermal Properties of Some Plastic Panels," WADD TR 60-657, January 1961
- 3-12 Kreith, F., "Principles of Heat Transfer," International Textbook Co., Scranton, Pa., 1960
- 3-13 Hodgman, C. D., Editor in Chief, "Handbook of Chemistry and Physics," Chemical-Rubber Publishing Co., Cleveland, Ohio, 1944
- 3-14 McAdams, W. H., "Heat Transmission," McGraw-Hill Book Co., Inc., N.Y., 1954
- 3-15 Mackay, D. B., "Design of Space Powerplants," Prentice-Hall Inc., Englewood Cliffs, N.J., 1963
- 3-16 Mell, C. W., and Hostetler, K. E., "New and Improved Heat Transfer Fluids," AFML-TDR-64-24A, WPAFB, Ohio, February 1964
- 3-17 Mell, C. W., and Hostetler, K. E., "New and Improved Heat Transfer Fluids," AFML-TR-65-36, WPAFB, Ohio, February 1965
- 3-18 Kaye, J., et al., "Final Report on Heat Storage Cooling of Electronic Equipment," WADC TR-56-473, February 1957
- 3-19 Williams, W. S., "Survey of Literature on Latent Heat Sink Materials for Electronic Cooling Applications," 27 June 1963, Lockheed Missiles and Space Co. Internal Document.

- 3-20 Wooten, R. W., and Merz, E. J., "Mars-Voyager Systems," Preprints of Papers Presented at the AIAA Unmanned Spacecraft Meeting, Los Angeles, California, March 1-4, 1965
- 3-21 "Conceptual Design Studies of an Advanced Mariner Spacecraft," AVCO Corporation Report RAD-TR-64-36, AVCO Corp., Wilmington, Mass. 28 October 1964
- 3-22 Fixler, S. Z., "Analytical and Experimental Investigation of Satellite Passive Thermal Control Using Phase Change Materials," Preprints of Papers Presented at the AIAA Unmanned Spacecraft Meeting, Los Angeles, California, March 1-4, 1965
- 3-23 Tenney, J. B., and Fried, E., "Thermal Sterilization of Spacecraft Structures," Preprints of Papers Presented at the AIAA Unmanned Spacecraft Meeting, Los Angeles, Calif., March 1-4, 1965
- 3-24 Fried, E., and Kepple, R. J., "Spacecraft Sterilization - Thermal Considerations," AIAA Paper No. 65-427, July 1965
- 3-25 Tenney, J. B., and Crawford, R. G., "Design Requirements for the Sterilization Containers of Planetary Landers," AIAA Paper No. 65-387, July 1965
- 3-26 JPL Specification No. XSO-30275-TST-A, Environmental Test Specification, Compatibility Test for Planetary Dry Heat Sterilization Requirements, dated 24 May 1963
- 3-27 Lockheed Missiles & Space Company, "Experimental Study of Sterile Assembly Techniques," LMSC M-56-65-1, Final Report Under Contract No. JPL-950993, 21 March 1965
- 3-28 "NASA Management Manual," Chapter 4-4-1, NASA Unmanned Spacecraft Decontamination Policy
- 3-29 Nicks, O. W., "Sterilization of Mars Spacecraft," Astronautics and Aeronautics, Volume 2, No. 10, p. 21, October 1964
- 3-30 K. H. Hanson, "A Preliminary Study of the Thermal Integration of Electrical Power and Life Support Systems for Manned Space Vehicles," AIAA Paper No. 64-722, 14 September 1964

- 3-31 E. R. G. Eckert & R. M. Drake, "Heat and Mass Transfer," McGraw-Hill
- 3-32 W. H. Geidt, "Principles of Engineering Heat Transfer," Van Nostrand
- 3-33 W. H. McAdams, "Heat Transmission," 34d Ed., McGraw-Hill, 1954
- 3-34 "Physical Properties of the Planet Mars" Douglas Rpt. SM 43634, August 1963
- 3-35 "Manned Mars Exploration in the Unfavorable (1975-85) Time Period, Vol. VIII, Life Support & Environmental Control, Douglas Aircraft Co. SM-45582, Santa Monica, Calif., February 1964
- 3-36 Mechanics of Heat Pumps and Absorption Refrigeration: An Annotated Bibliography, Special Bibliography, SB-62-16, LMSC, April 1962
- 3-37 Air Force Materials Laboratory, "New & Improved Heat Transfer Fluids," MLTDR-64-24, February 1964
- 3-38 "The Optimization of an Actively Cooled Heat Shield," Ling-Temco-Vought Rpt No. 000256, 17 July 1963
- 3-39 Loffe, A. F., "Semiconductor Thermoelements and Thermoelectric Cooling," Infosearch Limited, London, 1957.
- 3-40 Green, W. B. (Editor), "Westinghouse Thermoelectric Handbook, Westinghouse Electric Corporation, Semiconductor Division, Youngwood, Pennsylvania, 1962
- 3-41 Hawkins, S. R., "Thermoelectric Heat Rejection in Spacecraft - Preliminary Study," LMSC IDC, 28 October 1964
- 3-42 "Study of Thermal Isolation Techniques - Technical Summary Report, Phase I, Feasibility Study", LMSC A772585, October 1965

## Section 4

## PHASE II - DEFINITION OF PROBLEM AREAS AND METHODS OF SOLUTION

Although all of the problem areas associated with the implementation of isolation schemes may be considered to fall into the general category of systems integration problems, some items can be singled out as primarily affecting the payload system, the sterilization system, or the isolation system. Thus, three general categories of isolation problem areas were established in Phase II - those pertaining to specific details of the sterilization facility design and operation, those affecting spacecraft systems design, and those affecting isolation systems design.

Figure 4-1 is the schematic diagram that evolved indicating the interaction between thermal isolation system design and payload and sterilization facility design. This diagram also illustrates the planned sequence in which these interactions and design problems were to be considered in Phase III studies. The basis for evaluating the magnitude of these interface effects was to define a preliminary design of isolation devices for components which are presently being considered for early Voyager Lander systems. These components have been described in Section 3; preliminary design of isolation devices would be based on the same types of components, but referenced to the specification of an actual component. Thus, a vidicon tube isolation system, for example, would be designed for a specific type and model of vidicon tube, mounted in a scanning camera system.

Sufficient latitude should be allowed, however, in the selection of the components and their mounting and installation in the Lander, so that a range of interaction effects could be obtained. For the purpose of estimating the total effect of isolation system interaction with the payload system, a Lander configuration was selected which appears to be representative of the current approach to Voyager systems design.

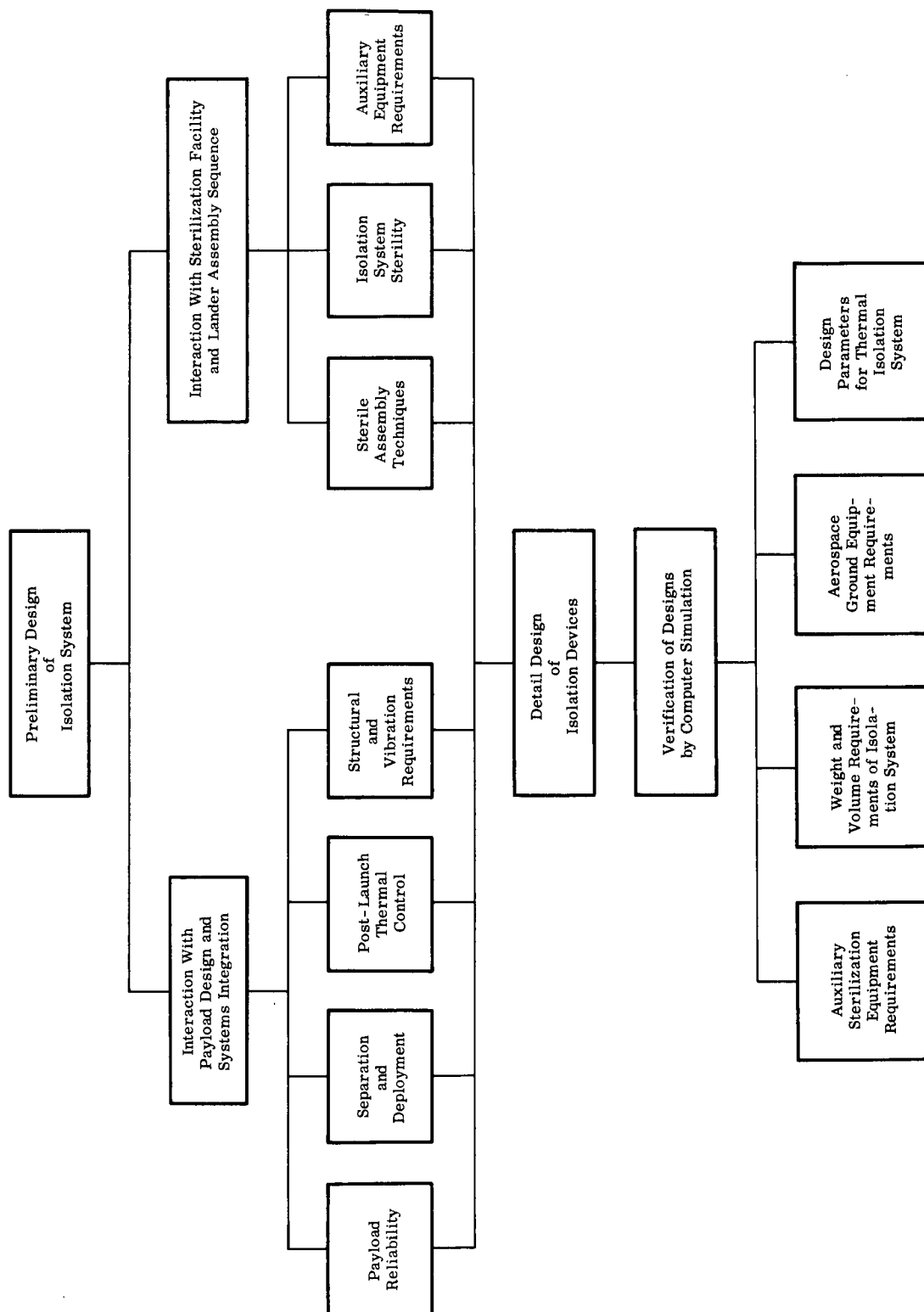


Fig. 4-1 Design Considerations and Interface Effects



#### 4.1 PRELIMINARY DESIGN OF ISOLATION SYSTEMS

Preliminary design of isolation devices should be based on the use of specific temperature-sensitive components, as noted above. A preliminary selection of these components was made; their detailed specifications are shown in Table 4-1.

Table 4-1  
DETAILED LANDER COMPONENT SPECIFICATIONS

Component	Manufacturer/Type	Weight (lb)	Volume (in. <sup>3</sup> )	Upper Temperature Limit (°C)
Nickel-Cadmium Battery	Sonotone Corporation	25.3	194	60
Life Detection Experiment-Culture Medium	NASA/JPL - Radioisotope, Optical Density or Microscopic Growth Detection	6.0	204	50
Life Detection Experiment - Vidicon Tube	RCA 8573	0.8*	23*	71
Life Detection Experiment - Photomultiplier Tube	RCA 8575	0.38	20	85
Tape Recorder	Raymond Engineering Lab.	16.8	486	70

\*Includes magnetic focussing and deflection coils.

The preliminary design of isolation devices for components which are to be isolated solely by the use of fluid circulation cooling involves only the design of a suitable shield, single or double walled, to carry the coolant fluid around the component. It was assumed that allowances for electrical penetrations and structural attachment of the shield would not provide any complex design problems. The design of isolation devices for components which are to be isolated by the use of both fluid circulation and thermoelectric cooling requires a more sophisticated design approach and integration

with the payload system, in order to allow for removal of the thermoelectric device from the component after completion of terminal sterilization.

For components which cannot remain completely enclosed by the isolation device, consideration was also given to mechanisms for the removal of a portion of the fluid circulation shield from the component, or the removal of the component from the shield. The desirability of enclosing several components within a single shield was also to be investigated.

#### 4.2 INTERACTION WITH PAYLOAD DESIGN AND SYSTEMS INTEGRATION

Although the preliminary design of the isolation system should be performed with a view toward integrating the isolated components into the Voyager-Lander design, a thorough evaluation of several mechanisms of interaction cannot be made until the preliminary design has been accomplished. Subsequent to the preliminary isolation system design it was planned that typical components, fitted with their isolation devices, would be designed into the prototype Lander configuration to provide a basis for the evaluation of interaction effects.

Conceptual design studies of Advanced Mariner and Mars-Voyager spacecraft have shown that the most probable Lander configuration is either a sphere surrounded by an outer crushable sphere, or a conical configuration conforming to an outer conical re-entry shield (see Refs. 4-1 through 4-4). For the purposes of this study, a prototype configuration similar to that described in Ref. 4-1 was used. Sufficient thermal design information is given in Ref. 4-1 so that the interactions of the isolation system with the landed payload could be determined.

In order to evaluate the magnitude of these interactions it is necessary to describe the payload in detail. However, to make the results of the study general and applicable to a range of vehicles, it was planned to use an idealized model of the Mars Lander described in Ref. 4-1. A general thermal network for this configuration is shown in Fig. 4-2.

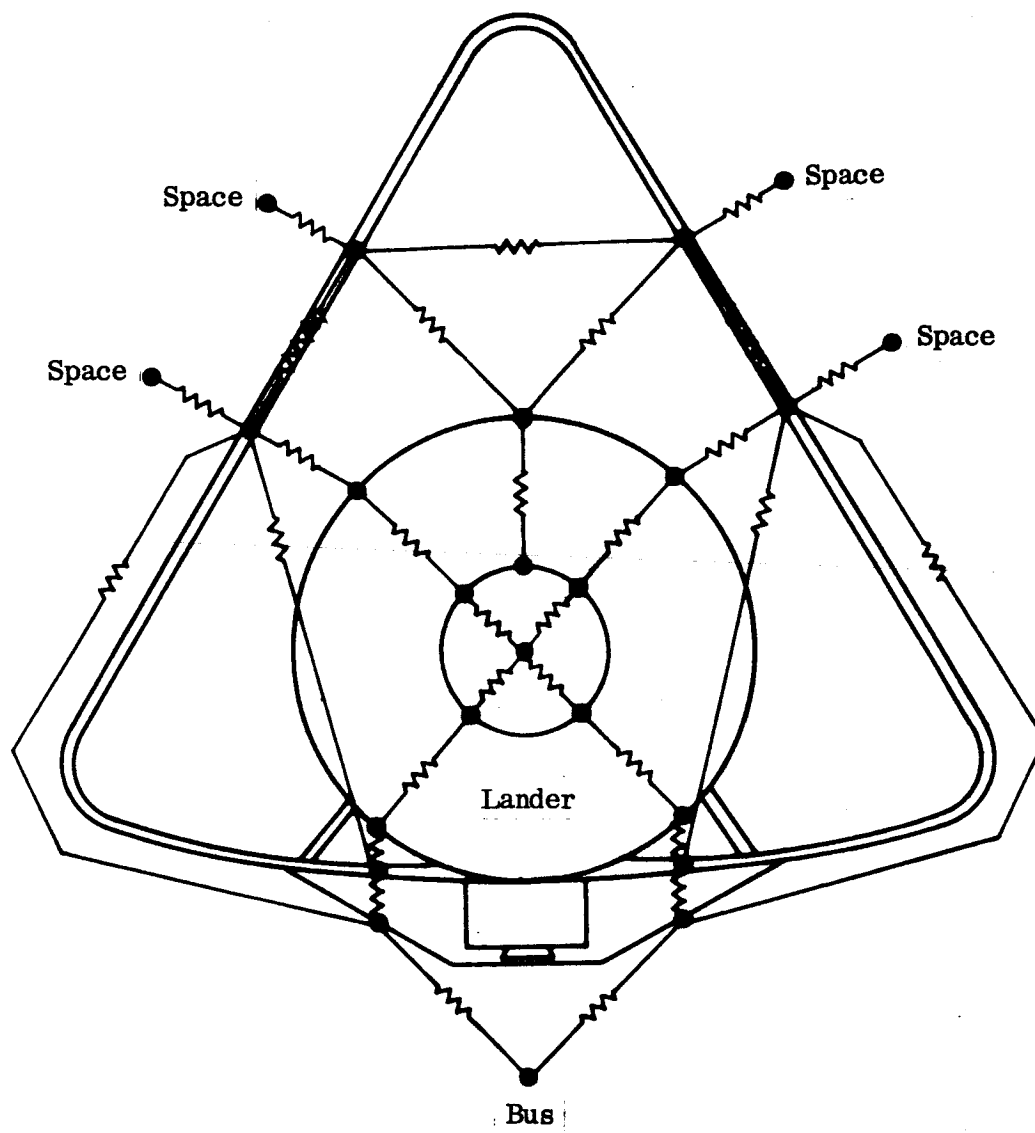


Fig. 4-2 Thermal Analog Network for Simulation of Heat Flow Paths in Idealized Lander Configuration

#### 4.3 INTERACTION WITH STERILIZATION FACILITY AND LANDER ASSEMBLY SEQUENCE

The design of a thermal isolation system is affected by general sterilization requirements and will, in turn, affect the design of the sterilization facility and the Lander assembly and sterilization sequence. The sterilization facility must be able to provide sterile coolant fluid for fluid circulation isolation devices and must regulate the flow rate of coolant to maintain isolated packages within allowable temperature ranges. This implies the use of a sterile coolant pump (and coolant heat exchanger if a very large reservoir of coolant is not available), which in turn imposes restrictions on the types of pumps and construction materials which can be used in the sterilization facility. Similarly, since the external surface of coolant shields will be exposed to the sterilization environment, as well as outer surfaces of coolant tubing, it may be necessary to use non-metallic materials for these items to insure their sterility. Also, any surfaces which are conductively coupled to coolant tubing and coolant shields may possibly remain at a temperature lower than that required for adequate sterilization when exposed to the terminal sterilization environment.

It was anticipated that the vehicle temperature distribution during terminal sterilization, which is determined by using the thermal network described previously, would reveal areas where the Lander structure adjacent to isolation devices, or the outer surfaces of isolation devices, remains at prohibitively low temperature during terminal sterilization. Appropriate changes in material or structural design must then be incorporated into the thermal model and the adequacy of the design solution verified.

Similarly, using the experience gained in the study of sterile assembly techniques (Ref. 4-5), it was planned to educe a recommended assembly sequence for the Lander and isolation system to insure aseptic assembly of pre-sterilized components and isolation devices.

#### 4.4 DETAIL DESIGN OF ISOLATION DEVICES

Subsequent to the resolution of the design problems discussed in Sections 4.1, 4.2, and 4.3, a detailed design evaluation of isolation systems was planned with the objective of

minimizing overall weight and volume requirements of the isolated payload components. The purpose of this study was to evaluate the weight and volume requirements associated with the thermal isolation of a selected range of sizes and shapes of given components. The isolation of a biological nutrient solution must be examined, for example, assuming the nutrient to be packaged in an ampoule, on a flat plate, or a similar extended surface. Similarly, a small range of shapes and sizes of batteries must be examined. In addition to the calculation of weight and volume requirements for the proposed range of vehicle component specifications, the adequacy of the detailed isolation system designs must be verified for the configurations in which the component combinations of size and shape result in the highest and lowest isolation system weight and volume penalties. The major results of such an evaluation can be utilized in defining:

- Design Parameters for the Thermal Isolation System (materials, construction and assembly techniques)
- Weight, Volume and Reliability Penalties of the Thermal Isolation System
- Auxiliary Sterilization Equipment Requirements
- Aerospace Ground Equipment Requirements

The overall results will be a range of isolation system requirements, corresponding to a selected range of Lander components, which can be incorporated into the preliminary design of Mars Lander systems and the design of a sterilization facility for planetary landers.

#### 4.5 PROGRAM PLAN AND MILESTONES FOR PHASE III

Presented below is the study plan for Phase III of the Thermal Isolation Study. This plan outlines the specific items of study and indicates the sequence in which these problems should be considered.

##### Task 1 – Preliminary Design of Isolation System

Perform preliminary design of isolation devices for application to the selected components shown in Table 4-1, with materials selection and design for minimization of weight and volume. Mechanisms for removal of portions of isolation device and hybrid systems such as fluid circulation combined with thermoelectric cooling are to be included.

### Task 2 - Interaction With Payload System

Construct thermal network for computer analysis of temperature distribution in the isolated payload system and use these results to evaluate:

- Temperature distribution and thermal stresses during terminal sterilizations, and
- Effects of isolation devices on post-launch thermal control.

Perform a preliminary analysis of the structural adequacy of isolation devices exposed to launch acceleration, preliminary design of mechanisms for separation of coolant lines and electrical feed-throughs at the payload and sterilization shield interfaces, and a qualitative analysis of the effects of the isolation system on payload systems reliability.

### Task 3 - Interaction With Sterilization Facility and Lander Assembly Sequence

Utilize the payload temperature distribution during sterilization (determined in Task 2) to locate areas which may remain cool and unsterilized and implement design changes to provide higher local temperatures. Construct recommended assembly sequence for pre-sterilized components into payload assembly and specify requirements for design of sterilization facility.

### Task 4 - Detail Design of Isolation Devices

Utilizing the results of studies performed in Tasks 1, 2, and 3, perform detailed design of isolation devices for a range of component sizes and shapes and evaluate the adequacy of at least two of these designs using the thermal analyzer network computer program. Compile the following results for the range of component sizes and shapes studied:

- Design Parameters for the Thermal Isolation System
- Weight, Volume and Reliability Penalties of the Thermal Isolation System
- Auxiliary Sterilization Equipment Requirements
- Aerospace Ground Equipment Requirements

#### 4.6 CONCLUSIONS - PHASE II

The major problem areas, design considerations, and interface effects involved in the design of a thermal isolation system for a candidate planetary lander configuration have been delineated. Methods of solution to these problems and a plan for the design of isolation systems have been outlined which will result in design procedures for a limited range of component configurations. The results of this program would be available for use in the design of the payload system as well as the design of the sterilization facility and lander assembly procedures.

#### 4.7 REFERENCES - PHASE II

- 4-1 "Conceptual Design Studies of an Advanced Mariner Spacecraft," AVCO Corporation Report, RAD-TR-64-36, AVCO Corp., Wilmington, Massachusetts, 28 October 1964
- 4-2 Tenny, J. B., and Fried, B., "Thermal Sterilization of Spacecraft Structures," Preprints of Papers presented at the AIAA Unmanned Spacecraft Meeting, Los Angeles, Calif., 1-4 March, 1965
- 4-3 Tenney, J. B., and Crawford, R. G., "Design Requirements for the Sterilization Containers of Planetary Landers," AIAA Paper No. 65-387, July 1965
- 4-4 Wooten, R. W., and Merz, E. J., "Mars-Voyager Systems," Preprints of Papers presented at the AIAA Unmanned Spacecraft Meeting, Los Angeles, Calif., 1-4 March, 1965
- 4-5 "Experimental Study of Sterile Assembly Techniques," LMSC M-56-65-1, Final Report under Contract No. JPL 950993, dated 21 March 1965
- 4-6 "Study of Thermal Isolation Techniques - Technical Summary Report, Phase II - Study Program and Milestones For Detailed Isolation Study," LMSC-A775430, October 1965
- 4-7 "A Study of Design Guidelines for Sterilization of Spacecraft Structures," NASA CR-61005, Contract No. NAS 8-11107, August 1964

## Section 5

PHASE III - PARAMETRIC STUDY OF SELECTED ISOLATION TECHNIQUES  
FOR TYPICAL CRITICAL COMPONENTS

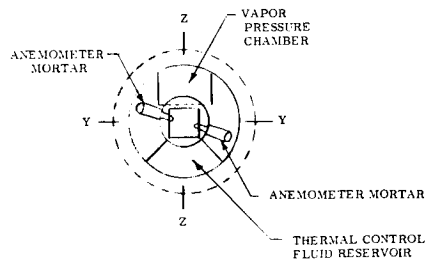
## 5.1 PRELIMINARY DESIGN OF AN ISOLATION SYSTEM

In order to evaluate the effects of terminal heat sterilization and post-launch thermal environments on temperature-sensitive components it was first necessary to describe a prototype lander configuration. The prototype lander configuration shown in Figs. 5-1 and 5-2 is based on an Advanced Mariner configuration described in Ref. 5-1. It includes the major structural elements which are likely to be found in a typical lander, and provides a basic framework into which must be packaged the candidate lander components.

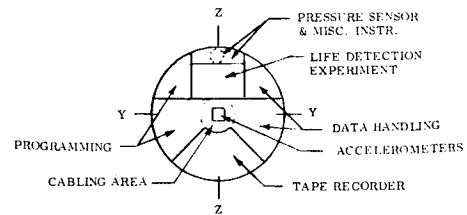
Detailed specifications of temperature-sensitive components (those requiring thermal isolation) were presented in Table 4-1 of Section 4. Techniques for mounting components within the idealized lander are shown in Figs. 5-3 through 5-6. Joints and package configurations were sufficiently well defined to permit thermal idealization, but no detail design work was performed. In particular, the life detection experiment has been defined so that it may incorporate either a photomultiplier or vidicon tube. Growth media containment has been envisioned in the form of ampoules or on planchets (Ref. 5-2).

Since fluid circulation cooling is the selected method of thermal isolation, all heat-sensitive components will be enclosed by an isolation shield whose purpose is to guide the fluid coolant around the component so as to provide fluid circulation over the entire component surface to be protected. Fluid coolant is supplied to the lander capsule through an umbilical containing explosively actuated valves and disconnects.

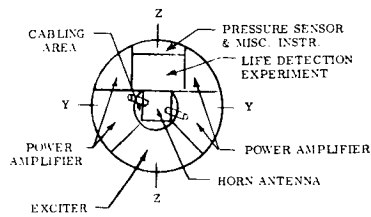




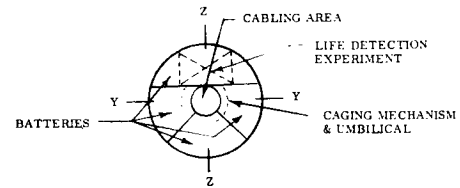
SECTION J-J



SECTION G-G



SECTION H-H



SECTION F-F

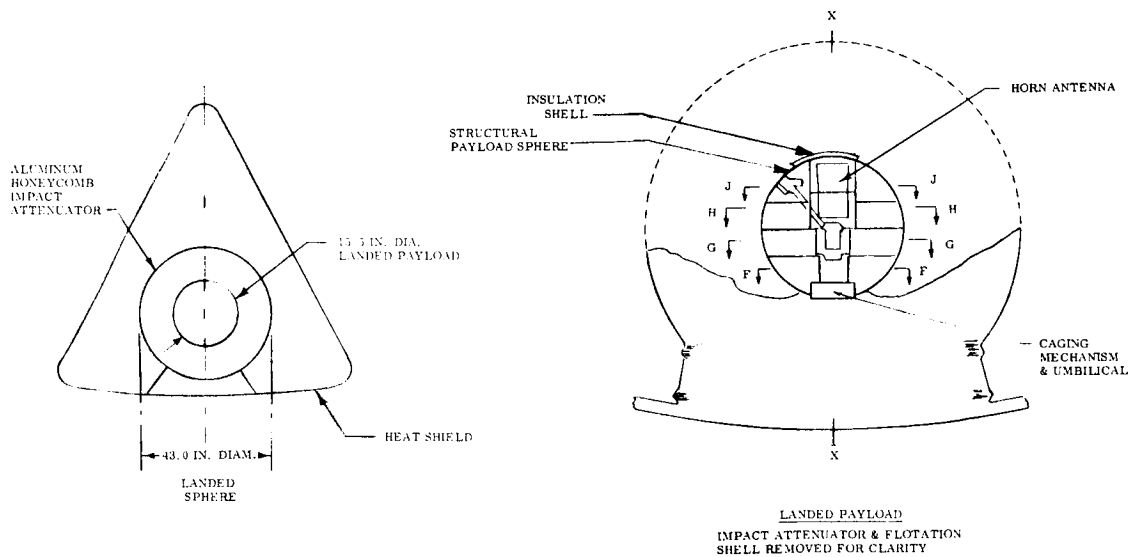


Fig. 5-1 Voyager-Lander Conceptual Design

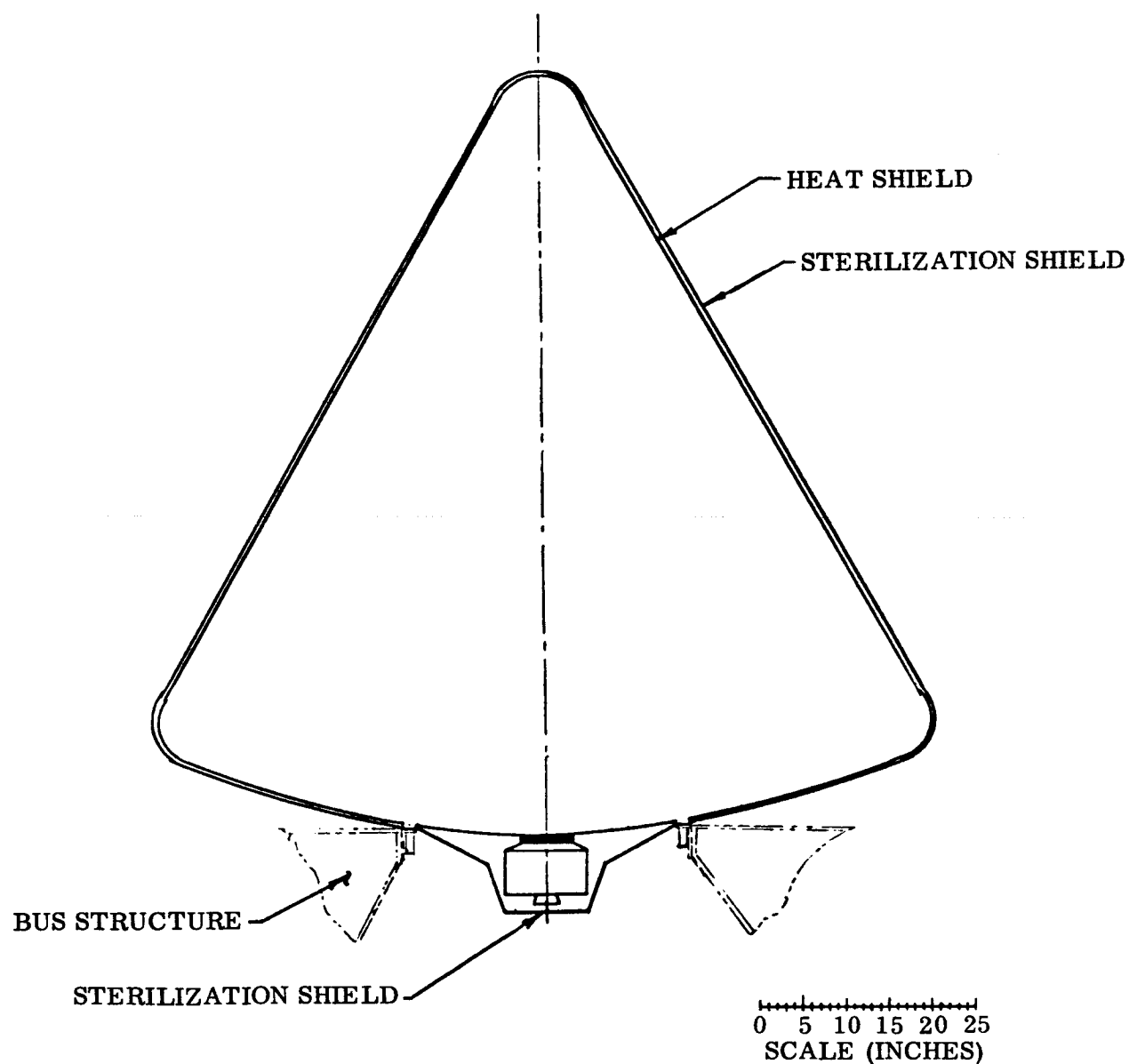


Fig. 5-2 Sterilization Shield Configuration

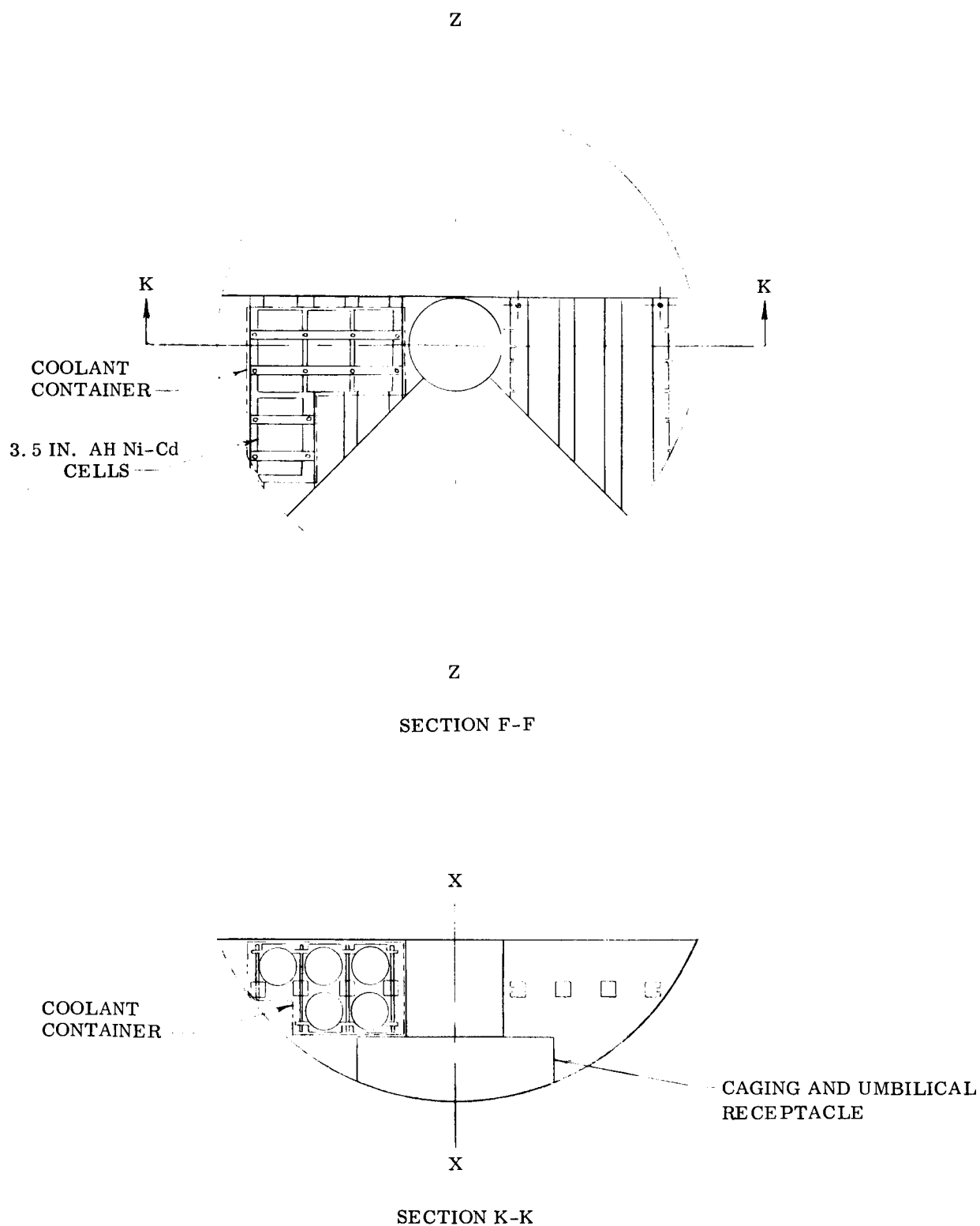


Fig. 5-3 Battery Installation in Landed Payload

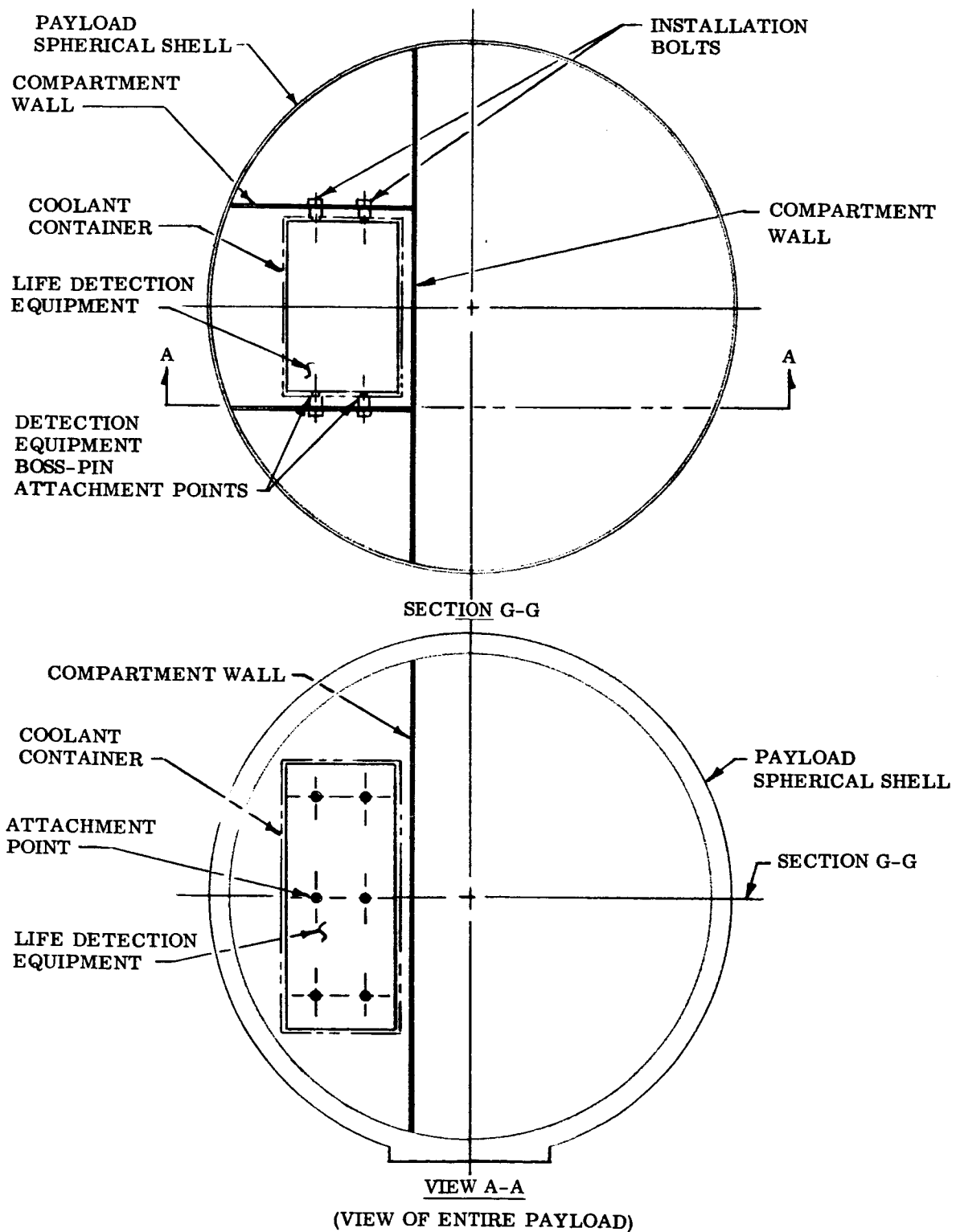


Fig. 5-4 Life Detection Equipment in Landed Payload

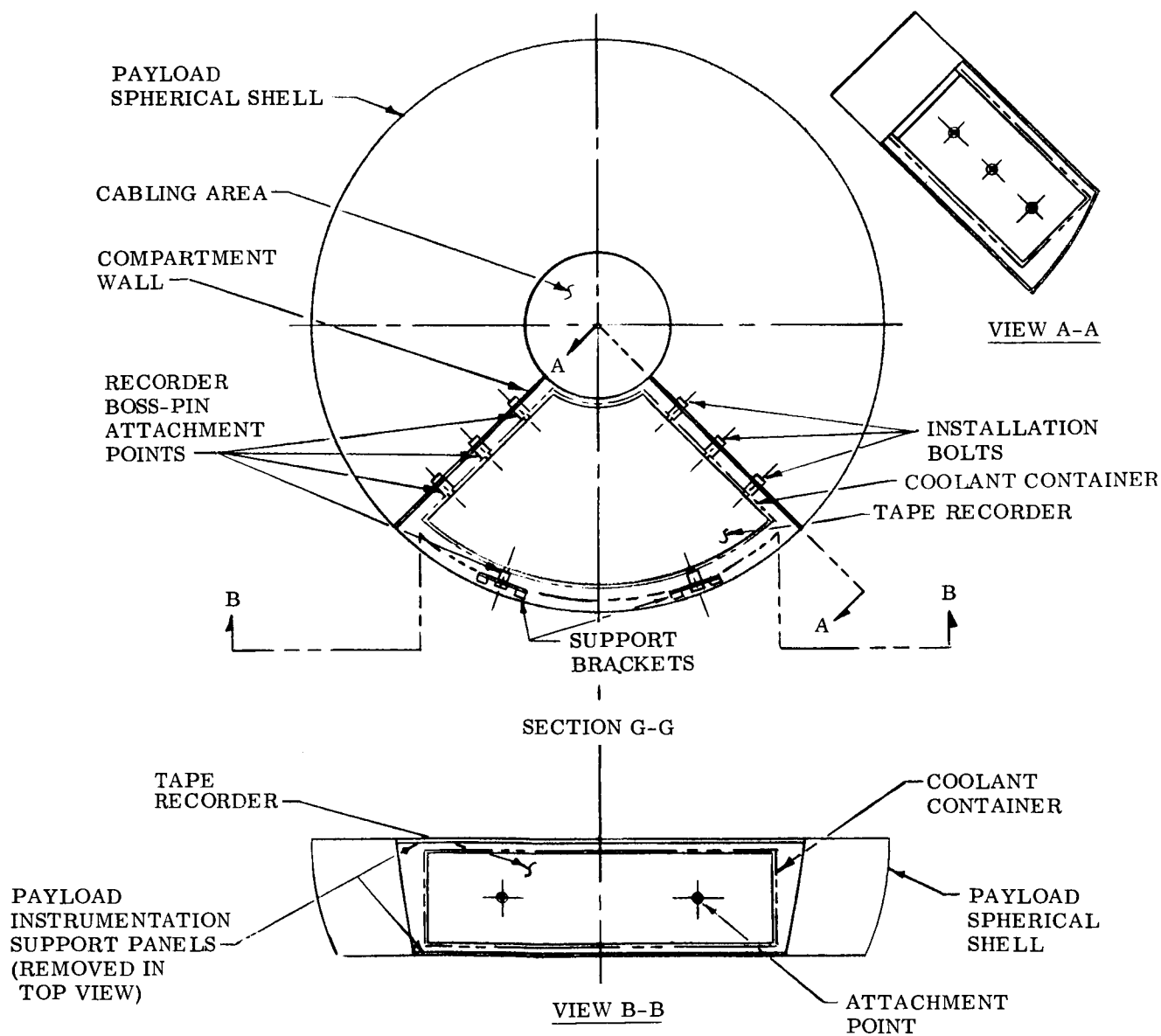


Fig. 5-5 Tape Recorder Installation in Landed Payload

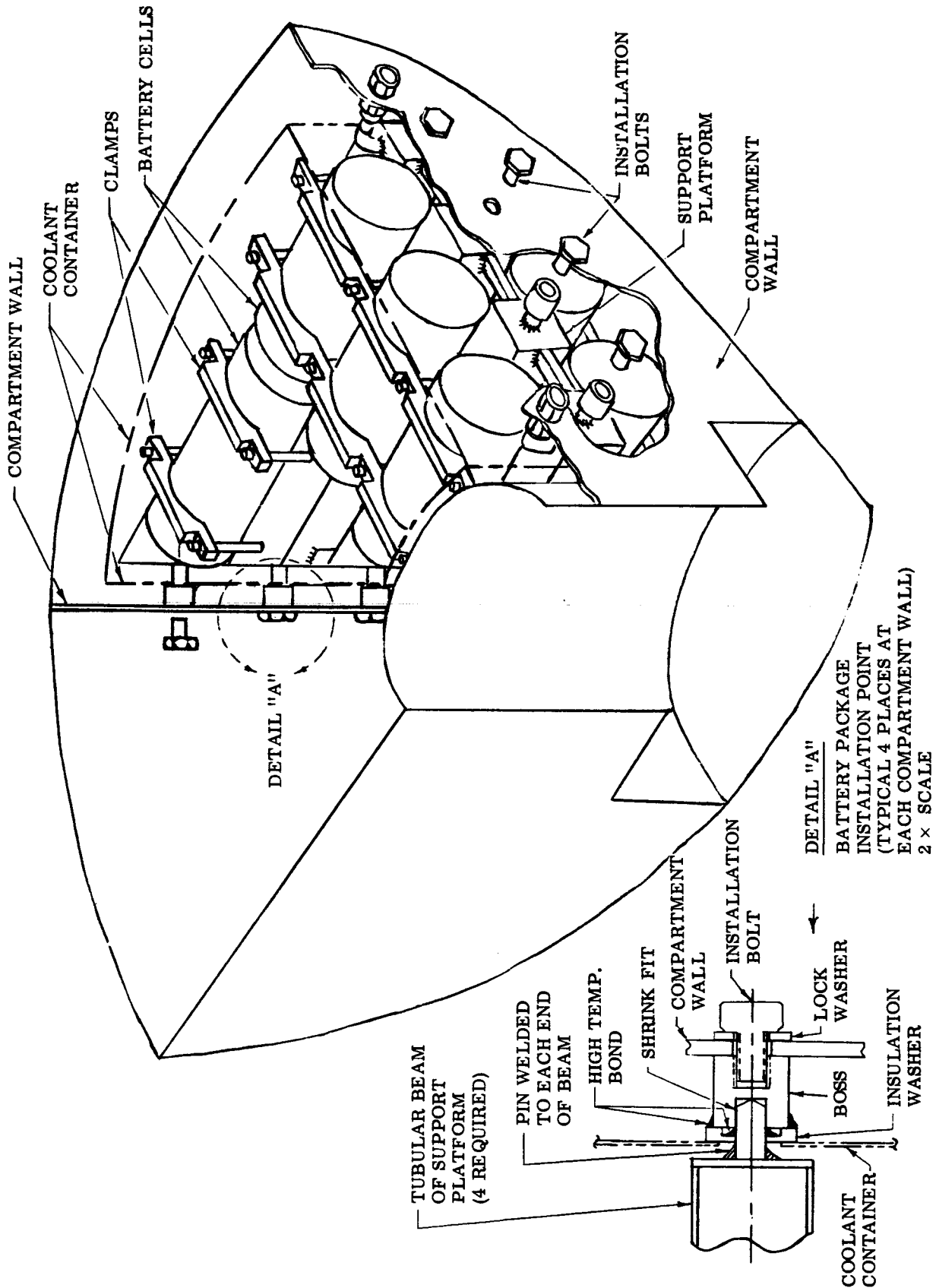


Fig. 5-6 Isolated Battery Installation

### 5.1.1 Coolant Shield Design

It is anticipated that the coolant shield will be aseptically assembled to the presterilized component prior to the installation of the component in the lander. The coolant shield will thus function as a biological barrier to prevent contamination of the component during handling and assembly of the component into the lander structure (a study of available sterile assembly techniques and an evaluation of their effectiveness has been performed at LMSC; the results are described in Ref. 5-3).

The preliminary design of a coolant shield was directed toward satisfying the following requirements:

- The coolant shield must be sterilizable and capable of sterile assembly to the component.
- The coolant shield should provide uniform coolant flow over the component surfaces.
- The coolant shield attachments to the component mounting structure should be designed to minimize cooling of adjacent structure which must be heated during terminal sterilization.
- The coolant shield should provide a biological barrier against contamination of the component by dirt, dust, or viable microorganisms.
- The coolant shield must be capable of withstanding ground handling and flight environments.
- The coolant shield design should minimize interference with post-launch thermal control. Weight and volume penalties associated with the isolation system should also be minimized.

The requirement that the coolant shield be sterilizable on its outer surface during terminal sterilization implies that at least the outer surface layer (that surface which is exposed to the hot sterilization gas) must be a good thermal insulator. The shield material may be made of either rigid or flexible materials (plastic films) or a combination of both.

Rigid materials, while heavier than relatively thin plastic films, have the advantage of being less susceptible to handling damage. A rigid isolation container, however, has the disadvantage of requiring a larger volume and more complex fabrication techniques than flexible containers. Flexible film materials are commonly used for germ-free isolators and may be easily fabricated to conform to complex geometrical shapes thus providing uniform flow passages for circulating fluid coolants. The use of a flexible film container for pre-sterilized lander components also allows manipulation of the component and permits the isolated component to be seen.

A combination of rigid and flexible materials may be used for the containment of components which require that a portion of the coolant container be removed or displaced after terminal sterilization. A list of properties of candidate flexible film materials which can withstand the proposed dry heat sterilization environment is shown in Table 5-1.

Table 5-1  
FILM MATERIALS FOR COOLANT CONTAINER CONSTRUCTION

Material	Maximum Service Temperature (° F)	Specific Gravity	Burst Strength (psi)
Cellulose Acetate	250-300	1.25-1.35	30-80
Nylon 6	380	1.12	—
Polypropylene	300	0.90	—
CFE Fluorocarbon	300-395	2.11	42
Polyester	300-360	1.23	56
Cellulose Triacetate	300-400	1.28	100-150
Polyimide ("H-Film")	500+	1.20	—

The use of a flexible film material for the coolant container will meet the requirements listed above providing that (1) adequate support is provided when fluid is circulating and (2) the film is sufficiently thick to allow its exterior surface to attain the sterilization temperature. For the range of thermal conductivities found in most plastic film materials this requires a fairly large single film thickness, on the order of 0.3 inches.



However, as stated in Ref. 5-4, terminal heat sterilization may not be an absolute requirement, as long as exposed component surfaces can be sterilized by gaseous sterilants and the sterility of electrical and mechanical devices within that component can be guaranteed.

In the event that terminal sterilization of the coolant shield outer surface is a firm requirement, a double-walled coolant shield may be used wherein the space between the coolant shield inner and outer walls is filled with an inert gas. The highly effective thermal resistance of this gas layer would insure high temperatures on the outer wall of the coolant shield during terminal sterilization.

In order to illustrate the conceptual design of a coolant container using a flexible film material, a mockup of an isolated component was constructed. The completed mockup, representing a cylindrical component surrounded by a plastic coolant container spaced 0.2 inches from the component surface, is illustrated in Fig. 5-7. Under pressure, due to the coolant flow, the plastic container is inflated so that reasonably uniform flow occurs over the component surface. When terminal sterilization has been completed, the space between the component and coolant container may be evacuated, to make the plastic film conform to the component surface thus minimizing any displacement of the coolant container during launch vibration. Also, due to its low density when compared to solid insulation or metallic materials, the use of plastic films for coolant container materials will minimize launch vibration and acceleration effects on the coolant container.

Because of the foregoing considerations, a flexible film material was selected for coolant containers in the prototype lander configuration.

#### 5.1.2 Component Attachment to Adjacent Structure

The design of component attachments to adjacent lander structure must be directed toward the satisfaction of several fairly unique requirements. These attachments must, of course, be able to transmit the acceleration and vibration loads to the lander structure,

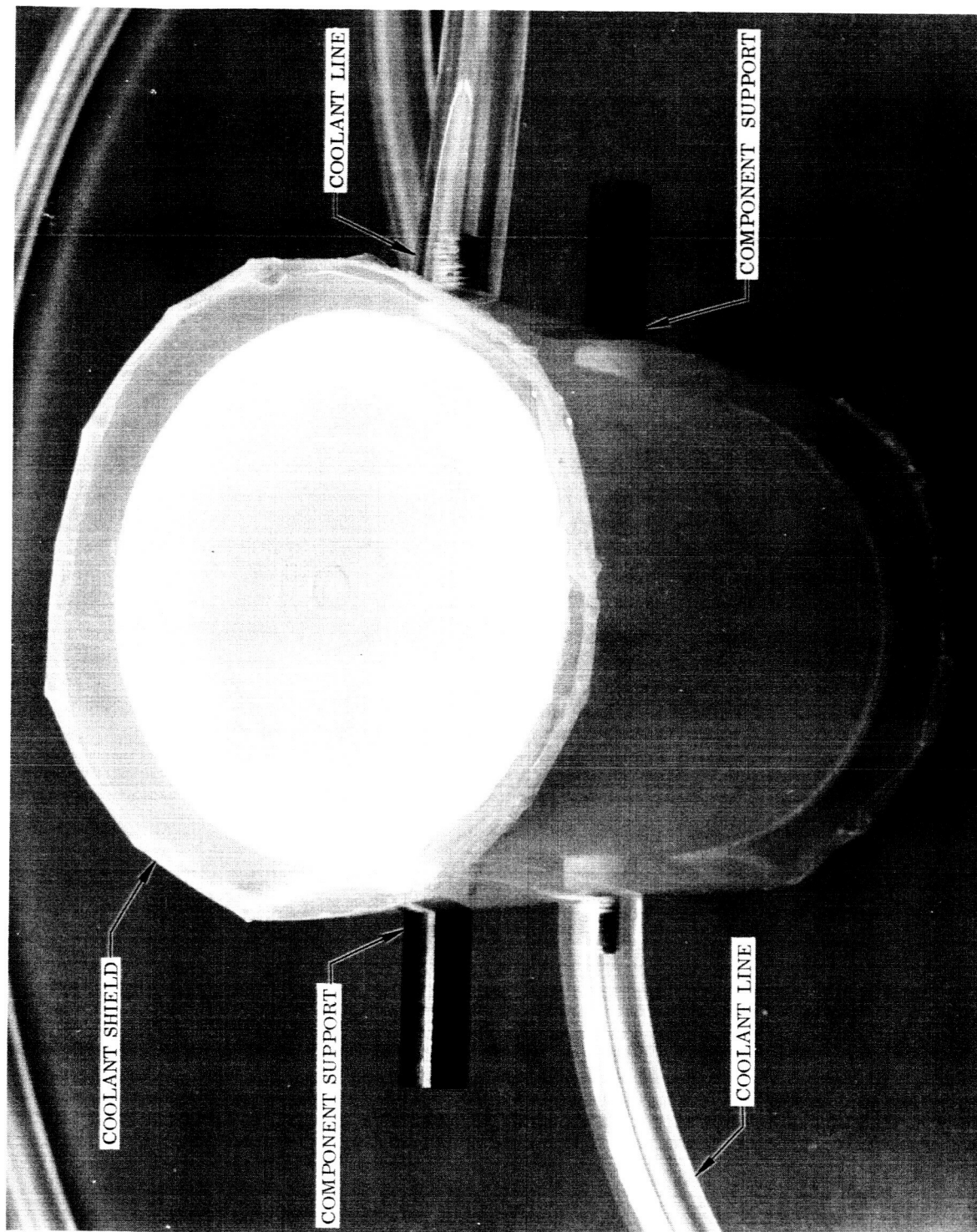


Fig. 5-7 Isolated Component Concept Mockup

and should not require assembly techniques which would compromise the effectiveness of sterile component assembly techniques. For adequate thermal control after landing on Mars, heat generated within the component during component operation must be allowed to flow into the adjacent structure; thus component attachments must provide a fairly low thermal resistance between the component and the lander structure. This requirement is in opposition to that for a high thermal resistance during sterilization. The latter requirement is due not only to the need for keeping heat flow into temperature sensitive components to a minimum during terminal sterilization, but also to the necessity for preventing cooling of adjacent lander structure below the temperature required for sterilization.

Some concepts which have been developed to satisfy the above requirements are illustrated in Figs. 5-8, 5-9, and 5-10. The first two of three concepts shown depend on achieving a high thermal resistance between the component and the structure to which it is mounted. It requires, therefore, some means of establishing a good path for conductive heat transfer subsequent to terminal sterilization. The first concept features a cross-section of material having a low thermal conductivity which is protected from both cooling by the circulating coolant fluid and from heating by the sterilization gas. This protection is accomplished by constructing the coolant shield so that it is locally "double-walled" to provide an insulating region around a portion of the connector.

The second concept, shown in Fig. 5-9, provides a high thermal resistance by means of a long heat transfer path. The connector is insulated from coolant flow near the coolant shield and well exposed to cooling near the component. It is evident that, while both of these configurations may be implemented with a fair degree of success, they would result in fairly large weight and volume penalties in comparison to conventional connectors.

The third concept, illustrated in Fig. 5-10, was selected as being the most practicable and economical connector which was capable of satisfying the requirements stated earlier in this section. It has the virtue of not requiring an auxiliary heat transfer path to recouple the component to the adjacent structure when post-launch thermal

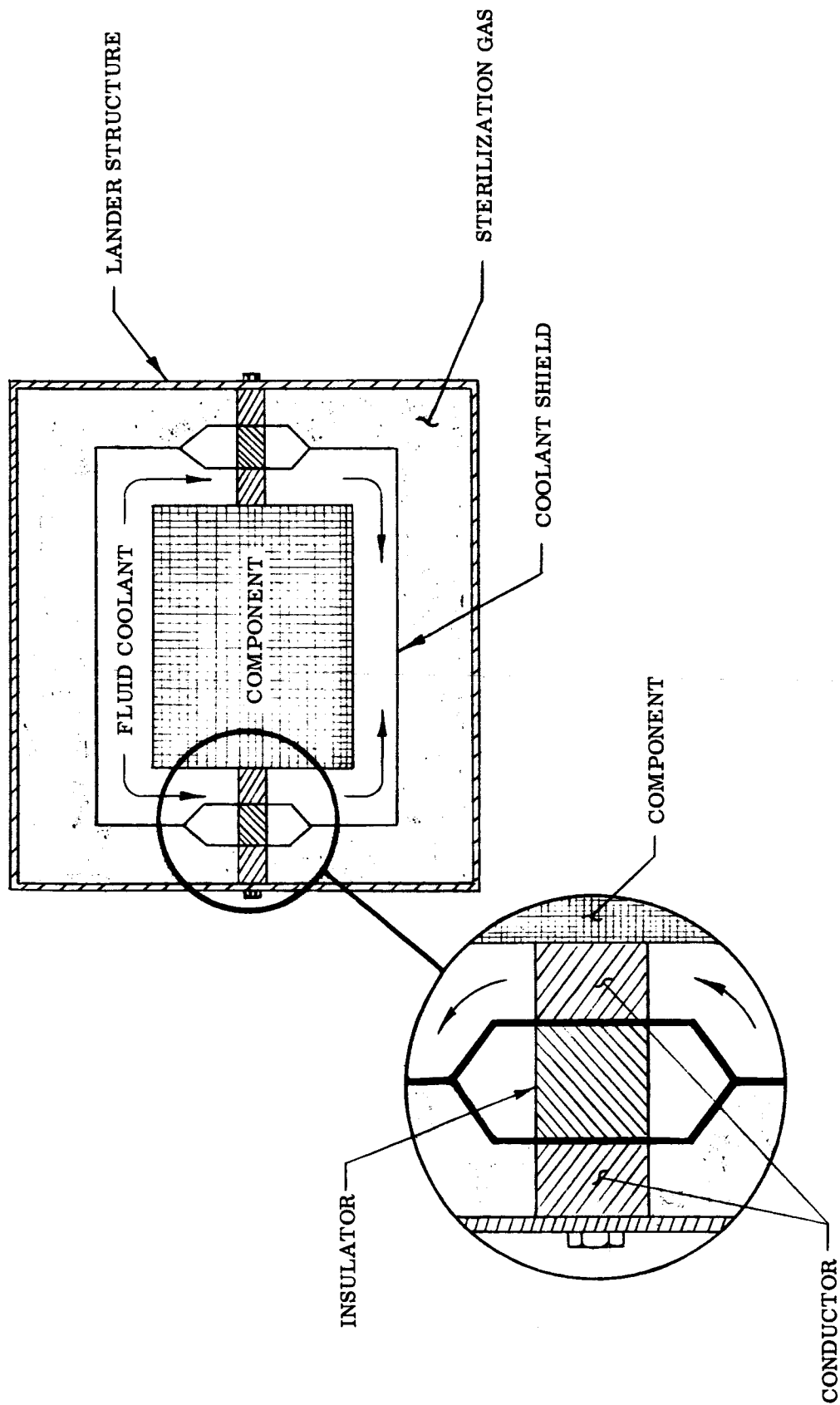


Fig. 5-8 High Thermal Resistance Connection

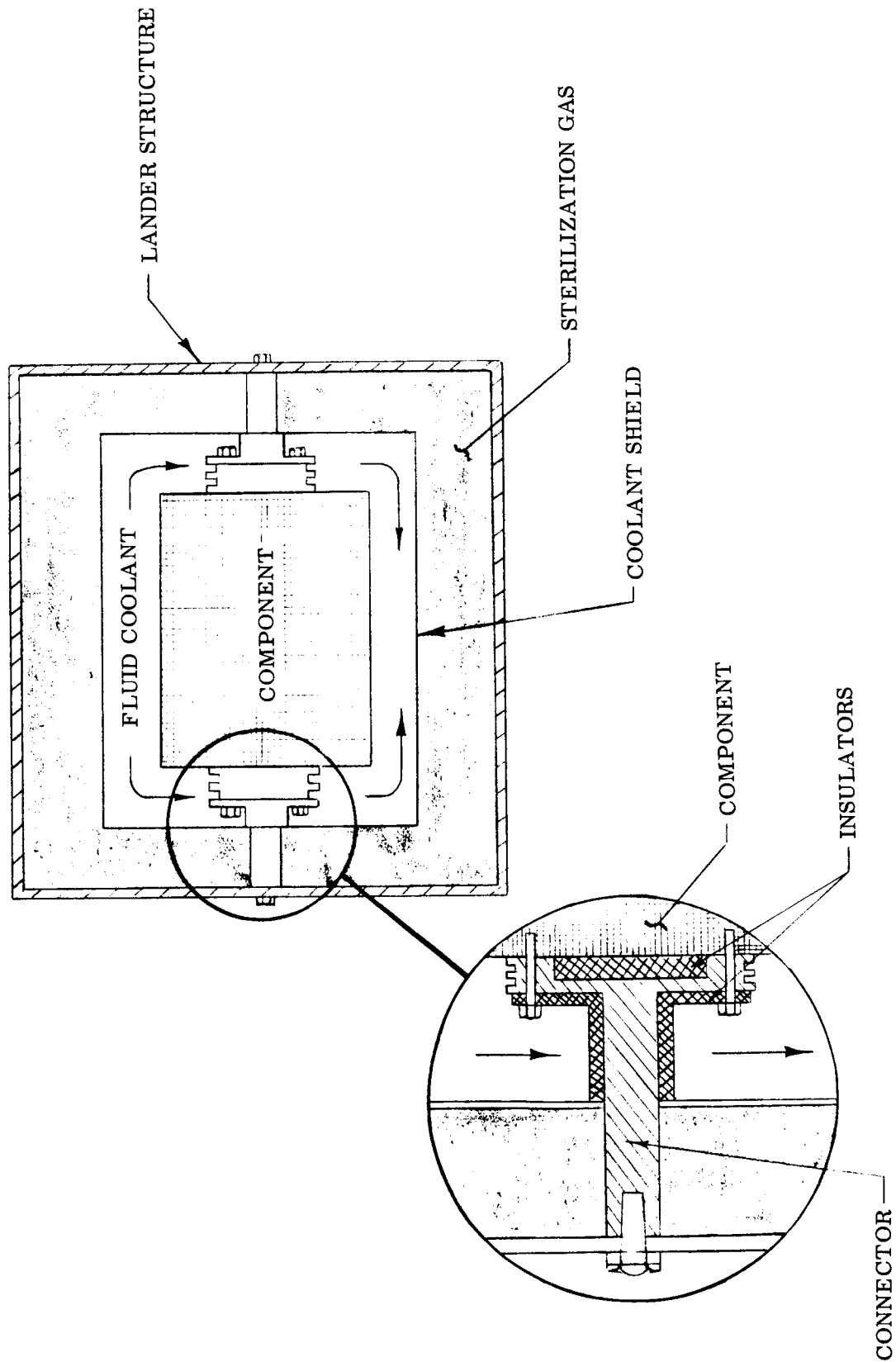


Fig. 5-9 High Thermal Resistance Connection

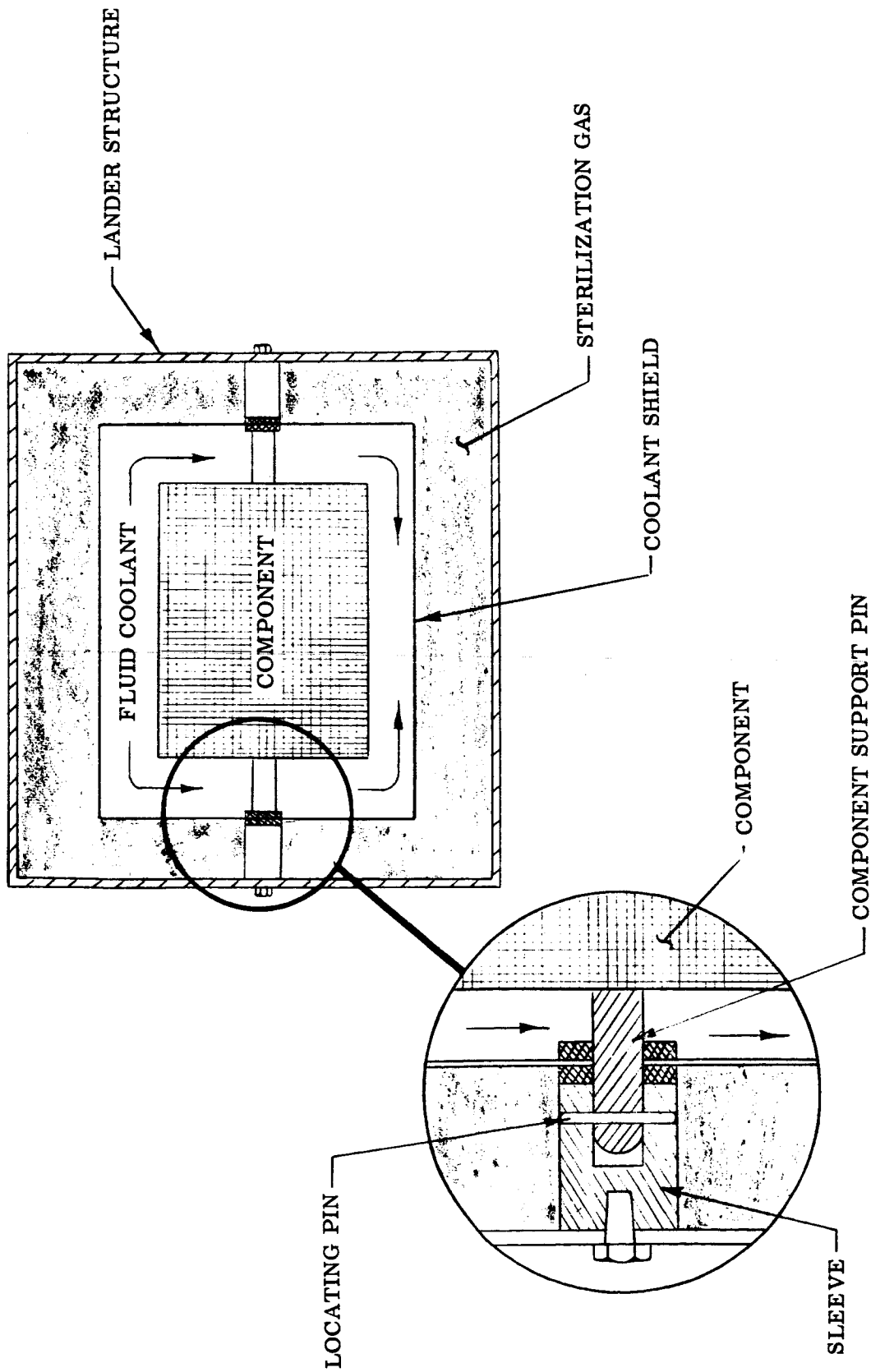


Fig. 5-10 Thermal Expansion Joint Connection

control is required. In this scheme, an inner pin constructed of a material having a low coefficient of thermal expansion is fitted to the component. An outer sleeve, of a material having a high coefficient of thermal expansion, is shrunkfit onto the inner pin, and is attached to the adjacent lander structure. At normal equipment temperature, intimate contact is achieved between the pin and its sleeve, providing an adequate heat transfer path as well as rigid structural support. During terminal heat sterilization the outer sleeve expands away from the inner pin and a large increase in the thermal resistance between the component and lander structure is effected. A small pin transverse to the axis of the sleeve serves to provide structural support during sterilization.

### 5.1.3 Coolant Line Connection and Separation System

The use of fluid circulation cooling for component isolation during terminal sterilization requires that coolant inlet and outlet tubes be plumbed to these components.

Figure 5-11 is a schematic diagram of a coolant supply system which makes use of a single tube for the coolant inlet supply to the lander and a separate tube for coolant outlet.

An alternative to the dual coolant tube system (using separate tubes for coolant inlet and outlet) is the use of two concentric tubes wherein the inner tube is used for coolant inlet and the annular space between the inner and outer tubes is used for coolant outlet.

Connection of tubing to the landed payload occurs in the coolant umbilical connector at the interface between the lander flotation shell and the separation shell adjacent to the impact attenuator. Due to the separation sequence required for this lander concept during planetary entry, coolant tubing separation must be provided at the interfaces shown in Fig. 5-11, namely, external to the impact attenuator and the heat shield. For maximum reliability, coolant tubing separation should be executed at these interfaces shortly after terminal sterilization, with the disconnect or separation devices being operated remotely. Disconnection of the coolant tubing external to the sterilization shield may be performed manually with standard quick-disconnect couplings

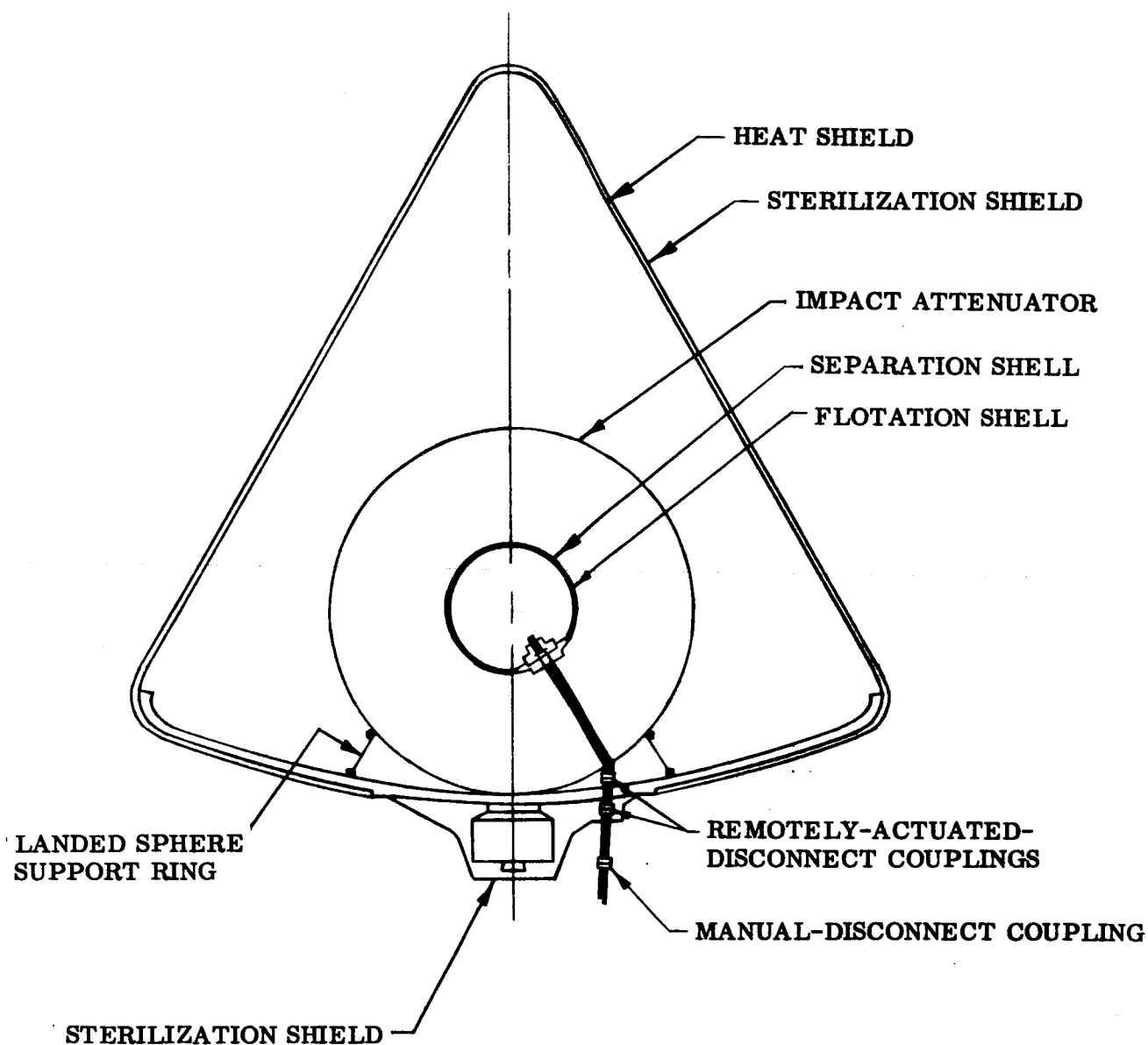


Fig. 5-11 Coolant Supply Line and Coolant Line Disconnect System



providing that the disconnection between the heat shield and the sterilization shield incorporates a biological barrier (in the form of a self-sealing check valve, for example).

Figure 5-11 shows a linear coolant line path between the outer surface of the impact attenuator and the landed payload sphere. In practice, coolant tubes may require routing in a serpentine path or may be required to contain an offset or loop. Such a nonlinear path would insure that the impact attenuation system would be relatively unaffected by the incorporation of a poor energy absorbing material. The use of flexible plastic tubing for coolant supply lines would allow for flexing of the coolant lines during compression of the impact attenuator at planetary impact.

Since the design of components associated with the isolation system is directed toward incurring minimum weight and volume penalties, the most economical form of coolant supply would feature single coolant inlet and outlet tubes which supply coolant to the interior of the landed payload, and which are then manifolded to supply coolant to individual components.

The coolant line umbilical connection and connections at separation interfaces require the use of remotely actuated disconnect couplings. Two types of fluid disconnect couplings have been investigated for the application: explosively actuated and electrically actuated (solenoid) release couplings. The criteria for evaluation of these devices are similar to those for the isolation system in general, and may be summarized by the following list of desirable characteristics:

- Low weight and volume
- High reliability
- Sterilizability
- Capable of operation after exposure to terminal sterilization environment
- Minimum interference with payload system operation

Explosively actuated release couplings generally impose smaller weight and volume penalties than solenoid actuated couplings and may be designed to provide a positive

metal-to-metal seal in the disconnected collant line which would form a highly effective biological barrier. The reliability of explosively actuated release couplings may be enhanced over that of solenoid actuated couplings due to the use of non-metallic seals in the latter. Conversely, the reliability of operations of the explosive charge in explosive devices may be degraded by exposure to the sterilization environment. Manufacturers of these devices claim, however, that they may be designed to operate reliably up to 300° F.

A limited investigation of the availability of suitable explosive and solenoid actuated release couplings has shown that a variety of these devices are commercially available in the small size required for this application; final selection of a specific device would rely, of course, on qualification testing of candidate devices after exposure to the sterilization environment.

## 5.2 INTERACTION BETWEEN THE PAYLOAD AND THERMAL ISOLATION SYSTEMS

The interaction between the isolation system and the lander payload system was evaluated with the use of a thermal model of the combined systems. Thermal properties of each isolated component, its associated coolant shield, and its attachments to the adjacent lander structure were determined and integrated into a thermal analog of the overall lander module.

Basic to the thermal analysis is the assumption that the lander thermal characteristics can be described by a lumped parameter "thermal network." Using the idealized network one considers temperature as a potential and thermal resistance as a branch resistance between two nodes. Once such a network has been established for the major heat flow paths within the lander the network characteristics are programmed into a digital computer to obtain a solution for the network. The node allocations for the network used, and a listing of the data inputs for the terminal sterilization case, are presented in Appendix B.

The following sections describe the results of the computer thermal analyses and the implications of these results for several phases in the life cycle of the lander.

### 5.2.1 Dry Heat Terminal Sterilization

The analysis of the lander thermal response during terminal sterilization was directed toward obtaining the transient temperature response of the lander components during heating and cooling of the lander. This was accomplished by programming the sterilization shield temperature to simulate heating and cooling of the shield when exposed to heating and cooling by forced convection from sterile nitrogen gas within the sterilization chamber. Heat is transferred between the sterilization shield and the internal components by convection, conduction and radiation. In order to simulate the operation of the differential thermal expansion connections between thermally isolated components and their adjacent structure, a variation in conductive thermal resistance between each of the isolated components and the structure to which they are attached was input to the network. This variation was programmed to yield a large increase in the aforementioned thermal resistance with an increase in connector temperature.

The results of the simulation are illustrated in Fig. 5-12 where the temperature response of several lander components is shown as a function of time. The most significant result of the analysis is the length of time required to bring non-isolated lander components up to the sterilization temperature even though an aluminum lander structure was assumed. This is in contrast to the relatively short heating times required for the configuration investigated in Ref. 5-5. Heating times for the referenced configuration were on the order of 6 to 7 hours, whereas the heating times for the configuration analyzed herein are approximately 10 times greater. The heat up time during terminal sterilization can be shortened by activating the thermal control heaters incorporated in this configuration for post-launch temperature control or by installing a small fan inside the heat shield structure.

Another approach would be to heat that portion of the lander exterior to the impact attenuator to an initial temperature higher than the selected sterilization temperature (i. e. , allowing the shield temperature to "overshoot" the desired sterilization temperature for 2 or 3 hours) to facilitate more rapid heating of the landed payload. This

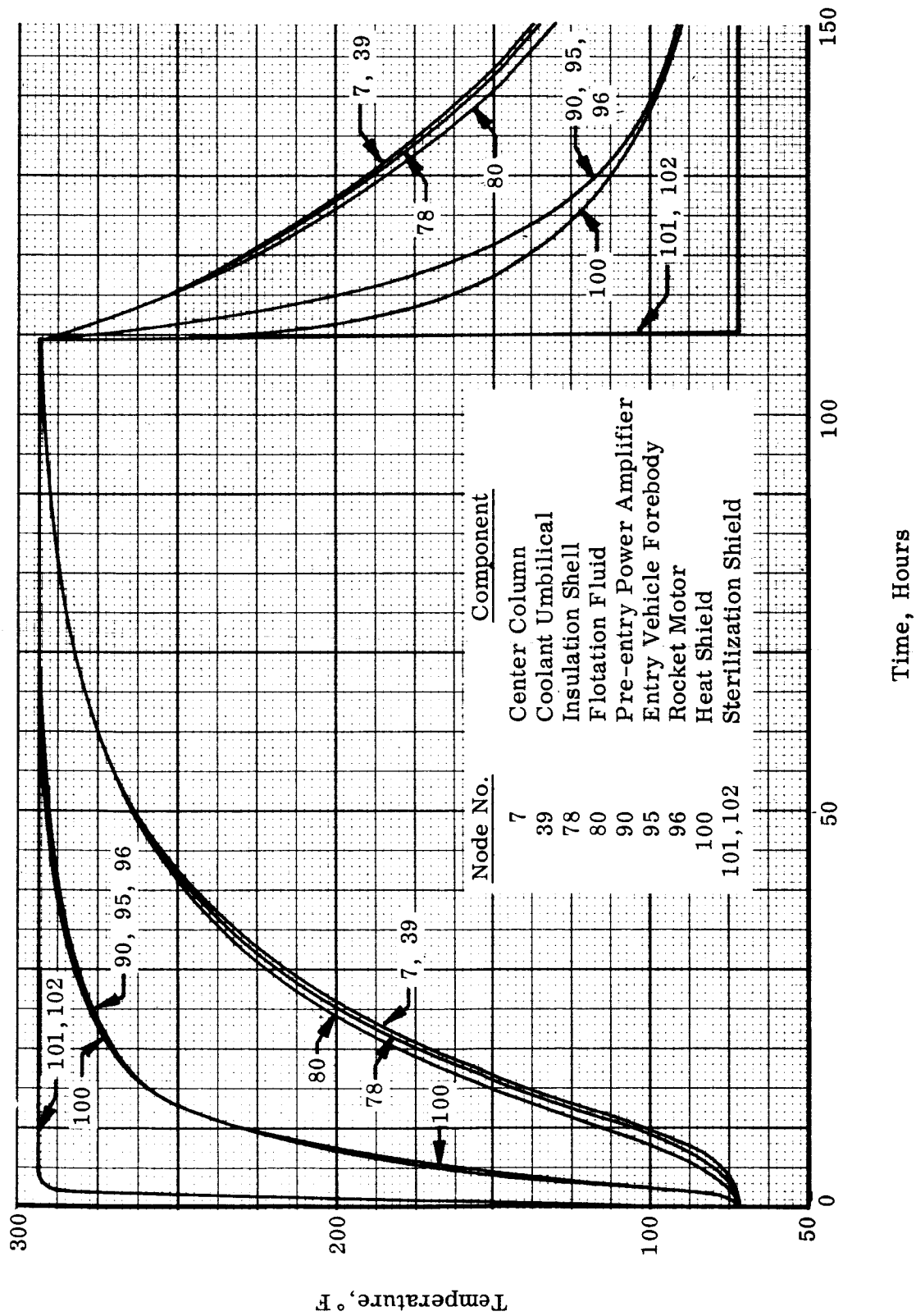


Fig. 5-12 Thermal Response of Lander During Terminal Sterilization

technique was not recommended in the studies reported in Ref. 5-5 for two reasons: (1) because of possible overheating of components which are thermally well-coupled to the sterilization shield, and (2) because of the possibility of local hot spots and severe thermal gradients occurring at or near the interface between the sterilization shield and the payload. The first of these possibilities may be evaluated only after specific components and materials have been selected for a lander design; the second possibility must also be evaluated for each lander design before final material specifications can be made. The foregoing considerations are discussed more fully in subsequent sections.

Structural Requirements During Sterilization. Previous studies (Ref. 5-6) have dealt with structural design considerations for a general lander structure which must undergo a dry-heat terminal sterilization environment. These studies have considered only major structural elements, rather than detailed design of components and instrument mounting, and have shown that proper design for the sterilization environment requires an increase in size and weight for some structural elements. Many of the structural materials which were investigated, if actually exposed to the sterilization environment, would have undergone significant irreversible degradation.

For the present study, materials and structural elements associated with the isolation system were selected with a view toward meeting the demands of the sterilization environment. Thus, as shown in Table 5-1, the preferred material for the coolant container would be a polyimide film ("H"-film). Also, due to the characteristics of the thermal expansion joints between isolated components and the bulkheads to which they are mounted, no stresses are incurred due to differential expansion at these joints. Additional areas which may suffer structural deformation due to thermal stresses or differential thermal expansion are

- The bond between the heat shield and the entry vehicle forebody
- The solid propellant rocket grain
- Component mounting panels, bulkheads and spherical shell structures
- Explosively actuated fasteners, valves and pin-pullers

Differential thermal expansion stresses in the bond between the heat shield and the entry vehicle forebody have been evaluated in Ref. 5-5 for a heat shield in the shape of a conical frustum. Application of a similar analysis to the present configuration shows that an increase in bond thickness of 0.211 inches would be required so that the bond will not fail in tension during terminal sterilization. This increase in bond thickness represents an additional weight penalty of about 40 pounds for a typical bonding material.

Depending on the shape of the solid propellant rocket grain, as well as the manner in which it is restricted within the motor case, severe cracking or even gross fractures of the propellant grain may occur at elevated temperatures. An early study of transient temperature distribution and thermal stresses is presented in Ref. 5-7, wherein a method of evaluating thermal stresses in hollow cylindrical grains is presented. The results of this and similar studies point out the severity of thermal stress problems in solid rocket motors and support the specification of the terminal sterilization environment as a major factor in the design of such motors. In addition to structural effects, solid propellants and explosively actuated devices may be degraded by the high temperature sterilization environment. The adequacy of these components, after exposure to the sterilization environment, must ultimately be evaluated on the basis of qualification testing of individual components.

As pointed out in Ref. 5-5, the thermal distortion of flat panels and bulkheads is normally not a serious problem since these elements, even though they may wrinkle or buckle slightly, will return to nearly their original shape upon cooling. Thus, unless they are used for mounting alignment sensitive components, thermal distortion of these members appears to be a secondary problem. A more severe problem is that associated with the expansion of gases within the sterilization shield during heating and contraction of these gases upon cooling. In order to avoid structural damage to the sterilization shield provisions for venting and replacing the gas must be made in the design of the shield and of the sterilization facility.

Effect of Isolation Devices on Adjacent Structure. During Phase II it was anticipated that some areas of the lander structure adjacent to isolation devices might remain at prohibitively low temperatures during terminal sterilization (so that these areas would not be adequately sterilized). No such areas were detected using the (fairly detailed) network described in Appendix B. The only portions of the lander which did not, in fact, attain the sterilization temperature were the outer surface of the coolant shield and a small portion of the differential thermal expansion connection.

Methods of insuring sterilization of coolant containers were discussed in Section 5.1.1, and, as pointed out in Section 5.4.2, the sterility of the interior of the thermal expansion joint may be insured by pre-sterilization of the component. In the earlier discussion of coolant line connections it was recommended that coolant inlet and outlet lines be routed in a serpentine path through the impact attenuator in order to preserve the function of the crushable attenuator material. The proposed method of routing the coolant supply lines would also allow relief for an increase in length during sterilization.

#### 5.2.2 Launch and Planetary Impact

The design of isolation system components to withstand launch and planetary impact must consider the structural adequacy of the coolant container (and any additional removable isolation devices) and the connections between isolated components and their adjacent structure. The structural integrity of coolant containers, when exposed to launch vibration and launch acceleration forces, is greatly enhanced if a flexible film material is used for these containers. The inherent low density of these materials insures that relatively low body forces would be imposed on the container itself. In addition a flexible container material may be rigidized after completion of terminal sterilization. These rigidization can be accomplished in two ways: (1) by purging the liquid coolant from the container and pressurizing it with an inert, sterile gas or (2), by evacuating the container and causing it to conform to the surface of the component. The first method has the advantage of insuring a positive pressure within the coolant container and thus at the coolant line disconnect devices, insuring against contamination

of the isolated lander components through leaks in the disconnect devices. It would also provide a gaseous environment for temperature sensitive components throughout the life of the lander thus aiding in post-launch thermal control of these components.

The structural adequacy of the differential expansion connections, which have been proposed for isolated component mounting, may be assured by providing a sufficiently large load carrying cross-section in the two parts of the device since at ordinary (room) temperatures its structural behavior would be almost identical to that of a standard bolted connector.

Since shock loading on individual components is a function of the natural frequencies of each component, as well as the impact shock spectrum, an investigation of the structural requirements of the isolation system during planetary impact requires a more detailed specification of lander structure and component characteristics than is presently available. Due to the anticipated high impact levels anticipated for a Mars lander, they should be included as an important part of any detailed design study for specific lander configurations.

### 5.2.3 Earth-Mars Cruise

The equilibrium lander temperatures for the Earth-Mars transfer orbit were computed using the previously described thermal analyzer network. The resultant temperatures are shown in detailed print-outs in Appendix B and are summarized in Table 5-2 for selected lander components. Temperatures shown in this table are steady-state temperatures for the solar-oriented bus near Earth and near Mars. Since, in the cruise phase, the lander is in the shadow of the bus (except for brief periods during injection, acquisition and midcourse maneuvers) there is a steady decrease in lander temperatures as it moves from Earth to Mars. Following the general provisions for thermal control properties of the sterilization shield outlined in Ref. 5-1, it was found that all internal payload package temperatures were maintained within the temperature limits of 40° F to 100° F. These results, obtained with the inclusion of 20 watts of heater power, are identical with those cited in Ref. 5-1, indicating no adverse effect of isolation system components on thermal control during Earth-Mars transfer.



Table 5-2  
LANDER TEMPERATURES DURING CRUISE PHASE

<u>Item</u>	<u>Near Earth <sup>(1)</sup> Temperature, ° F</u>	<u>Near Mars <sup>(2)</sup> Temperature, ° F</u>
Gulliver Experiment Case	39.4	39.2
Thermal Control Fluid	38.9	38.8
Tape Recorder	40.0	40.0
Batteries	39.6	39.5
Insulation Shell	37.7	37.6
Flotation Fluid	33.2	32.8
Impact Attenuator	-16.5	-19.6
Entry Vehicle Forebody	-35.4	-41.8
Heat Shield	-34.6	-41.6
Afterbody	-60.5	-64.8
Sterilization Shield Forebody	-11.7	-38.0
Sterilization Shield Afterbody	-126.0	-129.6
Rocket Motor	-32.6	-41.3
Bus Structure	-11.7	-38.0

---

(1) Heater Power = 10 watts

(2) Heater Power = 20 watts

#### 5.2.4 Post-Landing

As described in Appendix B, a thermal analysis of the lander was performed from impact, just prior to Martian dawn, to local noon. At the end of this 6 hour period (the maximum life of the power system considered) many internal component temperatures had reached the upper package limit of 100° F. The temperatures of the isolated components were, however, well below this upper limit at that time, as shown in Table 5-3. This is attributed to the fact that the lander is being heated from the time of impact until Martian noon and the isolated components tend to be shielded from direct radiative exchange with adjacent lander structure during this period. Thus, during the first six hours after landing, the isolation system appears to aid in lander thermal control. For longer periods of time, gradients in the lander structure become smaller and the internal components achieve a nearly uniform temperature.

Table 5-3

#### LANDER COMPONENT TEMPERATURES SIX HOURS AFTER PLANETARY IMPACT

<u>Isolated Components</u>	<u>Temperature, °F</u>
Gulliver Experiment Case	54.2
Detector Case	49.2
Metabolite	43.8
Tape Recorder	82.8
Battery I	79.9
Battery II	81.2
Battery III	81.2
Battery IV	80.6
<u>Non-Isolated Components</u>	<u>Temperature, °F</u>
Exciter	103.6
Anemometer	103.1
Flotation Shell	123.1
Radome	102.2
Programmer	93.0
Horn Antenna	102.2

### 5.3 INTERACTION WITH STERILIZATION FACILITY AND LANDER ASSEMBLY SEQUENCE

#### 5.3.1 Sterilization Facility Design Requirements

As pointed out earlier, the sterilization environment is a primary consideration for material selection and structural design evaluation. This consideration must be applied to the design of the sterilization chamber as well as the lander and thermal isolation system components. In addition there are several requirements which are imposed on the sterilization chamber and sterilization system design which arise as a result of the implementation of a thermal isolation system.

Earlier studies (Refs. 5-3 and 5-8) have pointed out the need, for example, for special auxiliary sterilization facilities using gaseous ethylene oxide as a sterilant. This requirement arises because terminal sterilization alone is not sufficient to reduce biological contamination to desired levels without the use of intermediate cleaning and sterilizing procedures. In order to maintain the isolation system at a low contaminant count prior to terminal sterilization, auxiliary facilities are required to pre-sterilize both the coolant supply lines and the external surfaces of coolant containers (unless the latter are of the doubled walled type described earlier). In addition to providing a sterile coolant reservoir and pumping system, the following requirements may be identified for the sterilization facility:

- Capability for circulation of hot nitrogen gas
- Capability for heating nitrogen to 300° F with feedback control from sterilization shield and/or lander
- Provision for a source of high pressure sterilant to pressurize sterilization shield and coolant shields during cooldown portion of sterilization cycle
- Provision for feedthroughs for gaseous and liquid flow and electrical feedthroughs for control and heater systems
- Provisions for handling and mounting of payload and actuation of remote disconnect devices

The above considerations have been summarized in the schematic block diagram shown in Fig. 5-13. These requirements are, of course, in addition to the general requirement that the sterilization chamber must function as a high temperature pressure vessel and must itself maintain a low level of contamination.

### 5.3.2 Payload Assembly and Sterilization Processing

Since isolated components may be easily maintained in their presterilized condition (the coolant container acting as a contamination barrier), only normal clean room handling and installation precautions need be observed during assembly of these components into the lander. The major effect of the thermal isolation system on payload processing occurs in conjunction with the terminal sterilization process itself. The effect of the isolation system on the sequence of payload processing prior to and during terminal sterilization has been inferred from data given in Ref. 5-5. Figure 5-14 shows a proposed flow diagram of lander processing, where tasks associated with the implementation of the isolation system have been integrated into the sterilization sequence of operations.

## 5.4 DETAIL DESIGN OF ISOLATION DEVICES

The results of the thermal analyses described earlier have shown that the isolation system components for the lander configuration analyzed will perform satisfactorily throughout the sterilization cycle, during Earth-Mars transfer and Martian post-landing operation.

Some general requirements can be identified which must be satisfied in the design of isolation system components, namely:

- Materials must themselves be able to undergo dry heat sterilization, must be compatible with auxiliary sterilants and cleaning fluids. They must also be able to survive the space environment without prohibitive outgassing, degradation, etc.
- Isolation system components must be designed to support launch acceleration and vibration loads and should withstand normal handling environments.

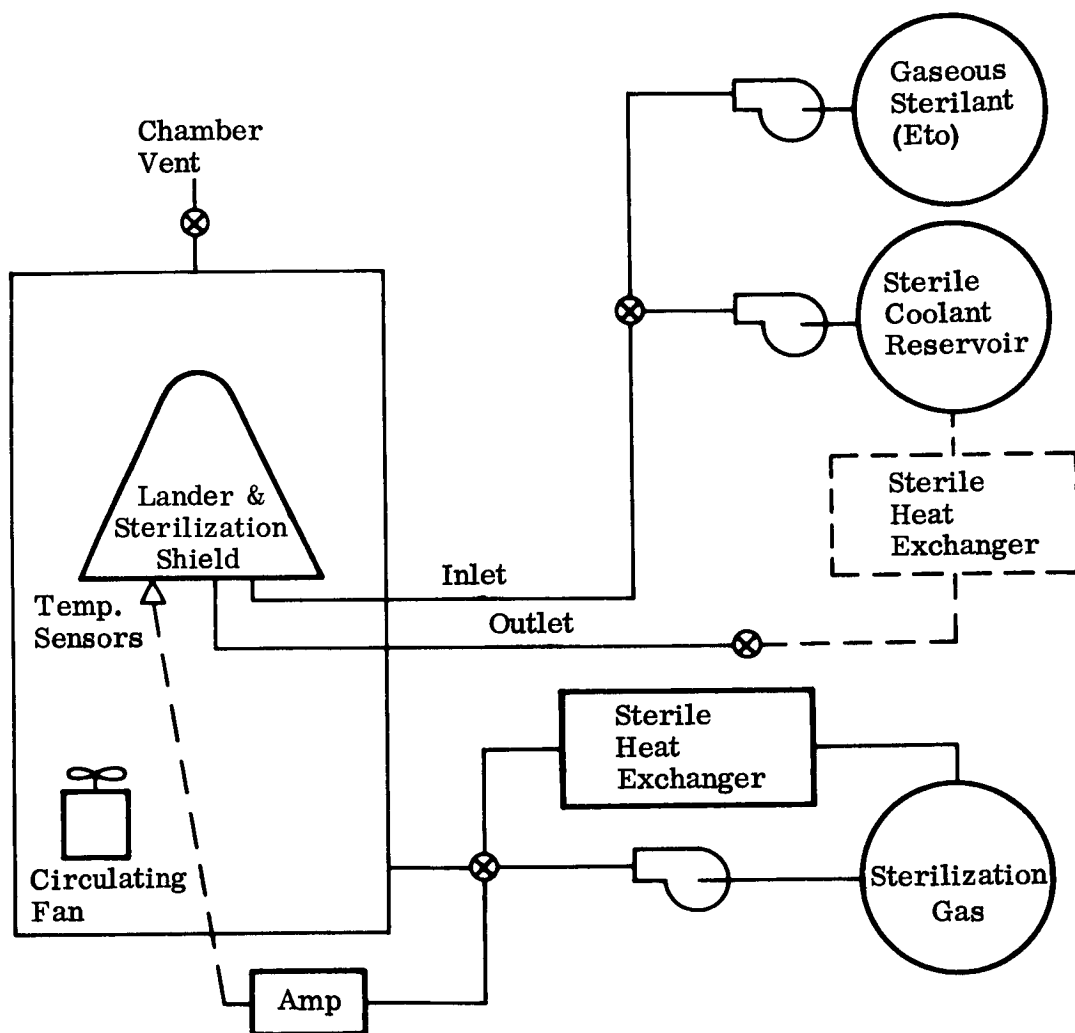


Fig. 5-13 Diagram of Sterilization Facility Functions

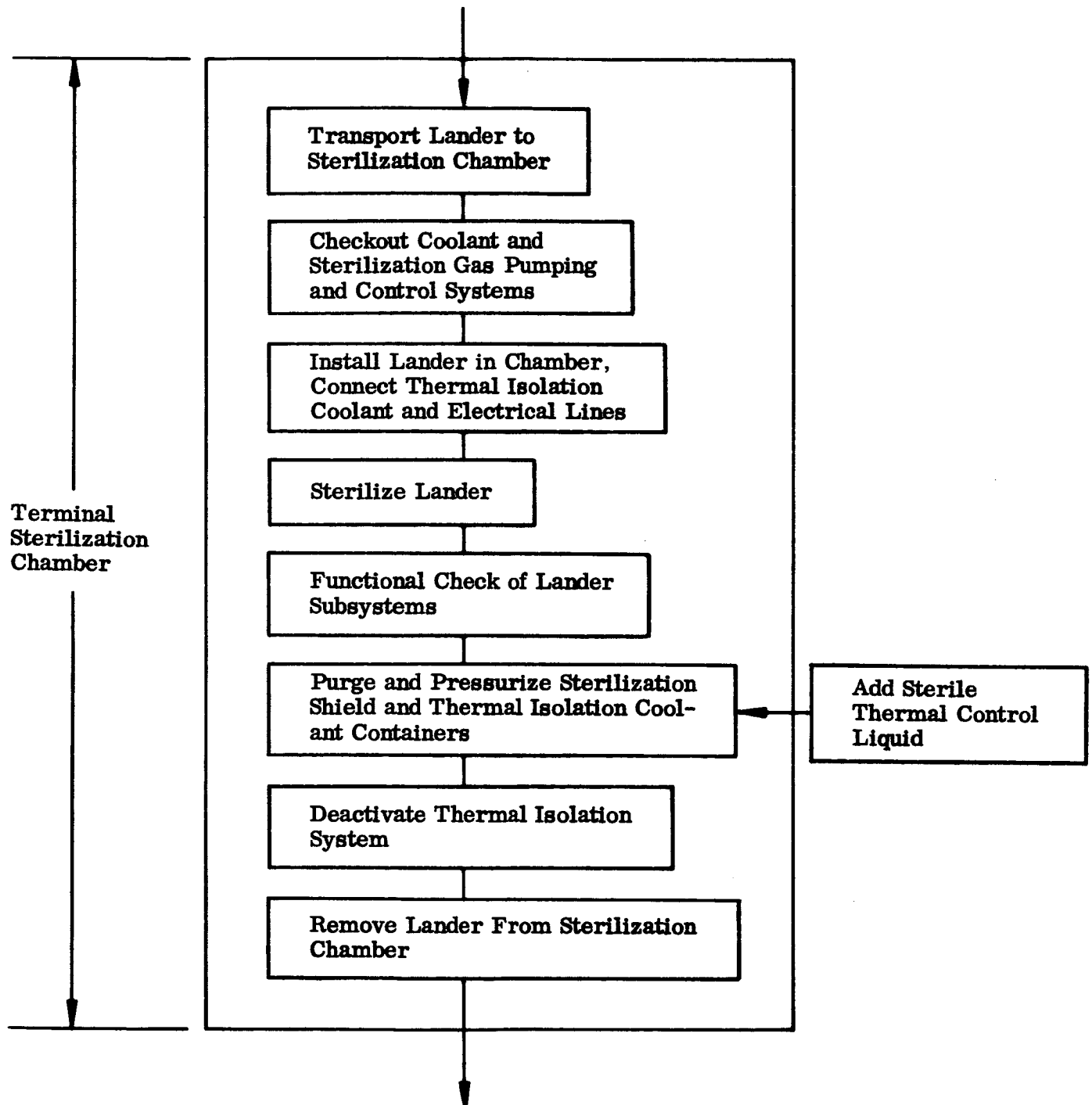


Fig. 5-14 Diagram of Lander Sterilization Process

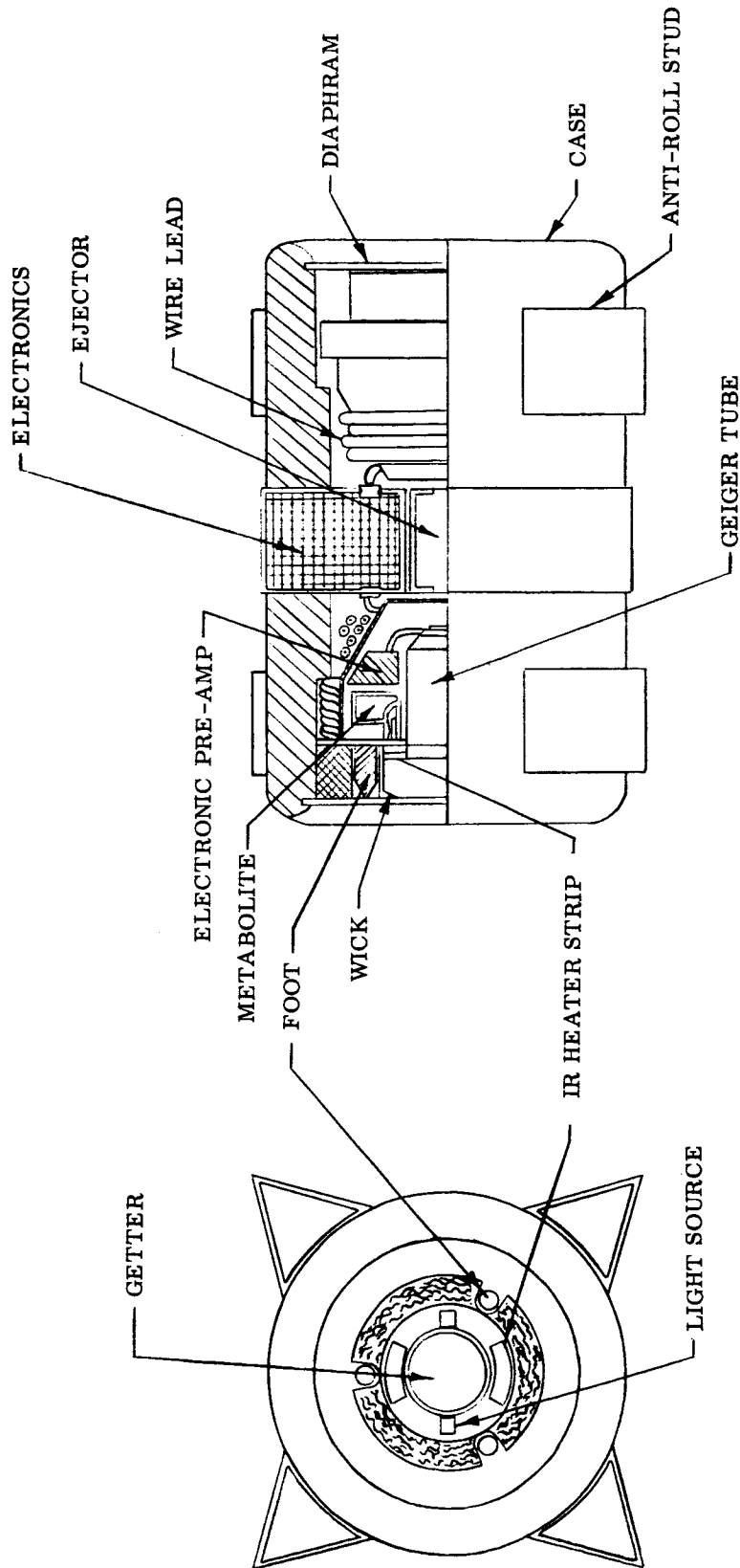
Further, more detailed requirements are imposed on specific components as outlined below.

#### 5.4.1 Coolant Shield and Auxiliary Isolation Mechanisms

Coolant shield construction and surface finish should provide a minimum of radiation coupling to adjacent, non-isolated components so that rapid heating of these components will be assured during terminal sterilization. The double-walled construction of coolant containers, wherein coolant flows in the space adjacent to the component and an inert gas remains in the outer space, will insure high outer surface temperatures on the coolant container and minimize cooling of adjacent components. Coolant shield construction for the isolation of individual life detection components may be achieved by techniques similar to those outlined earlier.

The design of the coolant container for the life detection experiment (Fig. 5-4) was based on completely isolating the "in situ" Gulliver configuration. This configuration, shown in Fig. 5-15, is virtually a self-contained unit and is ejected on the Martian surface after payload landing. In isolating portions of life detection experiments which are contained in the lander during the post-landing phase, such as biological nutrient solutions, the coolant container may again be of the double-walled type so that nutrients are not affected by contact with the isolation coolant. In this case special provisions must be made for the passage of tubing for sample collection through the coolant container. These provisions would take the form of solenoid or explosively actuated valves in the sample collection tube which would be normally closed during sterilization and opened at the end of the sterilization cycle.

In order to examine the isolation of portions of components whose function requires that they be unenclosed by a coolant container subsequent to sterilization, a brief investigation of the design of a removable isolation device was performed. This investigation was directed toward the design of a removable thermoelectric device which would isolate the face plate of a vidicon tube. Similar designs may be constructed for other components where the area to be uncovered is on the order of 10 or 20 square centimeters. The details of the design procedure are given in Appendix B.



(REPRODUCED FROM REFERENCE 5-2)

Fig. 5-15 "In-Situ" Gulliver Design



The first design, shown in Fig. 5-16, features an explosively actuated pin puller. During the sterilization cycle, the thermoelectric device is held against the fluid circulation shield by rigid guide rails. Following the sterilization cycle, the pin puller is remotely actuated moving the thermoelectric device into position free of the vidicon tube face where it is locked into place by virtue of the self-locking action of the pin-puller. The second method, shown in Fig. 5-17, allows the thermoelectric device to rotate by means of a remotely actuated servo-motor or coil spring, into a stowage well where it is locked into place.

#### 5.4.2 Auxiliary Sterilization and Ground Equipment Requirements

The ground equipment requirements associated with the operation of the isolation system have been discussed in Section 5.3; however, provisions must be made for certain auxiliary sterilization equipment to be used during assembly of coolant containers to heat sensitive components. Since only a portion of the thermal expansion joint connection will be exposed to the terminal sterilization environment, and since the coolant container must be sterilized on its interior surface, an auxiliary dry-heat sterilization facility should be provided within the component assembly area. This facility may be a small oven with an attached glove box for handling for isolation system components during assembly to their related lander components.

#### 5.4.3 Weight, Volume and Reliability Penalties for the Thermal Isolation System

As a result of the design details presented earlier, an estimate of weight and volume penalties of thermal isolation system components may be made. A breakdown of these weight penalties is shown in Table 5-4, for the lander configuration considered in Section 5.1. These weight and volume requirements have been summarized for all the isolated components in the lander; no penalties were attributed to thermal expansion connections since they are approximately equivalent in weight and volume to standard connectors. Inclusion of the thermal isolation system in this lander configuration represents an increase from 627.1 pounds to 636.6 pounds in the weight of the separated payload.

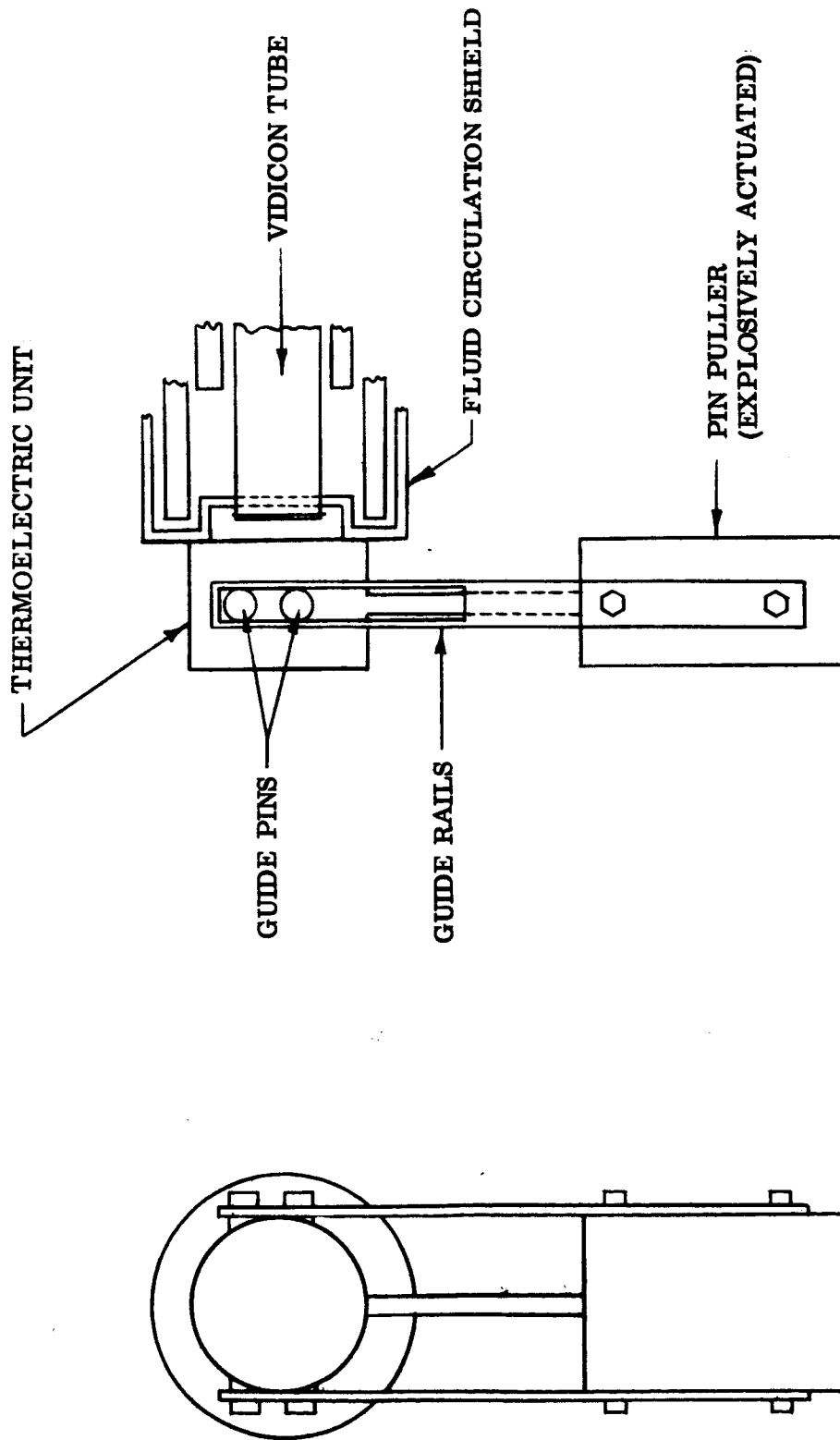


Fig. 5-16 Thermoelectric Isolation Device for Vidicon Tube Face

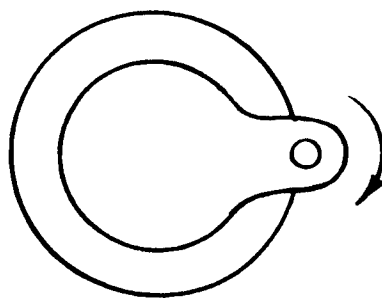
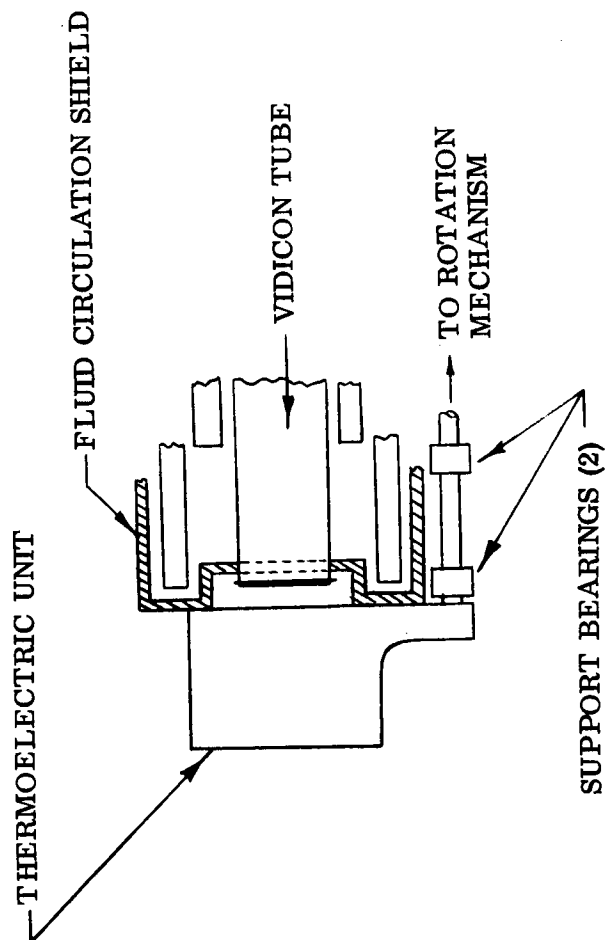


Fig. 5-17 Thermoelectric Isolation Device, Second Concept

Table 5-4

## ISOLATION SYSTEM WEIGHT AND VOLUME REQUIREMENTS\*

<u>Item</u>	<u>Weight, lb</u>	<u>Volume, in<sup>3</sup></u>
Coolant Containers	4.78	63.7
Coolant Tubing	1.92	14.4
Valves and Disconnect Devices	<u>2.80</u>	<u>7.3</u>
TOTALS	9.50	85.4

\*Weight and volume requirements shown are those associated only with isolation equipment which remains with the lander after sterilization.

As indicated by the foregoing analyses, the interactions between the deactivated thermal isolation system are virtually negligible for fluid circulation isolation systems. However, the operation of removable isolation devices may be a basic factor in the reliable operation of certain lander components. The extent of the effect of removable isolation devices on over-all payload reliability is impossible to evaluate without the specification of a specific experiment configuration. It is estimated, therefore, that the only payload reliability degradation which may be incurred by installation of thermal isolation devices would be referenced to operation of a few easily identified components, and the reliable operation of these components and their associated isolation devices may be verified immediately after the terminal sterilization cycle.

## 5.5 CONCLUSIONS - PHASE III

1. Flexible film materials appear to be a logical choice for coolant containers.
2. Flexible film coolant containers used for thermal isolation have no adverse effect on thermal control during the Earth-Mars transfer orbit.
3. The coolant shield can also act as a biological barrier for the isolated component during the last stages of assembly.
4. A small dry-heat sterilization chamber should be available in the component assembly area for presterilizing isolation system component parts.

5. Non-isolated components adjacent to those that are isolated can be made to reach the sterilization temperatures if proper attention is paid to conduction limiting connections and proper surface finishes.
6. Heat transfer by conduction between the isolated component and adjacent structure can be minimized by taking advantage of the differential thermal expansion of different metals when designing the supporting mechanism.
7. Differential thermal expansion between various structural materials results in a weight penalty to provide the strength needed.
8. Auxiliary facilities are required to presterilize the coolant supply lines and the external surfaces of coolant containers.
9. The sterilization facility itself must be maintained at the low level of contamination specified for the assembly rooms.
10. Lengthy heat up times will be required for lander designs where the payload is completely enclosed in a layer of crushable materials.
11. Internal circulation fans within the lander sterilization shield will shorten the time required to reach temperature stabilization.
12. The spacecraft should be vented during sterilization to relieve the pressure buildup. During cool down sterile gas must be added to maintain a positive pressure within the sterilization shield surrounding the spacecraft.
13. Coolant containers should be evacuated after sterilization and then filled with an inert sterile gas.
14. Thermoelectric devices can be used for isolating small areas that must be later exposed for normal operation.
15. The thermal isolation system aids in landed payload thermal control on the Martian surface.
16. Thermal isolation system effects on reliability are confined to a small number of components whose integrity can be established by suitable tests.
17. The weight and volume penalties for the isolation system analyzed are 9.50 pounds and 85.4 cubic inches respectively.

## 5.6 REFERENCES - PHASE III

- 5-1 "Conceptual Design Studies of an Advanced Mariner Spacecraft," AVCO Corporation Report, RAD-TR-64-36, AVCO Corp., Wilmington, Massachusetts, 28 October 1964
- 5-2 "Fourth Annual Progress Report - Radioisotope Biochemical Probe For Extraterrestrial Life," Hazelton Laboratories Inc., Contract NASr-10, March 1965, NASA CR 62911
- 5-3 Air Force Materials Laboratory, "New and Improved Heat Transfer Fluids," MLTDR-64-24, February 1964
- 5-4 "An Analysis of the Extraterrestrial Life Detection Problem," Ames Research Center, NASA SP-75, 1965
- 5-5 "A Study of Design Guidelines for Sterilization of Spacecraft Structures," NASA CR-61005, Contract No. NAS 8-11107, August 1964
- 5-6 Tenny, J. B. and Fried, B., "Thermal Sterilization of Spacecraft Structures," Preprints of Papers presented at the AIAA Unmanned Spacecraft Meeting, Los Angeles, Calif., 1 - 4 March 1965
- 5-7 Geckler, R. D., "Transient Radial Heat Conduction in Hollow Circular Cylinders," Jet Propulsion, v. 25, 1955
- 5-8 Jaffee, L. D., "Sterilizing Unmanned Spacecraft," Astronautics & Aeronautics, August 1963

## Appendix A

## BASIC HEAT TRANSFER AND THERMOELECTRIC EQUATION DEVELOPMENT

This appendix provides a summary of calculations which were omitted from the main body of the report but which provide additional insight into the physical processes involved in the application of various thermal isolation techniques.

## A.1 CONVECTIVE HEAT TRANSFER TO NON-ISOLATED COMPONENTS

In the following section relations are developed for several component shapes to allow the calculation of natural convection heat transfer to the component in question.

## A.1.1 Cubical Volumes

Following a procedure similar to that outlined in Ref. 3-12, we establish a characteristic length  $L^*$  given by

$$\frac{1}{L^*} = \frac{1}{L_{\text{CUBE}}} + \frac{1}{L_{\text{CUBE}}} = \frac{2}{L_{\text{CUBE}}} \quad (\text{A. 1})$$

where  $L_{\text{CUBE}}$  is the length of one side of the cubical volume. The arithmetic mean gas temperature is taken as

$$\bar{T} = \frac{293 + T_j}{2} \quad (\text{A. 2})$$

The product of the Grashof and Prandtl numbers for nitrogen is

$$(\text{Gr Pr})_{\text{CUBE}} = \frac{1}{8} \left[ A (293 - T_j) L^3 \right] \text{Pr} \quad (\text{A. 3})$$

where

$$A = \rho^2 g \beta / \mu^2$$

and  $Pr$  are evaluated for nitrogen at the mean temperature  $T$ . For values of  $T$  between 50°F and 400°F, the Prandtl number is virtually constant,

$$(Pr)_{N_2} = 0.71$$

thus, for a cube whose sides have length  $L_{CUBE}$

$$(Gr Pr)_{CUBE} = 0.0887 A L_{CUBE}^3 (293 - T_j) \quad (A. 4)$$

where the value of  $A$  is plotted as a function of  $T_j$  in Fig. 3-1, as well as the value of the thermal conductivity of nitrogen. Also, for a cube, the Nusselt number is

$$(Nu)_{CUBE} = \frac{\bar{h} L^*}{K_f} = \frac{\bar{h} L_{CUBE}}{2 K_f} \quad (A. 5)$$

So that,

$$\left( Q_{CUBE} \right)_{UNP} = \frac{2 K_f (Nu)_{CUBE}}{L_{CUBE}} \left[ 6 L_{CUBE}^2 (293 - T_{CUBE}) \right]$$

or

$$\left( Q_{CUBE} \right)_{UNP} = 12 K_f L_{CUBE} (Nu)_{CUBE} (293 - T_{CUBE}) \quad (A. 6)$$



where  $(Nu)_{CUBE}$  is determined from the relation

$$(Nu)_{CUBE} = \phi (GrPr)_{CUBE} \quad (A.7)$$

### A.1.2 Spherical Volumes

For spheres,  $L^* = D_{SPHERE}/2$ , where  $D_{SPHERE}$  is the diameter of the sphere; therefore

$$(GrPr)_{SPHERE} = 0.0887 A D_{SPHERE} (293 - T_{SPHERE}) \quad (A.8)$$

$$(Nu)_{SPHERE} = \frac{\bar{h} D_{SPHERE}}{2 K_f} \quad (A.9)$$

and

$$(Q_{SPHERE})_{UNP} = \frac{2 K_f (Nu)_{SPHERE}}{D_{SPHERE}} (\pi D_{SPHERE}^2) (293 - T_{SPHERE})$$

or

$$(Q_{SPHERE})_{UNP} = 2 \pi K_f D_{SPHERE} (Nu)_{SPHERE} (293 - T_{SPHERE}) \quad (A.10)$$

### A.1.3 Long ( $L/D > 5$ ) Horizontal Cylinders

For horizontal cylindrical volumes (length to diameter ratio greater than 5), the characteristic length is the diameter,  $D_{CYL}$ , so that

$$(\text{GrPr})_{\text{CYL}} = 0.71 A D_{\text{CYL}}^3 (293 - T_{\text{CYL}}) \quad (\text{A. 11})$$

$$(\text{Nu})_{\text{CYL}} = \bar{h} D_{\text{CYL}} / K_f \quad (\text{A. 12})$$

and

$$(Q_{\text{UNP}})_{\text{CYL}} = \frac{K_f}{D_{\text{CYL}}} (\text{Nu})_{\text{CYL}} \pi D_{\text{CYL}} L_{\text{CYL}} (293 - T_{\text{CYL}})$$

or

$$(Q_{\text{UNP}})_{\text{CYL}} = \pi K_f L_{\text{CYL}} (\text{Nu})_{\text{CYL}} (293 - T_{\text{CYL}}) \quad (\text{A. 13})$$

#### A. 1.4 Short Horizontal or Vertical Cylinders

The characteristic length is

$$\frac{1}{L^*} = \frac{1}{L_{\text{CYL}}} + \frac{1}{D_{\text{CYL}}}$$

or

$$L_{\text{CYL}}^* = \frac{L_{\text{CYL}}}{\left[ 1 + \left( \frac{L}{D} \right)_{\text{CYL}} \right]} \quad (\text{A. 14})$$

so that

$$(\text{GrPr})_{\text{CYL}} = 0.71 A \frac{L_{\text{CYL}}^3}{\left[ 1 + \left( \frac{L}{D} \right)_{\text{CYL}} \right]^3} (293 - T_{\text{CYL}}) \quad (\text{A. 15})$$

$$(Nu)_{CYL} = \frac{\bar{h} L_{CYL}}{K_f \left[ 1 + \left( \frac{L}{D} \right)_{CYL} \right]} \quad (A.16)$$

and

$$(Q_{UNP})_{CYL} = \frac{K_f \left[ 1 + \left( \frac{L}{D} \right)_{CYL} \right]}{L_{CYL}} (Nu)_{CYL} \left( \pi D_{CYL} L_{CYL} + \frac{\pi}{2} D_{CYL}^2 \right) (293 - T_{CYL}) \quad (A.17)$$

#### A.1.5 Long Vertical Cylinders

For long vertical cylinders, the characteristic length is the height of the cylinder

$$L^* = H_{CYL} \quad (A.18)$$

so that

$$(GrPr)_{CYL} = 0.71 A H_{CYL}^3 (293 - T_{CYL})$$

$$(Nu)_{CYL} = \bar{h} L_{CYL} K_f \quad (A.20)$$

and

$$(Q_{UNP})_{CYL} = \frac{K_f}{H_{CYL}} (Nu)_{CYL} (\pi D_{CYL} H_{CYL}) (293 - T_{CYL})$$

or

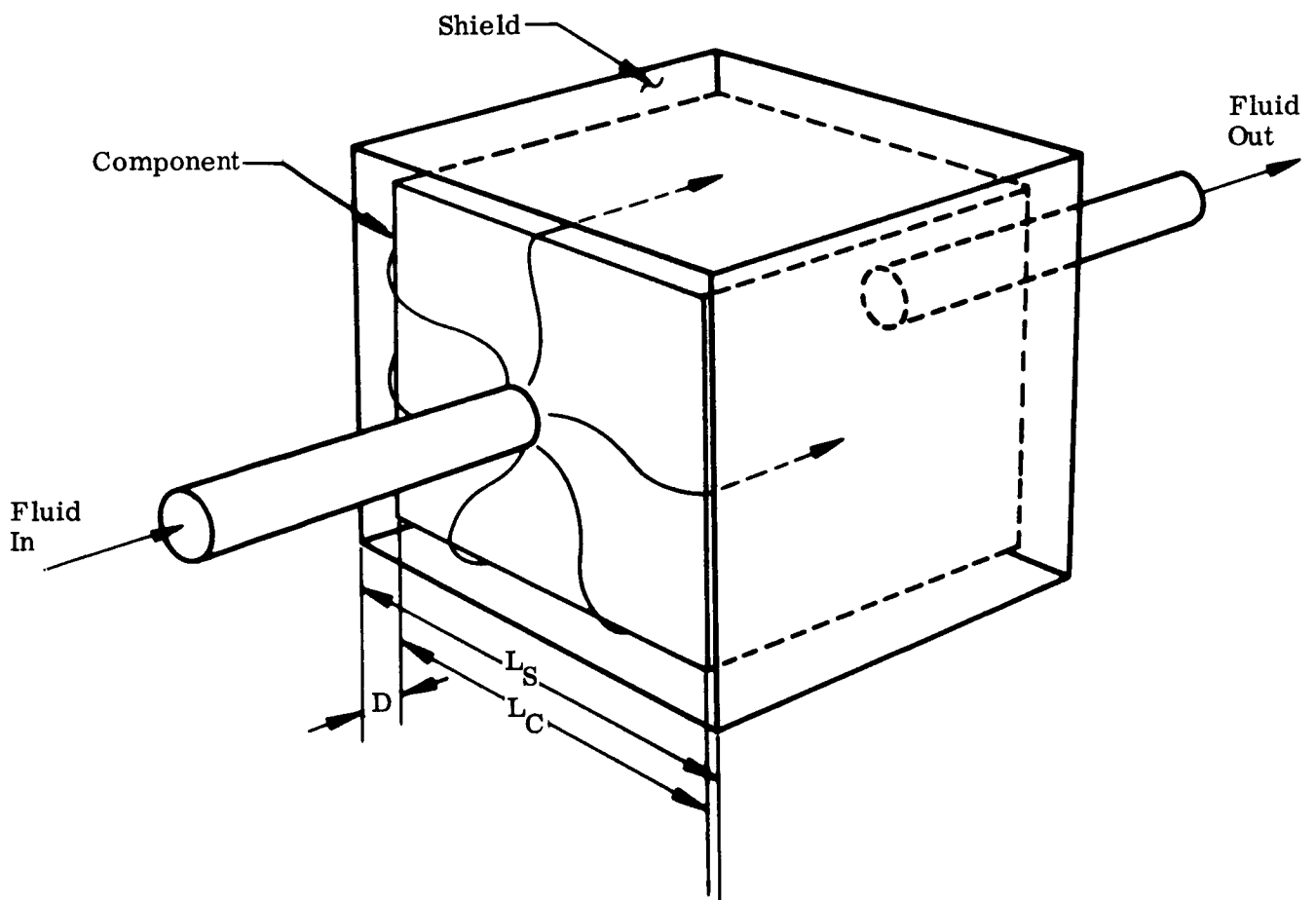
$$\left( Q_{\text{UNP}} \right)_{\text{CYL}} = \pi D_{\text{CYL}} K_f (\text{Nu})_{\text{CYL}} (293 - T_{\text{CYL}}) \quad (\text{A. 21})$$

where  $(\text{Nu})_{\text{CYL}}$  is now evaluated from

$$(\text{Nu})_{\text{CYL}} = 0.555 \left( \text{Gr Pr} \right)_{\text{CYL}}^{1/4} \quad (\text{A. 22})$$

## A.2 SUMMARY OF RELATIONS FOR FLUID CIRCULATION COOLING

Assuming a cubical component enclosed in a cubical shield, as shown below,



an energy balance on the fluid gives

$$Q_f = Q_S = \dot{W}_f C_{P_f} (T_{f_{MAX}} - T_{f_{IN}}) \quad (A. 23)$$

The heat transferred from the hot sterilization gas to the shield is

$$Q_S = \frac{A_S (293 - \bar{T}_S)^{1.25}}{4 (L_S^*)^{0.27}} \quad (A. 24)$$

The heat transferred from the shield to the coolant fluid is

$$Q'_S = h_{S_f} A_S (\bar{T}_S - T_b) \quad (A. 25)$$

where

$$T_b = \frac{T_{f_{IN}} + T_{f_{MAX}}}{2}$$

The Pohlhausen relationship for laminar coolant flow is

$$h_{S_f} = \frac{2}{3} \frac{\dot{W}_f C_{P_f}}{A_a Re^{1/2} Pr^{1/2}} \quad (A. 26)$$

where  $A_a$  is the annular cross-section area for coolant flow.

### A.3 FEASIBILITY ANALYSIS OF THERMOELECTRIC COOLING

The following sections contain a development of the fundamental relations used for the analyses of thermoelectric cooling devices, as well as a specification of the thermoelectric

material properties used in obtaining the numerical results, a sample calculation using the analysis presented in Section 3.7, and an alternate, but complex, method of analysis whose results substantiate those given in Section 3.7.

#### A.3.1 Basic Relations for Analysis of Thermoelectric Cooling

The following analysis is based on a single p-n couple; therefore, the total voltage and heat rates for a given system are found by multiplying the equations given below by the number of p-n couples used.

The voltage required to produce a current flow through the couple is given by

$$V = \alpha \Delta T + IR \quad (A.27)$$

The power (or heat) input to the couple is found by multiplying Eq. (A.27) by the current input:

$$P_{IN} = Q_{IN} = I \alpha \Delta T + I^2 R \quad (A.28)$$

The net heat absorbed by the couple at the cold junction and the heat rejected at the hot junction are given by

$$Q_C = I \alpha T_C - K \Delta T - \frac{1}{2} I^2 R \quad (A.29)$$

and

$$Q_H = I \alpha T_H - K \Delta T + \frac{1}{2} I^2 R \quad (A.30)$$

where

$$\alpha = |\alpha_n| + |\alpha_p| = \text{Seebeck Coefficient, Volts/}^\circ\text{K}$$

$$I = \text{Input Current, Amperes}$$

$$K = K_n + K_p + K_I = K_n \frac{A_n}{L_n} + K_p \frac{A_p}{L_p} + K_I \frac{A_I}{L_I}$$

$$= \text{Thermal Conductance, Watts/}^\circ\text{K}$$

$$R = R_n + R_p = \rho_n \frac{L_n}{A_n} + \rho_p \frac{L_p}{A_p} = \text{Electrical Resistance, Ohms}$$

$$T_C = \text{Cold Junction Temperature, } ^\circ\text{K}$$

$$T_H = \text{Hot Junction Temperature, } ^\circ\text{K}$$

$$\Delta T = T_H - T_C, ^\circ\text{K}$$

In Eq. (A.28),  $I\alpha\Delta T$  represents the power consumed in producing the Seebeck effect  $\alpha\Delta T$ , and  $I^2R$  represents the power consumed in moving the current  $I$  through the resistance  $R$ , (Joule heating). It is assumed that the Joule heat is distributed evenly between the hot and cold junctions. In Eqs. (A.29) and (A.30),  $I\alpha T_C$  and  $I\alpha T_H$  is the Peltier heat absorbed and rejected, respectively,  $K\Delta T$  is the heat leak through the thermoelectric pellets and surrounding insulation from the hot side, and  $1/2 I^2 R$  is the Joule heat at the cold and hot junctions.

If Eq. (A.29) is solved for  $\Delta T$ ,

$$\Delta T = \frac{I\alpha T_C - \frac{1}{2} I^2 R - Q_C}{K} \quad (\text{A.31})$$

it is seen that for a given input current, the maximum value of  $\Delta T$  is obtained for  $Q_C = 0$ .

The current which produces a maximum  $\Delta T$  is termed the optimum current  $I_{OPT}$ , and may be found by setting  $Q_C = 0$ , holding  $T_C$  constant, and differentiating Eq. (A.31) with respect to  $I$ , giving

$$I_{OPT} = \frac{\alpha T_C}{R} \quad (A.32)$$

The maximum temperature differential may then be found by substituting the optimum current into Eq. (A.31) with  $Q_C = 0$ , giving

$$\Delta T_{MAX} = \frac{1}{2} \frac{\alpha^2 T_C^2}{RK} \quad (A.33)$$

$\Delta T_{MAX}$  may also be expressed as

$$\Delta T_{MAX} = \frac{1}{2} Z T_C^2 \quad (A.34)$$

where

$$Z = \frac{\alpha^2}{RK} \quad (A.35)$$

is the thermoelectric figure of merit.

It is seen from Eq. (A.29) that for a given input current, the heat absorbed is a maximum for  $\Delta T = 0$ . The current producing  $(Q_C)_{MAX}$  may be found by setting  $\Delta T = 0$  and differentiating Eq. (A.29) with respect to  $I$ , giving

$$I(Q_C)_{MAX} = I_{OPT} = \frac{\alpha T_C}{R} \quad (A.36)$$



The maximum heat absorbed may then be found by substituting  $I_{OPT}$  into Eq. (A.29) giving

$$(Q_C)_{MAX} = \frac{1}{2} \frac{\alpha^2 T_C^2}{R} - K\Delta T \quad (A.37)$$

Combining Eqs. (A.33) and (A.37), we find that

$$(Q_C)_{MAX} = K (\Delta T_{MAX} - \Delta T) = K\Delta T_{MAX} \left(1 - \frac{\Delta T}{\Delta T_{MAX}}\right) \quad (A.38)$$

Similarly, substituting  $I_{OPT}$  into Eqs. (A.28) and (A.30) and combining with Eq. (A.33) gives

$$(Q_{IN})_{OPT} = 2K \frac{T_H}{T_C} \Delta T_{MAX} \quad (A.39)$$

and

$$(Q_H)_{OPT} = 2K \frac{T_H}{T_C} \Delta T_{MAX} + K (\Delta T_{MAX} - \Delta T) \quad (A.40)$$

### A.3.2 Typical Material Parameters

Thermoelectric material properties used in obtaining numerical results were as follows:

$$|\alpha_n| = |\alpha_p| = 175 \times 10^{-6} \text{ volts/}^\circ\text{K}$$

$$K = K_n = K_p = 0.0115 \text{ watts/cm}^\circ\text{K}$$

$$\rho = \rho_n = \rho_p = 0.001 \text{ ohm-cm}$$

$$K_I = 0.00026 \text{ watts/cm}^\circ\text{K}$$

$$\rho_{\text{Cu}} = 8.94 \text{ gm/cm}^3$$

$$\rho_{\text{I}} = 0.15 \text{ gm/cm}^3$$

$$\rho_{\text{n}} = \rho_{\text{p}} = 8.0 \text{ gm/cm}^3$$

The thermoelectric material figure of merit, based on the value of  $\alpha$ ,  $K$ , and  $\rho$  given above is

$$Z = 2.66 \times 10^{-3} \text{ }^\circ\text{K}^{-1}$$

### A.3.3 Sample Calculations

Assume the following values for a component to be protected:

Geometry: cube

Dimensions: Length per side = 1 ft = 30.48 cm

Characteristic length =  $L_{\text{S}}^* = 0.5 \text{ ft} = 15.24 \text{ cm}$

Volume =  $V_{\text{S}}^* = 1 \text{ ft}^3 = 28,320 \text{ cm}^3$

Weight:  $W_{\text{S}}^* = 100 \text{ lb} = 45360 \text{ gm}$

Upper Temperature Limit:  $T_{\text{C}} = 200^\circ\text{F} = 366^\circ\text{K}$

From Fig. 3-18:  $X_{\text{OPT}} = 31$

From Fig. 3-16 at  $X = 31$ :  $(T_{\text{H}})_{\text{OPT}} = 471^\circ\text{K}$ ,  $(\Delta T_{\text{MAX}})_{\text{OPT}} = 105^\circ\text{K}$

From Fig. 3-19 at  $L_{\text{S}}^* = 15.24 \text{ cm}$ :  $L_{\text{MIN}} = 6.4 \text{ cm}$ ,  $L_{\text{S}} = 21.6 \text{ cm}$

For a cube,  $A_S = 6(L)^2$  and  $V_S = (L)^3$ , where  $L = 2L_S$

$$\text{Total area exposed to sterilization gas} = A_S = 11,200 \text{ cm}^2$$

$$\text{Total volume} = V_S = 81,000 \text{ cm}^3$$

From  $X = 31$  and  $A_S = 11,200 \text{ cm}^2$ ;

$$\text{Thermoelectric pellet area} = 350 \text{ cm}^2$$

$$\text{Insulation area} = 10,850 \text{ cm}^2$$

From  $L = 6.4 \text{ cm}$  and above areas:

$$\text{Thermoelectric pellet volume} = 1,650 \text{ cm}^3$$

$$\text{Insulation volume} = 51,050 \text{ cm}^3$$

From volumes calculated above and densities listed in A.3.2:

$$\text{Thermoelectric pellet weight} = 13,200 \text{ gm} = 29.1 \text{ lb}$$

$$\text{Insulation weight} = 7,670 \text{ gm} = 16.9 \text{ lb}$$

Assuming the amount of copper utilized is approximately equivalent to  $1/32 \text{ in.}$  covering outside surface area:

$$\text{Copper weight} = 7,960 \text{ gm} = 17.6 \text{ lb}$$

$$\text{Total weight of thermoelectric unit} = W_{T/E} = 63.6 \text{ lb}$$

Total weight of system consisting  
of a component surrounded by a

$$\text{thermoelectric unit} = W_S = W_S^* + W_{T/E} = 163.6 \text{ lb}$$

From definitions of weight and volume measures given in Section 3

$$\eta_W = \frac{W_S^*}{W_S} = 0.612 \quad , \quad \eta_V = \frac{V_S^*}{V_S} = 0.350$$

Selecting  $n = 60$  couples = 10 couples per side:

From Eq. 3.46 (Section 3)

$$\text{Cross-sectional area per pellet} = A = 2.92 \text{ cm}^2$$

From Eqs. (A. 27) and (A. 28)

$$\text{Voltage required} = V = 9.90 \text{ volts}$$

$$\text{Operating current} = I_{\text{OPT}} = 29.2 \text{ Amperes}$$

From Eqs. (A. 30) and (A. 33)

Convective heat transfer rate,  $Q_S$ , is equal to the heat rejected

$$Q_H, \text{ i.e., } Q_S = Q_H = 290 \text{ watts}$$

#### A.3.4 Alternative Method of Analysis

The basic equations shown in Section A.3.1 apply to the alternative method of analysis with the exception of the definition of thermal conductance,  $K$ . The thermoelectric heat pump model analyzed in Section A.3.1 consisted of two dissimilar thermoelectric pellets surrounded by insulation, whereas the alternative method is based on a model consisting of thermoelectric pellets alone. The definition of thermal conductance is now given by

$$K = K_n + K_p \tag{A.41}$$

For total thermoelectric pellet and insulation cross-sectional areas and lengths equal, i.e.,  $2nA = nA_I$  and  $L = L_I$ , the heat leak through the insulation from hot to cold side is given by

$$Q_L = 2n \frac{A}{L} K_I (T_H - T_C) \quad (A. 42)$$

which for a constant component temperature, is equal to the heat absorbed at the cold junction,  $Q_C$ . Combining Eqs. (A. 29) and (A. 42) yields:

$$T_H = T_C + C_1 T_C \frac{L}{A} I - C_2 \left( \frac{L}{A} I \right)^2 \quad (A. 43)$$

or

$$I \frac{L}{A} = C_3 T_C \pm \left[ C_4 T_C^2 - C_5 (T_H - T_C) \right]^{1/2} \quad (A. 44)$$

Substituting Eq. (A. 43) in Eq. (A. 30) gives

$$Q_H = \left[ C_6 T_C I + C_7 T_C \frac{L}{A} I^2 + C_8 \frac{L}{A} I^2 - C_9 \left( \frac{L}{A} I \right)^2 \right] n \quad (A. 45)$$

A relationship between the convective heat transfer rate,  $Q_S$ , by the sterilization gas and the heat pump parameters  $L/A I$  is determined by plotting,  $Q_S$ , [Eq. (A. 40)] and  $L/A I$  [Eq. (A. 44)], vs. the hot junction temperature,  $T_H$ , for several values of the cold junction (or component) temperature  $T_C$ .

The intersection of curves for  $Q_S$  and  $Q_H$  plotted vs.  $L/A I$  now represent solutions giving thermoelectric heat pump parameters such that the heat rejected would be removed by natural convection while maintaining a constant component temperature  $T_C$ . The obvious drawback to this analysis is the number of variables ( $I, L, A, A_S$ ,

n and  $T_C$ ) involved. Separate plots of  $Q_S$  and  $Q_H$  versus  $(L/A)$  must be made for the full range of each variable, and possible solutions evaluated. This has been done for a limited number of cases, and a sample plot is shown in Fig. A-1. The intersection of the curves for  $Q_S$  and  $Q_H$  for parameters listed on the figure occurs at a value of  $L = 8.63 \text{ in.} = 21.9 \text{ cm.}$

The method of analysis discussed above preceded that given in Section 3.7 and the choice of simplifying the analysis by assuming equal insulation and thermoelectric pellet areas (equivalent to  $X = 1$  in Section 3.7) was therefore made before the significance of a specific ratio,  $X_{OPT}$  for  $L_{MIN}$  corresponding to a specific component temperature was apparent. This can be illustrated for the operation with  $I = I_{OPT}$  from Fig. 3-18, when the value of  $X$  corresponding to a minimum  $L$  is 31 for a component temperature of  $200^\circ\text{F.}$  In view of this, the large value of  $L$  determined in the example given above is not surprising.

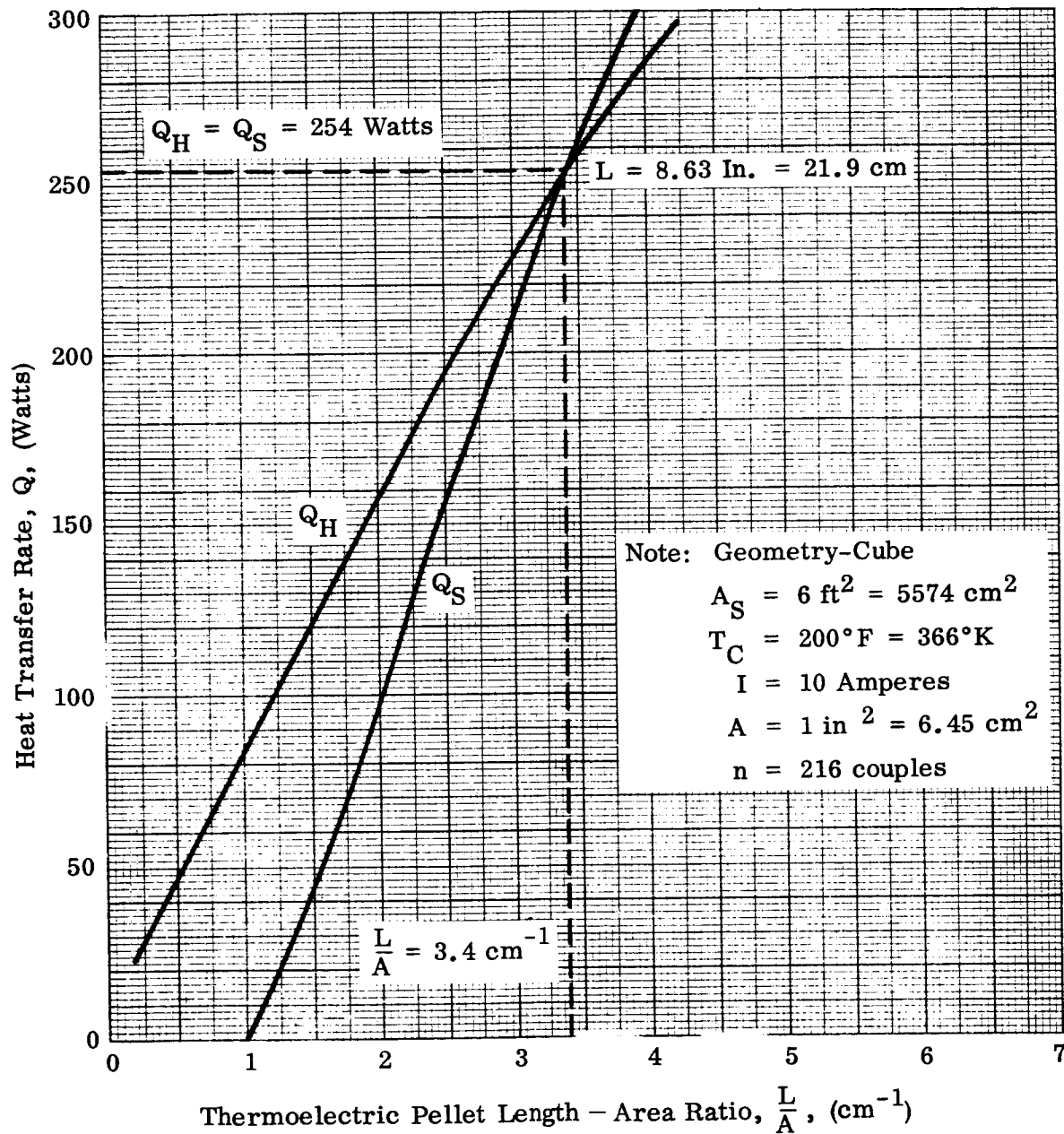


Fig. A-1 Heat Rejected and Convective Heat Transfer Rate vs. Thermoelectric Pellet Length-Area Ratio

## Appendix B

### PHASE III ANALYTICAL OPERATIONS

#### B.1 COMPUTER THERMAL ANALYSES

Using the lander configuration illustrated in Figs. 5-1 through 5-6, a thermal model was constructed for use in the network thermal analyzer program described in Ref. B-1. The node allocation for the network is shown in Table B-1. Nodes 101 and 102 represent the sterilization canister; nodes 103 and 104 represent the bus structure. The nodes representing the bus structure were active only during the cruise phases of the analyses. Separate computer runs were made for the following cases:

- Dry Heat Terminal Sterilization
- Near Earth Cruise Phase
- Near Mars Cruise Phase
- Mars Post-Landing Phase

The analyses of the lander thermal response were directed toward obtaining the transient response of the structure for heatup and cooldown periods during terminal sterilization. This was accomplished by subjecting the nodes representing the sterilization canister to a programmed temperature rise to 293° F. After all non-isolated lander components had reached 293° F (as determined by a test in the computer program) the canister temperature was decreased to 70° F. The significant computer results for the sterilization case were presented in Fig. 5-12. A listing of computer input data for this case is shown in Fig. B-1.

Computer output listings for the near-Earth and near-Mars portions of the cruise phase are shown in Figs. B-2 and B-3. Since these environments produce almost equilibrium temperature distributions in the lander, only results for a single time during each portion of the cruise phase are shown.



Table B-1  
NODE ALLOCATION FOR VOYAGER-LANDER NETWORK

Node No.	Item
1	S-Band Horn Antenna
2	Antenna Mounting Flange
3	Accelerometers
4	Upper Accelerometer Flange
5	Lower Accelerometer Flange
6	Center Column, Upper
7	Center Column, Intermediate
8	Center Column, Lower
9	Forward Ring
10	Bulkhead 1
11	Bulkhead 2
12	Bulkhead 3
13	Bulkhead 4
14	Bulkhead 5
15	Bulkhead 6
16	Bulkhead 7
17	Structural Payload Sphere - Segment J
18	Bulkhead 8
19	Bulkhead 9
20	Bulkhead 10
21	Bulkhead 11
22	Bulkhead 12
23	Bulkhead 13
24	Structural Payload Sphere - Segment H
25	Bulkhead 14
26	Bulkhead 15
27	Bulkhead 16
28	Bulkhead 17

Table B-1 (Continued)

Node No.	Item
29	Bulkhead 18
30	Bulkhead 19
31	Structural Payload Sphere - Segment G
32	Bulkhead 20
33	Bulkhead 21
34	Bulkhead 22
35	Bulkhead 23
36	Umbilical Receptable
37	Radome
38	Structural Payload Sphere - Segment F
39	Coolant Umbilical
40	Anemometer I
41	Anemometer Mortar I
42	Anemometer Mortar Mount I
43	Gas Generator I
44	
45	Anemometer II
46	Anemometer Mortar II
47	Anemometer Mortar Mount II
48	Gas Generator II
49	
50	Thermal Control Fluid <sup>1</sup>
51	Life Detection Experiment Coolant Container
52	Gulliver Experiment Case ("In Situ" Design)
53	Detector Case
54	Pre-Amplifier
55	Metabolite Container

---

<sup>1</sup>Not included in thermal network during terminal sterilization.

Table B-1 (Continued)

Node No.	Item
56	Metabolite
57	Geiger-Muller Tube
58	Exciter
59	Power Amplifier I
60	Power Amplifier II
61	Power Amplifier III
62	Power Amplifier IV
63	Pressure Sensor
64	Data Handling I
65	Tape Recorder
66	Tape Recorder Coolant Container
67	Data Handling II
68	Programmer I
69	Programmer II
70	Battery I
71	Battery II
72	Battery III
73	Battery IV
74	Battery Coolant Container I
75	Battery Coolant Container II
76	Battery Coolant Container III
77	Battery Coolant Container IV
78	Insulation Shell
79	Caging and Electrical Umbilical Mechanism
80	Flotation Fluid
81	Flotation Shell
82	Separation Shell <sup>2</sup>

---

<sup>2</sup>Not included in thermal network for Martian Post-Landed phase.

Table B-1 (Continued)

Node No.	Item
83	Impact Attenuator <sup>2</sup>
84	Descent Antenna <sup>2</sup>
85	Landed Sphere Support Ring <sup>2</sup>
86	Temperature Sensors (3) <sup>2</sup>
87	Pressure Transducer I <sup>2</sup>
88	Pressure Transducers II (2) <sup>2</sup>
89	Pre-Entry Exciter <sup>2</sup>
90	Pre-Entry Power Amplifier <sup>2</sup>
91	Pre-Entry Slot Antenna <sup>2</sup>
92	Multi-Channel Radiometer <sup>2</sup>
93	Descent Power Amplifier <sup>2</sup>
94	Descent Exciter <sup>2</sup>
95	Entry Vehicle Forebody <sup>2</sup>
96	Rocket Motor <sup>2</sup>
97	Main Chute System <sup>2</sup>
98	Drogue Chute System <sup>2</sup>
99	Afterbody <sup>2</sup>
100	Heat Shield <sup>2</sup>
101	Sterilization Shield Afterbody <sup>2</sup>
102	Sterilization Shield Forebody <sup>2</sup>
103	Bus Structure <sup>2, 3</sup>
104	Solar Panels (Backface) <sup>2, 3</sup>

---

<sup>2</sup>Not included in thermal network for Martian Post-Landed phase.

<sup>3</sup>Not included in thermal network during terminal sterilization.

## C10 DRY HEAT TERMINAL STERILIZATION

DEC 1,70.

DEC 120,70.

NSK

## RESISTOR BLOCK

DEC 1,1,2,300.

DEC 2,1,9,2500.

DEC 3,2,9,300.

DEC 4,9,6,1364.

DEC 5,9,17,931.

DEC 6,9,78,10000.

DEC 7,3,4,300.

DEC 8,3,5,300.

DEC 9,4,6,300.

DEC 10,4,7,150.

DEC 11,4,11,700.

DEC 12,5,7,150.

DEC 13,5,8,100.

DEC 14,5,12,600.

DEC 15,6,10,110.

DEC 16,8,30,100.

DEC 17,10,17,1000.

DEC 18,10,24,1000.

DEC 19,11,24,1000.

DEC 20,11,31,1000.

DEC 21,12,38,1000.

DEC 22,12,31,1000.

DEC 23,13,6,250.

DEC 24,13,10,100.

DEC 25,13,17,200.

DEC 26,17,70,100.

DEC 27,18,6,250.

DEC 28,18,10,100.

DEC 29,18,24,200.

DEC 30,18,11,100.

DEC 31,19,6,250.

DEC 32,19,10,100.

DEC 33,19,24,200.

DEC 34,19,11,100.

DEC 35,20,6,200.

DEC 36,20,10,100.

DEC 37,20,24,150.

DEC 38,20,11,100.

DEC 39,21,6,200.

DEC 40,21,10,100.

DEC 41,21,24,200.

DEC 42,21,11,100.

DEC 43,22,6,200.

DEC 44,22,10,100.

DEC 45,22,24,200.

DEC 46,22,11,100.

DEC 47,23,6,200.

DEC 48,23,10,100.

DEC 49,23,24,150.

DEC 50,23,11,100.

DEC 51,24,78,100.

DEC 52,25,7,300.

DEC 53,25,11,100.

DEC 54,25,31,300.

DEC 55,25,12,10.

DEC 56,26,7,300.

DEC 57,26,11,100.

Fig. B-1 Thermal Analyzer Input Data Listing for Terminal Sterilization Analysis

DEC 67,20,31,300.  
 DEC 68,20,12,100.  
 DEC 69,27,7,300.  
 DEC 70,27,11,100.  
 DEC 71,27,31,300.  
 DEC 72,27,12,100.  
 DEC 73,28,7,300.  
 DEC 74,28,11,100.  
 DEC 75,28,31,300.  
 DEC 76,28,12,100.  
 DEC 77,29,7,300.  
 DEC 78,29,11,100.  
 DEC 79,29,31,300.  
 DEC 80,29,12,100.  
 DEC 81,30,7,300.  
 DEC 82,30,11,100.  
 DEC 83,30,31,300.  
 DEC 84,30,12,100.  
 DEC 85,31,78,100.  
 DEC 86,32,8,200.  
 DEC 87,32,36,100.  
 DEC 88,32,38,200.  
 DEC 89,32,12,100.  
 DEC 90,33,8,250.  
 DEC 91,33,12,100.  
 DEC 92,33,38,200.  
 DEC 93,33,36,100.  
 DEC 94,34,8,250.  
 DEC 95,34,12,100.  
 DEC 96,34,38,200.  
 DEC 97,34,36,100.  
 DEC 98,35,8,250.  
 DEC 99,35,12,100.  
 DEC 100,35,38,200.  
 DEC 101,36,38,250.  
 DEC 102,35,36,100.  
 DEC 103,36,79,500.  
 DEC 104,36,39,200.  
 DEC 105,37,1,100.  
 DEC 106,42,10,200.  
 DEC 107,42,17,550.  
 DEC 108,47,10,200.  
 DEC 109,47,17,550.  
 DEC 110,51,52,6.0E+07  
 DEC 111,52,53,20000.  
 DEC 112,53,54,20000.  
 DEC 113,53,55,20000.  
 DEC 114,55,56,20000.  
 DEC 115,55,57,10000.  
 DEC 116,58,21,1000.  
 DEC 117,58,22,1000.  
 DEC 118,58,23,1000.  
 DEC 119,66,05,3.0E+07  
 DEC 120,74,70,3.0E+07  
 DEC 121,75,71,3.0E+07  
 DEC 122,76,72,3.0E+07  
 DEC 123,77,73,3.0E+07  
 DEC 124,78,80,255.  
 DEC 125,79,82,1.0E+06  
 DEC 126,80,81,338.  
 DEC 127,81,82,1500.  
 DEC 128,82,83,800.  
 DEC 129,83,84,100.  
 DEC 130,83,85,200.  
 DEC 131,85,86,50.  
 DEC 132,85,87,100

Fig. B-1 (Cont.)

DEC 158,85,88,50.	
DEC 159,95,89,200.	
DEC 160,95,90,200.	
DEC 161,95,91,50.	
DEC 162,95,92,50.	
DEC 163,85,93,200.	
DEC 164,85,94,200.	
DEC 165,85,95,200.	
DEC 166,95,100,100.	
DEC 167,96,100,50.	
DEC 168,95,99,7200.	
DEC 169,97,99,300.	
DEC 170,98,99,300.	
DEC 171,99,101,100000.	
DEC 172,100,102,10000.	
DEC 179,52,25,50.	
DEC 180,52,26,50.	
DEC 181,65,28,50.	
DEC 182,65,29,50.	
DEC 183,70,33,50.	
DEC 184,70,38,50.	
DEC 185,71,33,50.	
DEC 186,71,34,50.	
DEC 187,72,34,50.	
DEC 188,72,35,50.	
DEC 189,73,32,50.	
DEC 190,73,35,50.	
DEC 400,99,111,7.78E-3	CONVECTION RESISTORS
DEC 401,111,101,.78E-3	CONVECTION RESISTORS
DEC 402,100,112,1.	CONVECTION RESISTORS
DEC 403,112,102,1.	CONVECTION RESISTORS
DEC 404,096,113,1.	CONVECTION RESISTORS
DEC 405,113,102,1.	CONVECTION RESISTORS
DEC 406,83,114,1.0E6	CONVECTION RESISTORS
INC 1,1,0,0.,16	CONVECTION RESISTORS
DEC 500,19,20,600.	
DEC 501,20,21,600.	
DEC 502,22,23,600.	
DEC 503,23,24,600.	
DEC 504,29,30,600.	
DEC 505,30,25,500.	
DEC 506,25,26,1200.	
DEC 507,26,27,600.	
DEC 508,27,28,600.	
NBK	
DEC 1,0.39	
DEC 2,0.	
DEC 3,0.24	
DEC 4,0.	
DEC 5,0.	
DEC 6,.99	
DEC 7,.72	
DEC 8,.8	
DEC 9,0.	
DEC 10,1.5	
DEC 11,2.56	
DEC 12,2.2	
DEC 13,0.	
DEC 17,.5	
DEC 18,.6	
DEC 19,.8	
DEC 20,.84	
DEC 21,.8	
DEC 22,.8	
DEC 23,.84	
DEC 24,1.	

Fig. B-1 (Cont.)

DEC 25,0.	
DEC 26,1.06	
DEC 27,1.24	
DEC 28,.0	
DEC 29,1.08	
DEC 30,.03	
DEC 31,.75	
DEC 32,0.0	
DEC 33,0.	
DEC 34,0.	
DEC 35,0.	
DEC 36,1.2	
DEC 37,0.2	
DEC 38,1.	
DEC 39,0.	
DEC 42,.27	
DEC 47,.27	
DEC 51,0.3	
DEC 56,1.86	
DEC 64,0.10	
DEC 66,0.30	
DEC 68,1.2	
DEC 74,0.24	
DEC 75,0.21	
DEC 76,0.21	
DEC 77,0.22	
DEC 78,0.86	
DEC 79,0.6	
DEC 80,.152	
DEC 81,3.55	
DEC 82,0.9	
DEC 83,31.3	
DEC 84,0.32	
DEC 85,3.34	
DEC 86,.4	
DEC 87,.20	
DEC 88,.4	
DEC 89,0.9	
DEC 90,1.36	
DEC 91,.4	
DEC 92,.4	
DEC 93,1.88	
DEC 94,0.9	
DEC 95,13.75	
DEC 96,5.	
DEC 97,5.	
DEC 98,5.	
DEC 99,3.	
DEC 100,24.2	
DEC 111,0.	
DEC 112,.0	
DEC 113,0.	
DEC 114,0.	
NBK	
DEC 1	STERILIZATION SHIELD TEMP
DEC 6.,70.	
DEC 7056.,288.	
DEC 7200.,290.	
DEC 14400.,293.	
DEC 216000.,293.	
DEC 219600.,70.	
DEC 500000.,70.	
DEC 0.	
DEC -1	
DEC 2	
DEC -200.,50.	

Fig. B-1 (Cont.)



DEC 100.,50.	
DEC 300.,1.0E+06	
DEC 600.,1.0E+06	
DEC 0.	
DEC -2	
DEC 50	
DEC 17850.	
DEC 1.E10	
DEC 0	
INC 0,80	
DEC .0001	
DEC 290.0	50K85
DEC 218000.	50K86
DEC 300.0	50K87
DEC 292.99	50K88
DEC 80.	50K89
DEC 500.	50K90
DEC -50	
DEC 51	
DEC -256.,4462.5	
DEC -81.,5950.	
DEC -16.,8925.	
DEC -9.,10300.	
DEC -4.,14200.	
DEC -1.,17850.	
DEC 0.,1.E10	
DEC 1.,17850.	
DEC 4.,14200.	
DEC 9.,10300.	
DEC 16.,8925.	
DEC 81.,5950.	
DEC 256.,4462.5	
DEC 0	
DEC -51	
NBK	
CFR T42,T40	
CFR T42,T41	
CFR T42,T43	
CFR T42,T44	
CFR T47,T45	
CFR T47,T46	
CFR T47,T48	
CFR T47,T49	
CFR T19,T59	
CFR T18,T60	
CFR T20,T61	
CFR T23,T62	
CFR T30,T67	
CFR T26,T69	
TSW T20,50K85,5	A001
TSW 50K85,T68,468	A002
CFR 50K87,50K85	A003
CFR 50K86,M1	A004
CFR 50K88,T1	A005
INC 0,1,113	A006
CFR 50K89,50K90	A007
SUB T114,T63,50K3	5001
INC 0,1,1,16	5002
LIIN 50K3,R4.6,51	
INC 1,1,0,16	
CFR 50K2,R419	5007
SUB T99,T111,50K40	5100
SUB T111,T101,50K41	5101
SUB T100,T112,? 42	5102
SUB T112,T102,50K43	5103
SUB T90,T113,50K44	5104

Fig. B-1 (Cont.)

SUB T113,T102,50K45 5105  
 LIN 50K40,K400,  
 INC 1,1,0,5  
 LIN M1,T101,1  
 LIN M1,T102,1  
 LIN T25,R179,2  
 LIN T20,R180,2  
 LIN T28,R181,2  
 LIN T29,R182,2  
 LIN T33,R183,2  
 LIN T30,R184,2  
 LIN T33,R185,2  
 LIN T34,R186,2  
 LIN T34,R187,2  
 LIN T35,R188,2  
 LIN T32,R189,2  
 LIN T35,R190,2  
 RAD 201,01,02,0.25E- 5  
 RAD 202,01,37,0.25E- 4  
 RAD 203,01,03,0.25E- 5  
 RAD 204,01,00,0.18E- 3  
 RAD 205,06,17,0.25E- 5  
 RAD 207,42,6,.1E-5  
 RAD 208,0,47,.1E-5  
 RAD 209,00,51,0.25E- 4  
 RAD 210,0,20,.1E-4  
 RAD 211,0,23,.1E-4  
 RAD 212,05,58,0.10E- 4  
 RAD 213,06,24,0.25E- 5  
 RAD 214,07,51,0.10E- 5  
 RAD 215,07,68,0.10E- 4  
 RAD 216,07,04,0.10E- 4  
 RAD 217,07,66,0.10E- 4  
 RAD 218,08,75,0.10E- 4  
 RAD 219,08,76,0.10E- 4  
 RAD 220,08,74,0.10E- 4  
 RAD 221,08,03,0.15E- 5  
 RAD 222,08,39,0.80E- 6  
 RAD 223,42,17,.6E-4  
 RAD 224,42,13,.2E-4  
 RAD 225,42,10,.4E-4  
 RAD 226,47,17,.6E-4  
 RAD 227,47,13,.2E-4  
 RAD 228,47,10,.4E-4  
 RAD 241,51,25,0.25E- 4  
 RAD 242,51,26,0.25E- 4  
 RAD 243,51,17,0.10E- 4  
 RAD 244,53,52,0.25E- 4  
 RAD 245,54,52,0.25E- 5  
 RAD 246,54,55,0.13E- 5  
 RAD 247,54,57,0.12E- 5  
 RAD 248,58,21,0.25E- 4  
 RAD 249,58,22,0.25E- 4  
 RAD 250,58,10,0.25E- 4  
 RAD 251,58,24,0.25E- 4  
 RAD 252,58,11,0.25E- 4  
 RAD 254,20,19,.2E-4  
 RAD 255,24,19,.2E-4  
 RAD 256,10,19,.2E-4  
 RAD 257,11,19,.2E-4  
 RAD 259,21,20,.2E-4  
 RAD 260,24,20,.2E-4  
 RAD 261,10,20,.2E-4  
 RAD 262,11,10,.2E-4  
 RAD 263,22,23,.2E-4  
 RAD 264,24,23,.2E-4

Fig. B-1 (Cont.)

RAD 265,10,23,.2E-4  
 RAD 266,11,23,.2E-4  
 RAD 269,23,18,.2E-4  
 RAD 270,24,18,.2E-4  
 RAD 271,10,18,.2E-4  
 RAD 272,11,18,.2E-4  
 RAD 273,25,24,.1E-4  
 RAD 275,30,29,.2E-4  
 RAD 275,31,29,.2E-4  
 RAD 277,11,29,.2E-4  
 RAD 278,12,29,.2E-4  
 RAD 279,00,20,.20E- 4  
 RAD 280,06,29,.20E- 4  
 RAD 281,00,31,.0.20E- 4  
 RAD 282,06,11,.0.20E- 4  
 RAD 283,00,12,.0.20E- 4  
 RAD 284,65,06,.0.25E- 3  
 RAD 285,51,52,.0.13E- 3  
 RAD 286,50,25,.0.65E- 3  
 RAD 287,28,00,.2E-3  
 RAD 288,31,30,.10E-4  
 RAD 289,11,30,.13E-4  
 RAD 290,12,30,.13E-4  
 RAD 292,20,27,.10E-4  
 RAD 293,31,27,.15E-4  
 RAD 294,11,27,.2E-4  
 RAD 295,12,27,.2E-4  
 RAD 297,27,26,.065E-4  
 RAD 298,26,31,.0.10E- 4  
 RAD 299,11,26,.135E-4  
 RAD 300,12,26,.135E-4  
 RAD 301,70,74,.0.20E- 3  
 RAD 302,71,75,.0.15E- 3  
 RAD 303,72,76,.0.15E- 3  
 RAD 304,73,77,.0.15E- 3  
 RAD 305,74,32,.0.20E- 4  
 RAD 306,74,33,.0.20E- 4  
 RAD 307,74,38,.0.10E- 3  
 RAD 308,74,12,.0.10E- 3  
 RAD 309,74,36,.0.25E- 3  
 RAD 310,75,33,.0.20E- 4  
 RAD 311,75,34,.0.20E- 4  
 RAD 312,75,38,.0.10E- 3  
 RAD 313,75,12,.0.10E- 3  
 RAD 314,75,36,.0.25E- 3  
 RAD 315,76,34,.0.20E- 4  
 RAD 316,76,35,.0.20E- 4  
 RAD 317,76,38,.0.10E- 3  
 RAD 318,76,12,.0.10E- 3  
 RAD 319,76,36,.0.25E- 3  
 RAD 320,77,32,.0.20E- 4  
 RAD 321,77,35,.0.20E- 4  
 RAD 322,77,38,.0.10E- 3  
 RAD 323,77,12,.0.10E- 3  
 RAD 324,77,36,.0.25E- 3  
 RAD 325,38,79,.0.90E- 3  
 RAD 326,37,78,.0.50E- 4  
 RAD 327,17,78,.0.31E- 3  
 RAD 328,24,70,.0.31E- 3  
 RAD 329,31,78,.0.31E- 3  
 RAD 330,36,70,.0.31E- 3  
 RAD 331,78,81,.0.13E- 2  
 RAD 332,81,82,.0.14E- 2  
 RAD 333,84,83,.0.1E- 3  
 RAD 334,85,85,.0.11E- 2  
 RAD 335,85,99,.0.11E- 2

Fig. B-1 (Cont.)

```

RAD 336,85,99,0.20E- 2
RAD 337,85,85,0.10E- 4
RAD 338,85,95,0.10E- 4
RAD 339,84,99,0.10E- 3
RAD 340,87,85,0.10E- 4
RAD 341,87,85,0.10E- 4
RAD 342,88,85,0.20E- 4
RAD 343,88,85,0.20E- 4
RAD 344,89,95,0.70E- 4
RAD 345,89,83,0.70E- 4
RAD 346,90,95,0.80E- 4
RAD 347,90,83,0.80E- 4
RAD 348,93,85,0.90E- 4
RAD 349,93,95,0.90E- 4
RAD 350,94,85,0.70E- 4
RAD 351,94,95,0.70E- 4
RAD 352,95,85,1.075E-4
RAD 353,95,99,1.075E-4
RAD 354,100,90,2.77E-4
RAD 355,102,90,2.77E-4
RAD 356,97,99,0.40E- 3
RAD 357,97,95,0.40E- 3
RAD 358,97,83,0.40E- 3
RAD 359,98,99,0.30E- 3
RAD 360,98,95,0.35E- 3
RAD 362,100,102,3.61E-3
RAD 363,99,101,2.21E-3
NEK
DEC T1,T3,T7,T8,T9
DEC T17,T24,T31,T36
DEC T37,T38,T39,T40
DEC T43,T45,T48,T50
DEC T51,T52,T53,T54,T55,T56,T57
INC 7,7,7,7,7,7,6
DEC T100,T101,T102,T103,T104
DEC T111
INC 1,9
NEK
END OUTPUT BLOCK
DEC 0.,0.,500000.,1000.,0.
DEC 0.,80,100.,0.,1.
NEK

```

3750 WORDS OF STORAGE HAVE BEEN USED.

Fig. B-1 (Cont.)

## MARS CRUISE PHASE NEAR EARTH

TIME	RCMIN	MINND	RCMAX	MAXND	DTHEFA	NCYC
0.	0.50000E+01	0	0.	0	0.	2
0.39157E+02	T1	0.39007E+02	T6	0.39275E+02	T7	0.39511E+02
0.39175E+02	T9	0.38560E+02	T17	0.38750E+02	T24	0.38767E+02
0.39545E+02	T36	0.39167E+02	T37	0.39695E+02	T38	0.39500E+02
0.39999E+02	T40	0.39999E+02	T43	0.39999E+02	T45	0.39999E+02
0.39874E+02	T50	0.39209E+02	T51	0.39367E+02	T52	0.39478E+02
0.39489E+02	T54	0.39519E+02	T55	0.39533E+02	T56	0.39492E+02
0.39037E+02	T58	0.39999E+02	T59	0.39999E+02	T60	0.39999E+02
0.39599E+02	T62	0.39999E+02	T63	0.39999E+02	T64	0.39999E+02
0.39208E+02	T66	0.39999E+02	T67	0.39999E+02	T68	0.39999E+02
0.39575E+02	T70	0.39509E+02	T71	0.39569E+02	T72	0.39570E+02
0.39580E+02	T74	0.39554E+02	T75	0.39554E+02	T76	0.39555E+02
0.37740E+02	T78	0.39545E+02	T79	0.39545E+02	T80	0.26724E+02
0.45299E+01	T82	-0.16477E+02	T83	-0.34184E+02	T86	-0.34183E+02
-0.16042E+02	T84	-0.34263E+02	T85	-0.35150E+02	T90	-0.35316E+02
-0.34163E+02	T88	-0.35170E+02	T89	-0.34192E+02	T94	-0.35350E+02
-0.35510E+02	T92	-0.34194E+02	T93	-0.59265E+02	T98	-0.60490E+02
-0.32631E+02	T96	-0.56844E+02	T97	-0.11708E+02	T102	-0.11696E+02
-0.34010E+02	T100	-0.12598E+03	T101	-0.12598E+03	T102	-0.11696E+02
-0.12678E+02	T104	-0.12598E+03	T101	-0.12598E+03	T102	-0.11696E+02
0.50000E+01	0.92307E+00	5	0.20851E+05	1	0.26153E+00	5
0.39154E+02	T1	0.38996E+02	T6	0.39263E+02	T7	0.39496E+02
0.39793E+02	T9	0.38568E+02	T17	0.38732E+02	T24	0.38753E+02
0.39523E+02	T36	0.39163E+02	T37	0.39686E+02	T38	0.39551E+02
0.39999E+02	T40	0.39999E+02	T43	0.39999E+02	T45	0.39999E+02
0.38874E+02	T50	0.39209E+02	T51	0.39367E+02	T52	0.39477E+02
0.39489E+02	T54	0.39519E+02	T55	0.39533E+02	T56	0.39492E+02
0.39037E+02	T58	0.39999E+02	T59	0.39999E+02	T60	0.39999E+02
0.39599E+02	T62	0.39999E+02	T63	0.39999E+02	T64	0.39999E+02
0.39208E+02	T66	0.39999E+02	T67	0.39999E+02	T68	0.39999E+02
0.39575E+02	T70	0.39509E+02	T71	0.39569E+02	T72	0.39570E+02
0.39580E+02	T74	0.39554E+02	T75	0.39554E+02	T76	0.39555E+02
0.37736E+02	T78	0.39544E+02	T79	0.39544E+02	T80	0.26724E+02
0.45292E+01	T82	-0.16477E+02	T83	-0.34224E+02	T86	-0.34241E+02
-0.16051E+02	T84	-0.34209E+02	T85	-0.35150E+02	T90	-0.35319E+02
-0.34157E+02	T88	-0.35171E+02	T89	-0.34194E+02	T94	-0.35350E+02
-0.35518E+02	T92	-0.34195E+02	T93	-0.59265E+02	T98	-0.60490E+02
-0.32631E+02	T96	-0.56844E+02	T97	-0.11708E+02	T102	-0.11696E+02
-0.34010E+02	T100	-0.12598E+03	T101	-0.12598E+03	T102	-0.11696E+02
-0.12678E+02	T104	-0.12598E+03	T101	-0.12598E+03	T102	-0.11696E+02
0.10000E+02	0.92307E+00	5	0.20851E+05	1	0.26153E+00	5
TIME	RCMIN	MINND	RCMAX	MAXND	DTHEFA	NCYC
0.	0.92307E+00	5	0.20851E+05	1	0.26153E+00	5

Fig. B-2 Thermal Analyzer Output

## MARKS CRUISE PHASE NEAR CAPSULE RELEASE

TIME	RCMIN	MINND	RCMAX	MAXND	DTHETA	NCYC
0.0	0.50000E+01	0	0.	0	0.	2
0.38993E+02	T1	0.38993E+02	T0	0.39209E+02	T7	0.39451E+02
0.39093E+02	T9	0.38993E+02	T17	0.38662E+02	T24	0.38677E+02
0.39189E+02	T30	0.38993E+02	T37	0.39642E+02	T38	0.39499E+02
0.39289E+02	T40	0.39189E+02	T43	0.39999E+02	T45	0.39999E+02
0.39389E+02	T50	0.39189E+02	T51	0.39208E+02	T52	0.39282E+02
0.39489E+02	T54	0.39389E+02	T55	0.39319E+02	T56	0.39291E+02
0.39589E+02	T59	0.39489E+02	T59	0.39999E+02	T60	0.39999E+02
0.39689E+02	T62	0.39589E+02	T63	0.39999E+02	T64	0.39999E+02
0.39789E+02	T66	0.39689E+02	T67	0.39999E+02	T68	0.39999E+02
0.39889E+02	T70	0.39789E+02	T71	0.39516E+02	T72	0.39518E+02
0.39989E+02	T74	0.39889E+02	T75	0.39506E+02	T76	0.39508E+02
0.40089E+02	T78	0.39989E+02	T79	0.39840E+02	T80	0.395970E+02
0.40189E+02	T82	0.40089E+02	T83			
0.40289E+02	T84	0.40189E+02	T85	0.38633E+02	T86	0.38632E+02
0.40389E+02	T88	0.40289E+02	T89	0.41505E+02	T90	0.41694E+02
0.40489E+02	T92	0.40389E+02	T93	0.38654E+02	T94	0.41771E+02
0.40589E+02	T96	0.40489E+02	T97	0.03715E+02	T98	0.64816E+02
0.40689E+02	T100	0.40589E+02	T101	0.38010E+02	T102	0.37969E+02
0.40789E+02	T104					

TIME	RCMIN	MINND	RCMAX	MAXND	DTHETA	NCYC
0.50000E+01	0.92307E+00	5	0.20853E+05	1	0.26153E+00	5
0.38993E+02	T1	0.38993E+02	T6	0.39201E+02	T7	0.39442E+02
0.39093E+02	T9	0.38993E+02	T17	0.38650E+02	T24	0.38668E+02
0.39189E+02	T30	0.39093E+02	T37	0.39656E+02	T38	0.39499E+02
0.39289E+02	T40	0.39189E+02	T43	0.39999E+02	T45	0.39999E+02
0.39389E+02	T50	0.39289E+02	T51	0.39208E+02	T52	0.39281E+02
0.39489E+02	T54	0.39389E+02	T55	0.39319E+02	T56	0.39291E+02
0.39589E+02	T59	0.39489E+02	T59	0.39999E+02	T60	0.39999E+02
0.39689E+02	T62	0.39589E+02	T63	0.39999E+02	T64	0.39999E+02
0.39789E+02	T66	0.39689E+02	T67	0.39999E+02	T68	0.39999E+02
0.39889E+02	T70	0.39789E+02	T71	0.39516E+02	T72	0.39518E+02
0.39989E+02	T74	0.39889E+02	T75	0.39506E+02	T76	0.39508E+02
0.40089E+02	T78	0.39989E+02	T79	0.39840E+02	T80	0.395970E+02
0.40189E+02	T82	0.40089E+02	T83			
0.40289E+02	T84	0.40189E+02	T85	0.38674E+02	T86	0.38690E+02
0.40389E+02	T88	0.40289E+02	T89	0.41505E+02	T90	0.41701E+02
0.40489E+02	T92	0.40389E+02	T93	0.38654E+02	T94	0.41771E+02
0.40589E+02	T96	0.40489E+02	T97	0.03715E+02	T98	0.64816E+02
0.40689E+02	T100	0.40589E+02	T101	0.38010E+02	T102	0.37969E+02
0.40789E+02	T104					

TIME	RCMIN	MINND	RCMAX	MAXND	DTHETA	NCYC
0.10000E+02	0.92307E+00	5	0.20853E+05	1	0.26153E+00	5

Fig. B-3 Thermal Analyzer Output

A listing of lander temperatures during the first 6 hours after planetary impact, from Martian dawn to local noon, is included as Fig. B-4. In addition to solar radiation and conduction from the Martian surface, the effects of convection from an atmosphere having an eleven (11) millibar surface pressure have been included. Basic input data are shown in Figs. B-5 and B-6.

#### B.1.1 References

Bible, A. E., et al., "Thermal Analyzer Control System for IBM 709-7090-7094 Computer-Engineering Utilization Manual," LMSC 3-56-65-8, Lockheed Missiles & Space Co., Sunnyvale, Calif., 1 September 1965.

### B.2 REMOVABLE THERMOELECTRIC HEAT SHIELD

The following sections relate the mathematical development of a method for achieving thermal isolation of small areas using thermoelectric cooling devices. A thermoelectric device can be used where the protected component function necessitates removing a portion of the thermal isolation hardware following terminal sterilization.

This analysis utilizes the basic relations presented in Appendix A and is similar to the general analysis of Section 3.7. The primary difference is concerned with the heat rejection surface configuration.

Application of this method in thermally isolating a vidicon tube face is discussed in Section 5.4.2.

#### B.2.1 Heat Rejection Requirements

It has been assumed that the heat rejection surface for the small areas under consideration are planes oriented vertically during terminal sterilization. As noted in Section 3.7.2, natural convection heat transfer has been assumed as the primary means of removing heat rejected by the thermoelectric unit to the sterilization gas.

## MARS LANDER ON SURFACE\*

TIME	RCMIN	MINND	RCMAX	MAXND	DTHETA	NCYC
0.20399E+05	0.97844E+01	21	0.23406E+05	1	0.	1
0.39999E+02	T1	0.39999E+02	T2	0.39999E+02	T3	0.39999E+02
0.39999E+02	T5	0.39999E+02	T6	0.39999E+02	T7	0.39999E+02
0.39999E+02	T9	0.39999E+02	T10	0.39999E+02	T11	0.39999E+02
0.40229E+02	T13	0.39999E+02	T14	0.39999E+02	T15	0.39999E+02
0.39999E+02	T17	0.39999E+02	T18	0.39999E+02	T19	0.39999E+02
0.39999E+02	T21	0.39999E+02	T22	0.39999E+02	T23	0.39999E+02
0.39999E+02	T25	0.39999E+02	T26	0.39999E+02	T27	0.39999E+02
0.39999E+02	T29	0.39999E+02	T30	0.39999E+02	T31	0.39999E+02
0.39999E+02	T33	0.39999E+02	T34	0.39999E+02	T35	0.39999E+02
0.39999E+02	T37	0.39999E+02	T38	0.39999E+02	T39	0.39999E+02
0.39999E+02	T41	0.39999E+02	T42	0.39999E+02	T43	0.39999E+02
0.39999E+02	T45	0.39999E+02	T46	0.39999E+02	T47	0.39999E+02
0.39999E+02	T49	0.69999E+02	T50			
0.39999E+02	T51	0.39999E+02	T52	0.39999E+02	T53	0.39999E+02
0.39999E+02	T55	0.39999E+02	T56	0.39999E+02	T57	0.39999E+02
0.39999E+02	T59	0.39999E+02	T60	0.39999E+02	T61	0.39999E+02
0.39999E+02	T63	0.39999E+02	T64	0.39999E+02	T65	0.39999E+02
0.39999E+02	T67	0.39999E+02	T68	0.39999E+02	T69	0.39999E+02
0.39999E+02	T71	0.39999E+02	T72	0.39999E+02	T73	0.39999E+02
0.39999E+02	T75	0.39999E+02	T76	0.39999E+02	T77	0.39999E+02
0.39999E+02	T79	0.39999E+02	T80	0.39999E+02	T81	0.39999E+02
0.15906E+03	T129	-0.45999E+03	T130	0.39999E+02	T81	0.42006E+03
0.10000E+01	T133	0.	T134	-0.10246E+03	T131	-0.11906E+03
				0.	T135	
0.21599E+05	0.97842E+01	21	0.23253E+05	1	0.24130E+01	155
0.41813E+02	T1	0.42129E+02	T2	0.41989E+02	T3	0.42161E+02
0.41986E+02	T5	0.42458E+02	T6	0.42089E+02	T7	0.41919E+02
0.42707E+02	T9	0.42502E+02	T10	0.42275E+02	T11	0.42042E+02
0.42864E+02	T13	0.39999E+02	T14	0.39999E+02	T15	0.39999E+02
0.43144E+02	T17	0.42516E+02	T18	0.42521E+02	T19	0.42493E+02
0.42451E+02	T21	0.42433E+02	T22	0.42397E+02	T23	0.42678E+02
0.42138E+02	T25	0.42154E+02	T26	0.42149E+02	T27	0.42133E+02
0.42154E+02	T29	0.42158E+02	T30	0.42557E+02	T31	0.41949E+02
0.41950E+02	T33	0.41950E+02	T34	0.41950E+02	T35	0.41909E+02
0.41772E+02	T37	0.41916E+02	T38	0.41903E+02	T39	0.39999E+02
0.39999E+02	T41	0.42581E+02	T42	0.39999E+02	T43	0.39999E+02
0.39999E+02	T45	0.39999E+02	T46	0.42581E+02	T47	0.39999E+02

\*NOTES: 1. Planetary impact at 5:40 AM = 20,400 seconds  
 2. Sunrise at 5:42 AM = 20,520  
 3. Noon at 42,120 seconds

Fig. B-4 Thermal Analyzer Output



## MARS LANDER ON SURFACE

TIME	RCMIN	MINND	RCMAX	MAXND	DTHETA	NCYC
0.21599E+05	0.97842E+01	21	0.23253E+05	1	0.24130E+01	155
0.39999E+02	T49	0.69993E+02	T50			
0.40242E+02	T51	0.40006E+02	T52	0.40001E+02	T53	0.40000E+02
0.40000E+02	T55	0.39999E+02	T56	0.40000E+02	T57	0.43296E+02
0.39999E+02	T59	0.39999E+02	T60	0.39999E+02	T61	0.39999E+02
0.39999E+02	T63	0.40044E+02	T64	0.39999E+02	T65	0.40714E+02
0.39999E+02	T67	0.39999E+02	T68	0.39999E+02	T69	0.40977E+02
0.41134E+02	T71	0.41134E+02	T72	0.41133E+02	T73	0.40763E+02
0.40830E+02	T75	0.40830E+02	T76	0.40794E+02	T77	0.43573E+02
0.39999E+02	T79	0.47443E+02	T80	0.53257E+02	T81	0.43086E+03
0.16394E+03	T129	-0.45999E+03	T130	-0.91847E+02	T131	-0.11070E+03
0.10000E+01	T133	0.60770E+07	T134	0.61799E+09	T135	
TIME	RCMIN	MINND	RCMAX	MAXND	DTHETA	NCYC
0.22799E+05	0.97839E+01	21	0.22994E+05	1	0.24462E+01	309
0.45244E+02	T1	0.45636E+02	T2	0.45475E+02	T3	0.45691E+02
0.45470E+02	T5	0.46043E+02	T6	0.45608E+02	T7	0.45382E+02
0.46471E+02	T9	0.46120E+02	T10	0.45844E+02	T11	0.45543E+02
0.46537E+02	T13	0.39999E+02	T14	0.39999E+02	T15	0.39999E+02
0.47106E+02	T17	0.46130E+02	T18	0.46135E+02	T19	0.46106E+02
0.46055E+02	T21	0.46034E+02	T22	0.46010E+02	T23	0.46438E+02
0.45747E+02	T25	0.45704E+02	T26	0.45696E+02	T27	0.45611E+02
0.45705E+02	T29	0.45712E+02	T30	0.46332E+02	T31	0.45417E+02
0.45419E+02	T33	0.45419E+02	T34	0.45419E+02	T35	0.45367E+02
0.45194E+02	T37	0.45367E+02	T38	0.45359E+02	T39	0.39999E+02
0.39999E+02	T41	0.46282E+02	T42	0.39999E+02	T43	0.39999E+02
0.39999E+02	T45	0.39999E+02	T46	0.46282E+02	T47	0.39999E+02
0.39999E+02	T49	0.69991E+02	T50			
0.41038E+02	T51	0.40055E+02	T52	0.40014E+02	T53	0.40003E+02
0.40002E+02	T55	0.40000E+02	T56	0.40006E+02	T57	0.46589E+02
0.39999E+02	T59	0.39999E+02	T60	0.39999E+02	T61	0.39999E+02
0.39999E+02	T63	0.40238E+02	T64	0.39999E+02	T65	0.42948E+02
0.39999E+02	T67	0.39999E+02	T68	0.39999E+02	T69	0.42015E+02
0.42321E+02	T71	0.42321E+02	T72	0.42311E+02	T73	0.42745E+02
0.43005E+02	T75	0.43005E+02	T76	0.42908E+02	T77	0.47875E+02
0.39999E+02	T79	0.53737E+02	T80	0.62346E+02	T81	0.47875E+02
0.16468E+03	T129	-0.45999E+03	T130	-0.81231E+02	T131	0.43959E+03
0.10000E+01	T133	0.13228E+08	T134	0.61799E+09	T135	-0.10234E+03
TIME	RCMIN	MINND	RCMAX	MAXND	DTHETA	NCYC
0.23999E+05	0.97836E+01	21	0.22701E+05	1	0.24787E+01	463

Fig. B-4 (Cont.)

## MAKS LANDER ON SURFACE

TIME	RCMIN	MINND	RCMAX	MAXND	DTHETA	NCYC	
0.23999E+05	0.97836E+01	21	0.22701E+05	1	0.24787E+01	463	
0.49135E+02	T1	0.49540E+02	T2	0.49365E+02	T3	0.49595E+02	T4
0.49356E+02	T5	0.49961E+02	T6	0.49510E+02	T7	0.49255E+02	T8
0.50456E+02	T9	0.50050E+02	T10	0.49763E+02	T11	0.49432E+02	T12
0.50465E+02	T13	0.39999E+02	T14	0.39999E+02	T15	0.39999E+02	T16
0.51154E+02	T17	0.50063E+02	T18	0.50068E+02	T19	0.50040E+02	T20
0.49983E+02	T21	0.49962E+02	T22	0.49944E+02	T23	0.50427E+02	T24
0.49660E+02	T25	0.49616E+02	T26	0.49608E+02	T27	0.49504E+02	T28
0.49616E+02	T29	0.49626E+02	T30	0.50329E+02	T31	0.49291E+02	T32
0.49292E+02	T33	0.49293E+02	T34	0.49292E+02	T35	0.49237E+02	T36
0.49083E+02	T37	0.49226E+02	T38	0.49229E+02	T39	0.39999E+02	T40
0.39999E+02	T41	0.50244E+02	T42	0.39999E+02	T43	0.39999E+02	T44
0.39999E+02	T45	0.39999E+02	T46	0.50244E+02	T47	0.39999E+02	T48
0.39999E+02	T49	0.69992E+02	T50				
0.42271E+02	T51	0.40186E+02	T52	0.40057E+02	T53	0.40019E+02	T54
0.40014E+02	T55	0.40002E+02	T56	0.40032E+02	T57	0.50369E+02	T58
0.39999E+02	T59	0.39999E+02	T60	0.39999E+02	T61	0.39999E+02	T62
0.39999E+02	T63	0.40617E+02	T64	0.39999E+02	T65	0.46229E+02	T66
0.39999E+02	T67	0.39999E+02	T68	0.39999E+02	T69	0.43225E+02	T70
0.43665E+02	T71	0.43665E+02	T72	0.43642E+02	T73	0.45301E+02	T74
0.45794E+02	T75	0.45794E+02	T76	0.45648E+02	T77	0.52064E+02	T78
0.39999E+02	T79	0.58623E+02	T80	0.68206E+02	T81	0.44670E+02	T128
0.16218E+03	T129	-0.45999E+03	T130	-0.70615E+02	T131	-0.93990E+02	T132
0.10000E+01	T133	0.20379E+08	T134	0.61799E+09	T135		
0.25199E+05	0.97834E+01	21	0.22396E+05	1	0.25126E+01	617	
0.53108E+02	T1	0.53507E+02	T2	0.53321E+02	T3	0.53556E+02	T4
0.53306E+02	T5	0.53923E+02	T6	0.53470E+02	T7	0.53198E+02	T8
0.54445E+02	T9	0.54017E+02	T10	0.53732E+02	T11	0.53383E+02	T12
0.54411E+02	T13	0.39999E+02	T14	0.39999E+02	T15	0.39999E+02	T16
0.55159E+02	T17	0.54035E+02	T18	0.54040E+02	T19	0.54013E+02	T20
0.55954E+02	T21	0.53933E+02	T22	0.53917E+02	T23	0.54423E+02	T24
0.53622E+02	T25	0.53579E+02	T26	0.53572E+02	T27	0.53467E+02	T28
0.53579E+02	T29	0.53590E+02	T30	0.54329E+02	T31	0.53231E+02	T32
0.53233E+02	T33	0.53233E+02	T34	0.53233E+02	T35	0.53177E+02	T36
0.53057E+02	T37	0.53155E+02	T38	0.53169E+02	T39	0.39999E+02	T40
0.39999E+02	T41	0.54223E+02	T42	0.39999E+02	T43	0.39999E+02	T44
0.39999E+02	T45	0.39999E+02	T46	0.54223E+02	T47	0.39999E+02	T48

Fig. B-4 (Cont.)

## MARS LANDER ON SURFACE

TIME	RCMIN	MINND	RCMAX	MAXND	DTHEIA	NCYC
0.25199E+05	0.97834E+01	21	0.22396E+05	1	0.25126E+01	617
0.39999E+02	T49	0.69993E+02	T50			
0.43783E+02	T51	0.40417E+02	T52	0.40146E+02	T53	0.40061E+02
0.40043E+02	T55	0.40009E+02	T56	0.40095E+02	T57	0.54311E+02
0.39999E+02	T59	0.39999E+02	T60	0.39999E+02	T61	0.39999E+02
0.39999E+02	T63	0.41187E+02	T64	0.39999E+02	T65	0.50002E+02
0.39999E+02	T67	0.39999E+02	T68	0.39999E+02	T69	0.44637E+02
0.45200E+02	T71	0.45200E+02	T72	0.45160E+02	T73	0.48097E+02
0.48818E+02	T75	0.48818E+02	T76	0.48635E+02	T77	0.56142E+02
0.39999E+02	T79	0.62958E+02	T80	0.72900E+02	T81	0.45322E+03
0.15852E+03	T129	-0.45999E+03	T130	-0.59999E+02	T131	-0.85632E+02
0.10000E+01	T133	0.27261E+08	T134	0.61799E+09	T135	
TIME	RCMIN	MINND	RCMAX	MAXND	DTHEIA	NCYC
0.26399E+05	0.97831E+01	21	0.22087E+05	1	0.25478E+01	771
0.57047E+02	T1	0.57435E+02	T2	0.57238E+02	T3	0.57475E+02
0.57219E+02	T5	0.57840E+02	T6	0.57390E+02	T7	0.57104E+02
0.58374E+02	T9	0.57935E+02	T10	0.57656E+02	T11	0.57295E+02
0.58302E+02	T13	0.39999E+02	T14	0.39999E+02	T15	0.39999E+02
0.59089E+02	T17	0.57959E+02	T18	0.57965E+02	T19	0.57938E+02
0.57878E+02	T21	0.57858E+02	T22	0.57843E+02	T23	0.58361E+02
0.57541E+02	T25	0.57499E+02	T26	0.57494E+02	T27	0.57394E+02
0.57499E+02	T29	0.57512E+02	T30	0.58269E+02	T31	0.57135E+02
0.57137E+02	T33	0.57137E+02	T34	0.57137E+02	T35	0.57081E+02
0.56997E+02	T37	0.57048E+02	T38	0.57073E+02	T39	0.39999E+02
0.39999E+02	T41	0.58147E+02	T42	0.39999E+02	T43	0.39999E+02
0.39999E+02	T45	0.39999E+02	T46	0.58147E+02	T47	0.39999E+02
0.39999E+02	T49	0.69994E+02	T50			
0.45469E+02	T51	0.40760E+02	T52	0.40294E+02	T53	0.40144E+02
0.40100E+02	T55	0.40026E+02	T56	0.40209E+02	T57	0.58252E+02
0.39999E+02	T59	0.39999E+02	T60	0.39999E+02	T61	0.39999E+02
0.39999E+02	T63	0.41942E+02	T64	0.39999E+02	T65	0.53945E+02
0.39999E+02	T67	0.39999E+02	T68	0.39999E+02	T69	0.46252E+02
0.46925E+02	T71	0.46925E+02	T72	0.46866E+02	T73	0.51005E+02
0.51935E+02	T75	0.51935E+02	T76	0.51721E+02	T77	0.60120E+02
0.39999E+02	T79	0.67047E+02	T80	0.77143E+02	T81	0.45953E+03
0.15440E+03	T129	-0.45999E+03	T130	-0.48666E+02	T131	-0.77273E+02
0.10000E+01	T133	0.33923E+08	T134	0.61799E+09	T135	
TIME	RCMIN	MINND	RCMAX	MAXND	DTHEIA	NCYC
0.27599E+05	0.97828E+01	21	0.21777E+05	1	0.25832E+01	925

Fig. B-4 (Cont.)

## MAKS LANDER ON SURFACE

TIME	RCMIN	MINND	RCMAX	MAXND	DTHETA	NCYC
0.27599E+05	0.97828E+01	21	0.21777E+05	1	0.25832E+01	925
0.60917E+02	T1	0.61293E+02	T2	0.61088E+02	T3	0.61325E+02
0.61064E+02	T5	0.61686E+02	T6	0.61241E+02	T7	0.60944E+02
0.62222E+02	T9	0.61781E+02	T10	0.61510E+02	T11	0.61139E+02
0.62119E+02	T13	0.39999E+02	T14	0.39999E+02	T15	0.39999E+02
0.62938E+02	T17	0.61812E+02	T18	0.61817E+02	T19	0.61792E+02
0.61732E+02	T21	0.61711E+02	T22	0.61696E+02	T23	0.62223E+02
0.61391E+02	T25	0.61349E+02	T26	0.61347E+02	T27	0.61253E+02
0.61349E+02	T29	0.61364E+02	T30	0.62135E+02	T31	0.60973E+02
0.60974E+02	T33	0.60975E+02	T34	0.60975E+02	T35	0.60919E+02
0.60868E+02	T37	0.60875E+02	T38	0.60911E+02	T39	0.39999E+02
0.39999E+02	T41	0.61996E+02	T42	0.39999E+02	T43	0.39999E+02
0.39999E+02	T45	0.39999E+02	T46	0.61996E+02	T47	0.39999E+02
0.39999E+02	T49	0.69996E+02	T50			
0.47269E+02	T51	0.41214E+02	T52	0.40510E+02	T53	0.40277E+02
0.40192E+02	T55	0.40060E+02	T56	0.40386E+02	T57	0.62135E+02
0.39999E+02	T59	0.39999E+02	T60	0.39999E+02	T61	0.39999E+02
0.39999E+02	T63	0.42873E+02	T64	0.39999E+02	T65	0.57904E+02
0.39999E+02	T67	0.39999E+02	T68	0.39999E+02	T69	0.48059E+02
0.48831E+02	T71	0.48831E+02	T72	0.48750E+02	T73	0.53978E+02
0.55094E+02	T75	0.55094E+02	T76	0.54853E+02	T77	0.64010E+02
0.39999E+02	T79	0.71001E+02	T80	0.81185E+02	T81	0.46573E+03
0.15009E+03	T129	-0.45999E+03	T130	-0.37333E+02	T131	-0.68915E+02
0.10000E+01	T133	0.40586E+08	T134	0.61799E+09	T135	
0.28799E+05	0.97825E+01	21	0.21467E+05	1	0.26184E+01	1079
0.64711E+02	T1	0.65076E+02	T2	0.64865E+02	T3	0.65101E+02
0.64837E+02	T5	0.65437E+02	T6	0.65019E+02	T7	0.64711E+02
0.66005E+02	T9	0.65533E+02	T10	0.65289E+02	T11	0.64910E+02
0.65861E+02	T13	0.39999E+02	T14	0.39999E+02	T15	0.39999E+02
0.66710E+02	T17	0.65590E+02	T18	0.65595E+02	T19	0.65571E+02
0.65910E+02	T21	0.65490E+02	T22	0.65475E+02	T23	0.66010E+02
0.65167E+02	T25	0.65126E+02	T26	0.65126E+02	T27	0.65038E+02
0.65126E+02	T29	0.65143E+02	T30	0.65925E+02	T31	0.64738E+02
0.64739E+02	T33	0.64740E+02	T34	0.64740E+02	T35	0.64685E+02
0.64665E+02	T37	0.64632E+02	T38	0.64677E+02	T39	0.39999E+02
0.39999E+02	T41	0.65770E+02	T42	0.39999E+02	T43	0.39999E+02
0.39999E+02	T45	0.39999E+02	T46	0.65770E+02	T47	0.39999E+02

Fig. B-4 (Cont.)

## MAKS LANDER ON SURFACE

TIME	RCMIN	MINND	RCMAX	MAXND	DTHETA	NCYC
0.26799E+05	0.97825E+01	21	0.21467E+05	1	0.26184E+01	1079
0.39999E+02	T49	0.69997E+02	T50			
0.49149E+02	T51	0.41778E+02	T52	0.40798E+02	T53	0.40473E+02
0.40327E+02	T55	0.40116E+02	T56	0.40632E+02	T57	0.65947E+02
0.39999E+02	T59	0.39999E+02	T60	0.39999E+02	T61	0.39999E+02
0.39999E+02	T63	0.43974E+02	T64	0.39999E+02	T65	0.61816E+02
0.39999E+02	T67	0.39999E+02	T68	0.39999E+02	T69	0.50043E+02
0.50904E+02	T71	0.50904E+02	T72	0.50801E+02	T73	0.56996E+02
0.58276E+02	T75	0.58276E+02	T76	0.58011E+02	T77	0.67821E+02
0.39999E+02	T79	0.74861E+02	T80	0.85112E+02	T81	0.47187E+03
0.14566E+03	T129	-0.45999E+03	T130	-0.25999E+02	T131	-0.60557E+02
0.10000E+01	T133	0.47015E+08	T134	0.61799E+09	T135	

T54  
T58  
T62  
T66  
T70  
T74  
T78  
T128  
T132

TIME	RCMIN	MINND	RCMAX	MAXND	DTHETA	NCYC
0.29999E+05	0.97822E+01	21	0.21157E+05	1	0.26533E+01	1233
0.68432E+02	T11	0.68786E+02	T12	0.68569E+02	T13	0.68805E+02
0.68538E+02	T5	0.69155E+02	T6	0.68725E+02	T7	0.68408E+02
0.69709E+02	T9	0.69251E+02	T10	0.68996E+02	T11	0.68610E+02
0.69531E+02	T13	0.39999E+02	T14	0.39999E+02	T15	0.39999E+02
0.70407E+02	T17	0.69295E+02	T18	0.69300E+02	T19	0.69276E+02
0.69216E+02	T21	0.69196E+02	T22	0.69181E+02	T23	0.69723E+02
0.68871E+02	T25	0.68831E+02	T26	0.68833E+02	T27	0.68751E+02
0.68830E+02	T29	0.68849E+02	T30	0.69642E+02	T31	0.68433E+02
0.68434E+02	T33	0.68435E+02	T34	0.68435E+02	T35	0.68380E+02
0.68387E+02	T37	0.68319E+02	T38	0.68372E+02	T39	0.39999E+02
0.39999E+02	T41	0.69471E+02	T42	0.39999E+02	T43	0.39999E+02
0.39999E+02	T45	0.39999E+02	T46	0.69471E+02	T47	0.39999E+02

T4  
T8  
T12  
T16  
T20  
T24  
T28  
T32  
T36  
T40  
T44  
T48

TIME	RCMIN	MINND	RCMAX	MAXND	DTHETA	NCYC
0.39999E+02	T49	0.69998E+02	T50			
0.51091E+02	T51	0.42449E+02	T52	0.41163E+02	T53	0.40737E+02
0.40510E+02	T55	0.40202E+02	T56	0.40952E+02	T57	0.69684E+02
0.39999E+02	T59	0.39999E+02	T60	0.39999E+02	T61	0.39999E+02
0.39999E+02	T63	0.45234E+02	T64	0.39999E+02	T65	0.65658E+02
0.39999E+02	T67	0.39999E+02	T68	0.39999E+02	T69	0.52191E+02
0.53131E+02	T71	0.53131E+02	T72	0.53005E+02	T73	0.60050E+02
0.61472E+02	T75	0.61472E+02	T76	0.61186E+02	T77	0.71556E+02
0.39999E+02	T79	0.78639E+02	T80	0.88950E+02	T81	0.47806E+03
0.14096E+03	T129	-0.45999E+03	T130	-0.17166E+02	T131	-0.52018E+02
0.10000E+01	T133	0.52762E+08	T134	0.61799E+09	T135	

T54  
T58  
T62  
T66  
T70  
T74  
T78  
T128  
T132

Fig. B-4 (Cont.)

## MARS LANDER ON SURFACE

TIME	RCMIN	MINND	RCMAX	MAXND	DTHETA	NCYC	
0.31199E+05	0.97819E+01	21	0.20847E+05	1	0.26877E+01	1387	
0.72083E+02	T1	0.72425E+02	T2	0.72205E+02	T3	0.72440E+02	T4
0.72171E+02	T5	0.72784E+02	T6	0.72362E+02	T7	0.72037E+02	T8
0.73343E+02	T9	0.72880E+02	T10	0.72634E+02	T11	0.72242E+02	T12
0.73131E+02	T13	0.39999E+02	T14	0.39999E+02	T15	0.39999E+02	T16
0.74035E+02	T17	0.72930E+02	T18	0.72935E+02	T19	0.72912E+02	T20
0.72851E+02	T21	0.72832E+02	T22	0.72817E+02	T23	0.73366E+02	T24
0.72506E+02	T25	0.72467E+02	T26	0.72471E+02	T27	0.72395E+02	T28
0.72466E+02	T29	0.72486E+02	T30	0.73290E+02	T31	0.72060E+02	T32
0.72062E+02	T33	0.72063E+02	T34	0.72062E+02	T35	0.72008E+02	T36
0.72039E+02	T37	0.71939E+02	T38	0.72000E+02	T39	0.39999E+02	T40
0.39999E+02	T41	0.73101E+02	T42	0.39999E+02	T43	0.39999E+02	T44
0.39999E+02	T45	0.39999E+02	T46	0.73101E+02	T47	0.39999E+02	T48
0.39999E+02	T49	0.70000E+02	T50				
0.53084E+02	T51	0.43222E+02	T52	0.41608E+02	T53	0.41074E+02	T54
0.40748E+02	T55	0.40323E+02	T56	0.41350E+02	T57	0.73351E+02	T58
0.39999E+02	T59	0.39999E+02	T60	0.39999E+02	T61	0.39999E+02	T62
0.39999E+02	T63	0.46647E+02	T64	0.39999E+02	T65	0.69427E+02	T66
0.39999E+02	T67	0.39999E+02	T68	0.39999E+02	T69	0.54488E+02	T70
0.55497E+02	T71	0.55497E+02	T72	0.55348E+02	T73	0.63132E+02	T74
0.64677E+02	T75	0.64677E+02	T76	0.64371E+02	T77	0.75221E+02	T78
0.39999E+02	T79	0.82345E+02	T80	0.92712E+02	T81	0.48421E+03	T128
0.13617E+03	T129	-0.45999E+03	T130	-0.83333E+01	T131	-0.43467E+02	T132
0.10000E+01	T133	0.58508E+08	T134	0.61799E+09	T135		
0.32399E+05	0.97816E+01	21	0.20540E+05	1	0.27224E+01	1541	
0.75666E+02	T1	0.75999E+02	T2	0.75777E+02	T3	0.76010E+02	T4
0.75739E+02	T5	0.76348E+02	T6	0.75934E+02	T7	0.75603E+02	T8
0.76911E+02	T9	0.76443E+02	T10	0.76207E+02	T11	0.75810E+02	T12
0.76660E+02	T13	0.39999E+02	T14	0.39999E+02	T15	0.39999E+02	T16
0.77599E+02	T17	0.76500E+02	T18	0.76505E+02	T19	0.76483E+02	T20
0.76422E+02	T21	0.76403E+02	T22	0.76388E+02	T23	0.76944E+02	T24
0.76077E+02	T25	0.76039E+02	T26	0.76045E+02	T27	0.75974E+02	T28
0.76038E+02	T29	0.76059E+02	T30	0.76873E+02	T31	0.75624E+02	T32
0.75625E+02	T33	0.75627E+02	T34	0.75626E+02	T35	0.75573E+02	T36
0.75624E+02	T37	0.75497E+02	T38	0.75565E+02	T39	0.39999E+02	T40
0.39999E+02	T41	0.76667E+02	T42	0.39999E+02	T43	0.39999E+02	T44
0.39999E+02	T45	0.39999E+02	T46	0.76667E+02	T47	0.39999E+02	T48

Fig. B-4 (Cont.)

## MAKS LANDER ON SURFACE

TIME	RCMIN	MINND	RCMAX	MAXND	DTHETA	NCYC
0.32599E+05	0.97816E+01	21	0.20540E+05	1	0.27224E+01	1541
0.39999E+02	T49	0.70001E+02	T50			
0.55121E+02	T51	0.44095E+02	T52	0.42132E+02	T53	0.41488E+02
0.41043E+02	T55	0.40486E+02	T56	0.41827E+02	T57	0.76950E+02
0.39999E+02	T59	0.39999E+02	T60	0.39999E+02	T61	0.39999E+02
0.39999E+02	T63	0.48203E+02	T64	0.39999E+02	T65	0.73123E+02
0.39999E+02	T67	0.39999E+02	T68	0.39999E+02	T69	0.56921E+02
0.57991E+02	T71	0.57991E+02	T72	0.57819E+02	T73	0.66238E+02
0.67889E+02	T75	0.67889E+02	T76	0.67565E+02	T77	0.78821E+02
0.39999E+02	T79	0.85986E+02	T80	0.96410E+02	T81	0.49034E+03
0.13131E+03	T129	-0.45999E+03	T130	0.50000E+00	T131	-0.34915E+02
0.10000E+01	T133	0.64255E+08	T134	0.61799E+09	T135	
TIME	RCMIN	MINND	RCMAX	MAXND	DTHETA	NCYC
0.33599E+05	0.97814E+01	21	0.20234E+05	1	0.27680E+01	1695
0.79188E+02	T1	0.79511E+02	T2	0.79288E+02	T3	0.79520E+02
0.79248E+02	T5	0.79850E+02	T6	0.79446E+02	T7	0.79109E+02
0.80419E+02	T9	0.79946E+02	T10	0.79719E+02	T11	0.79318E+02
0.80140E+02	T13	0.39999E+02	T14	0.39999E+02	T15	0.39999E+02
0.81101E+02	T17	0.80009E+02	T18	0.80014E+02	T19	0.79993E+02
0.79932E+02	T21	0.79913E+02	T22	0.79898E+02	T23	0.80461E+02
0.79588E+02	T25	0.79550E+02	T26	0.79558E+02	T27	0.79492E+02
0.79549E+02	T29	0.79572E+02	T30	0.80395E+02	T31	0.79129E+02
0.79130E+02	T33	0.79132E+02	T34	0.79131E+02	T35	0.79078E+02
0.79148E+02	T37	0.78997E+02	T38	0.79070E+02	T39	0.39999E+02
0.39999E+02	T41	0.80171E+02	T42	0.39999E+02	T43	0.39999E+02
0.39999E+02	T45	0.39999E+02	T46	0.80171E+02	T47	0.39999E+02
0.39999E+02	T49	0.70002E+02	T50			
0.57200E+02	T51	0.45062E+02	T52	0.42738E+02	T53	0.41980E+02
0.41400E+02	T55	0.40696E+02	T56	0.42385E+02	T57	0.80486E+02
0.39999E+02	T59	0.39999E+02	T60	0.39999E+02	T61	0.39999E+02
0.39999E+02	T63	0.49896E+02	T64	0.39999E+02	T65	0.76750E+02
0.39999E+02	T67	0.39999E+02	T68	0.39999E+02	T69	0.59477E+02
0.60601E+02	T71	0.60601E+02	T72	0.60405E+02	T73	0.69363E+02
0.71103E+02	T75	0.71103E+02	T76	0.70764E+02	T77	0.82361E+02
0.39999E+02	T79	0.89560E+02	T80	0.10004E+03	T81	0.49643E+03
0.12640E+03	T129	-0.45999E+03	T130	0.93333E+01	T131	-0.26364E+02
0.10000E+01	T133	0.68768E+08	T134	0.61799E+09	T135	
TIME	RCMIN	MINND	RCMAX	MAXND	DTHETA	NCYC
0.34799E+05	0.97811E+01	21	0.19930E+05	1	0.28198E+01	1849

Fig. B-4 (Cont.)

MARS LANDER ON SURFACE						
TIME	RCMIN	MINND	RCMAX	MAXND	DTHETA	NCYC
0.34799E+05	0.97811E+01	21	0.19930E+05	1	0.28198E+01	1849
0.82052E+02	T1	0.82966E+02	T2	0.82743E+02	T3	0.82973E+02
0.82702E+02	T5	0.83296E+02	T6	0.82902E+02	T7	0.82560E+02
0.83809E+02	T9	0.83391E+02	T10	0.83175E+02	T11	0.82771E+02
0.83558E+02	T13	0.39999E+02	T14	0.39999E+02	T15	0.39999E+02
0.84547E+02	T17	0.83461E+02	T18	0.83467E+02	T19	0.83446E+02
0.83384E+02	T21	0.83366E+02	T22	0.83351E+02	T23	0.83921E+02
0.83042E+02	T25	0.83005E+02	T26	0.83015E+02	T27	0.82954E+02
0.83004E+02	T29	0.83028E+02	T30	0.83861E+02	T31	0.82579E+02
0.82580E+02	T33	0.82581E+02	T34	0.82581E+02	T35	0.82528E+02
0.82613E+02	T37	0.82442E+02	T38	0.82520E+02	T39	0.39999E+02
0.39999E+02	T41	0.83619E+02	T42	0.39999E+02	T43	0.39999E+02
0.39999E+02	T45	0.39999E+02	T46	0.83619E+02	T47	0.39999E+02
0.39999E+02	T49	0.70003E+02	T50			
0.59315E+02	T51	0.46120E+02	T52	0.43424E+02	T53	0.42552E+02
0.41820E+02	T55	0.40957E+02	T56	0.43023E+02	T57	0.83963E+02
0.39999E+02	T59	0.39999E+02	T60	0.39999E+02	T61	0.39999E+02
0.39999E+02	T63	0.51717E+02	T64	0.39999E+02	T65	0.80312E+02
0.39999E+02	T67	0.39999E+02	T68	0.39999E+02	T69	0.62144E+02
0.63313E+02	T71	0.63313E+02	T72	0.63096E+02	T73	0.72505E+02
0.74319E+02	T75	0.74319E+02	T76	0.73966E+02	T77	0.85844E+02
0.39999E+02	T79	0.93090E+02	T80	0.10362E+03	T81	0.50250E+03
0.12143E+03	T129	-0.45999E+03	T130	0.18166E+02	T131	-0.17813E+02
0.10000E+01	T133	0.73226E+08	T134	0.61799E+09	T135	
0.39999E+05	0.97808E+01	21	0.19628E+05	1	0.28295E+01	2003
0.86002E+02	T1	0.6367E+02	T2	0.86145E+02	T3	0.86374E+02
0.86103E+02	T5	0.6689E+02	T6	0.86306E+02	T7	0.85959E+02
0.87267E+02	T9	0.6784E+02	T10	0.86577E+02	T11	0.86172E+02
0.86924E+02	T13	0.39999E+02	T14	0.39999E+02	T15	0.39999E+02
0.87940E+02	T17	0.86861E+02	T18	0.86866E+02	T19	0.86846E+02
0.86784E+02	T21	0.86785E+02	T22	0.86751E+02	T23	0.87329E+02
0.86444E+02	T25	0.36408E+02	T26	0.86420E+02	T27	0.86363E+02
0.86407E+02	T29	0.36432E+02	T30	0.87275E+02	T31	0.85977E+02
0.85978E+02	T33	0.35980E+02	T34	0.85979E+02	T35	0.85927E+02
0.86024E+02	T37	0.35836E+02	T38	0.85919E+02	T39	0.39999E+02
0.39999E+02	T41	0.87013E+02	T42	0.39999E+02	T43	0.39999E+02
0.39999E+02	T45	0.39999E+02	T46	0.87013E+02	T47	0.39999E+02

Fig. B-4 (Cont.)



## MARS LANDER ON SURFACE

TIME	RCMIN	MINND	RCMAX	MAXND	DTHETA	NCYC
0.35999E+05	0.97808E+01	21	0.19628E+05	1	0.28295E+01	2003
0.39999E+02	T49	0.70005E+02	T50			
0.61465E+02	T51	0.47267E+02	T52	0.44190E+02	T53	0.43205E+02
0.42307E+02	T55	0.41272E+02	T56	0.43741E+02	T57	0.87385E+02
0.39999E+02	T59	0.39999E+02	T60	0.39999E+02	T61	0.39999E+02
0.39999E+02	T63	0.53661E+02	T64	0.39999E+02	T65	0.83815E+02
0.39999E+02	T67	0.39999E+02	T68	0.39999E+02	T69	0.64910E+02
0.66119E+02	T71	0.66119E+02	T72	0.65880E+02	T73	0.75658E+02
0.77534E+02	T75	0.77534E+02	T76	0.77169E+02	T77	0.89274E+02
0.39999E+02	T79	0.96561E+02	T80	0.10715E+03	T81	0.50854E+03
0.11640E+03	T129	-0.45999E+03	T130	0.26999E+02	T131	-0.92616E+01
0.10000E+01	T133	0.77684E+08	T134	0.61799E+09	T135	
TIME	RCMIN	MINND	RCMAX	MAXND	DTHETA	NCYC
0.37199E+05	0.97805E+01	21	0.19329E+05	1	0.28945E+01	2157
0.89422E+02	T1	0.89719E+02	T2	0.89499E+02	T3	0.89726E+02
0.89455E+02	T5	0.90032E+02	T6	0.89660E+02	T7	0.89310E+02
0.90614E+02	T9	0.90127E+02	T10	0.89931E+02	T11	0.89524E+02
0.90240E+02	T13	0.39999E+02	T14	0.39999E+02	T15	0.39999E+02
0.91283E+02	T17	0.90210E+02	T18	0.90215E+02	T19	0.90197E+02
0.90134E+02	T21	0.90116E+02	T22	0.90101E+02	T23	0.90686E+02
0.89797E+02	T25	0.89762E+02	T26	0.89775E+02	T27	0.89722E+02
0.89761E+02	T29	0.89787E+02	T30	0.90638E+02	T31	0.89327E+02
0.89328E+02	T33	0.89329E+02	T34	0.89329E+02	T35	0.89277E+02
0.89385E+02	T37	0.89182E+02	T38	0.89269E+02	T39	0.39999E+02
0.39999E+02	T41	0.90358E+02	T42	0.39999E+02	T43	0.39999E+02
0.39999E+02	T45	0.39999E+02	T46	0.90358E+02	T47	0.39999E+02
0.39999E+02	T49	0.70006E+02	T50			
0.63649E+02	T51	0.48498E+02	T52	0.45036E+02	T53	0.43938E+02
0.42862E+02	T55	0.41647E+02	T56	0.44540E+02	T57	0.90757E+02
0.39999E+02	T59	0.39999E+02	T60	0.39999E+02	T61	0.39999E+02
0.39999E+02	T63	0.55719E+02	T64	0.39999E+02	T65	0.87262E+02
0.39999E+02	T67	0.39999E+02	T68	0.39999E+02	T69	0.67765E+02
0.69007E+02	T71	0.69007E+02	T72	0.68747E+02	T73	0.78822E+02
0.80746E+02	T75	0.80746E+02	T76	0.80371E+02	T77	0.92654E+02
0.39999E+02	T79	0.99977E+02	T80	0.11062E+03	T81	0.51455E+03
0.11132E+03	T129	-0.45999E+03	T130	0.32499E+02	T131	-0.71028E+00
0.10000E+01	T133	0.80981E+08	T134	0.61799E+09	T135	
TIME	RCMIN	MINND	RCMAX	MAXND	DTHETA	NCYC
0.38399E+05	0.97802E+01	21	0.19033E+05	1	0.28945E+01	2311

Fig. B-4 (Cont.)

## MARS LANDER ON SURFACE

TIME	RCMIN	MINND	RCMAX	MAXND	DTHETA	NCYC
0.38399E+05	0.97802E+01	21	0.19033E+05	1	0.28945E+01	2311
0.52730E+02	T1	0.93018E+02	T2	0.92801E+02	T3	0.93026E+02
0.92757E+02	T5	0.93322E+02	T6	0.92963E+02	T7	0.92612E+02
0.93907E+02	T9	0.93417E+02	T10	0.93232E+02	T11	0.92826E+02
0.93502E+02	T13	0.93999E+02	T14	0.93999E+02	T15	0.93999E+02
0.94568E+02	T17	0.93507E+02	T18	0.93512E+02	T19	0.93494E+02
0.93431E+02	T21	0.93413E+02	T22	0.93398E+02	T23	0.93988E+02
0.93098E+02	T25	0.93064E+02	T26	0.93079E+02	T27	0.93031E+02
0.93033E+02	T29	0.93090E+02	T30	0.93947E+02	T31	0.92627E+02
0.92628E+02	T33	0.92630E+02	T34	0.92629E+02	T35	0.92578E+02
0.92694E+02	T37	0.92480E+02	T38	0.92570E+02	T39	0.93999E+02
0.93999E+02	T41	0.93648E+02	T42	0.93999E+02	T43	0.93999E+02
0.93999E+02	T45	0.93999E+02	T46	0.93648E+02	T47	0.93999E+02
0.39999E+02	T49	0.70007E+02	T50			
0.65863E+02	T51	0.49811E+02	T52	0.45961E+02	T53	0.44751E+02
0.43487E+02	T55	0.42083E+02	T56	0.45418E+02	T57	0.94077E+02
0.39999E+02	T59	0.39999E+02	T60	0.39999E+02	T61	0.39999E+02
0.39999E+02	T63	0.57885E+02	T64	0.39999E+02	T65	0.90654E+02
0.39999E+02	T67	0.39999E+02	T68	0.39999E+02	T69	0.70698E+02
0.71968E+02	T71	0.71968E+02	T72	0.71688E+02	T73	0.81991E+02
0.83953E+02	T75	0.83953E+02	T76	0.83568E+02	T77	0.95970E+02
0.39999E+02	T79	0.10329E+03	T80	0.11394E+03	T81	0.51804E+03
0.11099E+03	T129	-0.45999E+03	T130	0.37999E+02	T131	0.29487E+01
0.10000E+01	T133	0.83680E+08	T134	0.61799E+09	T135	
0.39599E+05	0.97800E+01	21	0.18742E+05	1	0.29648E+01	2465
0.95971E+02	T1	0.96250E+02	T2	0.96038E+02	T3	0.96258E+02
0.95993E+02	T5	0.96544E+02	T6	0.96199E+02	T7	0.95847E+02
0.97125E+02	T9	0.96637E+02	T10	0.96465E+02	T11	0.96061E+02
0.96692E+02	T13	0.39999E+02	T14	0.39999E+02	T15	0.39999E+02
0.97775E+02	T17	0.96734E+02	T18	0.96740E+02	T19	0.96722E+02
0.96659E+02	T21	0.96641E+02	T22	0.96627E+02	T23	0.97218E+02
0.96331E+02	T25	0.96298E+02	T26	0.96315E+02	T27	0.96273E+02
0.96297E+02	T29	0.96325E+02	T30	0.97182E+02	T31	0.95862E+02
0.95863E+02	T33	0.95864E+02	T34	0.95864E+02	T35	0.95814E+02
0.95937E+02	T37	0.95712E+02	T38	0.95806E+02	T39	0.39999E+02
0.39999E+02	T41	0.96867E+02	T42	0.39999E+02	T43	0.39999E+02
0.39999E+02	T45	0.39999E+02	T46	0.96867E+02	T47	0.39999E+02

Fig. B-4 (Cont.)

## MARS LANDER ON SURFACE

TIME	RCMIN	MINND	RCMAX	MAXND	DTHETA	NCYC
0.39599E+05	0.97800E+01	21	0.18742E+05	1	0.29648E+01	2465
0.39999E+02	T49	0.70008E+02	T50			
0.68101E+02	T51	0.51203E+02	T52	0.46964E+02	T53	0.45643E+02
0.44181E+02	T55	0.42583E+02	T56	0.46375E+02	T57	0.97335E+02
0.39999E+02	T59	0.39999E+02	T60	0.39999E+02	T61	0.39999E+02
0.39999E+02	T63	0.60151E+02	T64	0.39999E+02	T65	0.93986E+02
0.39999E+02	T67	0.39999E+02	T68	0.39999E+02	T69	0.73699E+02
0.74992E+02	T71	0.74992E+02	T72	0.74693E+02	T73	0.85154E+02
0.87144E+02	T75	0.87144E+02	T76	0.86752E+02	T77	0.99199E+02
0.39999E+02	T79	0.10649E+03	T80	0.11708E+03	T81	0.52083E+03
0.11169E+03	T129	-0.45999E+03	T130	0.43499E+02	T131	0.53846E+01
0.10000E+01	T133	0.86379E+08	T134	0.61799E+09	T135	
TIME	RCMIN	MINND	RCMAX	MAXND	DTHETA	NCYC
0.40799E+05	0.97797E+01	21	0.18455E+05	1	0.29692E+01	2619
0.99137E+02	T11	0.99405E+02	T12	0.99199E+02	T13	0.99416E+02
0.99155E+02	T5	0.99690E+02	T16	0.99360E+02	T7	0.99010E+02
0.10026E+03	T9	0.99782E+02	T10	0.99622E+02	T11	0.99222E+02
0.99807E+02	T13	0.39999E+02	T14	0.39999E+02	T15	0.39999E+02
0.10090E+03	T17	0.99886E+02	T18	0.99891E+02	T19	0.99874E+02
0.99811E+02	T21	0.99794E+02	T22	0.99778E+02	T23	0.10037E+03
0.99489E+02	T25	0.99457E+02	T26	0.99475E+02	T27	0.99440E+02
0.99456E+02	T29	0.99485E+02	T30	0.10034E+03	T31	0.99023E+02
0.99024E+02	T33	0.99026E+02	T34	0.99025E+02	T35	0.98976E+02
0.99104E+02	T37	0.98872E+02	T38	0.98968E+02	T39	0.39999E+02
0.39999E+02	T41	0.10000E+03	T42	0.39999E+02	T43	0.39999E+02
0.39999E+02	T45	0.39999E+02	T46	0.10000E+03	T47	0.39999E+02
0.39999E+02	T49	0.70009E+02	T50			
0.70356E+02	T51	0.52670E+02	T52	0.48044E+02	T53	0.46614E+02
0.44947E+02	T55	0.43149E+02	T56	0.47410E+02	T57	0.10052E+03
0.39999E+02	T59	0.39999E+02	T60	0.39999E+02	T61	0.39999E+02
0.39999E+02	T63	0.62510E+02	T64	0.39999E+02	T65	0.97245E+02
0.39999E+02	T67	0.39999E+02	T68	0.39999E+02	T69	0.76758E+02
0.78068E+02	T71	0.78068E+02	T72	0.77752E+02	T73	0.88300E+02
0.90306E+02	T75	0.90306E+02	T76	0.89909E+02	T77	0.10234E+03
0.39999E+02	T79	0.10959E+03	T80	0.12011E+03	T81	0.52356E+03
0.11228E+03	T129	-0.45999E+03	T130	0.48999E+02	T131	0.78205E+01
0.10000E+01	T133	0.88429E+08	T134	0.61799E+09	T135	
TIME	RCMIN	MINND	RCMAX	MAXND	DTHETA	NCYC
0.41999E+05	0.97794E+01	21	0.18175E+05	1	0.30219E+01	2773

Fig. B-4 (Cont.)

## MARS LANDER ON SURFACE

TIME	RCMIN	MINND	RCMAX	MAXND	DTHETA	NCYC
0.41999E+05	0.97794E+01	21	0.18175E+05	1	0.30219E+01	2773
0.10222E+03	T1	0.10248E+03	T2	0.10228E+03	T3	0.10249E+03
0.10224E+03	T5	0.10276E+03	T6	0.10244E+03	T7	0.10209E+03
0.10333E+03	T9	0.10285E+03	T10	0.10270E+03	T11	0.10230E+03
0.10284E+03	T13	0.39999E+02	T14	0.39999E+02	T15	0.39999E+02
0.10395E+03	T17	0.10296E+03	T18	0.10296E+03	T19	0.10295E+03
0.10288E+03	T21	0.10287E+03	T22	0.10285E+03	T23	0.10344E+03
0.10257E+03	T25	0.10254E+03	T26	0.10256E+03	T27	0.10253E+03
0.10254E+03	T29	0.10257E+03	T30	0.10342E+03	T31	0.10211E+03
0.10211E+03	T33	0.10211E+03	T34	0.10211E+03	T35	0.10206E+03
0.10219E+03	T37	0.10195E+03	T38	0.10205E+03	T39	0.39999E+02
0.39999E+02	T41	0.10307E+03	T42	0.39999E+02	T43	0.39999E+02
0.39999E+02	T45	0.39999E+02	T46	0.10307E+03	T47	0.39999E+02
0.39999E+02	T49	0.70010E+02	T50			
0.72623E+02	T51	0.54209E+02	T52	0.49199E+02	T53	0.47662E+02
0.45785E+02	T55	0.43782E+02	T56	0.48520E+02	T57	0.10363E+03
0.39999E+02	T59	0.39999E+02	T60	0.39999E+02	T61	0.39999E+02
0.39999E+02	T63	0.64953E+02	T64	0.39999E+02	T65	0.10042E+03
0.39999E+02	T67	0.39999E+02	T68	0.39999E+02	T69	0.79861E+02
0.81184E+02	T71	0.81184E+02	T72	0.80853E+02	T73	0.91423E+02
0.93435E+02	T75	0.93435E+02	T76	0.93035E+02	T77	0.10541E+03
0.39999E+02	T79	0.11261E+03	T80	0.12305E+03	T81	0.52625E+03
0.11278E+03	T129	-0.45999E+03	T130	0.54499E+02	T131	0.10256E+02
0.10303E+01	T133	0.89333E+08	T134	0.61799E+09	T135	
0.43199E+05	0.97792E+01	21	0.17900E+05	1	0.30439E+01	2927
0.10524E+03	T1	0.10549E+03	T2	0.10530E+03	T3	0.10551E+03
0.10525E+03	T5	0.10575E+03	T6	0.10546E+03	T7	0.10511E+03
0.10632E+03	T9	0.10584E+03	T10	0.10571E+03	T11	0.10532E+03
0.10581E+03	T13	0.39999E+02	T14	0.39999E+02	T15	0.39999E+02
0.10693E+03	T17	0.10596E+03	T18	0.10597E+03	T19	0.10595E+03
0.10589E+03	T21	0.10587E+03	T22	0.10585E+03	T23	0.10645E+03
0.10558E+03	T25	0.10555E+03	T26	0.10557E+03	T27	0.10555E+03
0.10555E+03	T29	0.10558E+03	T30	0.10643E+03	T31	0.10512E+03
0.10512E+03	T33	0.10513E+03	T34	0.10513E+03	T35	0.10508E+03
0.10521E+03	T37	0.10497E+03	T38	0.10507E+03	T39	0.39999E+02
0.39999E+02	T41	0.10607E+03	T42	0.39999E+02	T43	0.39999E+02
0.39999E+02	T45	0.39999E+02	T46	0.10607E+03	T47	0.39999E+02

Fig. B-4 (Cont.)

NOTE: 60 DAYS TO PERIHELION  
20.7° NORTH LATITUDE

REFERENCE: G. DeVaucouleurs,  
"The Physical Environment on Mars,"  
in "Physics and Medicine of the Upper  
Atmosphere and Space," Edited by  
O. O. Benson and H. Strughold,  
John Wiley & Sons, Inc., New York,  
1960

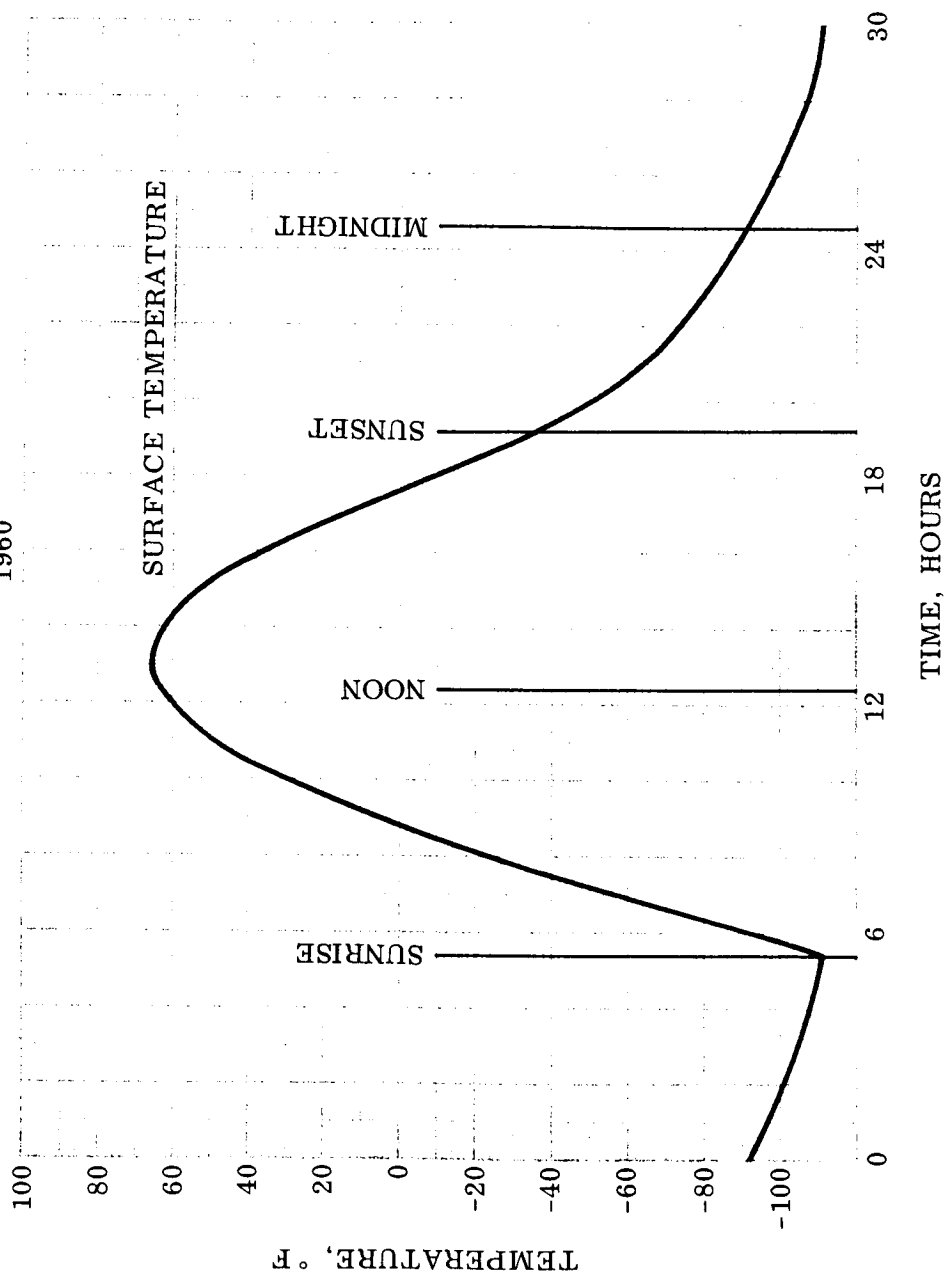


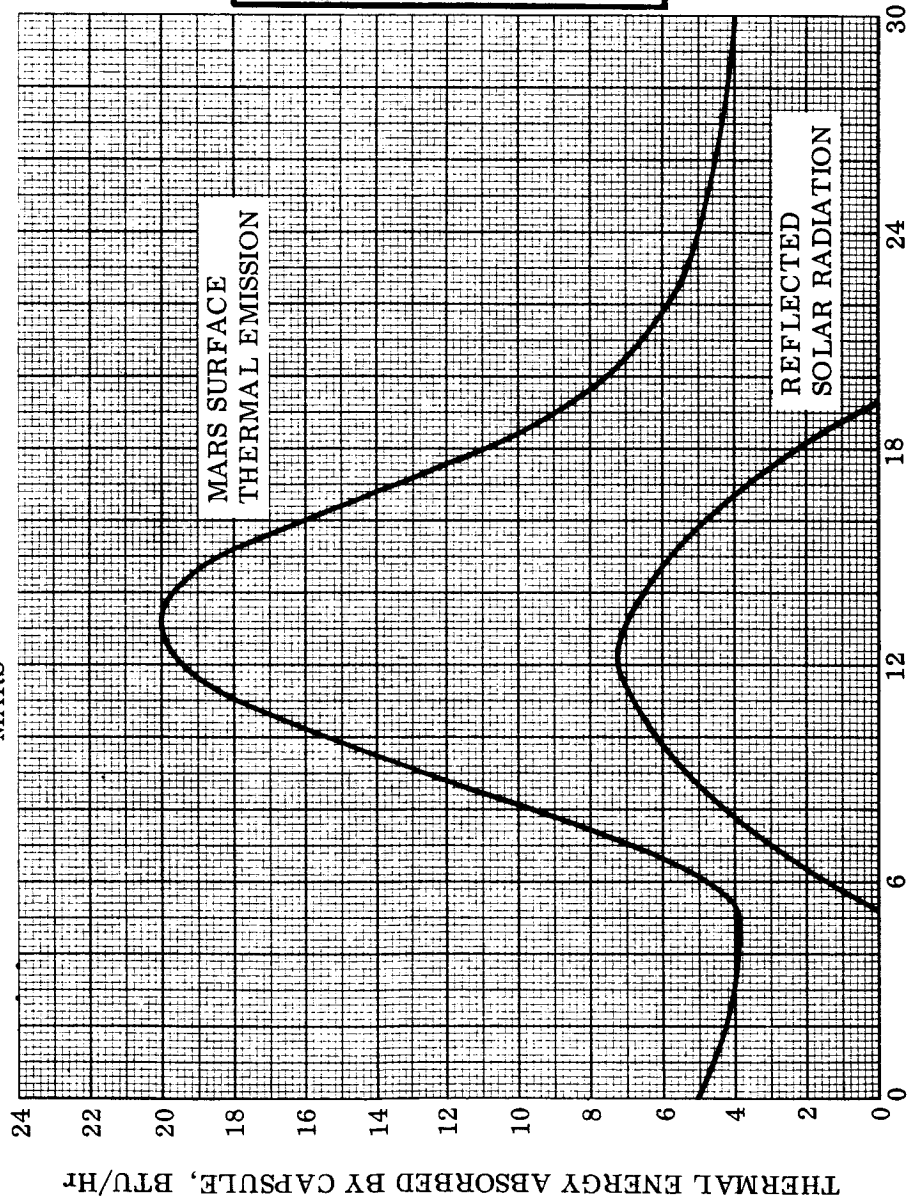
Fig. B-5 Martian Surface Temperature vs. Time

NOTE: 60 DAYS TO PERIHELION  
20.7° NORTH LATITUDE  
CAPSULE AT 10° NORTH LATITUDE.

$$\epsilon_{\text{CAPSULE}} = 0.053$$

$$\alpha_{\text{CAPSULE}} = 0.083$$

$$\rho_{\text{MARS}} = 0.15$$



HOURS AFTER MIDNIGHT ON MARS AT 10° NORTH LATITUDE

Fig. B-6 Solar and Infrared Radiation Absorbed by Landed Payload Capsule

The Nusselt number (Nu) for natural convection heat transfer between a fluid and short vertical planes in a laminar regime is given by Ref. 3-14 as

$$\text{Nu}_f = 0.59 \left[ \text{Gr}_f \text{Pr}_f \right]^{0.25} \quad (\text{B. 1})$$

where all properties are evaluated at the film temperature. At ordinary temperature and atmospheric pressure, Eq. (B.1) reduces to

$$h_c = 0.29 \left( \frac{\Delta T}{L_p} \right)^{0.25} = 0.29 \frac{(T_H - 293)^{0.25}}{(L_p)^{0.25}} \quad (\text{B. 2})$$

Equation (B.2) deviates less than 10% from Eq. (B.1) for the temperatures involved during sterilization and is considered adequate for this analysis. (See Fig. B-7).

The natural convection heat transfer rate,  $Q_S$  (BTU/Hr), is given by

$$Q_S = h_{\text{CONV}} A_S (T_H - 293) \quad (\text{B. 3})$$

which, after substitution of Eq. (B.2), becomes

$$Q_S = 0.29 A_S \frac{(T_H - 293)^{1.25}}{(L_p)^{0.25}} \quad (\text{B. 4})$$

where

$A_S$  = Surface area exposed to nitrogen gas,  $\text{ft}^2$

$L_p$  = Flat plate length, ft

$T_H$  = Hot junction (surface) temperature, °F

293 = Temperature of nitrogen gas, °F

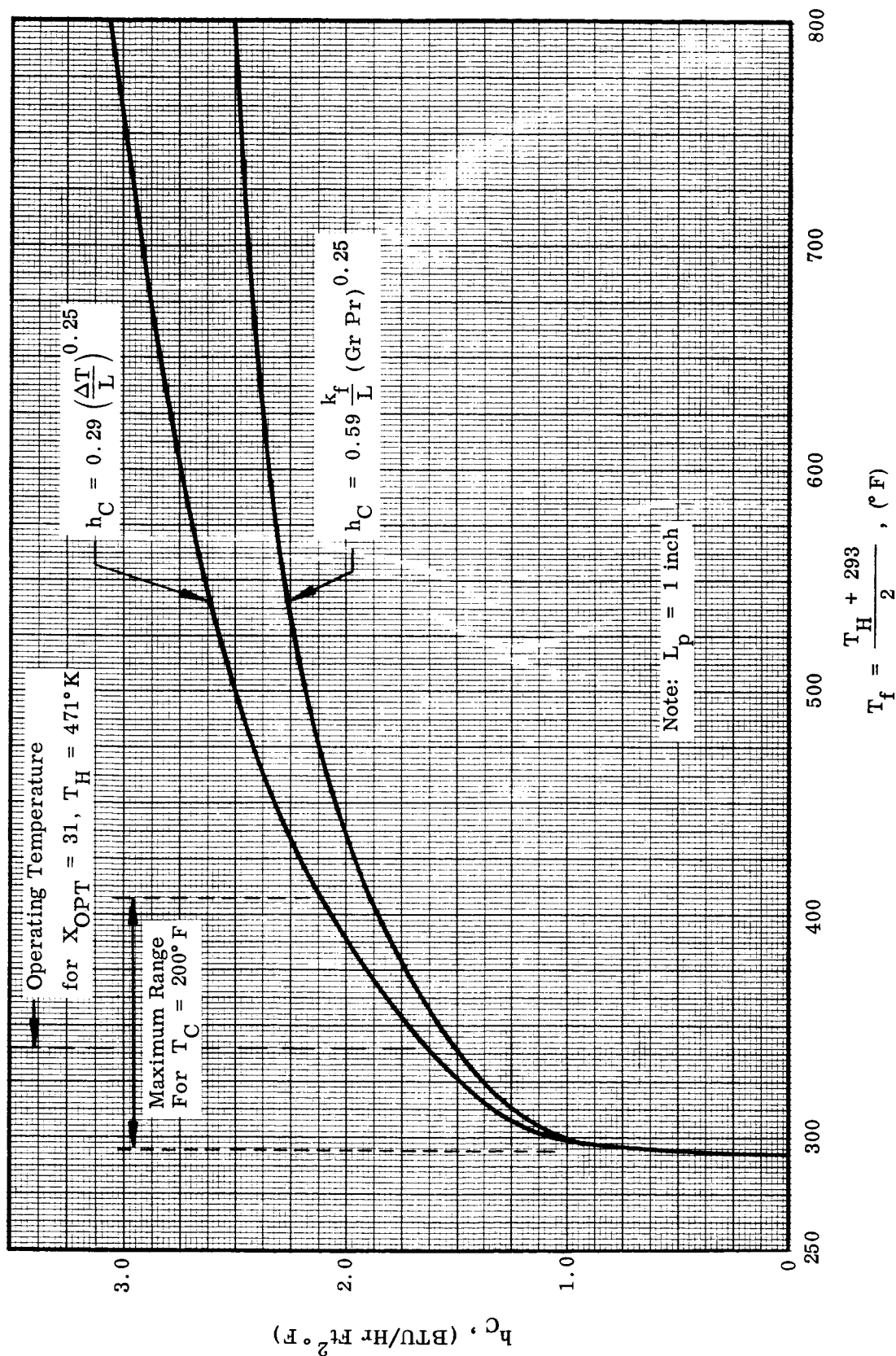


Fig. B-7 Convective Heat Transfer Coefficient vs. Film Temperature



Converting Eq. (B.4) to metric units, ( $Q_S$  watts) is given by

$$Q_S = 4.50 \times 10^{-4} A_S \frac{(T_H - 418)^{1.25}}{(L_p)^{0.25}} \quad (B.5)$$

where  $A_S$  is in  $\text{cm}^2$ ,  $L_p$  in cm, and  $T_H$  in  $^\circ\text{K}$ .

### B.2.2. Sizing the Thermoelectric Unit

The relation for thermoelectric pellet length was given by Eq. (3.49) as

$$L = 3.06 \times 10^{-5} \frac{A_S T_C T_H}{Q_H^* (1+X)}$$

Imposing the condition that the natural convection heat rate,  $Q_S$ , of the nitrogen gas must be equal to the heat rejected,  $Q_H^*$ , by the thermoelectric heat pump device, Eqs. (B.5) and (3.49) may be combined to give

$$L = \frac{0.0680 T_C T_H (L_p)^{0.25}}{(T_H - 418)^{1.25} (1+X)} \quad (B.6)$$

The relationship between  $T_C$ ,  $T_H$  and  $X$  for  $\Delta T_{\text{MAX}}$  was given by Eq. (3.51) as

$$(T_H - T_C)_{\text{MAX}} = \frac{1.333 \times 10^{-3} T_C^2}{1 + 0.0226 X}$$

It is shown graphically in Figs. 3-15 and 3-16 for two values of  $T_C$ . Equation (3.51) can be solved for  $T_H$  and substituted in Eq. (B.6) to give  $L = L(L_p, T_C, X)$ . This relationship is shown graphically in Fig. B-8 for  $L_p = 1$  inch. It will be noted that  $X_{\text{OPT}}(X \text{ for } L_{\text{MIN}})$  is approximately 31 for  $T_C$  equal to  $200^\circ\text{F}$ .

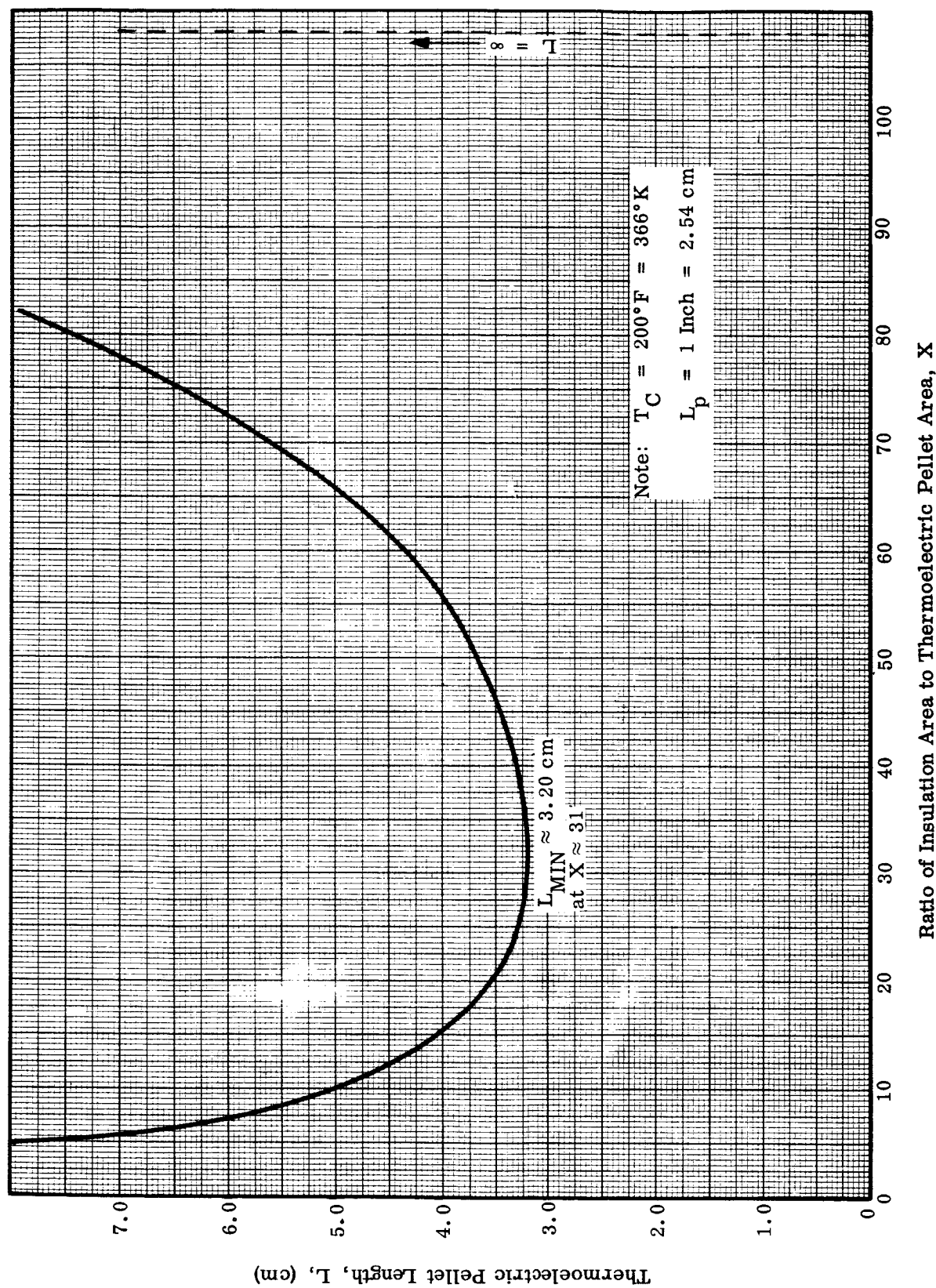


Fig. B-8 Thermoelectric Pellet Length vs. Ratio of Insulation Area to Thermoelectric Pellet Area

As related in Section 3.7,  $X_{OPT}$  is not a function of plate length, thus an optimum ratio of insulation area to thermoelectric pellet area may be found based only on the upper temperature limit of the area to be isolated.

Using the value of  $X$  determined above and the corresponding value of  $T_H$  from Fig. 3-16, the minimum thermoelectric pellet length,  $L_{MIN}$ , may be derived from Eq. (B.6) as a function of plate length,  $L_p$ , only. Thus, for  $T_C = 200^\circ F$ ,

$$(L_{MIN})_{T_C = 200^\circ F} = 2.54 (L_p)^{0.25} \quad (B.7)$$

Equation (B.7) is shown graphically in Fig. B-9.

#### B.2.3. Application to Vidicon Tube Face

We are now ready to consider the problem of thermally isolating a small area using a removable thermoelectric cooling device. A vidicon tube is assumed to be enclosed in a fluid circulation cooling shield with the exception of its face. A thermoelectric device for isolating the face will be designed utilizing the method presented in the foregoing section. Typical material parameters given in Appendix A have been used in this example.

Thermoelectric Unit Design. Assume a square thermoelectric unit with the following dimensions:

$$\begin{aligned} \text{Length per side} &= L_p = 2 \text{ in.} = 5.08 \text{ cm} \\ \text{Surface area} &= A_S = 4 \text{ in.}^2 = 25.8 \text{ cm}^2 \end{aligned}$$

The vidicon tube upper temperature limit is  $212^\circ F$ , therefore let  $T_C = 200^\circ F = 366^\circ K$ .

From Fig. B-8 for  $T_C = 200^\circ F$ ;  $X_{OPT} = 31$

From Fig. 3-16 at  $X = 31$ ;  $(T_H)_{OPT} = 471^\circ K$ ,  $(\Delta T_{MAX})_{OPT} = 105^\circ K$ .

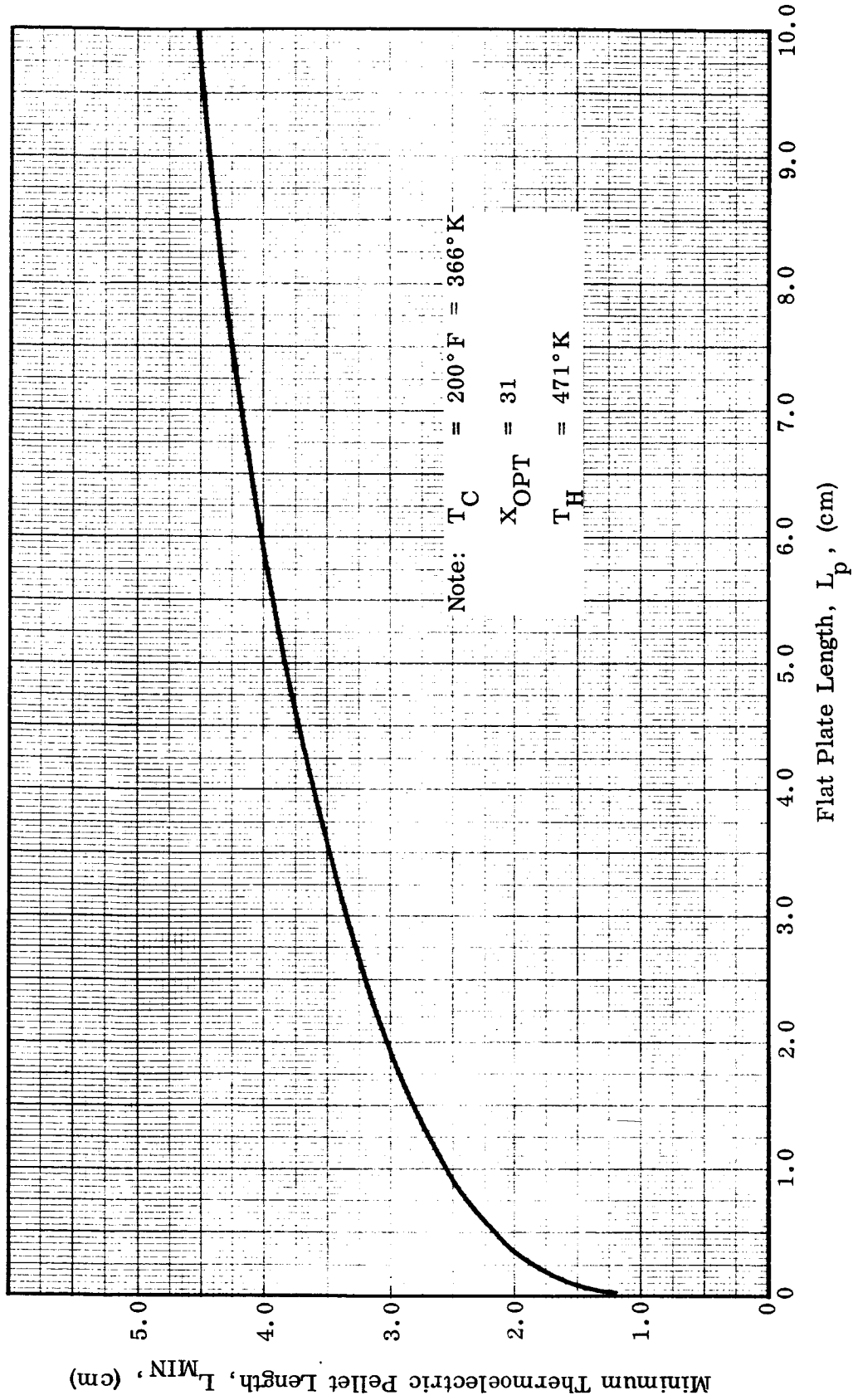


Fig. B-9 Minimum Thermoelectric Pellet Length vs. Flat Plate Length

From Fig. B-9 at  $L_p = 5.08 \text{ cm}$ ;  $L_{\text{MIN}} = 3.82 \text{ cm} = 1.50 \text{ in}$

Since  $X = 31$  and  $A_S = 25.8 \text{ cm}^2$ ;

Thermoelectric material cross-sectional area =  $0.806 \text{ cm}^2$

Insulation cross-sectional area =  $25.0 \text{ cm}^2$

For  $A_S = 25.8 \text{ cm}^2$ ,  $X = 31$  and choosing  $n = 2$  couples; then from Eq. (3.46),

$A_S = 2nA(1+X)$ :

Cross-sectional area per pellet =  $A = 0.2016 \text{ cm}^2$

From Eq. (A.32) ;  $I_{\text{OPT}} = 3.38 \text{ amperes}$

From Eq. (A.27) ;  $V = 0.330 \text{ volts}$

From Eq. (A.28) ;  $P_{\text{IN}} = Q_{\text{IN}} = 1.114 \text{ watts}$

From Eq. (A.29) ;  $Q_C = 0$

From Eq. (A.30) ;  $Q_H = Q_H^* = 1.114 \text{ watts}$   
and (3.43)

From Eq. (B.4) ;  $Q_S = 1.114 \text{ watts}$